

University of Chicago
Concepts in Biophysical Chemistry

Andrei Tokmakoff

This text is disseminated via the Open Education Resource (OER) LibreTexts Project (<https://LibreTexts.org>) and like the hundreds of other texts available within this powerful platform, it is freely available for reading, printing and "consuming." Most, but not all, pages in the library have licenses that may allow individuals to make changes, save, and print this book. Carefully consult the applicable license(s) before pursuing such effects.

Instructors can adopt existing LibreTexts texts or Remix them to quickly build course-specific resources to meet the needs of their students. Unlike traditional textbooks, LibreTexts' web based origins allow powerful integration of advanced features and new technologies to support learning.



The LibreTexts mission is to unite students, faculty and scholars in a cooperative effort to develop an easy-to-use online platform for the construction, customization, and dissemination of OER content to reduce the burdens of unreasonable textbook costs to our students and society. The LibreTexts project is a multi-institutional collaborative venture to develop the next generation of open-access texts to improve postsecondary education at all levels of higher learning by developing an Open Access Resource environment. The project currently consists of 14 independently operating and interconnected libraries that are constantly being optimized by students, faculty, and outside experts to supplant conventional paper-based books. These free textbook alternatives are organized within a central environment that is both vertically (from advance to basic level) and horizontally (across different fields) integrated.

The LibreTexts libraries are Powered by [NICE CXOne](#) and are supported by the Department of Education Open Textbook Pilot Project, the UC Davis Office of the Provost, the UC Davis Library, the California State University Affordable Learning Solutions Program, and Merlot. This material is based upon work supported by the National Science Foundation under Grant No. 1246120, 1525057, and 1413739.

Any opinions, findings, and conclusions or recommendations expressed in this material are those of the author(s) and do not necessarily reflect the views of the National Science Foundation nor the US Department of Education.

Have questions or comments? For information about adoptions or adaptations contact info@LibreTexts.org. More information on our activities can be found via Facebook (<https://facebook.com/Libretexts>), Twitter (<https://twitter.com/libretexts>), or our blog (<http://Blog.Libretexts.org>).

This text was compiled on 03/09/2025

TABLE OF CONTENTS

Licensing

1: Water and Aqueous Solutions

- 1: Fluids
 - 1.1: What is a Fluid?
 - 1.2: Radial Distribution Function
 - 1.3: Excluded Volume
- 2: Lattice Model of a Fluid
 - 2.1: Lattice Models
 - 2.2: Ideal Lattice Gas
 - 2.3: Binary Fluid
- 3: Water's Physical Properties
 - 3.1: Water Structure
 - 3.2: Water Dynamics
 - 3.3: Electrical Properties of Pure Water
- 4: Solvation
 - 4.1: Solvation
 - 4.2: Solvation Thermodynamics
 - 4.3: Solvation Dynamics and Reorganization Energy
- 5: Hydrophobicity
 - 5.1: Hydrophobic Solvation - Thermodynamics
 - 5.2: Hydrophobic Solvation- Solute Size Effect
 - 5.3: Hydrophobic Collapse
- 6: Electrical Properties of Water and Aqueous Solutions
 - 6.1: Electrostatics
 - 6.2: Dielectric Constant and Screening
 - 6.3: Free Energy of Ions in Solution
 - 6.4: Ion Distributions in Electrolyte Solution
 - 6.5: Poisson–Boltzmann Equation
 - 6.6: Debye–Hückel Theory
 - 6.7: Ion Distributions Near a Charged Interface
 - 6.8: Ion Distributions Near a Charged Sphere

2: Macromolecules

- 7: Statistical Description of Macromolecular Structure
 - 7.1: Segment Models
 - 7.2: Excluded Volume Effects
 - 7.3: Polymer Loops
- 8: Polymer Lattice Models
 - 8.1: Entropy of Single Polymer Chain
 - 8.2: Self-Avoiding Walks
 - 8.3: Conformational Changes with Temperature
 - 8.4: Flory–Huggins Model of Polymer Solutions
 - 8.5: Polymer–Solvent Interactions

- 9: Macromolecular Mechanics
 - 9.1: Force and Work
 - 9.2: Worm-like Chain
 - 9.3: Polymer Elasticity and Force–Extension Behavior

3: Diffusion

- 10: Diffusion
 - 10.1: Continuum Diffusion
 - 10.2: Solving the Diffusion Equation
 - 10.3: Steady-State Solutions
- 11: Brownian Motion
 - 11.1: Random Walk and Diffusion
 - 11.2: Markov Chain and Stochastic Processes
 - 11.3: Fluorescence Correlation Spectroscopy
 - 11.4: Orientational Diffusion
- 12: Diffusion in a Potential
 - 12.1: Diffusion with Drift
 - 12.2: Biased Random Walk
 - 12.3: Diffusion in a Potential
- 13: Friction and the Langevin Equation
 - 13.1: Langevin Equation
 - 13.2: Brownian Dynamics

4: Transport

- 14: Hydrodynamics
 - 14.1: Newtonian Fluids
 - 14.2: Stokes' Law
 - 14.3: Laminar and Turbulent Flow
- 15: Passive Transport
 - 15.1: Dimensionality Reduction
 - 15.2: Facilitated Diffusion
 - 15.3: Search Times in Facilitated Diffusion
- 16: Targeted Diffusion
 - 16.1: Diffusion to Capture
 - 16.2: Diffusion to Capture with Interactions
 - 16.3: Mean First Passage Time
- 17: Directed and Active Transport
 - 17.1: Motor Proteins
 - 17.2: Passive vs Active Transport
 - 17.3: Brownian Ratchet
 - 17.4: Polymerization Ratchet and Translocation Ratchet

5: Cooperativity

- 18: Cooperativity
 - 18.1: Helix–Coil Transition
 - 18.2: Two-State Thermodynamics
- 19: Self-Assembly

- [19.1: Micelle Formation](#)
- [19.2: Classical Nucleation Theory](#)
- [19.3: Why Are Micelles Uniform in Size?](#)
- [19.4: Shape of Self-Assembled Amphiphiles](#)

6: Dynamics and Kinetics

- [20: Protein Folding](#)
 - [20.1: Models for Simulating Folding](#)
 - [20.2: Perspectives on Protein Folding Dynamics](#)
- [21: Binding and Association](#)
 - [21.1: Thermodynamics and Biomolecular Reactions](#)
 - [21.2: Statistical Thermodynamics of Biomolecular Reactions](#)
 - [21.3: DNA Hybridization](#)
 - [21.4: Biomolecular Kinetics](#)
 - [21.5: Diffusion-Limited Reactions](#)
 - [21.6: Protein Recognition and Binding](#)
 - [21.7: Forces Guiding Binding](#)
 - [21.8: Specificity in Recognition and Binding](#)
- [22: Biophysical Reaction Dynamics](#)
 - [22.1: Concepts and Definitions](#)
 - [22.2: Computing Dynamics](#)
 - [22.3: Representations of Dynamics](#)
 - [22.4: Analyzing Trajectories](#)
 - [22.5: Time-Correlation Functions](#)
- [23: Barrier Crossing and Activated Processes](#)
 - [23.1: Transition State Theory](#)
 - [23.2: Kramers' Theory](#)

[Index](#)

[Glossary](#)

[Detailed Licensing](#)

Licensing

A detailed breakdown of this resource's licensing can be found in [Back Matter/Detailed Licensing](#).

SECTION OVERVIEW

1: Water and Aqueous Solutions

1: Fluids

- 1.1: What is a Fluid?
- 1.2: Radial Distribution Function
- 1.3: Excluded Volume

2: Lattice Model of a Fluid

- 2.1: Lattice Models
- 2.2: Ideal Lattice Gas
- 2.3: Binary Fluid

3: Water's Physical Properties

- 3.1: Water Structure
- 3.2: Water Dynamics
- 3.3: Electrical Properties of Pure Water

4: Solvation

- 4.1: Solvation
- 4.2: Solvation Thermodynamics
- 4.3: Solvation Dynamics and Reorganization Energy

5: Hydrophobicity

- 5.1: Hydrophobic Solvation - Thermodynamics
- 5.2: Hydrophobic Solvation- Solute Size Effect
- 5.3: Hydrophobic Collapse

6: Electrical Properties of Water and Aqueous Solutions

- 6.1: Electrostatics
- 6.2: Dielectric Constant and Screening
- 6.3: Free Energy of Ions in Solution
- 6.4: Ion Distributions in Electrolyte Solution
- 6.5: Poisson–Boltzmann Equation
- 6.6: Debye–Hückel Theory
- 6.7: Ion Distributions Near a Charged Interface
- 6.8: Ion Distributions Near a Charged Sphere

This page titled [1: Water and Aqueous Solutions](#) is shared under a [CC BY-NC-SA 4.0](#) license and was authored, remixed, and/or curated by [Andrei Tokmakoff](#) via [source content](#) that was edited to the style and standards of the LibreTexts platform.

CHAPTER OVERVIEW

1: Fluids

[1.1: What is a Fluid?](#)

[1.2: Radial Distribution Function](#)

[1.3: Excluded Volume](#)

This page titled [1: Fluids](#) is shared under a [CC BY-NC-SA 4.0](#) license and was authored, remixed, and/or curated by [Andrei Tokmakoff](#) via [source content](#) that was edited to the style and standards of the LibreTexts platform.

1.1: What is a Fluid?

Fluids

What is a fluid? Almost everything that we will discuss is soft matter under physiological temperature conditions: liquids and solutions, cytoplasm and cytosol, DNA and proteins in solution, membranes, micelles, colloids, gels... All of these materials can in some respect be considered a fluid. So, what is a fluid?

- A substance that flows, deforms, and changes shape when subject to a force, or stress.
- It has no fixed shape, but adapts its surface to the shape of its container. Gasses are also fluids, but we will focus on fluids that are mostly incompressible.

For physicists, fluids are commonly associated with flow—a non-equilibrium property—and how matter responds to forces (i.e., "Newtonian fluids"). This topic—"rheology"—will be discussed in more detail later. From this perspective, all soft condensed matter can be considered a fluid. For chemists, fluids most commonly appear as liquids and solutions. Chemists typically use a molecular description for the solute, but less so for the solvent. However, chemists have a clear appreciation of how liquids influence chemical behavior and reactivity, a topic commonly called "solvation". The most common perspective of fluids is as continuous dielectric media, however fluids can be multicomponent heterogeneous mixtures. For our biophysical purposes, we use the perspectives above, with a particular interest in the uniquely biological fluid: water. Since we are particularly interested in molecular-scale phenomena, we will add some additional criteria:

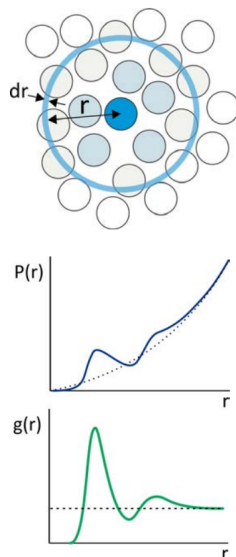
- **Composition:** Fluids are dense media composed of particulate matter (atoms, molecules, proteins...) that can interact with one another. Since no two particles can occupy the same volume, each particle in a fluid has "excluded volume" that is not available to the remaining particles in the system.
- **"Structure":** Fluids are structured locally on the distance scale of the particle size by their packing and cohesive interactions, but are macroscopically disordered.
- **The midrange or mesoscale distances** involve interactions between multiple particles, leading to correlated motions of the constituents.
- **"Flow"** is a manifestation of these correlated structural motions in the mesoscale structure.
- **Most important:** The cohesive forces (intermolecular interactions) between the constituents of a fluid, and the energy barriers to changing structure, are on the order of $k_B T$ ("thermal energy"). Thermal forces are enough to cause spontaneous flow on a microscopic level even at equilibrium.

Fluids may appear time-invariant at equilibrium, but they are microscopically dynamic. In many cases, "structure" (the positioning of constituents in space) and the "dynamics" (time-dependent changes to position) are intimately coupled.

This page titled [1.1: What is a Fluid?](#) is shared under a [CC BY-NC-SA 4.0](#) license and was authored, remixed, and/or curated by [Andrei Tokmakoff](#) via [source content](#) that was edited to the style and standards of the LibreTexts platform.

1.2: Radial Distribution Function

"Structure" implies that the positioning of particles is regular and predictable. This is possible in a fluid to some degree when considering the short-range position and packing of particles. The local particle density variation should show some structure in a statistically averaged sense. Structure requires a reference point, and in the case of a fluid we choose a single particle as the reference and describe the positioning of other particles relative to that. Since each particle of a fluid experiences a different local environment, this information must be statistically averaged, which is our first example of a correlation function. For distances longer than a "correlation length", we should lose the ability to predict the relative position of a specific pair of particles. On this longer length scale, the fluid is homogeneous.



The radial distribution function, $g(r)$, is the most useful measure of the "structure" of a fluid at molecular length scales. Although it invokes a continuum description, by "fluid" we mean any dense, disordered system which has local variation in the position of its constituent particles but is macroscopically isotropic. $g(r)$ provides a statistical description of the local packing and particle density of the system, by describing the average distribution of particles around a central reference particle. We define the radial distribution function as the ratio of $\langle \rho(r) \rangle$, the average local number density of particles at a distance r , to the bulk density of particles, ρ :

$$g(r) = \frac{\langle \rho(r) \rangle}{\rho}$$

In a dense system, $g(r)$ starts at zero (since it does not count the reference particle), rises to a peak at the distance characterizing the first shell of particles surrounding the reference particle (i.e., the 1st solvation shell), and approaches 1 for long distances in isotropic media. The probability of finding a particle at a distance r in a shell of thickness dr is $P(r) = 4\pi r^2 g(r) dr$, so integrating $\rho \cdot g(r)$ over the first peak in gives the average number of particles in the first shell.

The radial distribution function is most commonly used in gasses, liquids, and solutions, since it can be used to calculate thermodynamic properties such as the internal energy and pressure of the system. But is relevant at any size scale, such as packing of colloids, and is useful in complex heterogeneous media, such as the distribution of ions around DNA. For correlating the position of different types of particles, the radial distribution function is defined as the ratio of the local density of "b" particles at a distance r from "a" particles, $g_{ab}(r) = \langle \rho_{ab}(r) \rangle / \rho$. In practice, $\rho_{ab}(r)$ is calculated by looking radially from an "a" particle at a shell at distance r and of thickness dr , counting the number of "b" particles within that shell, and normalizing the count by the volume of that shell.

Two-Particle Density Correlation Function¹

Let's look a little deeper, considering particles of the same type, as in an atomic liquid or granular material. If there are N particles in a volume V , and the position of the i^{th} particle is \vec{r}_i , then the number density describes the position of particles,

$$\rho(\bar{r}) = \sum_{i=1}^N \delta(\bar{r} - \bar{r}_i)$$

The average of a radially varying property given by $X(r)$ is determined by

$$\langle X(r) \rangle = \frac{1}{V} \int_V X(r) 4\pi r^2 dr$$

Integrating $\rho(\bar{r})$ over a volume gives the particle number in that volume.

$$\int_V \rho(r) 4\pi r^2 dr = N$$

When the integral is over the entire volume, we can use this to obtain the average particle density:

$$\frac{1}{V} \int_0^\infty \rho(r) 4\pi r^2 dr = \frac{N}{V} = \rho$$

Next, we can consider the spatial correlations between two particles, i and j . The two-particle density correlation function is

$$\rho(\bar{r}, \bar{r}') = \left\langle \sum_{i=1}^N \delta(\bar{r} - \bar{r}_i) \sum_{j=1}^N \delta(\bar{r}' - \bar{r}_j) \right\rangle$$

This describes the conditional probability of finding particle i at position r_i and particle j at position r_j . We can expand and factor $\rho(\bar{r}, \bar{r}')$ into two terms depending on whether $i = j$ or $i \neq j$:

$$\begin{aligned} \rho(\bar{r}, \bar{r}') &= N \langle \delta(\bar{r} - \bar{r}_i) \delta(\bar{r} - \bar{r}_i) \rangle + N(N-1) \langle \delta(\bar{r} - \bar{r}_i) \delta(\bar{r}' - \bar{r}_j) \rangle \\ &= \rho^{(1)} + \rho^{(2)}(\bar{r}, \bar{r}') \end{aligned}$$

The first term describes the self-correlations, of which there are N terms: one for each atom.

$$\rho^{(1)} = N \langle \delta(\bar{r} - \bar{r}_i) \delta(\bar{r}' - \bar{r}_i) \rangle = \rho$$

The second term describes the two-body correlations, of which there are $N(N-1)$ terms.

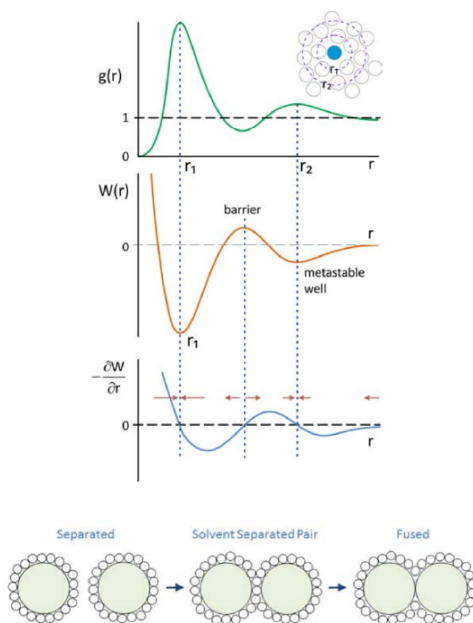
$$\begin{aligned} \rho^{(2)}(\bar{r}, \bar{r}') &= N(N-1) \langle \delta(\bar{r} - \bar{r}_i) \delta(\bar{r}' - \bar{r}_j) \rangle \\ &= \frac{N^2}{V^2} g(\bar{r}, \bar{r}') = \rho^2 g(\bar{r}, \bar{r}') \end{aligned}$$

$g() = \rho^{(2)}(\bar{r}, \bar{r}') / \rho^2$ is the two-particle distribution function, which describes spatial correlation between two atoms or molecules. For isotropic media, it depends only on distance between particles, $g(|\bar{r}, \bar{r}'|) = g(r)$, and is therefore also called the radial pair-distribution function.

We can generalize $g(r)$ to a mixture of a and b particles by writing $g_{ab}(r)$:

$$\begin{aligned} g_{ab}(r) &= \frac{\rho_{ab}(r)}{N_b/V} \\ N_b &= \int_V dr 4\pi r^2 \rho_{ab}(r) \end{aligned}$$

Potential of Mean Force



One can use $g(r)$ to describe the free energy for bringing two particles together as

$$W(r) = -k_B T \ln g(r)$$

$W(r)$ is known as the potential of mean force. We are taking a free energy which is a function of many internal variables and projecting it onto a single coordinate. $W(r)$ is a potential function that can be used to obtain the mean effective forces that a particle will experience at a given separation $f = -\partial W / \partial r$.

-
1. J. P. Hansen and I. R. McDonald, *Theory of Simple Liquids*, 2nd Ed. (Academic Press, New York, 1986); D. A. McQuarrie, *Statistical Mechanics*. (Harper & Row, New York, 1976).

This page titled [1.2: Radial Distribution Function](#) is shared under a [CC BY-NC-SA 4.0](#) license and was authored, remixed, and/or curated by [Andrei Tokmakoff](#) via [source content](#) that was edited to the style and standards of the LibreTexts platform.

1.3: Excluded Volume

Excluded Volume

One of the key concepts that arises from a particulate description of matter is excluded volume. Even in the absence of attractive interactions, at short range the particles of the fluid collide and experience repulsive forces. These repulsive forces are a manifestation of excluded volume, the volume occupied by one particle that is not available to another. This excluded volume gives rise to the structure of solvation shells that is reflected in the short-range form of $g(r)$ and $W(r)$. Excluded volume also has complex dynamic effects in dense fluids, because one particle cannot move far without many other particles also moving in some correlated manner.

The excluded volume can be related to $g(r)$ and $W(r)$, making note of the virial expansion. If we expand the equation of state in the density of the fluid (ρ):

$$\frac{p}{\rho k_B T} = 1 + B_2(T)\rho + \dots$$

The second virial coefficient B_2 is half of the excluded volume of the system. This is the leading source of non-ideality in gasses reflected in the van der Waals equation of state.

$$\begin{aligned} 2B_2(T) &= \int_0^\infty r^2 (1 - g(r)) dr \\ &= \int_0^\infty r^2 (1 - \exp[-W(r)/k_B T]) dr \end{aligned}$$

This page titled [1.3: Excluded Volume](#) is shared under a [CC BY-NC-SA 4.0](#) license and was authored, remixed, and/or curated by [Andrei Tokmakoff](#) via [source content](#) that was edited to the style and standards of the LibreTexts platform.

CHAPTER OVERVIEW

2: Lattice Model of a Fluid

[2.1: Lattice Models](#)

[2.2: Ideal Lattice Gas](#)

[2.3: Binary Fluid](#)

This page titled [2: Lattice Model of a Fluid](#) is shared under a [CC BY-NC-SA 4.0](#) license and was authored, remixed, and/or curated by [Andrei Tokmakoff](#) via [source content](#) that was edited to the style and standards of the LibreTexts platform.

2.1: Lattice Models

Lattice Models

Lattice models provide a minimalist, or coarse-grained, framework for describing the translational, rotational, and conformational degrees of freedom of molecules, and are particularly useful for problems in which entropy of mixing, configurational entropy, or excluded volume are key variables. The lattice forms a basis for enumerating different configurations of the system, or microstates. Each of these microstates may have a different energy, which is then used to calculate a partition function.

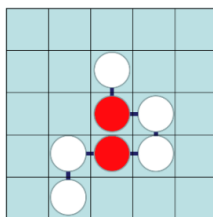
$$Q = \sum_i e^{-E_i/k_B T} \quad (2.1.1)$$

The thermodynamic quantities then emerge from

$$\begin{aligned} F &= -k_B T \ln Q \\ S &= -k_B \sum_i P_i \ln P_i \\ U &= \sum_i P_i E_i \end{aligned}$$

and other internal variables (X) can be statistically described from

$$\langle X \rangle = \sum_{i=1}^N P_i X_i \quad P_i(E_i) = \frac{e^{-E_i/k_B T}}{Q}$$



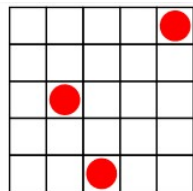
We will typically work with a macroscopic volume broken into cells, typically of a molecular size, which we can fill with the fundamental building blocks in our problem (atoms, molecules, functional groups) subject to certain constraints. In this section we will concern ourselves with the mixing of rigid particles, i.e., translational degrees of freedom. More generally, lattice models can include translational, rotational, and conformational degrees of freedom of molecules.

This page titled [2.1: Lattice Models](#) is shared under a [CC BY-NC-SA 4.0](#) license and was authored, remixed, and/or curated by [Andrei Tokmakoff](#) via [source content](#) that was edited to the style and standards of the LibreTexts platform.

2.2: Ideal Lattice Gas

Lattice Gas

The description of a weakly interacting fluid, gas, solution, or mixture is dominated by the translational entropy or entropy of mixing. In this case, we are dealing with how molecules occupy a volume, which leads to a translational partition function. We begin by defining a lattice and the molecules that fill that lattice:



Parameters:

Total volume: V

Cell volume: v

Number of sites: $M = V/v$

Number of particles: N ($N \leq M$)

Fill Factor: $x = N/M$ ($0 \leq x \leq 1$)

Number of contacts each cell has with adjacent cells: z

We begin by assuming that all microstates (configurations of occupied sites in the volume) are equally probable, i.e., $E_i = \text{constant}$. This is the microcanonical ensemble, so the entropy of the fluid is given by Boltzmann's equation

$$S = k_B \ln \Omega \quad (2.2.1)$$

where Ω is the number of microstates available to the system. If M is not equal to N , then the permutations for putting N indistinguishable particles into M sites is given by the binomial distribution:

$$\Omega = \frac{M!}{N!(M-N)!}$$

← Particles are indistinguishable
← Vacancies are indistinguishable

Also, on cubic lattice, we have 6 contacts that each cell makes with its neighbors. The contact number is z , which will vary for $2D$ ($z = 4$) and $3D$ ($z = 6$) problems.

How do we choose the size of v ? It has to be considered on a case-by-case basis. The objective of these models is to treat the cell as the volume that a particle excludes to occupation by other particles. This need not correspond to an actual molecular dimension in the atomic sense. In the case of the traditional derivation of the translational partition function for an ideal gas, v is equivalent to the quantization volume $\Lambda^3 = (h^2/2\pi m k_B T)^{3/2}$.

From Ω we can obtain the entropy of mixing from $S = k_B \ln \Omega$ with the help of Sterling's approximation $\ln(M!) \simeq M \ln(M) - M$:

$$\begin{aligned} S &= k_B (M \ln M - N \ln N - (M - N) \ln(M - N)) \\ &= -M k_B (x \ln x + (1 - x) \ln(1 - x)) \end{aligned} \quad (2.2.2)$$

In the last line, we introduced a particle fill factor

$$x = N/M$$

which quantifies the fraction of cells that are occupied by particles, and is also known as the mole fraction or the packing ratio. Since $x < 1$, the entropy of mixing is always positive.

For the case of a dilute solution or gas, $N \ll M$, and $(1 - x) \approx 1$, so

$$S_{\text{dilute}} \approx -N k_B \ln x \quad \text{or} \quad -n R \ln x$$

We can derive the ideal gas law $p = Nk_B T/V$ from this result by making use of the thermodynamic identity $p = T(\partial S/\partial V)_N$.

This page titled [2.2: Ideal Lattice Gas](#) is shared under a [CC BY-NC-SA 4.0](#) license and was authored, remixed, and/or curated by [Andrei Tokmakoff](#) via [source content](#) that was edited to the style and standards of the LibreTexts platform.

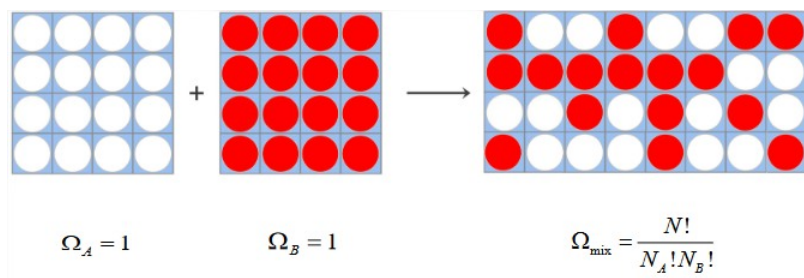
2.3: Binary Fluid

Entropy of Mixing

The thermodynamics of the mixing process is important to phase equilibria, hydrophobicity, solubility, and related solvation problems. The process of mixing two pure substances A and B is shown below. We define the composition of the system through the number of A and B particles: N_A and N_B and the total number of particles $N = N_A + N_B$, which also equals the number of cells. We begin with two containers of the homogeneous pure fluids and mix them together, keeping the total number of cells constant. In the case of the pure fluids before mixing, all cells of the container are initially filled, so there is only one accessible microstate, $\Omega_{\text{pure}} = 1$, and

$$S_{\text{pure}} = k_B \ln 1 = 0$$

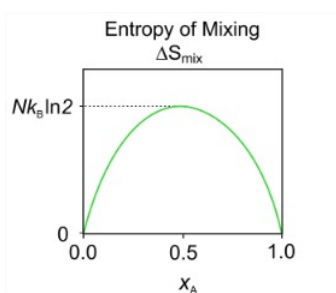
When the two containers are mixed, the number of possible microstates are given by the binomial distribution: $\Omega_{\text{mix}} = N! / N_A! N_B!$.



If these particles have no interactions, each microstate is equally probable, and similar to eq. (2.2.2) we obtain the entropy of the mixture as

$$S_{\text{mix}} = -Nk_B (x_A \ln x_A + x_B \ln x_B) \quad (2.3.1)$$

For the mixture, we define the mole fractions for the two components: $x_A = N_A/N$ and $x_B = N_B/N$. As before, since x_A and $x_B < 1$, the entropy for the mixture is always positive. The entropy of mixing is then calculated from $\Delta S_{\text{mix}} = S_{\text{mix}} - (S_{\text{pure A}} + S_{\text{pure B}})$. Since the entropy of the pure substances in this model is zero, $\Delta S_{\text{mix}} = S_{\text{mix}}$. A plot of this function as a function of mole fractions illustrates that the maximum entropy mixture has $x_A = x_B = 0.5$.

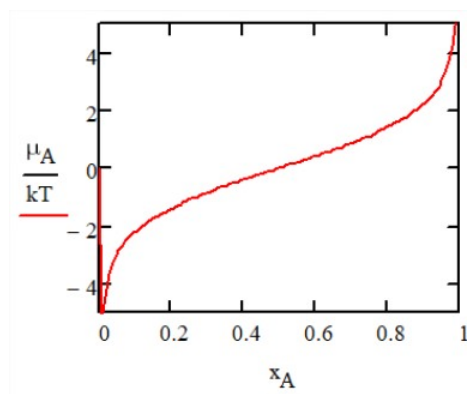


In the absence of interactions between particles, the free energy of mixing is purely entropic with $\Delta F_{\text{mix}} = -T \Delta S_{\text{mix}}$. The chemical potential of A particles μ_A describes the free energy needed to replace a particle B with an additional A particle, and is obtained from

$$\mu_i = \left(\frac{\partial F}{\partial N_i} \right)_{T, V, \{N_{j \neq i}\}}$$

$$\mu_A = -k_B T (\ln x_A - \ln x_B) = -\mu_B$$

This curve illustrates the increasing challenge of finding available space as the packing fraction increases.



Intermolecular Interaction

To look at real systems, we now add interactions between particles by assigning an interaction energy ω between two cells which are in contact. The interaction energy can be positive (destabilizing) or negative (favorable).



With the addition of intermolecular interactions, each microstate will have a distinct energy, the canonical partition function can be obtained from eq. (2.1.1), and other thermodynamic properties follow.

In the case of a mixture, we assign separate interaction energies for each adjoining $A-A$, $B-B$, or $A-B$ pair in a given microstate: ω_{AA} , ω_{BB} , ω_{AB} . How do we calculate the energy of a microstate? m is the total number of molecular contacts in the volume, and these can be divided into $A-A$, $B-B$, or $A-B$ contacts:

$$m = m_{AA} + m_{BB} + m_{AB}$$

While m is constant, the counts of specific contacts m_{ij} vary by microstate. Then the energy of the mixture for the single i^{th} microstate can be written as

$$E_{\text{mix}} = m_{AA}\omega_{AA} + m_{BB}\omega_{BB} + m_{AB}\omega_{AB} \quad (2.3.2)$$

and the internal energy comes from an ensemble average of this quantity. An exact calculation of the internal energy from the partition function would require a sum over all possible configurations with their individual contact numbers. Instead, we can use a simpler, approximate approach which uses a strategy that starts by expressing each term in eq. (2.3.2) in terms of m_{AB} . We know:

$$\begin{aligned} m_{AA} &= (\text{Total contacts for A}) - (\text{Contacts of A with B}) \\ &= \frac{zN_A}{2} - \frac{m_{AB}}{2} \end{aligned} \quad (2.3.3)$$

$$m_{BB} = \frac{zN_B}{2} - \frac{m_{AB}}{2} \quad (2.3.4)$$

Then we have

$$\begin{aligned} E_{\text{mix}} &= \left(\frac{z\omega_{AA}N_A}{2} \right) + \left(\frac{z\omega_{BB}N_B}{2} \right) + m_{AB} \left(\omega_{AB} - \frac{\omega_{AA} + \omega_{BB}}{2} \right) \\ &= U_{\text{pure A}} + U_{\text{pure B}} + m_{AB}\Delta\omega \end{aligned} \quad (2.3.5)$$

The last term in this expression is half the change of interaction energy to switch an $A-A$ and a $B-B$ contact to form two $A-B$ contacts:

$$\Delta\omega = \left(\omega_{AB} - \frac{\omega_{AA} + \omega_{BB}}{2} \right) \quad (2.3.6)$$

We also recognize that the first two terms are just the energy of the two pure liquids before mixing. These are calculated by taking the number of cells in the pure liquid (N_i) times the number of contacts per cell (z) and then divide by two, so you do not double

count the contacts.

$$U_{\text{pure}, i} = \frac{z\omega_{ii}N_i}{2} \quad (2.3.7)$$

With these expressions, eq. (2.3.5) becomes

$$E_{\text{mix}} = U_{\text{pure A}} + U_{\text{pure B}} + m_{AB}\Delta\omega$$

This equation describes the energy of a microstate in terms of the number of $A - B$ contacts present m_{AB} .

At this point, this is not particularly helpful because it is not practical to enumerate all of the possible microstates and their corresponding m_{AB} . To simplify our calculation of U_{mix} , we make a "mean field approximation," which replaces m_{AB} with its statistical average $\langle m_{AB} \rangle$:

$$\begin{aligned} \langle m_{AB} \rangle &= (\# \text{ of contact sites for A}) \times (\text{probability of contact site being B}) \\ &= (N_A z) \left(\frac{N_B}{N} \right) = z x_A x_B N \end{aligned} \quad (2.3.8)$$

Then for the energy for the mixed state $U_{\text{mix}} = \langle E_{\text{mix}} \rangle$, we obtain:

$$U_{\text{mix}} = U_{\text{pure A}} + U_{\text{pure B}} + x_A x_B N k_B T \chi_{AB} \quad (2.3.9)$$

Here we have introduced the unitless *exchange parameter*,

$$\chi_{AB} = \frac{z}{k_B T} \left(\omega_{AB} - \frac{\omega_{AA} + \omega_{BB}}{2} \right) = \frac{z\Delta\omega}{k_B T} \quad (2.3.10)$$

which expresses $\Delta\omega$ (the change in energy on switching a single A and B from the pure state to the other liquid) in units of $k_B T$. Dividing by z gives the average interaction energy per contact.

$$\chi_{AB} > 0 \rightarrow \text{unfavorable A-B interaction}$$

$$\chi_{AB} < 0 \rightarrow \text{favorable A-B interaction}$$

We can now determine the change in internal energy on mixing:

$$\begin{aligned} \Delta U_{\text{mix}} &= (U_{\text{mix}} - U_{\text{pure A}} - U_{\text{pure B}}) \\ &= x_A x_B N k_B T \chi_{AB} \end{aligned} \quad (2.3.11)$$

Note ΔU_{mix} as a function of composition has its minimum value for a mixture with $x_A = 0.5$, when $\chi_{AB} < 0$.

Note that in the mean field approximation, the canonical partition function is

$$Q = \frac{N!}{N_A! N_B!} q_A^{N_A} q_B^{N_B} \exp[-U_{\text{mix}}/k_B T]$$

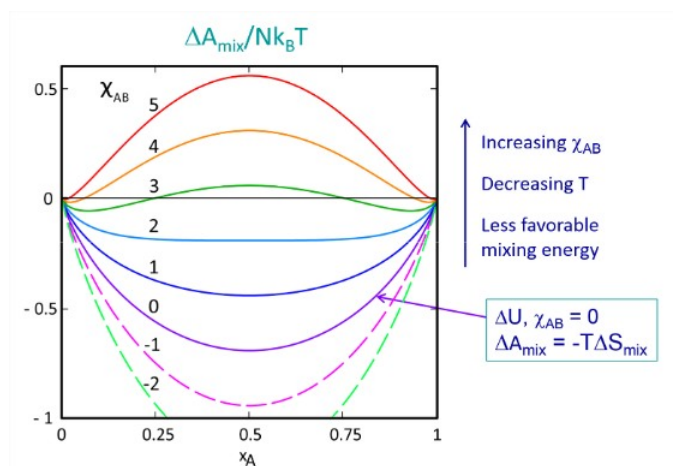
We kept the internal molecular partition functions here for completeness, but for the simple particles in this model $q_A = q_B = 1$.

Free Energy Mixing¹

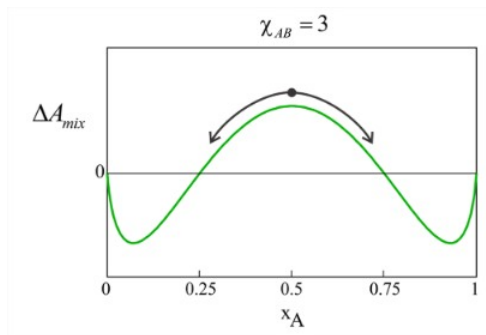
Using eqs. (2.3.1) and (2.3.11), we can now obtain the free energy of mixing

$$\begin{aligned} \Delta F_{\text{mix}} &= \Delta U_{\text{mix}} - T\Delta S_{\text{mix}} \\ &= N k_B T (x_A x_B \chi_{AB} + x_A \ln x_A + x_B \ln x_B) \end{aligned}$$

This function is plotted below as a function of mole fraction for different values of the exchange parameter. When there are no intermolecular interactions ($\chi_{AB} = 0$), the mixing is spontaneous for any mole fraction and purely entropic. Any strongly favorable $A - B$ interaction ($\chi_{AB} < 0$) only serves to decrease the free energy further for all mole fractions.



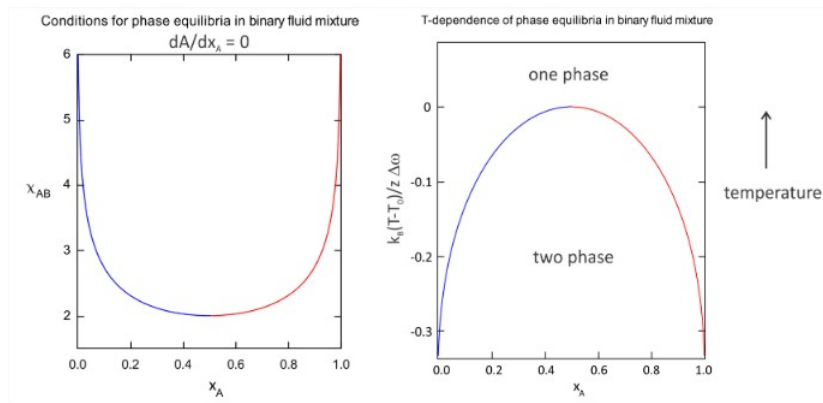
As χ_{AB} increases, we see the free energy for mixing rise, with the biggest changes for the 50/50 mixture. To describe the consequences, let's look at the curve for $\chi_{AB} = 3$, for which certain compositions are miscible ($\Delta F_{mix} < 0$) and others immiscible ($\Delta F_{mix} > 0$).



Consider what would happen if we prepare a 50/50 mixture of this solution. The free energy of mixing is positive at the equilibrium composition of the $x_A = 0.5$ homogeneous mixture, indicating that the two components are immiscible. However, there are other mixture compositions that do have a negative free energy of mixing. Under these conditions the solution can separate into two phases in such a way that (ΔF_{mix} is minimized. This occurs at mole fractions of $x_A = 0.07$ & 0.93 , which shows us that one phase will be characterized by $x_A \gg x_B$ and the other with $x_A \ll x_B$. If we prepare an unequal mixture with positive (ΔA_{mix} , for example ($x_A = 0.3$), the system will still spontaneously phase separate although mass conservation will dictate that the total mass of the fraction with ($x_A = 0.07$) will be greater than the mass of the fraction at ($x_A = 0.93$). As χ_{AB} increases beyond 3, the mole fraction of the lesser component decreases as expected for the hydrophobic effect. Consider if $A = \text{water}$ and $B = \text{oil}$. ω_{BB} and ω_{AB} are small and negative, ω_{AA} is large and negative, and $\chi_{AB} \gg 1$.

Critical Behavior

Note that 50/50 mixtures with ($2 < \chi_{AB} < 2.8$) have a negative free energy of mixing to create a single homogeneous phase, yet, the system can still lower the free energy further by phase separating. As seen in the figure, $\chi_{AB} = 2$ marks a crossover from one phase mixtures to two phase mixtures, which is the signature of a critical point. We can find the conditions for phase equilibria by locating the free energy minima as a function of χ_{AB} , which leads to the phase diagrams as a function of χ_{AB} and T below. The critical temperature for crossover from one- to two-phase behavior is T_0 , and $\Delta\omega$ is the average differential change in interaction energy defined in eq. (2.3.10).



Readings

1. K. Dill and S. Bromberg, *Molecular Driving Forces: Statistical Thermodynamics in Biology, Chemistry, Physics, and Nanoscience*. (Taylor & Francis Group, New York, 2010).
2. W. W. Graessley, *Polymeric Liquids and Networks: Structure and Properties*. (Garland Science, New York, 2004), Ch. 3.

1. J. H. Hildebrand and R. L. Scott, *Regular Solutions*. (Prentice-Hall, Englewood Cliffs, N.J., 1962).

This page titled [2.3: Binary Fluid](#) is shared under a [CC BY-NC-SA 4.0](#) license and was authored, remixed, and/or curated by [Andrei Tokmakoff](#) via [source content](#) that was edited to the style and standards of the LibreTexts platform.

CHAPTER OVERVIEW

3: Water's Physical Properties

[3.1: Water Structure](#)

[3.2: Water Dynamics](#)

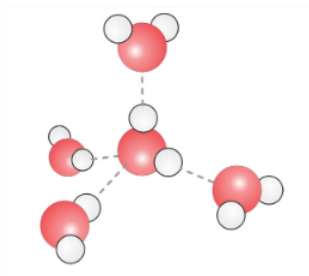
[3.3: Electrical Properties of Pure Water](#)

This page titled [3: Water's Physical Properties](#) is shared under a [CC BY-NC-SA 4.0](#) license and was authored, remixed, and/or curated by [Andrei Tokmakoff](#) via [source content](#) that was edited to the style and standards of the LibreTexts platform.

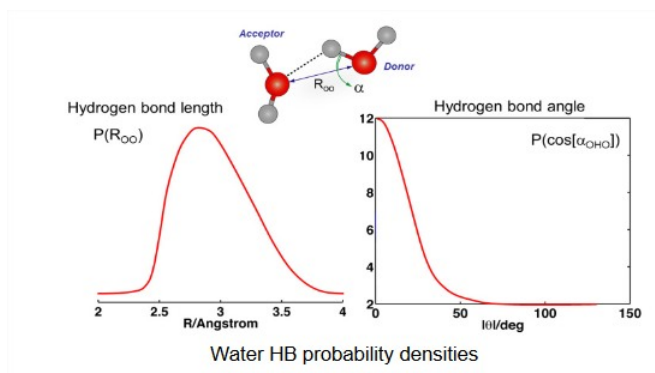
3.1: Water Structure

Water's Physical Properties

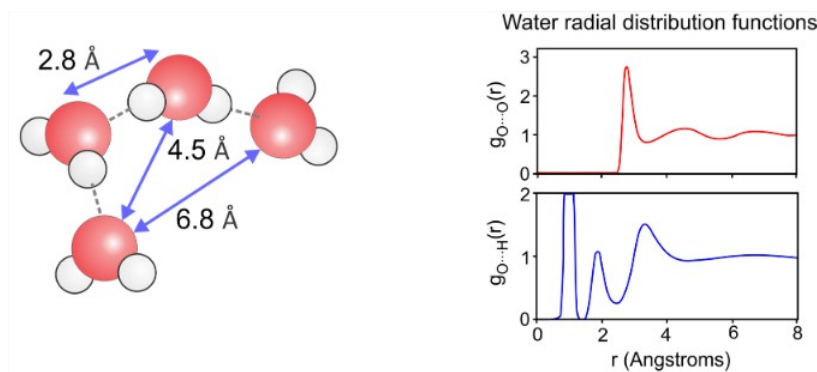
Water is a structured liquid. Its unique physical properties stem from its hydrogen bond network.



- On average, each molecule can donate two hydrogen bonds and accept two hydrogen bonds.
- Strong hydrogen bond (HB) interactions give preferential directionality along tetrahedral orientation.
- Large variation in HB distances and angles.



- Structural correlations last about 1–2 solvent shells, or <1 nm.

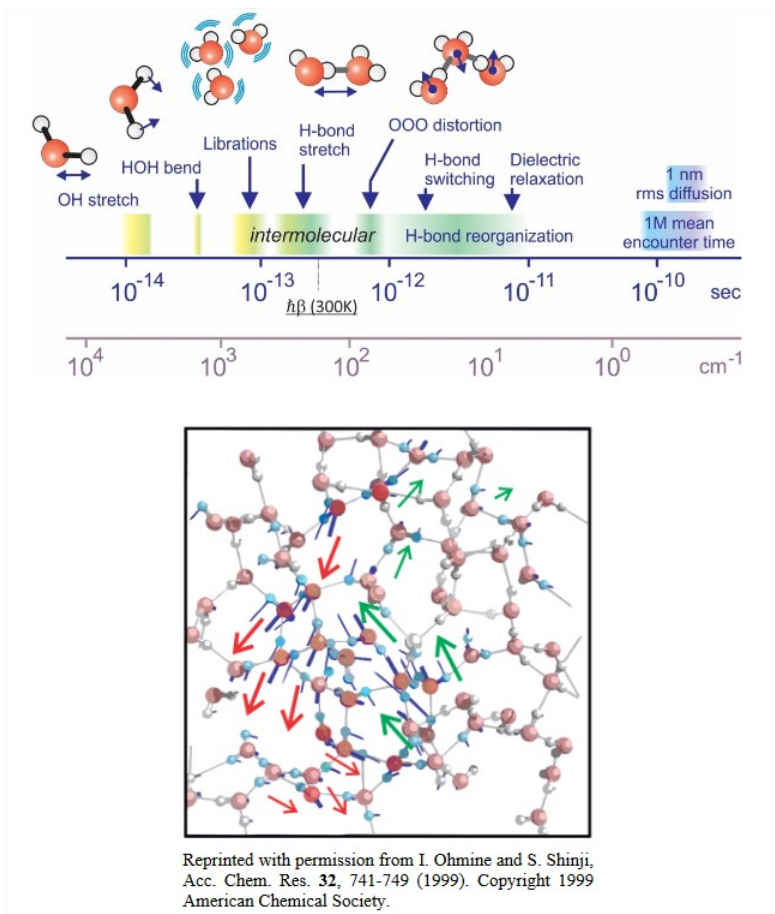


This page titled [3.1: Water Structure](#) is shared under a [CC BY-NC-SA 4.0](#) license and was authored, remixed, and/or curated by [Andrei Tokmakoff](#) via [source content](#) that was edited to the style and standards of the LibreTexts platform.

3.2: Water Dynamics

Water Dynamics

- Hydrogen bond distances and angles fluctuate with 200 and 60 femtosecond time scales, respectively.
- Hydrogen bonded structures reorganize in a collective manner on picosecond time scales (1–8 ps).



The water HB energy is tough to measure:

- 2-6 kcal mol⁻¹ depending on the method used.
- These are ΔH for reorganization, but we do not know how many HB broken or formed in the process.

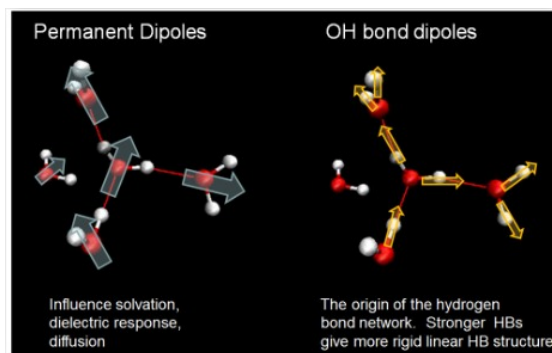
This page titled [3.2: Water Dynamics](#) is shared under a [CC BY-NC-SA 4.0](#) license and was authored, remixed, and/or curated by [Andrei Tokmakoff](#) via [source content](#) that was edited to the style and standards of the LibreTexts platform.

3.3: Electrical Properties of Pure Water

Electrical Properties of Pure Water

The motion of water's dipoles guide almost everything that happens in the liquid. Two important contributions:

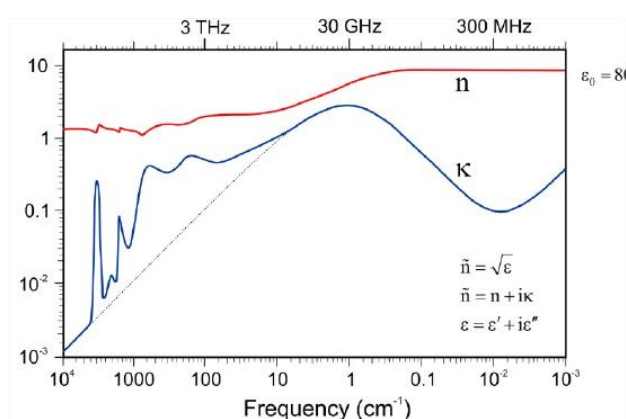
1. Permanent dipole moment of molecule lies along symmetry axis.
2. Induced dipole moments (polarization) along the hydrogen bonds. Strengthening hydrogen bond increases r_{OH} and decreases R_{OO} , which increases the dipole moment. The dipole moment per molecule changes from 1.7 to 3.0 D going from gas phase to liquid.



Water Dielectric Response

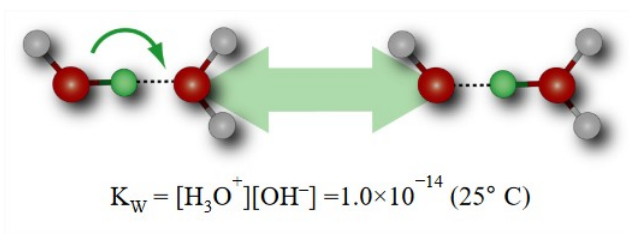
Pure water is a strong dielectric medium, meaning that long-range electrostatic forces acting between two charges in water are dramatically reduced. The static dielectric constant is $\epsilon = 80$, also known as the relative permittivity $\epsilon_r = \epsilon/\epsilon_0$. The dielectric response is strongly frequency and temperature dependent. Motion of water charges encoded in complex dielectric constant (ϵ) or index of refraction (\tilde{n}).

Dielectric Constant	
T(°C)	ϵ_r
0	88
20	80.1
100	55.3

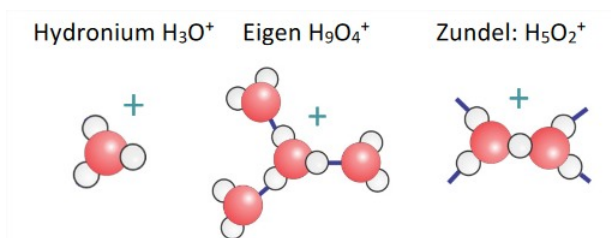


Water Autoionization and pH

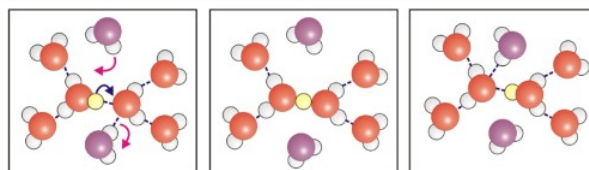
- Protons and hydroxide govern acid base chemistry.
- Any water molecule in the bulk lives about 10 hours before dissociating.
- In a liter, a water molecule dissociates every 30 microseconds.



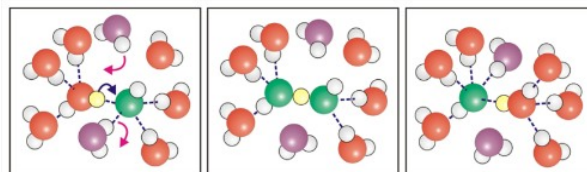
Protons in Water



- Structure of H^+ in water and the extent to which the excess charge is delocalized is still unresolved. It is associated strongly enough to describe as covalently interacting, but its time evolution is so rapid (<1 ps) that it is difficult to define a structure.



- Much higher mobility than expected by diffusion of a cation of similar size.
- Explained by Grotthuss mechanism for transfer of proton to neighboring water molecules.



- OH^- is also very mobile and acts as a proton acceptor from water.

Water Physical Properties

Property	Units	T (°C)				
		0	25	37	50	100
Heat Capacity	C_p $\text{J mol}^{-1} \text{K}^{-1}$	76.01	75.327		75.33	75.95
Density	ρ kg m^{-3}	999.82	997.13	993.37	988.02	958.4
Dielectric Relaxation Time	τ $\text{ps} = 10^{-12} \text{ s}$	14.5	8.1	5.0	4.5	0
Surface Tension	γ N m^{-1}	0.0756	0.07198			0.06
Self-Diffusion Constant	D $\text{cm}^2 \text{ s}^{-1}$	1.2E-05	2.1E-05	2.8E-05	4.0E-05	
Speed of Sound	c m s^{-1}	1402	1494	1525	1543	1543
Dynamic Viscosity	η mPa s ($10^{-3} \text{ N s m}^{-2}$)	1.792	0.893	0.692	0.547	0.283
Dielectric Constant	ϵ_r	87.7	78.3	73.9	69.88	55.3
Avg. dipole moment in liquid	D		2.95			

Protons and Hydroxide			25°C
H+ and OH- concentration	c	mol L ⁻¹	1.004E-07
Proton mobility	μ_{H^+}	cm ² V ⁻¹ s ⁻¹	0.00362
Hydroxide mobility	μ_{OH^-}	cm ² V ⁻¹ s ⁻¹	0.00198
Proton diffusion constant		Å ² ps ⁻¹	0.931
Hydroxide diffusion constant		Å ² ps ⁻¹	0.503

This page titled [3.3: Electrical Properties of Pure Water](#) is shared under a [CC BY-NC-SA 4.0](#) license and was authored, remixed, and/or curated by [Andrei Tokmakoff](#) via [source content](#) that was edited to the style and standards of the LibreTexts platform.

CHAPTER OVERVIEW

4: Solvation

[4.1: Solvation](#)

[4.2: Solvation Thermodynamics](#)

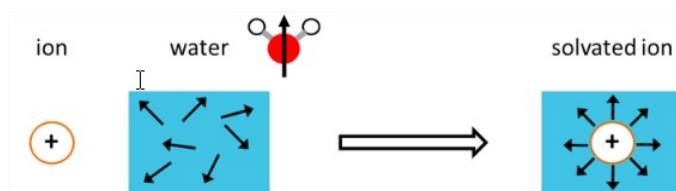
[4.3: Solvation Dynamics and Reorganization Energy](#)

This page titled [4: Solvation](#) is shared under a [CC BY-NC-SA 4.0](#) license and was authored, remixed, and/or curated by [Andrei Tokmakoff](#) via [source content](#) that was edited to the style and standards of the LibreTexts platform.

4.1: Solvation

Solvation describes the intermolecular interactions of a molecule or ion in solution with the surrounding solvent, which for our purposes will refer to water. Aqueous solvation influences an enormous range of problems in molecular biophysics, including (1) charge transfer and charge stabilization; (2) chemical and enzymatic reactivity; (3) the hydrophobic effect; (4) solubility, phase separation, and precipitation; (5) binding affinity; (6) self-assembly; and (7) transport processes in water. The terms solute and solvent commonly apply to dilute mixtures in the liquid phase in which the solute (minor component) is dispersed into the solvent (major component). For this reason, the concept of solvation is also at times extended to refer to the influence of any surrounding environment in which a biomolecule is embedded, for instance, a protein or membrane.

There are numerous types of interactions and dynamical effects that play a role in solvation. Typically, solute–solvent interactions are dominated by electrostatics (interactions of charges, dipoles, and induced dipoles), as well as hydrogen bonding and repulsion (both of which have electrostatic components). Therefore there is a tendency to think about solvation purely in terms of these electrostatic interaction energies. A common perspective—polar solvation—emphasizes how the dipoles of a polar liquid can realign themselves to energetically stabilize solute charges, as illustrated here for the case of ion solvation in water. The extent of solute stabilization in the liquid is the reorganization energy.



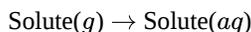
Unlike most solvents, the presence of water as a solvent for biological molecules fundamentally changes their properties and behavior from the isolated molecule. This means that water influences the conformation of flexible molecules, and sometimes hydrogen bonding interactions with water can be strong enough that it is hard to discern where the boundary of solute ends and water begins. But there is also a significant energetic cost to disrupting water's hydrogen bonding network in order to insert a solute into the liquid. Furthermore, the fluctuating hydrogen bond network of water introduces a significant entropy to the system which can be competitive or even the dominant contributor to the free energy of solvation. As a result, there are competing interactions involving both solute and water that act to restructure the solute and solvent relative to their isolated structures.

It is also important to remember that solvation is a highly dynamical process. Solvation dynamics refers to the time-dependent correlated motions of solute and solvent. How does a solvent reorganize in response to changes in solute charge distribution or structure? Conversely, how do conformational changes to the intermolecular configuration of the solvent (i.e., flow) influence changes in structure or charge distribution in the solute? The latter perspective views the solute as "slaved" to the solvent dynamics. These coupled processes result in a wide variety of time-scales in the solvation of biological macromolecules that span timescales from 10^{-14} to 10^{-7} seconds.

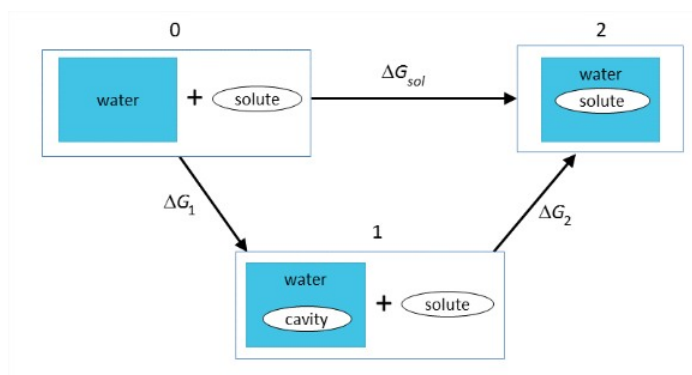
This page titled [4.1: Solvation](#) is shared under a [CC BY-NC-SA 4.0](#) license and was authored, remixed, and/or curated by [Andrei Tokmakoff](#) via [source content](#) that was edited to the style and standards of the LibreTexts platform.

4.2: Solvation Thermodynamics

Let's consider the thermodynamics of an aqueous solvation problem. This will help identify various physical processes that occur in solvation, and identify limitations to this approach. Solvation is described as the change in free energy to take the solute from a reference state, commonly taken to be the isolated solute in vacuum, into dilute aqueous solution:



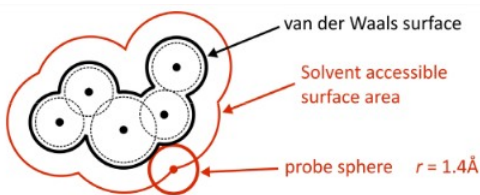
Conceptually, it is helpful to break this process into two steps: (1) the energy required to open a cavity in the liquid, and (2) the energy to put the solute into the cavity and turn on the interactions between solute and solvent.



Each of these terms has enthalpic and entropic contributions:

$$\begin{aligned} \Delta G_{\text{solv}} &= \Delta H_{\text{solv}} - T\Delta S_{\text{solv}} \\ \Delta G_{\text{solv}} &= \Delta G_1 + \Delta G_2 \\ &= \Delta H_1 - T\Delta S_1 + \Delta H_2 - T\Delta S_2 \end{aligned}$$

ΔG_1 : Free energy to open a cavity in water. We are breaking the strong cohesive intermolecular interactions in water (ΔH_1), creating a void against constant pressure, and reducing the configurational entropy of the water hydrogen-bond network (ΔS_1). Therefore ΔG_1 is large and positive. The hydrophobic effect is dominated by this term. In atomistic models, cavities for biomolecules are commonly defined through the solute's solvent accessible surface area (SASA). In order to account for excluded volume on the distance scale of a water molecule, the SASA can be obtained by rolling a sphere with radius 1.4 \AA over the solute's van der Waals surface.

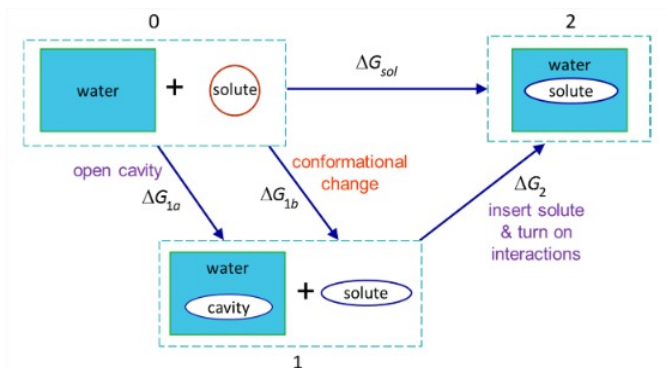


ΔG_2 : Free energy to insert the solute into the cavity, turn on the interactions between solute and solvent. Ion and polar solvation is usually dominated by this term. This includes the favorable electrostatic and H-bond interactions (ΔH_2). It also can include a restructuring of the solute and/or solvent at their interface due to the new charges. The simplest treatment of this process describes the solvent purely as a homogeneous dielectric medium and the solute as a simple sphere or cavity embedded with point charges or dipoles. It originated from the Born–Haber cycle first used to describe ΔH_{rxn} of gas-phase ions, and formed the basis for numerous continuum and cavity-in-continuum approaches to solvation.

Given the large number of competing effects involving solute, solvent, and intermolecular interactions, predicting the outcome of this process is complicated.

Looking at the cycle above illustrates many of the complications from this approach relevant to molecular biophysics, even without worrying about atomistic details. From a practical point of view, the two steps in this cycle can often have large magnitude but opposite sign, resulting in a high level of uncertainty about ΔG_{solv} —even its sign! More importantly, this simplified cycle assumes that a clean boundary can be drawn between solute and solvent—the solvent accessible surface area. It also assumes that the influence of the solvent is perturbative, in the sense that the solvent does not influence the structure of the solute or that there is

conformational disorder or flexibility in the solute and/or solvent. However, even more detailed thermodynamic cycles can be used to address some of these limitations:



ΔG_{1a} : Free energy to create a cavity in water for the final solvated molecule.

ΔG_{1b} : Free energy to induce the conformational change to the solute for the final solvated state.

ΔG_2 : Free energy to insert the solute into the cavity, turn on the interactions between solute and solvent. This includes turning on electrostatic interactions and hydrogen bonding, as well as allowing the solvent to reorganize around the solute:

$$\Delta G_2 = \Delta G_{\text{solute-solvent}} + \Delta G_{\text{solvent reorg}}$$

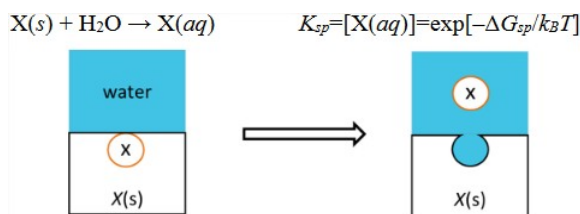
Configurational entropy may matter for each step in this cycle, and can be calculated using¹

$$S = -k_B \sum_i P_i \ln P_i$$

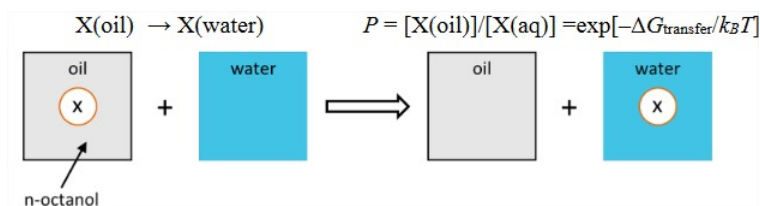
Here sum is over microstate probabilities, which can be expressed in terms of the joint probability of the solute with a given conformation and the probability of a given solvent configuration around that solute structure. In step 1, one can average over the conformational entropy of the solvent for the shape of the cavity (1a) and the conformation of the solute (1b). Step 2 includes solvent configurational variation and the accompanying variation in interaction strength.

With a knowledge of solvation thermodynamics for different species, it becomes possible to construct thermodynamic cycles for a variety of related solvation processes:

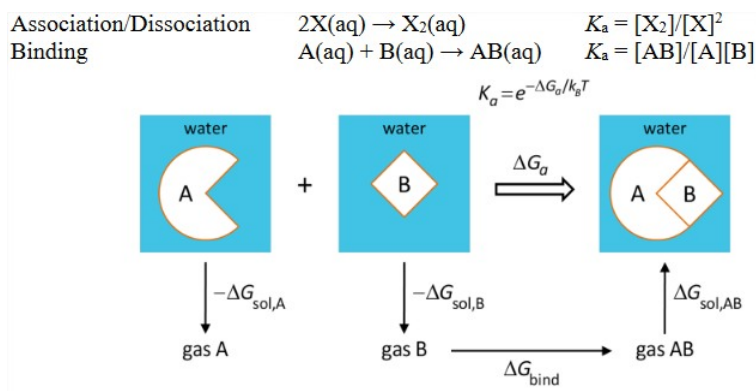
1) Solubility. The equilibrium between the molecule in its solid form and in solution is quantified through the solubility product K_{sp} , which depends on the free energy change of transferring between these phases



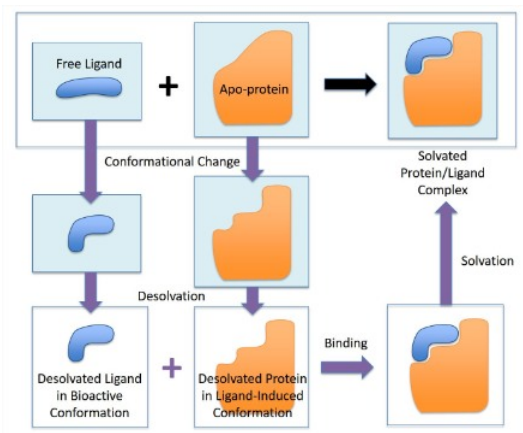
2) **Transfer free energy.** The most common empirical way of quantifying hydrophobicity is to measure the partitioning of a solute between oil and water. The partitioning coefficient P is related to the free energy needed to transfer a solute from the nonpolar solvent (typically octanol) to water



3) **Bimolecular association processes**



Binding with conformational selection

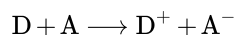


1. See C. N. Nguyen, T. K. Young and M. K. Gilson, Grid inhomogeneous solvation theory: Hydration structure and thermodynamics of the miniature receptor cucurbit[7]uril, *J. Chem. Phys.* 137 (4), 044101 (2012).

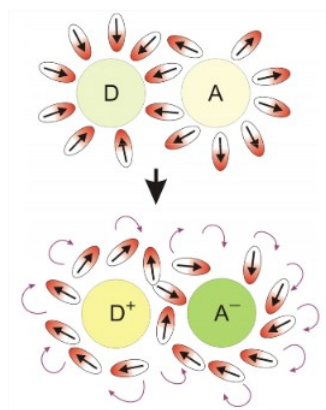
This page titled [4.2: Solvation Thermodynamics](#) is shared under a [CC BY-NC-SA 4.0](#) license and was authored, remixed, and/or curated by [Andrei Tokmakoff](#) via [source content](#) that was edited to the style and standards of the LibreTexts platform.

4.3: Solvation Dynamics and Reorganization Energy

Some of the practical challenges of describing solvation through thermodynamic cycles include dealing with strong solute–solvent interactions, flexible solutes, and explicit solvents. Additionally, it does not reflect the fact that solvation is a highly dynamic process involving motion of the solvent. Perhaps the most common example is in charge transfer processes (i.e., electrons and protons) in which water’s dipoles can act to drive and stabilize the position of the charge. For instance, consider the transfer of an electron from a donor to an acceptor in solution:



We most commonly consider electron transfer as dependent on a solvent coordinate in which solvent reorganizes its configuration so that dipoles or charges help to stabilize the extra negative charge at the acceptor site. This type of *collective* coordinate is illustrated in the figure below. These concepts are reflected in the [Marcus’ theory](#) of electron transfer. The free energy change to relax the solvent configuration after switching the charges in the initial configuration is known as the **reorganization energy** λ .



This page titled [4.3: Solvation Dynamics and Reorganization Energy](#) is shared under a [CC BY-NC-SA 4.0](#) license and was authored, remixed, and/or curated by [Andrei Tokmakoff](#) via [source content](#) that was edited to the style and standards of the LibreTexts platform.

CHAPTER OVERVIEW

5: Hydrophobicity

[5.1: Hydrophobic Solvation - Thermodynamics](#)

[5.2: Hydrophobic Solvation- Solute Size Effect](#)

[5.3: Hydrophobic Collapse](#)

This page titled [5: Hydrophobicity](#) is shared under a [CC BY-NC-SA 4.0](#) license and was authored, remixed, and/or curated by [Andrei Tokmakoff](#) via [source content](#) that was edited to the style and standards of the LibreTexts platform.

5.1: Hydrophobic Solvation - Thermodynamics

Why do oil and water not mix? What is hydrophobicity? First, the term is a misnomer. Greasy molecules that do not mix with water typically do have favorable interaction energies, i.e., $\Delta H_{int} < 0$. Walter Kauzmann first used the term "hydrophobic bonding" in 1954. This naming has been controversial from the beginning, but it has stuck presumably, because in this case ΔG is what determines the affinity of one substance for another rather than just ΔH . Generally speaking, the entropy of mixing governs the observation that two weakly interacting liquids will spontaneously mix. However, liquid water's intermolecular interactions are strong enough that it would prefer to hydrogen bond with itself than solvate nonpolar molecules. It will try to avoid disrupting its hydrogen bond network if possible.

The hydrophobic effect refers to the free energy penalty that one pays to solvate a weakly interacting solute. Referring to the thermodynamic cycle above, ΔG_{sol} , the reversible work needed to solvate a hydrophobic molecule, is dominated by step 1, the process of forming a cavity in water. The free energy of solvating a hydrophobic solute is large and positive, resulting from two factors:

1. $\Delta G_{sol} < 0$. The entropy penalty of creating a cavity in water. We restrict the configurational space available to the water within the cavity. This effect and the entropy of mixing (that applies to any solvation problem) contribute to ΔS_1 .
2. $\Delta G_{sol} > 0$. The energy penalty of breaking up the hydrogen bond network (ΔH_1) is the dominant contributor to the enthalpy. This can be estimated from a count of the net number of H-bonds that needs to be broken to accommodate the solute: ΔH_{sol} increases by 1-3 kcal mol⁻¹ of hydrogen bonds. The interaction energy between a hydrocarbon and water (ΔH_2) is weakly favorable as a result of dispersion interactions, but this is a smaller effect. (At close contact, van der Waals forces lower the energy by ~ 0.1 -1.0 kcal mol⁻¹). Therefore $\Delta H_{sol} \approx \Delta H_1$.

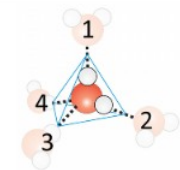
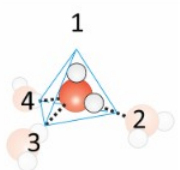
The net result is that ΔG_{sol} is large and positive, which is expected since water and oil do not mix.

These ideas were originally deduced from classical thermodynamics, and put forth by Frank and Evans (1945) in the "iceberg model", which suggested that water would always seek to fulfill as many hydrogen bonds as it could—wrapping the network around the solute. This is another misnomer, because the hydrophobic effect is a boundary problem about reducing configurational space, not actual freezing of fluctuations. Hydrogen bonds continue to break and reform in the liquid, but there is considerable excluded configurational space for this to occur. Let's think of this as solute-induced *hydrogen-bond network reorganization*.

Water Configurational Entropy

Let's make an estimate of ΔG_{sol} . Qualitatively, we are talking about limiting the configurational space that water molecules can adopt within the constraints of a tetrahedral potential.

Approximation							
Bulk water: 4 HBs/tetrahedron							
Within a tetrahedral lattice the orientation of an H ₂ O has:							
6 configurations:	<table border="0"> <tr> <td>1,2</td> <td>1,3</td> <td>1,4</td> </tr> <tr> <td>2,3</td> <td>2,4</td> <td>3,4</td> </tr> </table>	1,2	1,3	1,4	2,3	2,4	3,4
1,2	1,3	1,4					
2,3	2,4	3,4					
$\Omega_{bulk} = 6$							
At a planar interface, you satisfy the most hydrogen bonds by making one dangling hydrogen bond pointing toward the surface							
3 configurations	<table border="0"> <tr> <td>1,2</td> <td>1,3</td> <td>1,4</td> </tr> </table>	1,2	1,3	1,4			
1,2	1,3	1,4					
$\Omega_{surface} = 3$							

So an estimate for the entropy of hydrophobic solvation if these configurations are equally probable is $\Delta S_{sol} = k_B \ln(\Omega_{surf}/\Omega_{bulk}) = -k \ln 2$ per hydrogen bond of lost configurational space:

$$-T\Delta S_{sol} = k_B T \ln 2$$

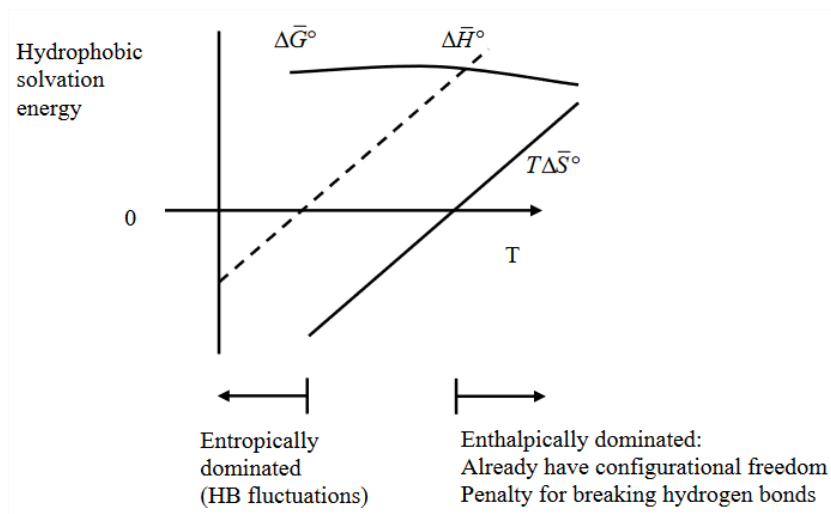
Evaluating at 300 K,

$$\begin{aligned} -T\Delta G_{sol} &= 1.7 \text{ kJ/mol water molecules @ 300 K} \\ &= 0.4 \text{ kcal/mol water molecules} \end{aligned}$$

This value is less than the typical enthalpy for hydrogen bond formation, which is another way of saying that the hydrogen bonds like to stay mostly intact, but have large amplitude fluctuations.

Temperature Dependence of Hydrophobic Solvation

From ΔS_{sol} we expect ΔG_{sol} to rise with temperature as a result of the entropic term. This is a classic signature of the hydrophobic effect: The force driving condensation or phase-separation increases with temperature. Since the hydrogen-bond strength connectivity and fluctuations in water's hydrogen-bond network change with temperature, the weighting of enthalpic and entropic factors in hydrophobic solvation also varies with T . Consider a typical temperature dependence of ΔG_{sol} for small hydrophobic molecules:



The enthalpic and entropic contributions are two strongly temperature-dependent effects, which compete to result in a much more weakly temperature-dependent free energy. Note, this is quite different from the temperature dependence of chemical equilibria described by the van 't Hoff equation, which assumes that ΔH is independent of temperature. The temperature dependence of all of these variables can be described in terms of a large positive heat capacity.

$$\begin{aligned}\Delta C_{p, \text{sol}} &= \frac{\partial \Delta H_{\text{sol}}^0}{\partial T} = T \frac{\partial \Delta S_{\text{sol}}^0}{\partial T} \\ &= -T \frac{\partial^2 G_{\text{sol}}^0}{\partial T^2} \quad (\text{Curvature of } \Delta G^0)\end{aligned}$$

At low temperatures, with a stronger, more rigid hydrogen-bond network, the ΔS term dominates. But at high temperature, approaching boiling, the entropic penalty is far less.

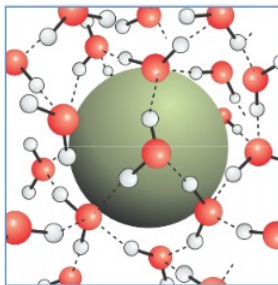
This page titled [5.1: Hydrophobic Solvation - Thermodynamics](#) is shared under a [CC BY-NC-SA 4.0](#) license and was authored, remixed, and/or curated by [Andrei Tokmakoff](#) via [source content](#) that was edited to the style and standards of the LibreTexts platform.

5.2: Hydrophobic Solvation- Solute Size Effect

To create a new interface there are enthalpic and entropic penalties. The influence of each of these factors depends on the size of the solute (R) relative to the scale of hydrogen bonding structure in the liquid (correlation length, ℓ , $\sim 0.5\text{--}1.0$ nm).

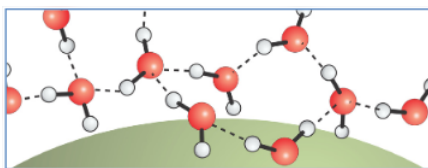
For small solutes ($R < \ell$): Network deformation

The solute can insert itself into the hydrogen bond network without breaking hydrogen bonds. It may strain the HBs ($\Delta H > 0$) and reduce the configurational entropy ($\Delta S < 0$), but the liquid mostly maintains hydrogen bonds intact. We expect the free energy of this process to scale as volume of the solute $\Delta G_{\text{sol}}(R < \ell) \propto R^3$.



For large solutes, $R > \ell$: Creating an interface

The hydrogen bond network can no longer maintain all of its HBs between water molecules. The low energy state involves dangling hydrogen bonds at the surface. One in three surface water molecules has a dangling hydrogen bond, i.e., on average five of six hydrogen bonds of the bulk are maintained at the interface.



We expect ΔG_{sol} to scale as the surface area $\Delta G_{\text{sol}}(R > \ell) \propto R^2$. Of course, large solutes also have a large volume displacement term. Since the system will always seek to minimize the free energy, there will be a point at which the R^3 term grows faster with solute radius than the R^2 term, so large solutes are dominated by the surface term.

Calculating ΔG for Forming a Cavity in Water

Let's investigate the energy required to form cavities in water using a purely thermodynamic approach. To put a large cavity ($R > \ell$) into water, we are creating a new liquid–vapor interface for the cavity. So we can calculate the energy to create a cavity using the surface tension of water. Thermodynamically, the surface tension γ is the energy required to deform a liquid–vapor interface: $\gamma = (\partial U / \partial a)_{N,V,T}$, where a is the surface area. So we can write the change in energy as a result of inserting a spherical cavity into water as the product of the surface tension of water times the surface area of the cavity,

$$U(R) = 4\pi R^2 \gamma$$

In principle, the experimentally determined γ should include entropic and enthalpic contributions to altering the hydrogen bond network at a surface, so we associate this with ΔG_{sol} . For water at 300 K, $\gamma = 72$ pN/nm. γ varies from 75 pN/nm at 0 °C to 60 pN/nm at 100 °C.

The surface tension can also be considered a surface energy per unit area: which can also be considered a surface energy, i.e., $\gamma = 72$ mJ/m². To relate this to a molecular scale quantity, we can estimate the surface area per water molecule in a spherical cavity. The molecular volume of bulk water deduced from its density is 3.0×10^{-26} L/molecule, and the corresponding surface area per molecule deduced from geometric arguments is $\sim 10 \text{ \AA}^2$. This area allows us to express $\gamma \approx 4.3$ kJ/mol, which is on the order of the strength of hydrogen bonds in water.

For small cavities ($R < \ell$), the considerations are different since we are not breaking hydrogen bonds. Here we are just constraining the configurational space of the cavity and interface, which should scale as volume. We define

$$\Delta G_{\text{sol}}(R < \ell) = \frac{4\pi R^3}{3} \rho_E$$

where ρ_E is an energy density¹.

$$\rho_E \approx 240 \times 10^{-9} \text{ pJ/nm}^3 = 240 \text{ pN/nm}^{-2}$$

Remembering that $-\partial G/\partial V|_{N,T} = p$, the energy density corresponds to units of pressure with a value $\rho_E = 2.4 \times 10^3$ atm. If we divide ρ_E by the molarity of water (55M), then we find it can be expressed as 4.4 kJ/mol , similar to the surface free energy value deduced.

So combining the surface and volume terms we write

$$\Delta G_{\text{sol}}(R) = 4\pi\gamma R^2 + \frac{4}{3}\pi R^3 \rho_E$$

Alternatively, we can define an effective length scale (radius) for the scaling of this interaction

$$\frac{\Delta G_{\text{sol}}}{k_B T} = \left(\frac{R}{R_{\text{surf}}}\right)^2 + \left(\frac{R}{R_V}\right)^3 \quad R_{\text{surf}} = \sqrt{\frac{k_B T}{4\pi\gamma}} \quad R_V = \left(\frac{3k_B T}{4\pi\rho_E}\right)^{1/3}$$

where $R_{\text{surf}} = 0.067 \text{ nm}$ and $R_V = 1.6 \text{ nm}$ at 300 K . We can assess the crossover from volume-dominated to area-dominated hydrophobic solvation effects by setting these terms equal and finding that this occurs when $R = 3\gamma/\rho_E = 0.9 \text{ nm}$. The figure below illustrates this behavior and compares it with results of MD simulations of a sphere in water.

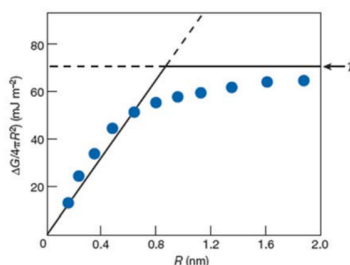


Figure 2 | Solvation free energy, ΔG , for a spherical cavity in water as a function of the cavity size. The results are for ambient conditions (room temperature and 1 atm pressure). The circles show the results of detailed microscopic calculations². The liquid-vapour surface tension is shown by γ . The solid lines show the approximate scaling behaviour of $\Delta G/4\pi R^2$ for small R , and the asymptotic behaviour for large R . This approach can be used to infer the typical length characterizing the crossover behaviour, but not the quantitative behaviour of ΔG in the crossover regime.

Reprinted by permission from Macmillan Publishers Ltd: D. Chandler, Nature 437, 640–647 (2005). Copyright 2005.

An alternate approach to describing the molar free energy of solvation for a hydrophobic sphere of radius r equates it with the probability of finding a cavity of radius r :

$$\begin{aligned} \Delta G &= -k_B T \ln P(r) \\ P(r) &= \frac{e^{-U(r)/k_B T}}{\int_0^\infty e^{-U(r)/k_B T} dr} = \frac{\exp\left[\frac{-4\pi\gamma r^2}{k_B T}\right]}{\frac{1}{2}\sqrt{\frac{k_B T}{4\gamma}}} \\ &= \frac{2}{\sqrt{\pi}R_{\text{surf}}} \exp[-r^2/R_{\text{surf}}^2] \end{aligned}$$

This leads to an expression much like we previously described for large cavities. It is instructive to determine for water @ 300 K :

$$\langle r \rangle = \int_0^\infty dr r P(r) = \pi^{-1/2} R_{\text{surf}} = \frac{1}{2\pi} \left(\frac{k_B T}{\gamma}\right)^{1/2} = 0.038 \text{ nm}$$

This is very small, but agrees well with simulations. (There is not much free volume in water!) However, when you repeat this to find the variance in the size of the cavities $\delta r = (\langle r^2 \rangle - \langle r \rangle^2)^{1/2}$, we find $\delta r = 0.028 \text{ nm}$. So the fluctuations in size are of the same scale as the average and therefore quite large in a relative sense, but still less than the size of a water molecule.

Simulations give the equilibrium distribution of cavities in water

$$\Delta\mu^0 = -k_B T \ln(P)$$

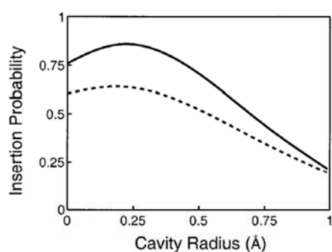


Figure 9. Free volume distributions from molecular dynamics simulations of a simple liquid, *n*-hexane (dashed line), and water (solid line). The probability of finding a cavity of a given radius is plotted. Water has more small cavities (<1 Å) than *n*-hexane. Data adapted from G. Hummer et al., *J. Phys. Chem. B* **1998**, *102*, 10 475.

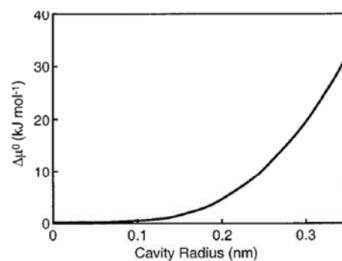


Figure 10. Free energy cost of creating a cavity, from molecular simulations. Data adapted from Hummer, G., et al. *J. Phys. Chem. B* **1998**, *102*, 10 475.

Reprinted with permission from N. T. Southall, K. A. Dill and A. D. J. Haymet, *J. Phys. Chem. B* **106**, 521–533 (2002). Copyright 2002 American Chemical Society.

1. D. Chandler, Interfaces and the driving force of hydrophobic assembly, *Nature* **437**, 640–647 (2005).

This page titled [5.2: Hydrophobic Solvation- Solute Size Effect](#) is shared under a [CC BY-NC-SA 4.0](#) license and was authored, remixed, and/or curated by [Andrei Tokmakoff](#) via [source content](#) that was edited to the style and standards of the LibreTexts platform.

5.3: Hydrophobic Collapse

Hydrophobic Collapse¹

We see that hydrophobic particles in water will attempt to minimize their surface area with water by aggregating or phase separating. This process, known as hydrophobic collapse, is considered to be the dominant effect driving the folding of globular proteins.

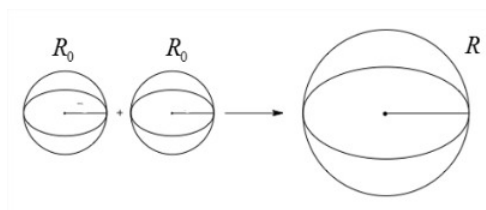
Let's calculate the free energy change for two oil droplets coalescing into one. The smaller droplets both have a radius R_0 and the final droplet a radius of R .

$$\Delta G_{\text{collapse}} = \Delta G_{\text{sol}}(R) - 2\Delta G_{\text{sol}}(R_0)$$

The total volume of oil is constant—only the surface area changes. If the total initial surface area is A_0 , and the final total surface area is A , then

$$\Delta G_{\text{collapse}} = (A - A_0)\gamma$$

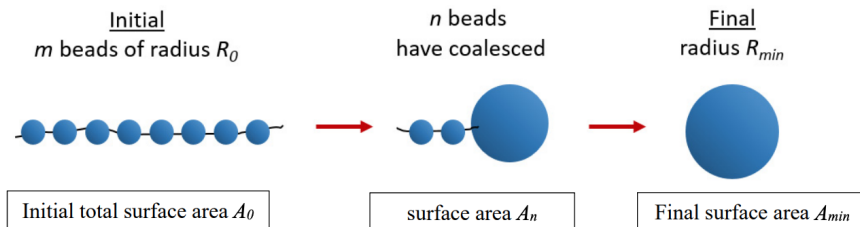
which is always negative since $A < A_0$ and γ is positive.



Initial State	Final State
Total Volume $V = 2\left(\frac{4}{3}\pi R_0^3\right)$	$V = \frac{4}{3}\pi R^3 \rightarrow R = 2^{1/3}R_0$
Initial surface area $A_0 = 2(4\pi R_0^2)$	$A = 4\pi R^2 = 4\pi(2^{1/3})^2 R_0^2 = 4\pi(1.59)R_0^2$
$\frac{A_0}{4\pi R_0^2} = 2$	$\frac{A}{4\pi R_0^2} = 1.59$
$\Delta G_{\text{collapse}} = (A - A_0)\gamma = (-0.41)4\pi R_0^2\gamma$	

This neglects the change in translational entropy due to two drops coalescing into one. Considering only the translational degrees of freedom of the drops, this should be approximately $\Delta S_{\text{collapse}} \approx k_B \ln(3/6)$. In other words, a small number compared to the surface term.

We can readily generalize this to a chain of n beads, each of radius R_0 , which collapse toward a single sphere with the same total volume. In this case, let's consider how the free energy of the system varies with the number of beads that have coalesced.



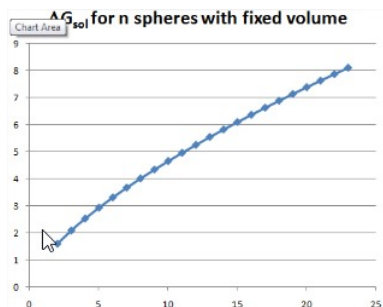
Again the total volume is constant, $V = n\left(\frac{4}{3}\pi R_0^3\right)$ and the surface area changes. The initial surface area is $A_0 = m4\pi R_0^2$ and the final surface area is $A_{\text{min}} = 4\pi(R_{\text{min}})^2 = m^{2/3}4\pi R_0^2$. Along the path, there is a drop of total surface area for each bead that coalesces. Let's consider one path, in which an individual bead coalesces with one growing drop. The total surface area once n of m particles have coalesced is

$A_n = (\text{surface area of drop formed by } n \text{ coalesced beads}) + (\text{total area of remaining } m - n \text{ beads})$

$$\begin{aligned} A_n &= (n^{2/3}4\pi R_0^2) + (m - n)4\pi R_0^2 \\ &= (m + n^{2/3} - n)4\pi R_0^2 \\ &= A_0 + (n^{2/3} - n)4\pi R_0^2 \end{aligned}$$

The free energy change for coalescing n beads is

$$\begin{aligned} \Delta G_{\text{coll}} &= (A_n - A_0)\gamma \\ &= (n^{2/3} - n)4\pi R_0^2\gamma \end{aligned}$$



This free energy is plotted as a function of the bead number at fixed volume. This is an energy landscape that illustrates that the downhill direction of spontaneous change leads to a smaller number of beads. The driving force for the collapse of this chain can be considered to be the decrease in free energy as a function of the number of beads in the chain:

$$\begin{aligned} f_{\text{coll}} &= -\frac{\partial \Delta G_{\text{coll}}}{\partial r} \propto -\frac{\partial \Delta G_{\text{coll}}}{\partial n} \\ -\frac{\partial \Delta G_{\text{coll}}}{\partial n} &= 4\pi R_0^2\gamma \left(1 - \frac{2}{3}n^{-1/3}\right) \end{aligned}$$

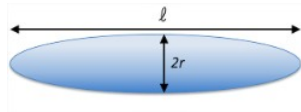
This is not a real force expressed in Newtons, but we can think of it as a pseudo-force, with the bead number acting as a proxy for the chain extension. If you want to extend a hydrophobic chain, you must do work against this. Written in terms of the extension of the chain x (not the drop area A)

$$w = -\int_{x_0}^x f_{\text{ext}} dx = \int_{x_0}^x \left(\frac{\partial \Delta G_{\text{coll}}}{\partial A_n}\right) \left(\frac{\partial A_n}{\partial x}\right) dx$$

Here we still have to figure out the relationship between extension and surface area, $\partial A_n / \partial x$.

Alternatively, we can think of the collapse coordinate as the number of coalesced beads, n .

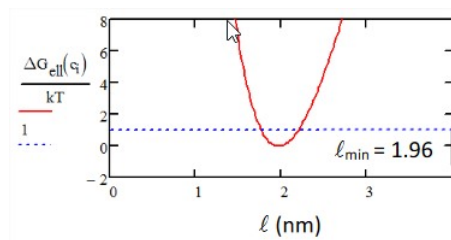
Hydrophobic Collapse and Shape Fluctuations



An alternate approach to thinking about this problem is in terms of the collapse of a prolate ellipsoid to a sphere as it seeks to minimize its surface area. We take the ellipsoid to have a longradius $\ell/2$ and a short radius r . The area and volume are then:

$$\begin{aligned} A &= 2\pi \left(r^2 + \frac{\ell^2}{4} \frac{\alpha}{\tan \alpha} \right) \quad \alpha = \cos^{-1} \left(\frac{2r}{\ell} \right) \\ V &= \frac{2}{3} \pi r^2 \ell \quad (\text{constant}) \\ \therefore r^2 &= 3V/2\pi\ell \\ A &= \left(\frac{3V}{\ell} + \pi \frac{\ell^2}{2} \frac{\alpha}{\tan \alpha} \right) \end{aligned}$$

Let's plot the free energy of this ellipsoid as a function of ℓ . For $V = 4 \text{ nm}^3$, $k_B T = 4.1 \text{ pN/nm}$ we find $\ell_{\text{min}} = 1.96 \text{ nm}$. Note that at $k_B T$ the dimensions of the ellipsoid can fluctuate over many $\sim 5 \text{ \AA}$.



Readings

1. N. T. Southall, K. A. Dill and A. D. J. Haymet, A view of the hydrophobic effect, *J. Phys. Chem. B* 106, 521–533 (2002).
2. D. Chandler, Interfaces and the driving force of hydrophobic assembly, *Nature* 437, 640–647 (2005).
3. G. Hummer, S. Garde, A. E. García, M. E. Paulaitis and L. R. Pratt, Hydrophobic effects on a molecular scale, *J. Phys. Chem. B* 102, 10469–10482 (1998).
4. B. J. Berne, J. D. Weeks and R. Zhou, Dewetting and hydrophobic interaction in physical and biological systems, *Annu. Rev. Phys. Chem.* 60, 85–103 (2009).

-
1. See K. Dill and S. Bromberg, *Molecular Driving Forces: Statistical Thermodynamics in Biology, Chemistry, Physics, and Nanoscience*. (Taylor & Francis Group, New York, 2010), p. 675.

This page titled [5.3: Hydrophobic Collapse](#) is shared under a [CC BY-NC-SA 4.0](#) license and was authored, remixed, and/or curated by [Andrei Tokmakoff](#) via [source content](#) that was edited to the style and standards of the LibreTexts platform.

CHAPTER OVERVIEW

6: Electrical Properties of Water and Aqueous Solutions

6.1: Electrostatics

6.2: Dielectric Constant and Screening

6.3: Free Energy of Ions in Solution

6.4: Ion Distributions in Electrolyte Solution

6.5: Poisson–Boltzmann Equation

6.6: Debye–Hückel Theory

6.7: Ion Distributions Near a Charged Interface

6.8: Ion Distributions Near a Charged Sphere

This page titled [6: Electrical Properties of Water and Aqueous Solutions](#) is shared under a [CC BY-NC-SA 4.0](#) license and was authored, remixed, and/or curated by [Andrei Tokmakoff](#) via [source content](#) that was edited to the style and standards of the LibreTexts platform.

6.1: Electrostatics

Electrical Properties of Water and Aqueous Solutions

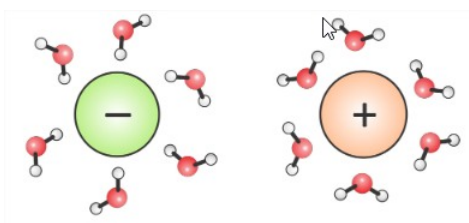
We want to understand the energy and electrical properties and transport of ions and charged molecules in water. These are strong forces. Consider an example of NaCl dissociation in gas phase dissociation energy $\Delta H_{\text{ionization}} \approx 270 \text{ kJ/mol}$:

$$K_{\text{ionization}}(\text{gas}) = \frac{[\text{Na}^+][\text{Cl}^-]}{[\text{NaCl}]} \approx 10^{-89}$$

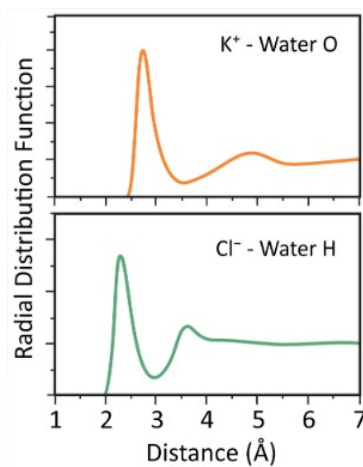
In solution, this process $[\text{NaCl}(\text{aq}) \rightarrow \text{Na}^+(\text{aq}) + \text{Cl}^-(\text{aq})]$ occurs spontaneously; the solubility product for NaCl is $K_{\text{sp}} = [\text{Na}^+(\text{aq})][\text{Cl}^-(\text{aq})]/[\text{NaCl}(\text{aq})] = 37$. Similarly, water molecules are covalently bonded hydrogen and oxygen atoms, but we know that the internal forces in water can autoionize a water molecule:

$$K_{\text{ionization}}(\text{gas}) = [\text{H}^+][\text{OH}^-] \approx 10^{-75} \text{ and } K_W(\text{H}_2\text{O}) = [\text{H}^+][\text{OH}^-] = 10^{-14}$$

These tremendous differences originate in the huge collective electrostatic forces that are present in water. “Polar solvation” refers to the manner in which water dipoles stabilize charges.

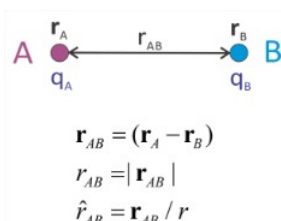


These dipoles are simplifications of the rearrangements of water's structure to accommodate and lower the energy of the ion. It is important to remember that water is a polarizable medium in which hydrogen bonding dramatically modifies the electrostatic properties.



Electrostatics

Let's review a number of results from classical electrostatics. The interactions between charged objects can be formulated using force, the electric field, or the electrostatic potential. The potential is our primary consideration when discussing free energies in thermodynamics and the Hamiltonian in statistical mechanics. Let's describe these, consider the interaction between two ions A and B , separated by a distance r_{AB} , with charges q_A and q_B .



Force and Work

Coulomb's Law gives the force that B exerts on A .

$$\mathbf{f}_{AB} = -\frac{1}{4\pi\epsilon} \frac{q_A q_B}{r_{AB}^2} \hat{r}_{AB}$$

\hat{r}_{AB} is a unit vector pointing from \mathbf{r}_B to \mathbf{r}_A . A useful identity to remember for calculations is

$$\frac{e^2}{4\pi\epsilon_0} = 230 \text{ pN/nm}^2$$

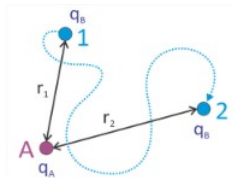
For thermodynamic purposes it is helpful to calculate the reversible work for a process. Electrical work comes from moving charges against a force

$$dw = -\mathbf{f} \cdot d\mathbf{r}$$

As long as q and ϵ are independent of r , and the process is reversible, then work only depends on r , and is independent of path. To move particle B from point 1 at a separation r_0 to point 2 at a separation r requires the following work

$$w_{1 \rightarrow 2} = \frac{1}{4\pi\epsilon} q_A q_B \left(\frac{1}{r_2} - \frac{1}{r_1} \right) \quad (6.1.1)$$

and if the path returns to the initial position, $w_{rev} = 0$.



Field, E

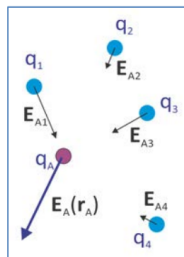
The electric field is a vector quantity that describes the action of charges at a point in space. The field from charged particle B at point A is

$$\mathbf{E}_{AB}(\mathbf{r}_A) = -\frac{1}{4\pi\epsilon} \frac{q_B}{r_{AB}^2} \hat{r}_{AB}$$

\mathbf{E}_{AB} is related to the force that particle B exerts on a charged test particle A with charge q_A through

$$\mathbf{f}_A = q_A \mathbf{E}_{AB}(\mathbf{r}_A)$$

While the force at point a depends on the sign and magnitude of the test charge, the field does not. More generally, the field exerted by multiple charged particles at point \mathbf{r}_A is the vector sum of the field from multiple charges (i):



$$\mathbf{E}(\mathbf{r}_A) = \sum_i \mathbf{E}_{Ai}(\mathbf{r}_A) = -\frac{1}{4\pi\epsilon} \sum_i \frac{q_i}{r_{Ai}^2} \hat{\mathbf{r}}_{Ai}$$

where $r_{Ai} = |\mathbf{r}_A - \mathbf{r}_i|$ and the unit vector $\hat{\mathbf{r}}_{Ai} = (\mathbf{r}_A - \mathbf{r}_i)/r_{Ai}$. Alternatively for a continuum charge density $\rho_q(\mathbf{r})$,

$$\mathbf{E}(\mathbf{r}_A) = -\frac{1}{4\pi\epsilon} \int \rho_q(\mathbf{r}) \frac{(\mathbf{r}_A - \mathbf{r})}{|\mathbf{r}_A - \mathbf{r}|^3} d\mathbf{r}$$

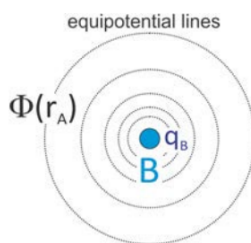
where the integral is over a volume.

Electrostatic Potential, Φ

For thermodynamics and statistical mechanics, we wish to express electrical interactions in terms of an energy or electrostatic potential. While the force and field are vector quantities, the electrostatic potential Φ is a scalar quantity which is related to the electric field through

$$\mathbf{E} = -\bar{\nabla}\Phi$$

It has units of energy per unit charge. The electrostatic potential at point \mathbf{r}_A , which results from a point charge at \mathbf{r}_B , is



$$\Phi(r_A) = \frac{1}{4\pi\epsilon} \frac{q_B}{r_{AB}} \quad (6.1.2)$$

The electric potential is additive in the contribution from multiple charges:

$$\Phi(r_A) = \frac{1}{4\pi\epsilon} \sum_i \frac{q_i}{r_{Ai}} \quad \text{or} \quad \Phi(r_A) = \frac{1}{4\pi\epsilon} \int \frac{\rho_q(\mathbf{r})}{|\mathbf{r}_A - \mathbf{r}|} d\mathbf{r}$$

The electrostatic energy of a particle A as a result of the potential due to particle B is

$$U_{AB}(r_A) = q_A \Phi(r_A) = \frac{1}{4\pi\epsilon} \frac{q_A q_B}{r_{AB}}$$

Note that $U_{AB} = q_A \Phi(r_A) = q_B \Phi(r_B) = \frac{1}{2}(q_A \Phi(r_A) + q_B \Phi(r_B))$, so we can generalize this to calculate the potential energy stored in a collection of multiple charges as

$$\begin{aligned} U &= \frac{1}{2} \sum_i q_i \Phi(r_{Ai}) \\ &= \frac{1}{2} \int \Phi_A(\mathbf{r}_A) \rho_q(\mathbf{r}_A) d\mathbf{r}_A \end{aligned}$$

This page titled [6.1: Electrostatics](#) is shared under a [CC BY-NC-SA 4.0](#) license and was authored, remixed, and/or curated by [Andrei Tokmakoff](#) via [source content](#) that was edited to the style and standards of the LibreTexts platform.

6.2: Dielectric Constant and Screening

Charge interactions are suppressed in a polarizable medium, which depends on the dielectric constant. The potential energy for interacting charges is long range, scaling as r^{-1} .

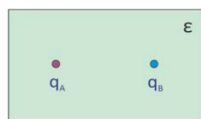
$$U(r) = \frac{q_A q_B}{4\pi \epsilon r}$$

You can think of ϵ as scaling the potential interaction distance $U \propto (\epsilon r)^{-1}$. Here we equate the dielectric constant and the relative permittivity $\epsilon_r = \epsilon/\epsilon_0$, which is a unitless quantity equal to the ratio of the sample permittivity ϵ to the vacuum permittivity ϵ_0 .

The dielectric constant is used to treat the molecular structure and dynamics of the charge environment in a mean sense, to give you a sense of how the polarizable medium screens the interaction of charges. Making use of a dielectric constant implies a separation of the charges of the system into a few important charges and the environment, which encompassed countless countless charges and their associated degrees of freedom.

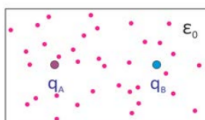
Two treatments of the electrostatic force that charge b exerts on charge a in a dense medium:

Continuum



$$f_A = \frac{1}{4\pi\epsilon_0} \frac{q_a q_b}{\epsilon_r r^2}$$

Explicit Charges



$$\begin{aligned} f_A &= \frac{1}{4\pi\epsilon_0} \left[\frac{q_a q_b}{r^2} + \sum_{i=1}^N \frac{q_a q_i}{r_{ai}^2} \right] \\ &= \frac{1}{4\pi\epsilon_0} \frac{q_a q_b}{r^2} \left[1 + \sum_{i=1}^N \frac{q_i}{q_b} \frac{r^2}{r_{ai}^2} \right] \end{aligned}$$

i : charged particles of the environment

This page titled [6.2: Dielectric Constant and Screening](#) is shared under a [CC BY-NC-SA 4.0](#) license and was authored, remixed, and/or curated by [Andrei Tokmakoff](#) via [source content](#) that was edited to the style and standards of the LibreTexts platform.

6.3: Free Energy of Ions in Solution

Returning to our continuum model of the solvation free energy, and apply this to solvating an ion. As discussed earlier, ΔG_{sol} will require forming a small cavity in water and turning on the interactions between the ion and water. We can calculate the energy for solvating an ion in a dielectric medium as the reversible work needed to charge the ion from a charge of 0 to its final value q within the dielectric medium:

$$w = \int_0^q \Phi_{\text{ion}} dq \quad (6.3.1)$$

As we grow the charge, it will induce a response from the dielectric medium (a polarization) that scales with electrostatic potential: $\Phi = q/4\pi\epsilon r$. We take the ion to occupy a spherical cavity with radius a . Although we can place a point charge at the center of the sphere, it is more easily solved assuming that the charge q is uniformly distributed over the surface of the sphere. Then the electrostatic potential at the surface of the sphere is $q/4\pi\epsilon a$ and the resulting work is

$$w = \frac{q^2}{8\pi\epsilon b}$$

In a similar manner, we can calculate the energy it takes to transfer an ion from one medium with ϵ_1 to another with ϵ_2 . We first discharge the ion in medium 1, transfer, and recharge the ion in medium 2. The resulting work, the Born transfer energy, is

$$\Delta w = \frac{q^2}{8\pi a} \left(\frac{1}{\epsilon_2} - \frac{1}{\epsilon_1} \right)$$

If you choose to distribute the charge uniformly through the spherical cavity, the prefactor $q^2/8\pi a$ becomes $3q^2/20\pi a$

This page titled [6.3: Free Energy of Ions in Solution](#) is shared under a [CC BY-NC-SA 4.0](#) license and was authored, remixed, and/or curated by [Andrei Tokmakoff](#) via [source content](#) that was edited to the style and standards of the LibreTexts platform.

6.4: Ion Distributions in Electrolyte Solution

To gain some insight into how ions in aqueous solution at physiological temperatures behave, we begin with the thermodynamics of homogeneous ionic solutions. Let's describe the distribution of ions relative to one another as a function of the concentration and charge of the ions. The free energy for an open system containing charged particles can be written

$$dG = -SdT + Vdp + \sum_{j=1}^{N_{\text{comp}}} \mu_j dN_j + \sum_{i=1}^{N_{\text{charges}}} \Phi(x) dq_i \quad (6.4.1)$$

μ_j and N_j are the chemical potential and the number of solutes of type j , in which the solute may or may not be charged and where the contribution of electrostatics is not included. This term primarily reflects the entropy of mixing in electrolyte solutions. The sum i only over charges q_i , under the influence of a spatially varying electrostatic potential. This reflects the enthalpic contribution to the free energy from ionic interactions.

In our case, we will assume that ions are the only solutes present, so that the sum over i and j are the same and this extends over all cations and anions in solution. We can relate the charge and number density through

$$q_i = z_i e N_i$$

where z is the valency of the ion ($\pm 1, 2, \dots$) and e is the fundamental unit of charge. Then expressing dq_i in terms of dN_i , we can write the free energy under constant temperature and pressure conditions as

$$dG|_{T,p} = \sum_i (\mu_i + z_i e \Phi) dN_i = \sum_i \mu'_i dN_i$$

Here μ'_i is known as the electrochemical potential.

To address the concentration dependence of the electrochemical potential, we remember that

$$\mu_i = \mu_i^\circ + k_B T \ln C_i$$

where C_i is the concentration of species i referenced to standard state, $C^\circ = 1M$. (Technically ionic solutions are not ideal and C_i is more accurately written as an activity.) Equivalently we can relate concentration to the number density of species i relative to standard state. Then the electrochemical potential of species i is

$$\mu'_i(x) = \mu_i^\circ + k_B T \ln C_i(x) + z_i e \Phi(x) \quad (6.4.2)$$

Here we write $C(x)$ to emphasize that there may be a spatial concentration profile. At equilibrium, the chemical potential must be the same at all points in space. Therefore, we equate the electrochemical potential at two points:

$$\mu'(x_2) = \mu'(x_1)$$

So from eq. (6.4.2)

$$\ln \frac{C(x_2)}{C(x_1)} = \frac{-ze\Delta\Phi}{k_B T} \quad (6.4.3)$$

where the potential difference is

$$\Delta\Phi = \Phi(x_2) - \Phi(x_1).$$

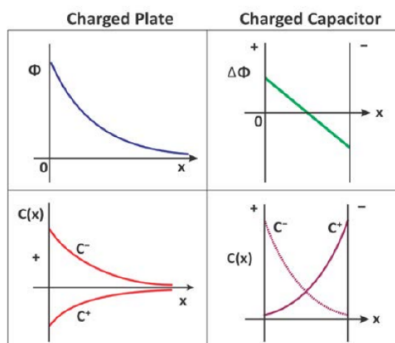
Equation (6.4.3) is one version of the Nernst Equation, which describes the interplay of the temperature-dependent entropy of mixing the ions and their electrostatic interactions. Rewriting it to describe $\Delta\Phi$ as a function of concentration is sometimes used to calculate the transmembrane potential as a function of ion concentrations on either side of the membrane.

The Nernst equation predicts Boltzmann statistics for the spatial distribution of charged species, i.e., that concentration gradients around charged objects drop away exponentially in space with in the interaction energy

$$\begin{aligned} \Delta U(x) &= ze\Delta\Phi(x) \\ C(x) &= C(x_0) e^{-\Delta U(x)/k_B T} \end{aligned} \quad (6.4.4)$$

This principle will hold whether we are discussing the ion concentration profile around a macroscopic object, like a charged plate, or for the average concentration profiles about a single ion. At short distances, oppositely charged particles will have their concentrations enhanced, whereas equally charged objects will be depleted. At short range, the system is dominated by the electrostatic interaction between charges, whereas at long distance, the entropy of mixing dominates.

For the case of charged plates:



Bjerrum Length, ℓ_B

The distance at which electrostatic interaction energy between two charges equals $k_B T$.

$$\text{For } \pm 1 \text{ charges } \ell_B = \frac{1}{4\pi\epsilon} \frac{e^2}{k_B T}$$

At $T = 300 \text{ K}$, $k_B T/e = 25 \text{ mV}$ and

For:	$\epsilon_r = 1 \quad \ell_B = 560 \text{ \AA}$ $\epsilon_r = 80 \quad \ell_B = 7.0 \text{ \AA}$
For $\ell > \ell_B$	Electrostatic interactions are largely screened, and motion is primarily Brownian
For $\ell < \ell_B$	Attractive and repulsive forces dominate. The Bjerrum length gives ion pairing threshold. For $\ell_B = 7.0 \text{ \AA}$, the ion concentrations are approximately, $6.9 \times 10^{26} \text{ m}^{-3}$ or $\sim 1 \text{ M}$.

This page titled [6.4: Ion Distributions in Electrolyte Solution](#) is shared under a [CC BY-NC-SA 4.0](#) license and was authored, remixed, and/or curated by [Andrei Tokmakoff](#) via [source content](#) that was edited to the style and standards of the LibreTexts platform.

6.5: Poisson–Boltzmann Equation

Poisson–Boltzmann Equation¹

The **Poisson–Boltzmann Equation** (PBE) is used to evaluate charge distributions for ions around charged surfaces. It brings together the description of the electrostatic potential around a charged surface with the Boltzmann statistics for the thermal ion distribution. Gauss' equation relates the flux of electric field lines through a closed surface to the charge density within the volume: $\nabla \cdot \vec{E} = \rho/\epsilon$. The Poisson equation can be obtained by expressing this in terms of the electrostatic potential using $\vec{E} = -\nabla\Phi$

$$-\nabla^2\Phi = \frac{\rho}{\epsilon} \quad (6.5.1)$$

Here ρ is the bulk charge density for a continuous medium.

We seek to describe the charge distribution of ions about charged surfaces of arbitrary geometry. The surface will be described by a surface charge density σ . We will determine $\rho(r)$, which is proportional to the number density or concentration of ions

$$\rho(r) = \sum_i z_i e C_i(r) \quad (6.5.2)$$

where the sum is over all ionic species in the solution, and z_i is the ion valency, which may take on positive or negative integer values. Drawing from the Nernst equation, we propose an ion concentration distribution of the Boltzmann form

$$C_i(r) = C_{0,i} e^{-z_i e \Phi(r)/k_B T} \quad (6.5.3)$$

Here we have defined the bulk ion concentration as $C_0 = C(r \rightarrow \infty)$, since $\Phi \rightarrow 0$ as $r \rightarrow \infty$. Note that the ionic composition is taken to obey the net charge neutrality condition

$$\sum_i z_i C_{0,i} = 0 \quad (6.5.4)$$

The expressions above lead to the general form of the PBE:

$$-\nabla^2\Phi = \frac{e}{\epsilon} \sum_i z_i C_{0,i} \exp[-z_i e \Phi/k_B T] \quad (6.5.5)$$

This is a nonlinear differential equation for the electrostatic potential and can be solved for the charge distribution of ions in solution for various boundary conditions. This can explain the ion distributions in aqueous solution about a charged structure. For instance:

- Surface (membrane) $\frac{\partial^2\Phi}{\partial x^2} = \frac{e}{\epsilon} \sum_i z_i C_{0,i} e^{-z_i e \Phi(x)/k_B T}$
- Sphere (protein) $\frac{1}{r^2} \frac{\partial}{\partial r} r^2 \frac{\partial\Phi}{\partial r} = \frac{e}{\epsilon} \sum_i z_i C_{0,i} e^{-z_i e \Phi(x)/k_B T}$
- Cylinder (DNA) $\frac{1}{r} \frac{\partial}{\partial r} r \frac{\partial\Phi}{\partial r} + \frac{\partial^2\Phi}{\partial z^2} = \frac{e}{\epsilon} \sum_i z_i C_{0,i} e^{-z_i e \Phi(x)/k_B T}$

These expressions only vary in the form of the Laplacian ∇^2 . They are solved by considering two boundary conditions: (1) $\Phi(\infty) = 0$ and (2) the surface charge density $\sigma/\epsilon = -\nabla\Phi$. We will examine the resulting ion distributions below.

In computational studies, the interactions of a solute with water and electrolyte solutions are often treated with "implicit solvent", a continuum approximation. Solving the PBE is one approach to calculating the effect of implicit solvent. The electrostatic free energy is calculated from $\Delta G_{\text{elec}} = \frac{1}{2} \sum_i e z_i \Phi_i$ and the electrostatic potential is determined from the PBE.

As a specific case of the PBE, let's consider the example of a symmetric electrolyte, obtained from dissolving a salt that has positive and negative ions with equal valence ($z_+ = -z_- = z$), resulting in equal concentration of the cations and anions ($C_{0,+} = C_{0,-} = C_0$), as for instance when dissolving NaCl. Equation (6.5.2) is used to describe the interactions of ions with the same charge (co-ions) versus the interaction of ions with opposite charge (counterions). For counterions, z and Φ have opposite signs and the ion concentration should increase locally over the bulk concentration. For co-ions, z and Φ have the same sign and we expect a lowering of the local concentration over bulk. Therefore, we expect the charge distribution to take a form

$$\begin{aligned}\rho &= -zeC_0(e^{ze\Phi/k_B T} - e^{-ze\Phi/k_B T}) \\ &= -2zeC_0 \sinh\left(\frac{ze\Phi}{k_B T}\right)\end{aligned}\tag{6.5.6}$$

Remember: $2\sinh(x) = e^x - e^{-x}$. Then substituting into eq. (6.5.1), we arrive at a common form of the PBE²

$$\nabla^2 \Phi = \frac{2zeC_0}{\epsilon} \sinh\left(\frac{ze\Phi}{k_B T}\right)\tag{6.5.7}$$

1. M. Daune, *Molecular Biophysics: Structures in Motion*. (Oxford University Press, New York, 1999); M. B. Jackson, *Molecular and Cellular Biophysics*. (Cambridge University Press, Cambridge, 2006).

2. Alternate forms in one dimension:

$$\frac{\partial^2 \Phi}{\partial x^2} = \frac{e}{\epsilon} C_0 2 \sinh\left(\frac{e\Phi}{k_B T}\right) = \frac{k_B T}{e} \frac{1}{\lambda_D^2} \sinh\left(\frac{e\Phi}{k_B T}\right) = \frac{4\pi k_B T}{e} \ell_B C_0 \sinh\left(\frac{e\Phi}{k_B T}\right)$$

This page titled [6.5: Poisson–Boltzmann Equation](#) is shared under a [CC BY-NC-SA 4.0](#) license and was authored, remixed, and/or curated by [Andrei Tokmakoff](#) via [source content](#) that was edited to the style and standards of the LibreTexts platform.

6.6: Debye–Hückel Theory

Since it is nonlinear, it is not easy to solve the PBE, but for certain types of problems, we can make approximations to help. The **Debye–Hückel approximation** holds for small electrostatic potential or high temperature conditions such that

$$\frac{ze\Phi}{k_B T} \ll 1$$

This is the regime in which the entropy of mixing dominates the electrostatic interactions between ions. In this limit, we can expand the exponential in eq. (6.5.5) as $\exp[-ze\Phi/k_B T] \approx 1 - ze\Phi/k_B T$. The leading term in the resulting sum drops because of the charge neutrality condition, eq. (6.5.4). Keeping the second term in the expansion leads to

$$\nabla^2 \Phi = \kappa^2 \Phi \quad (6.6.1)$$

where

$$\kappa^2 = \frac{2e^2}{\epsilon k_B T} I$$

and the ionic strength, I , is defined as

$$I = \frac{1}{2} \sum_i C_{0,i} z_i^2$$

Looking at eq. (6.6.1), we see that the Debye–Hückel approximation linearizes the PBE. It is known as the Debye–Hückel equation, or the linearized PBE. For the case of the 1:1 electrolyte solution described by eq. , we again obtain eq. (6.6.1) using $\sinh(x) \approx x$ as $x \rightarrow \infty$, with

$$\kappa^2 = \frac{2z^2 e^2 C_0}{\epsilon k_B T} = 8\pi z^2 C_0 \ell_B$$

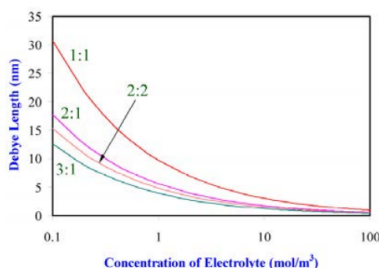
The constant κ has units of inverse distance, and its inverse is known as the **Debye length** $\lambda_D = \kappa^{-1}$. The Debye length sets the distance scale over which the electrostatic potential decays, i.e., the distance over which charges are screened from one another. For the symmetric electrolytes

$$\lambda_D = \kappa^{-1} = \sqrt{\frac{\epsilon k_B T}{2z^2 e^2 C_0}} \quad (6.6.2)$$

As an example: 1:1 electrolytes in H₂O: $\epsilon = 80$; $z_+ = -z_- = 1$; $T = 300 \text{ K}$ leads to

$$\begin{aligned} C_0 = 100 \text{ mM} & \quad \lambda_D = 9.6 \text{ \AA} \\ C_0 = 10 \text{ mM} & \quad \lambda_D = 30.4 \text{ \AA} \\ \lambda_D (\text{\AA}) & \approx 3.04 \cdot [C_0 (\text{M})]^{-1/2} \end{aligned}$$

The Debye approximation holds for small electrostatic potentials relative to $k_B T$ ($r > \lambda_D$). For instance, it's ok for ion distribution about large protein or vesicle but not for water in a binding pocket.



The variation of Debye length with concentrations of electrolytes. Reprinted from P. Ghosh
<http://nptel.ac.in/courses/103103033/module3/lecture3.pdf>.

This page titled [6.6: Debye–Hückel Theory](#) is shared under a [CC BY-NC-SA 4.0](#) license and was authored, remixed, and/or curated by [Andrei Tokmakoff](#) via [source content](#) that was edited to the style and standards of the LibreTexts platform.

6.7: Ion Distributions Near a Charged Interface

Debye–Hückel Approximation

Describing ions near a negatively charged plane is a way of describing the diffuse layer of cations that forms near the negatively charged interface in lipid bilayers. The simplest approach is to use the Debye–Hückel equation (linearized PBE) in one dimension. x is the distance away from the infinite charged plane with a surface charge density of $\sigma = q/a$.

$$\frac{\partial^2 \Phi(x)}{\partial x^2} = \frac{1}{\lambda_D^2} \Phi(x)$$

Generally, the solution is

$$\Phi(x) = a_1 e^{-x/\lambda_D} + a_2 e^{x/\lambda_D} \quad (6.7.1)$$

Apply boundary conditions:

1. $\lim_{x \rightarrow \infty} \Phi(x) = 0 \therefore a_2 = 0$
2. The electric field for surface with charge density σ (from Gauss' theorem)

$$E = -\left. \frac{\partial \Phi}{\partial x} \right|_{\text{surface}} = \frac{\sigma}{\epsilon} \quad (6.7.2)$$

Differentiate eq. (6.7.1) and compare with eq. (6.7.2):

$$a_1 = \frac{\sigma \lambda_D}{\epsilon}$$

The electrostatic potential decays exponentially away from the surface toward zero.

$$\Phi(x) = \frac{\sigma \lambda_D}{\epsilon} e^{-x/\lambda_D}$$

Nominally, the prefactor would be the "surface potential" at $x = 0$, but the Debye approximation would significantly underestimate this, as we will see later. Substituting Φ into the Poisson equation gives

$$\rho(x) = \frac{-\sigma}{\lambda_D} e^{-x/\lambda_D} \quad (6.7.3)$$

Ion distribution density in solution decays exponentially with distance. This description is valid for weak potentials, or $x > \lambda_D$. The potential and charge density are proportional as $\Phi(x) = -\lambda_D^2 \rho(x) / \epsilon$; both decay exponentially on the scale of the Debye length at long range.

Note:

Higher ion concentration \rightarrow smaller $\lambda_D \rightarrow$ Double layer less diffuse.

Higher temperature \rightarrow larger $\lambda_D \rightarrow$ Double layer more diffuse.

Note also that the surface charge is balanced by ion distribution in solution:

$$\sigma = -\int_0^{\infty} \rho(x) dx \quad (6.7.4)$$

which you can confirm by substituting eq. (6.7.3).

Gouy–Chapman Model¹

To properly describe the ion behavior for shorter distances ($x < \lambda_D$), one does not need to make the weak-potential approximation and can retain the nonlinear form of the Poisson–Boltzmann equation:

$$\frac{\partial^2 \Phi(x)}{\partial x^2} = \frac{2zeC_0}{\epsilon} \sinh\left(\frac{ze\Phi(x)}{kT}\right)$$

$$E = -\left. \frac{\partial \Phi}{\partial x} \right|_{\text{surf}} = \frac{4\pi \ell_B \sigma k_B T}{e^2}$$

In fact, this form does have an analytical solution. It is helpful to define a dimensionless reduced electrostatic potential, expressed in thermal electric units:

$$\underline{\Phi} = \frac{e}{k_B T} \Phi$$

and a reduced distance which is scaled by the Debye length

$$\underline{x} = x / \lambda_D$$

Then the PBE for a 1:1 electrolyte takes on a simple form

$$\nabla^2 \underline{\Phi}(x) = \sinh \underline{\Phi}(x)$$

with the solution:

$$\underline{\Phi}(x) = 2 \ln \left(\frac{1 + g e^{-x}}{1 - g e^{-x}} \right)$$

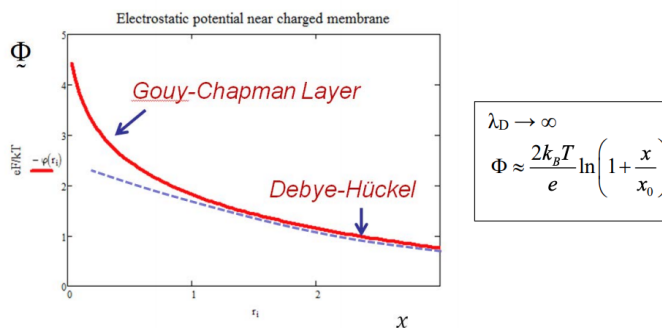
Here g is a constant, which we can relate to the surface potential, by setting x to zero.

$$\exp(-\underline{\Phi}(0)/2) = \frac{1-g}{1+g} = -\tanh(\ln(g)/2)$$

$\underline{\Phi}(0)$ is the scaled surface potential. Using the surface charge density σ we can find:

$$g = -\frac{x_0}{\lambda_D} + \sqrt{1 + \left(\frac{x_0}{\lambda_D}\right)^2} \quad \text{with } x_0 = \frac{e}{2\pi\ell_B\sigma}$$

Then you can get the ion distribution from Poisson equation: $\rho(x) = \varepsilon \nabla^2 \Phi(x)$.



The **Gouy–Chapman Layer**, which is $x < \lambda_D$, has strong enough ionic interactions that you will see an enhancement over Debye–Hückel.

Stern Layer

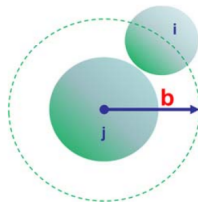
In immediate proximity to a strongly charged surface, one can form a direct contacts layer of counterions on surface: the **Stern layer**. The Stern Layer governs the slip plane for diffusion of charged particles. The zeta potential ζ is the potential energy difference between the Stern layer and the electroneutral region of the sample, and governs the electrophoretic mobility of particles. It is calculated from the work required to bring a charge from $x = \infty$ to the surface of the Stern layer.

-
1. H. H. Girault, *Analytical and Physical Electrochemistry*. (CRC Press, New York, 2004).; M. B. Jackson, *Molecular and Cellular Biophysics*. (Cambridge University Press, Cambridge, 2006), Ch. 11.; M. Daune, *Molecular Biophysics: Structures in Motion*. (Oxford University Press, New York, 1999), Ch. 18.; S. McLaughlin, The electrostatic properties of membranes, *Annu. Rev. Biophys. Biophys. Chem.* 18, 113-136 (1989).

This page titled [6.7: Ion Distributions Near a Charged Interface](#) is shared under a [CC BY-NC-SA 4.0](#) license and was authored, remixed, and/or curated by [Andrei Tokmakoff](#) via [source content](#) that was edited to the style and standards of the LibreTexts platform.

6.8: Ion Distributions Near a Charged Sphere

Ion Distributions Near a Charged Sphere¹



Now let's look at how ions will distribute themselves around a charged sphere. This sphere could be a protein or another ion. We assume a spherically symmetric charge distribution about ions, and a Boltzmann distribution for the charge distribution for the ions (i) about the sphere (j) of the form

$$\rho(r) = \sum_i e z_i C_{0,i} e^{-z_i e \Phi_j(r) / k_B T} \quad (6.8.1)$$

$\Phi_j(r)$ is the electrostatic potential at radius r which results from a point charge $z_j e$ at the center of the sphere. Additionally, we assume that the sphere is a hard wall, and define a radius of closest approach by ions in solution, b . The PBE becomes

$$\frac{1}{r^2} \frac{d}{dr} \left(r^2 \frac{d\Phi}{dr} \right) = \frac{1}{\epsilon} \sum_i e z_i C_{0,i} e^{-z_i e \Phi_j(r) / k_B T}$$

To simplify this, we again apply the Debye–Hückel approximation ($ze\Phi \ll k_B T$), expand the exponential in eq. , drop the leading term due to the charge neutrality condition, and obtain

$$\rho(r) = - \sum_i C_{0,i} z_i^2 e^2 \Phi_j(r) / k_B T \quad (6.8.2)$$

Then the linearized PBE in the Debye–Hückel approximation is

$$\frac{1}{r^2} \frac{d}{dr} \left(r^2 \frac{d\Phi}{dr} \right) = \kappa^2 \Phi \quad (6.8.3)$$

As before: $\kappa^2 = \lambda_D^{-2} = 2e^2 I / \epsilon k_B T$. Solutions to eq. (6.8.3) will take the form:

$$\Phi = A_1 \frac{e^{-\kappa r}}{r} + A_2 \frac{e^{\kappa r}}{r} \quad (6.8.4)$$

To solve this use boundary conditions:

1. $A_2 = 0$, since $\Phi \rightarrow 0$ at $r = \infty$.
2. The field at the surface of a sphere with charge $z_j e$ and radius b is determined from

$$4\pi b^2 E(b) = \frac{z_j e}{\epsilon} \quad (6.8.5)$$

Now, using

$$E(b) = - \left. \frac{d\Phi}{dr} \right|_{r=b} \quad (6.8.6)$$

Substitute eq. (6.8.4) into RHS and eq. (6.8.5) into LHS of eq. (6.8.6). Solve for A_1 .

$$A_1 = \frac{z_j e e^{\kappa b}}{4\pi \epsilon (1 + \kappa b)}$$

So, the electrostatic potential for $r \geq b$ is

$$\Phi(r) = \frac{z_j e}{\underbrace{4\pi\epsilon_0 r}_{\text{vacuum}}} \frac{e^{-\kappa(r-b)}}{\epsilon_r(1+\kappa b)} \quad (6.8.7)$$

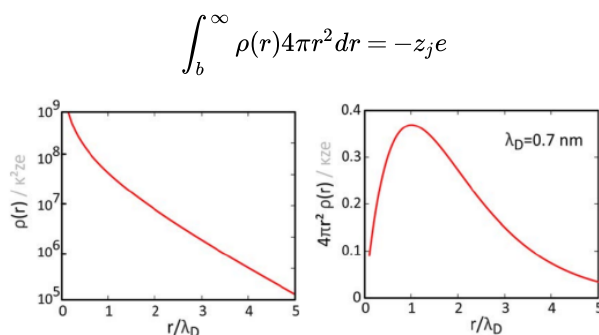
Setting $r = b$ gives us the surface potential of the sphere:

$$\Phi(b) = \frac{z_j e}{4\pi\epsilon b(1+\kappa b)}$$

Note the exponential factor in eq. (6.8.7) says that Φ drops faster than r^{-1} as a result of screening. Now substitute eq. (6.8.7) into eq. (6.8.2) we obtain the charge probability density

$$\rho(r) = \frac{-\kappa^2 z_j e}{4\pi r} \frac{e^{-\kappa(r-b)}}{1+\kappa b} \quad (6.8.8)$$

We see that the charge density about ion drops as $e^{-\kappa(r-b)}/r$, a rapidly decaying function that emphasizes the strong tendency for ions to attract or repel at short range. However, the charge density between r and $r + dr$ is $4\pi r^2 \rho(r)$ and therefore grows linearly with r before decaying exponentially: $r e^{-\kappa(r-b)}$. We plot this function to illustrate the thickness of the "ion cloud" around the sphere, which is peaked at $r = \lambda_D$. Additionally, note, that the charge distribution around that ion is equal and opposite to the charge of the sphere "j".



It is also possible to calculate radial distribution functions for ions in the Debye–Hückel limit.² The radial pair distribution function for ions of type i and j , $g_{ij}(r)$, is related to the potential of mean force W_{ij} as

$$g_{ij}(r) = \exp[-W_{ij}(r)/k_B T] \quad (6.8.9)$$

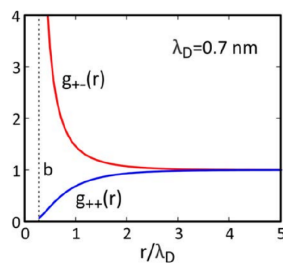
If only considering electrostatic effects, we can approximate W_{ij} as the interaction energy $U_{ij}(r) = z_i z_j \Phi_j(r)$. Using the Debye–Hückel result, eq. (6.8.7),

$$U_{ij}(r) = \frac{z_i z_j e^2}{4\pi\epsilon(1+\kappa b)} \frac{e^{-\kappa(r-b)}}{r}$$

Let's look at the form of $g(r)$ for two singly charged ions with $\lambda_D = 0.7 \text{ nm}$, $\epsilon = 80$, and $T = 300 \text{ K}$. The Bjerrum length is calculated as $\ell_B = e^2/4\pi\epsilon k_B T = 0.7 \text{ nm}$. Since the Debye–Hückel holds for $ze\Phi \ll k_B T$, we can expand the exponential in eq. as

$$g_{ij}(r) = 1 - \chi_{ij} + \frac{1}{2}\chi_{ij}^2 + \dots$$

where we define $\chi_{ij} = U_{ij}(r)/k_B T = \ell_B e^{-\kappa(r-b)} r^{-1} (1+\kappa b)^{-1}$. The resulting radial distribution function for co- and counterions calculated for $b = 0.15 \text{ nm}$ are shown below.



Readings

1. M. Daune, *Molecular Biophysics: Structures in Motion*. (Oxford University Press, New York, 1999), Ch. 16, 18.
2. D. A. McQuarrie, *Statistical Mechanics*. (Harper & Row, New York, 1976), Ch. 15.

-
1. See M. Daune, *Molecular Biophysics: Structures in Motion*. (Oxford University Press, New York, 1999), Ch. 16.; D. A. McQuarrie, *Statistical Mechanics*. (Harper & Row, New York, 1976), Ch. 15.; Y. Marcus, Ionic radii in aqueous solutions, *Chem. Rev.* 88 (8), 1475-1498 (1988).
 2. See D. A. McQuarrie, *Statistical Mechanics*. (Harper & Row, New York, 1976), Ch. 15.

This page titled [6.8: Ion Distributions Near a Charged Sphere](#) is shared under a [CC BY-NC-SA 4.0](#) license and was authored, remixed, and/or curated by [Andrei Tokmakoff](#) via [source content](#) that was edited to the style and standards of the LibreTexts platform.

SECTION OVERVIEW

2: Macromolecules

7: Statistical Description of Macromolecular Structure

7.1: Segment Models

7.2: Excluded Volume Effects

7.3: Polymer Loops

8: Polymer Lattice Models

8.1: Entropy of Single Polymer Chain

8.2: Self-Avoiding Walks

8.3: Conformational Changes with Temperature

8.4: Flory–Huggins Model of Polymer Solutions

8.5: Polymer–Solvent Interactions

9: Macromolecular Mechanics

9.1: Force and Work

9.2: Worm-like Chain

9.3: Polymer Elasticity and Force–Extension Behavior

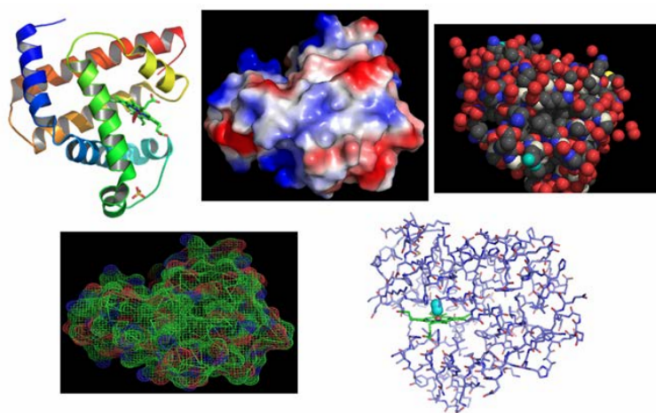
This page titled [2: Macromolecules](#) is shared under a [CC BY-NC-SA 4.0](#) license and was authored, remixed, and/or curated by [Andrei Tokmakoff](#) via [source content](#) that was edited to the style and standards of the LibreTexts platform.

CHAPTER OVERVIEW

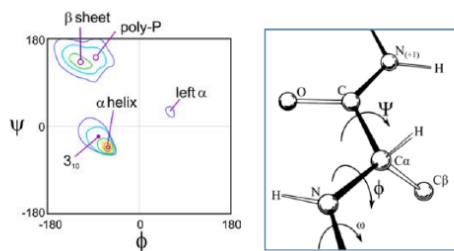
7: Statistical Description of Macromolecular Structure

There are a number of ways in which macromolecular structure is described in biophysics, which vary in type of information they are trying to convey. Consider these two perspectives on macromolecular structure that represent opposing limits: atomistic vs. statistical.

1. **Atomistic:** Use of atoms, small molecules, or functional groups as building blocks for biomolecular structure. This perspective is rooted in the dominant methods used for studying macromolecular structure (90% X-ray crystallography; 10% NMR). It has the most value for describing detailed Ångstrom to nanometer scale interactions of a chemical nature, but also tends to reinforce a unique and rigid view of structure, even though this cannot be the case at physiological temperatures. The atomistic perspective is inherent to molecular force fields used in computational biophysics, which allow us to explore time-dependent processes and molecular disorder. Even within the atomistic representation, there are many complementary ways of representing macromolecular structure. Below are several representations of myoglobin structure, each is used to emphasize specific physical characteristics of the protein.



2. **Statistical/physical:** More applicable for disordered or flexible macromolecules. Emphasis is on a statistical description of molecules that can have multiple configurations. Often the atomic/molecular structure is completely left out. These tools have particular value for describing configurational entropy and excluded volume, and are influenced by the constraints of covalent bonding linkages along the chain. This approach is equally important: 30–40% of primary sequences in PDB are associated with disordered or unstructured regions. Conformational preferences are described statistically.



Statistical Models

- Structure described in terms of spatial probability distribution functions.
- There may be constraints on geometry or energy functions that describe interactions between and within chains.
- We will discuss several models that emerge for a continuous chain in space that varies in stiffness, constraints on conformation, and excluded volume.
 - Segment models: random coils, feely jointed chain, freely rotating chain
 - Lattice models: Flory–Huggins theory

- Continuum model: worm-like chain

[7.1: Segment Models](#)

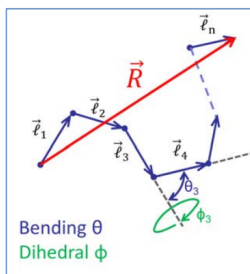
[7.2: Excluded Volume Effects](#)

[7.3: Polymer Loops](#)

This page titled [7: Statistical Description of Macromolecular Structure](#) is shared under a [CC BY-NC-SA 4.0](#) license and was authored, remixed, and/or curated by [Andrei Tokmakoff](#) via [source content](#) that was edited to the style and standards of the LibreTexts platform.

7.1: Segment Models

Segment Models¹



- $(n + 1)$ beads link by n segments or bonds of length ℓ .
- Each bead has a position \vec{r}_i .
- Each bond is assigned a vector, $\vec{\ell}_i = \vec{r}_i - \vec{r}_{i-1}$.
- The bending angle between adjacent segments i and $(i + 1)$ is θ_i : $\cos \theta = \vec{\ell}_i \cdot \vec{\ell}_{i-1}$
- For each bending angle there is an associated dihedral angle ϕ_i defined as the rotation of segment $(i + 1)$ out of the plane defined by segments i and $(i - 1)$.
- There are $n - 1$ separate bending and dihedral angles.

Statistical Variables for Macromolecules

End-to-end distance

The contour length is the full length of the polymer along the contour of the chain:

$$L_C = n\ell$$

Each chain has the same contour length, but varying dimensions in space that result from conformational flexibility. The primary structural variable for measuring this conformational variation is the end-to-end vector between the first and last bead, $\vec{R} = \vec{r}_n - \vec{r}_0$, or equivalently

$$\vec{R} = \sum_{i=1}^n \vec{\ell}_i$$

Statistically, the dimensions of a polymer can be characterized by the statistics of the end-to-end distance. Consider its mean-square value:

$$\langle \vec{R}^2 \rangle = \langle \vec{R} \cdot \vec{R} \rangle = \left\langle \left(\sum_{i=1}^n \vec{\ell}_i \right) \cdot \left(\sum_{j=1}^n \vec{\ell}_j \right) \right\rangle \quad (7.1.1)$$

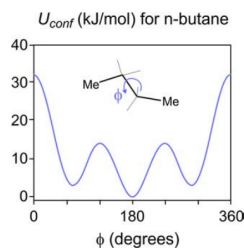
After expanding these sums, we can collect two sets of terms: (1) the self-terms with $i = j$ and (2) the interbond correlations ($i \neq j$):

$$\begin{aligned} \langle \vec{R}^2 \rangle &= n\ell^2 + \sum_{j \neq i} \langle \vec{\ell}_i \cdot \vec{\ell}_j \rangle \\ &= n\ell^2 + \ell^2 \sum_{j \neq i} \langle \cos \theta_{ij} \rangle \end{aligned} \quad (7.1.2)$$

Here θ_{ij} is the angle between segments i and j . This second term describes any possible conformational preferences between segments along the chain. We will call the factor $\langle \cos \theta_{ij} \rangle$ the segment orientation correlation function, which is also written

$$\begin{aligned} g(k) &= \langle \cos \theta_k \rangle \\ \theta_k &= \vec{\ell}_i \cdot \vec{\ell}_{i+k} \quad k = |j - i| \end{aligned} \quad (7.1.3)$$

Here k refers to the separation between two segments. This correlation function can vary in value from 1 to -1, where +1 represents a highly aligned or extended chain and negative values would be very condensed or compact. No interband correlations ($g = 0$) is expected for placement of segments by a random walk.



Interbond correlation can be inserted into segment models, both through ad hoc rules, or by applying an energy function that constrains the intersegment interactions. For instance, the torsional energy function below, U_{conf} , would be used to weight the probability that adjacent segments adopt a particular torsional angle. A general torsional energy function $U_{\text{conf}}(\Theta)$ involves all $2(n-1)$ possible angles $\Theta = \{\theta_1, \phi_1, \theta_2, \phi_2, \dots, \theta_{n-1}, \phi_{n-1}\}$, the joint probability density for adopting a particular conformation is

$$P(\Theta) = \frac{e^{-U_{\text{conf}}(\Theta)/k_B T}}{\int d\Theta e^{-U_{\text{conf}}(\Theta)/k_B T}}$$

The integral over Θ reflects $2(n-1)$ integrals over polar coordinates for all adjacent segments,

$$\int d\Theta = \int_0^\pi \int_0^{2\pi} \sin \theta_1 d\theta_1 d\phi_1 \cdots \int_0^\pi \int_0^{2\pi} \sin \theta_{n-1} d\theta_{n-1} d\phi_{n-1}$$

Then the alignment correlation function is

$$\langle \vec{\ell}_i \cdot \vec{\ell}_j \rangle = \ell^2 \int d\Theta \cos \theta_{ij} P(\Theta)$$

This is not a practical form, so we will make simplifying assumptions about the form of this probability distribution. For instance, if any segments configuration depends only on its nearest neighbors then $P(\Theta) = P(\theta, \phi)^{(n-1)}$.

Persistence Length

For any polymer, alignment of any pair of vectors in the chain becomes uncorrelated over a long enough sequence of segments. To quantify this distance we define a "persistence length" ℓ_p .

$$\ell_p = \langle \hat{\ell}_i \cdot \sum_{j=1}^n \hat{\ell}_j \rangle \quad \hat{\ell}_i = \frac{\vec{\ell}_i}{|\ell|}$$

This is the characteristic distance along the chain for the decay for the orientational correlation function between bond vectors,

$$g(k) = \ell^2 \langle \cos^k \theta \rangle$$

How will this behave? If you consider that $|\cos \theta| < 1$, then $\langle \cos^k \theta \rangle$ will drop with increasing k , approaching zero as $k \rightarrow \infty$. That is the memory of the alignment between two bond vectors drops with their separation, where the distance scale for the loss of correlation is ℓ_p . We thus expect a monotonically decaying form to this function:

$$g(k) = \ell^2 e^{-k\ell/\ell_p} \quad (7.1.4)$$

For continuous thin rod models of the polymer, this expression is written in terms of the contour distance s , the displacement along the contour of the chain (i.e., $s = \ell k$),

$$g(s) = \ell^2 e^{-|s|/\ell_p}$$

How do we relate θ and ℓ_p ?² Writing $\langle \cos^k \theta \rangle \approx \exp(k \ln \langle \cos \theta \rangle)$ and equating this with eq. (7.1.4) indicates that

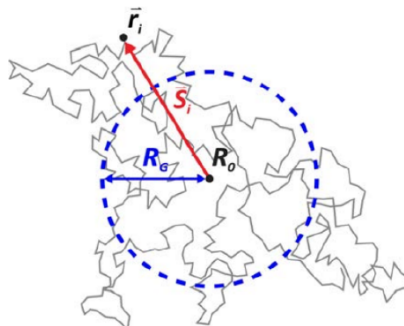
$$\ell_p = -\ell \ln \langle \cos \theta \rangle$$

For stiff chains, we can approximate $\ln(x) \approx (1 - x)$, so

$$\ell_p \approx \frac{\ell}{1 - \langle \cos \theta \rangle}$$

Radius of Gyration

The **radius of gyration** is another important structural variable that is closely related to experimental observables. Here the polymer dimensions are expressed as extension relative to the center of mass for the chain.



This proves useful for branched polymers and heteropolymers (such as proteins). Denoting the position and mass of the i^{th} bead as \vec{r}_i and m_i , we define the center of mass for the polymer as a mass-weighted mean position of the beads in space:

$$\vec{R}_0 = \frac{\sum_{i=0}^n m_i \vec{r}_i}{\sum_{i=0}^n m_i}$$

The sum index starting at 0 is meant to reflect the sum over $n + 1$ beads. The denominator of this expression is the total mass of the polymer $M = \sum_{i=0}^n m_i$. If all beads have the same mass, then $m_i/M = 1/(n + 1)$ and \vec{R}_0 is the geometrical mean of their positions.

$$\vec{R}_0 = \frac{1}{n + 1} \sum_{i=0}^n \vec{r}_i$$

The radius of gyration R_G for a configuration of the polymer describes the mass-weighted distribution of beads R_0 , and is defined through

$$\langle R_G^2 \rangle = \frac{1}{n + 1} \sum_{i=0}^n \langle \vec{S}_i^2 \rangle$$

where \vec{S}_i is gyration radius, i.e., the radial distance of the i^{th} bead from the center of mass

$$\vec{S}_i^2 = \frac{m_i}{M} (\vec{r}_i - \vec{R}_0)^2 \quad (\text{mass-weighted})$$

$$\vec{S}_i^2 = \frac{1}{n + 1} (\vec{r}_i - \vec{R}_0)^2 \quad (\text{equal mass beads})$$

Additionally, we can show that the mean-squared radius of gyration is related to the average separation of all beads of the chain.

$$\langle R_G^2 \rangle = \frac{1}{(n + 1)^2} \sum_{i=0}^n \sum_{j=0}^n \langle (\vec{r}_i - \vec{r}_j)^2 \rangle$$

Freely Jointed Chain

The freely jointed chain describes a macromolecule as a backbone for which all possible θ and ϕ are equally probable, and there are no correlations between segments. It is known as an "ideal chain" because there are no interactions between beads or excluded volume, and configuration of the polymer backbone follows a random walk. If we place the first bead at $r = 0$, we find that $\langle R \rangle = 0$, as expected for a random walk, and eq. (7.1.2) reduces to

$$\langle R^2 \rangle = n\ell^2$$

$$\text{or } R_{rms} = \langle R^2 \rangle^{1/2} = \sqrt{n}\ell$$

While the average end-to-end distance may be zero, the variance in the end-to-end distribution is

$$\sigma_r = \sqrt{\langle R^2 \rangle - \langle R \rangle^2} = \sqrt{n}\ell$$

The radius of gyration for an ideal chain is:

$$R_G = \sqrt{\frac{\langle R^2 \rangle}{6}} = \sqrt{\frac{n\ell^2}{6}}$$

Gaussian Random Coil

The freely jointed chain is also known as a Gaussian random coil, because the statistics of its configuration are fully described by $\langle R \rangle$ and $\langle R^2 \rangle$, the first two moments of a Gaussian end-to-end probability distribution $P(R)$. The end-to-end probability density in one dimension can be obtained from a random walk with n equally sized steps of length ℓ in one dimension, where forward and reverse steps are equally probable. If the first bead is set at $x_0 = 0$, then the last bead is placed by the last step at position x . In the continuous limit:

$$P(x, n) = \sqrt{\frac{1}{2\pi n\ell^2}} e^{-x^2/2n\ell^2} \quad (7.1.5)$$

$P(x, n)dx$ is the probability of finding the end of the chain with n beads at a distance between x and $x + dx$ from its first bead. Note this equates the rms end-to-end distance with the standard deviation for this distribution: $\langle R^2 \rangle = \sigma^2 = n\ell^2$.

To generalize eq. (7.1.5) to a three-dimensional chain, we recognize that propagation in the x , y , and z dimensions is equally probable, so that the 3D probability density can be obtained from a product of 1D probability densities $P(r) = P(x)P(y)P(z)$. Additionally, we need to consider the constraint that the distribution of end-to-end distances are equal in each dimension:

$$\langle \vec{R}^2 \rangle = \sigma_x^2 + \sigma_y^2 + \sigma_z^2 = n\ell^2$$

and since $\sigma_x^2 = \sigma_y^2 = \sigma_z^2$,

$$\langle \vec{R}^2 \rangle = 3\sigma_x^2 = n\ell^2$$

Therefore,

$$\begin{aligned} P(r, n) &= \sqrt{12\pi\sigma_x^2} e^{-x^2/2\sigma_x^2} \sqrt{12\pi\sigma_y^2} e^{-y^2/2\sigma_y^2} \sqrt{12\pi\sigma_z^2} e^{-z^2/2\sigma_z^2} \\ &= \left(\frac{3}{2\pi\sigma^2} \right)^{3/2} e^{-3r^2/2\sigma^2} \end{aligned}$$

To simplify, we define a scaling parameter with dimensions of inverse length

$$\beta = \sqrt{\frac{3}{2n\ell^2}} = \sqrt{\frac{3}{2}} \langle R^2 \rangle^{-1/2}$$

Then, the probability density in Cartesian coordinates,

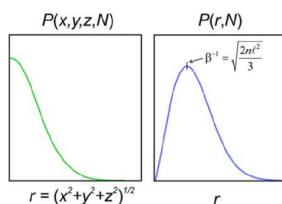
$$P(x, y, z, n) = \frac{\beta^3}{\pi^{3/2}} e^{-\beta^2 r^2} \quad \text{where } r^2 = x^2 + y^2 + z^2$$

Note the units of $P(x, y, z, n)$ are inverse volume or concentration. The probability of finding the end of a chain of n beads in a box of volume $dx dy dz$ at the position x, y, z is $P(x, y, z, n) dx dy dz$. This function illustrates that the most probable end-to-end distance for a random walk polymer is at the origin. On the other hand, we can also express this as a radial probability density that gives the probability of finding the end of a chain at a radius between r and $r + dr$ from the origin. Since the volume of a spherical shell grows in proportion to its surface area:

$$P(r, n)dr = 4\pi r^2 P(x, y, z, n)dr$$

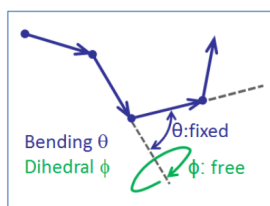
$$P(r, n) = 4\pi r^2 \left(\frac{3}{2\pi n \ell^2} \right)^{3/2} \exp \left[-\frac{3}{2} \frac{r^2}{n \ell^2} \right] \quad (7.1.6)$$

The units of $P(r, n)$ are inverse length. For the freely jointed chain, we see that $\beta^{-1} = \sqrt{2\langle R^2 \rangle / 3}$ is the most probable end-to-end distance.



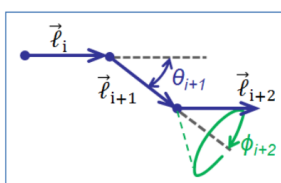
Freely Rotating Chain

An extension to the freely jointed chain that adds a single configurational constraint that better resembles real bonding in polymers is the freely rotating chain. In this case, the backbone angle θ has a fixed value, and the dihedral angle ϕ can rotate freely.



To describe the chain dimensions, we need to evaluate the angular bond correlations between segments. Focusing first on adjacent segments, we know that after averaging over all ϕ , the fixed θ assures that $\langle \vec{\ell}_i \cdot \vec{\ell}_{i+1} \rangle = \ell^2 \cos \theta$. For the next segment in the series, only the component parallel to $\vec{\ell}_{j+1}$ will contribute to sequential bond correlations as we average over ϕ_{i+2} :

$$\begin{aligned} \langle \vec{\ell}_i \cdot \vec{\ell}_{i+2} \rangle &= \langle \cos(\theta_i) \cos(\theta_{i+1}) - \sin(\theta_i) \sin(\theta_{i+1}) \cos(\phi_{i+1}) \rangle \\ &= \ell^2 \cos^2 \theta \end{aligned}$$



Extending this reasoning leads to the observation

$$\langle \vec{\ell}_i \cdot \vec{\ell}_j \rangle = \ell^2 (\cos \theta)^{j-i}$$

To evaluate the bond correlations in this expression, it is helpful to define an index for the separation between two bond vectors:

$$k = j - i$$

and

$$\alpha = \cos \theta$$

Then the segment orientation correlation function is

$$g(k) = \langle \vec{\ell}_i \cdot \vec{\ell}_j \rangle = \ell^2 \alpha^k$$

For a separation k on a chain of length n , there are $n - k$ possible combinations of bond angles,

$$\sum_{j \neq i} \langle (\cos \theta)^{j-i} \rangle = \sum_{k=1}^{n-1} (n-k) \alpha^k$$

$$\therefore \langle R^2 \rangle = n\ell^2 + \ell^2 \sum_{k=1}^{n-1} (n-k) \alpha^k$$

From this you can obtain

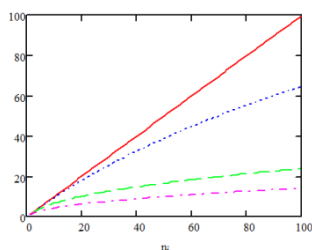
$$\langle R^2 \rangle = n\ell^2 \left(\frac{1+\alpha}{1-\alpha} - \frac{2\alpha(1-\alpha^n)}{n(1-\alpha)^2} \right)$$

In the limit of long chains ($n \rightarrow \infty$), we find

$$\langle R^2 \rangle \rightarrow n\ell^2 \left(\frac{1+\alpha}{1-\alpha} \right)$$

and

$$R_G = \sqrt{\frac{n\ell^2}{6} \left(\frac{1+\alpha}{1-\alpha} \right)}$$



$$\theta = \begin{pmatrix} 1 \\ 15 \\ 45 \\ 70.5 \end{pmatrix}$$

RMS end-to-end distance $\langle R^2 \rangle^{1/2}$ in units of ℓ as a function of n and θ

Restricted dihedrals

When the freely rotating chain is also amended to restrict the dihedral angle ϕ , we can solve the mean square end-to-end distance in the limit $n \rightarrow \infty$. Given an average dihedral angle,

$$\beta = \langle \cos \phi \rangle$$

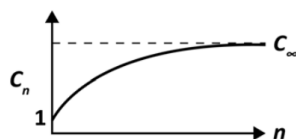
$$\langle R^2 \rangle = n\ell^2 \left(\frac{1+\alpha}{1-\alpha} \right) \left(\frac{1+\beta}{1-\beta} \right)$$

Nonideal Behavior

Flory characteristic ratio

Real polymers are stiff and have excluded volume, but the $R \sim \sqrt{n}$ scaling behavior usually holds at large n ($R \gg \ell_p$). To characterize non-ideality, we use the [Flory characteristic ratio](#):

$$C_n = \frac{\langle R^2 \rangle}{n\ell^2}$$



For freely jointed chains $C_n = 1$. For nonideal chains with angular correlations, $C_n > 1$. C_n depends on the chain length n , but should have an asymptotic value for large n : C_∞ . For example, if we examine long freely rotating chains

$$C_\infty = \lim_{n \rightarrow \infty} \frac{\langle R^2 \rangle}{n\ell^2} = \frac{1 + \alpha}{1 - \alpha} \quad \alpha = \cos \theta$$

(In practice, this limit typically holds for $n > 30$). Consider a tetrahedrally bonded polymer with full angle 109° ($\theta = 54^\circ$). then $\cos \theta = 1/3$, and $C_n = 2$. In practice, we reach the long chain limit C_∞ at $n \approx 10$. This relation works well for polyglycine and polyethylene glycol (PEG).

Statistical segment or Kuhn length

How stiff or flexible a polymer is depends on the length scale of observation. What is stiff on one scale is flexible for another. For an infinitely long polymer, one can always find a length scale for which its statistics are that of a Gaussian random coil. As a result for a segment polymer, one can imagine rescale continuous segments into one longer "effective segment" that may not represent atomic dimensions, but rather is defined in order to correspond to a random walk polymer, with $C_n = 1$. Then, the effective length of the segment is ℓ_e (also known as the Kuhn length) and the number of effective segments is n_e . Then the freely jointed chain equations apply:

$$L_C = n_e \ell_e$$

$$\langle R^2 \rangle = n_e \ell_e^2$$

From these equations, $\ell_e = \langle R^2 \rangle / L_C$. We see that $\ell_e \gg \ell$ applies to stiff chains, whereas $\ell_e \approx \ell$ are flexible.

We can also write the contour length as $L_C = \gamma n \ell$, where γ is a geometric factor < 1 that describes constraint on bond angles. For a freely rotating chain: $\gamma = \cos(\theta/2)$. Using the long chain chain expressions ($n \rightarrow \infty$): $\langle R^2 \rangle = C_\infty n \ell^2$, we find

$$\ell_e = \left(\frac{C_\infty}{\gamma} \right) \ell$$

$$n_e = \left(\frac{\gamma^2}{C_\infty} \right) n$$

$$\ell_p = \left(\frac{C_\infty + 1}{2} \right) \ell$$

Representative values for polymer segment models

	C_∞	(n_e/n)	ℓ (nm)	ℓ_e (nm)	γ	ℓ_p (nm)
Polyethylene	6.7	($n > 10$)	0.154	1.24	0.83	
PEG	3.8			0.34		
Polyalanine	9	($n > 70$)	0.38	3.6	0.95	0.5
Polyproline	90	($n > 700$)				5-10
dsDNA	86		0.35	30-100	1	50
ssDNA						1.5
Cellulose						6.2
Actin				16700		10000-20000

1. C. R. Cantor and P. R. Schimmel, *Biophysical Chemistry Part III: The Behavior of Biological Macromolecules*. (W. H. Freeman, San Francisco, 1980), Ch. 18.; K. Dill and S. Bromberg, *Molecular Driving Forces: Statistical Thermodynamics in Biology, Chemistry, Physics, and Nanoscience*. (Taylor & Francis Group, New York, 2010); P. J. Flory, *Principles of Polymer Chemistry*. (Cornell University Press, Ithaca, 1953).
2. C. R. Cantor and P. R. Schimmel, *Biophysical Chemistry Part III: The Behavior of Biological Macromolecules*. (W. H. Freeman, San Francisco, 1980), Ch. 19 p. 1033.

This page titled [7.1: Segment Models](#) is shared under a [CC BY-NC-SA 4.0](#) license and was authored, remixed, and/or curated by [Andrei Tokmakoff](#) via [source content](#) that was edited to the style and standards of the LibreTexts platform.

7.2: Excluded Volume Effects

Excluded Volume Effects

In real polymers, the chance of colliding with another part of the chain increases with chain length.

$$\langle R^2 \rangle = n\ell^2 + \sum_{i \neq j} \langle \vec{\ell}_i \cdot \vec{\ell}_j \rangle$$

$$\langle \vec{\ell}_i \cdot \vec{\ell}_j \rangle = g(s) = \langle \vec{\ell}_i \cdot \vec{\ell}_{i+s} \rangle \quad s = |i - j|$$

$g(s)$ gives the orientational correlations between polymer segments.

Flory, statistical mechanics of chain molecules

- If correlations are purely based on bond angles and rotational potential, then $g(s)$ decays exponentially with s . There is no excluded volume.
- With excluded volume, $g(s)$ does not vanish for large k . There are "long-range" interactions within the chain.
 - "Long range" means along long distance along contour, but short range in space.
- Excluded volume depends on chain + solvent and temperature.

Virial expansion

At low densities, thermodynamic functions can be expanded in a power series in the number of particles per unit volume: $n = N/V$ (density).

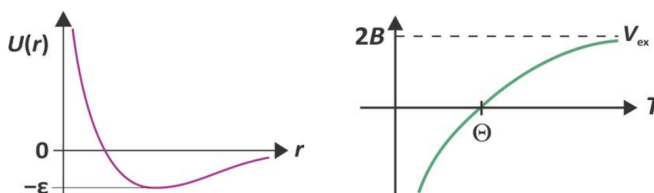
$$\begin{aligned} F &= F^0 + F_{\text{int}} \\ F_{\text{int}} &= N_p k_B T (nB + n^2 C + \dots) \end{aligned}$$

- F^0 refers to ideal chain
- N_p is # of polymer molecules
- B : units of volume

Excluded volume (repulsion) and attractive interactions are related to the second virial coefficient B . The excluded volume (or volume correlation relative to ideal behavior) for interacting beads of a polymer chain is calculated from

$$V_{\text{ex}} = \int d^3r (1 - \exp[-U(r)/k_B T])$$

$U(r)$ is the interaction potential. In the high temperature limit $V_{\text{ex}} = 2B$. So $2B$ can be associated with the excluded volume associated with one segment (bead) of the chain.



Temperature dependence

- At high T ($k_B T \gg \varepsilon$)
The attractive part of potential is negligible, and repulsions result in excluded volume. In this limit $2B \approx V_{\text{ex}}$.
- As $T \rightarrow 0$, the attractive part of potential matters more and more, resulting in collapse relative to ideal chain.
- Cross over: Theta point $T = \Theta$

$$\text{Near } \Theta \quad 2B \sim V_{\text{ex}} \left(\frac{T - \Theta}{\Theta} \right)$$

$T > \Theta$ High T . Repulsion dominates. Polymer swells (good solvent)

$T < \Theta$ Low T . Attractions dominate. Polymer collapses (globule, poor solvent)

Polymer swelling

At high temperatures ($T \gg \Theta$), the free energy of a coil can be expressed in terms interaction potential, which is dominated by repulsions that expand the chain, and the entropic elasticity that opposes it (see next chapter).

$$F = U - TS = nk_BTB \frac{3n}{4\pi R^3} + k_BT \frac{3R^2}{2n\ell^2} + \text{const.}$$

By minimizing F with respect to the end-to-end distance, R , and solving for R , we can find how the R scales with polymer size:

$$R \propto (B\ell^2)^{3/5} n^{3/5}$$

We see that the end-to-end distance of the chain with excluded volume scales with monomer number (n) with a slightly larger exponent than an ideal chain: $n^{3/5}$ rather than $n^{1/2}$. Generally, the relationship between R and n is expressed in terms of the Flory exponent, ν , which is related to several physical properties of polymer chains:

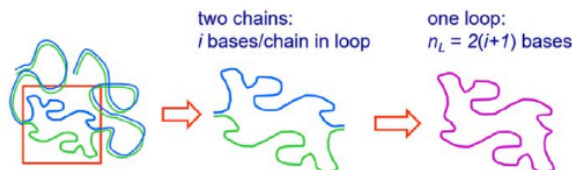
$$R \propto n^\nu$$

This page titled [7.2: Excluded Volume Effects](#) is shared under a [CC BY-NC-SA 4.0](#) license and was authored, remixed, and/or curated by [Andrei Tokmakoff](#) via [source content](#) that was edited to the style and standards of the LibreTexts platform.

7.3: Polymer Loops

For certain problems, we are concerned with cyclic polymers chains:

- Bubbles/loops in DNA melting
- Polypeptide and RNA hairpins
- DNA strand separation in transcription
- Cyclic DNA, chromosomal looping, and supercoiling



In describing macromolecules in closed loop form, the primary new variable that we need to address is the loop's configurational entropy. Because of configurational constraints that tie the ends of a loop together ($R_{ee} \rightarrow 0$) the loop has lower configurational entropy than an unrestrained coil.

Let's describe how the configurational entropy of a loop S_L depends on the size of the loop. We will consider the segment model with n_L segments in the loop. We start with the radial probability distribution for an unconstrained random coil, which is the reference state for our calculations:

$$P(r, n) = 4\pi r^2 \left(\frac{3}{2\pi n \ell^2} \right)^{3/2} \exp \left[-\frac{3}{2} \frac{r^2}{n \ell^2} \right] \quad (7.3.1)$$

The entropy of the loop S_L will reflect the constraints placed by holding the ends of the random coil together, which we describe by saying the ends of the chain must lie within a small distance Δr of each other. Since $R_{ee} < \Delta r$, $\Delta r^2 \ll n \ell^2$, and the exponential term in eq. (7.3.1) is ~ 1 . Then the probability of finding a random coil configuration with an end-to-end distance within a radius Δr is

$$\begin{aligned} P_L(n_L) &\approx \int_0^{\Delta r} dr 4\pi r^2 \left(\frac{3}{2\pi n_L \ell^2} \right)^{3/2} \\ &= \left(\frac{6}{\pi} \right)^{1/2} \left(\frac{\Delta r}{\ell} \right)^3 n_L^{-3/2} \\ &\equiv b n_L^{-3/2} \end{aligned}$$

In the last line we find that the probability of finding a looped chain decreases as $P_L \propto n_L^{-3/2}$, where b is the proportionality constant that emerges from integration. From the assumptions we made, $b \ll 1$, and $P_L < 1$.

To calculate the configurational entropy of the chain, we assume that the polymer (free or looped) can be quantified by Ω configurational states per segment of the chain. This reflects the fact that our segment model coarse-grains over many internal degrees of freedom of the macromolecule. Then, the entropy of a random coil of n segments is $S_C = k_B \ln \Omega^n$. To calculate the loop entropy, we correct the unrestrained chain entropy to reflect the constraints placed by holding the ends of the random coil together in the loop.

$$S_L = S_C + k_B \ln P_L$$

This expression reflects the fact that the number of configurations available to the constrained chain is taken to be $\Omega_L(n_L) = \Omega^{n_L} P_L(n_L)$, and each of these configurations are assumed to be equally probable ($S_L = k_B \ln \Omega_L$). Since $P_L < 1$, the second term is negative, lowering the loop entropy relative to the coil. We find that we can express the loop configurational entropy as

$$S_L(n_L) = k_B \left[n_L \ln \Omega - b - \frac{3}{2} \ln n_L \right]$$

Since this expression derives from the random coil, it does not account for excluded volume of the chain. However, regardless of the model used to obtain the loop entropy, we find that we can express it in the same form:

$$S_L(n_L) = k_B [n_L a - b + c \ln n_L]$$

where a , b , and c are constants. For the random coil $c = 1.50$, and for a self-avoiding random walk on a cubic lattice we find that it increases to $c = 1.77$. In 2D, a random coil results in $c = 1.0$, and a SAW gives $c = 1.44$.

Readings

1. M. Rubinstein and R. H. Colby, *Polymer Physics*. (Oxford University Press, New York, 2003).
2. K. Dill and S. Bromberg, *Molecular Driving Forces: Statistical Thermodynamics in Biology, Chemistry, Physics, and Nanoscience*. (Taylor & Francis Group, New York, 2010).
3. C. R. Cantor and P. R. Schimmel, *Biophysical Chemistry Part III: The Behavior of Biological Macromolecules*. (W. H. Freeman, San Francisco, 1980).
4. R. Phillips, J. Kondev, J. Theriot and H. Garcia, *Physical Biology of the Cell*, 2nd ed. (Taylor & Francis Group, New York, 2012).
5. P. J. Flory, *Principles of Polymer Chemistry*. (Cornell University Press, Ithaca, 1953).

This page titled [7.3: Polymer Loops](#) is shared under a [CC BY-NC-SA 4.0](#) license and was authored, remixed, and/or curated by [Andrei Tokmakoff](#) via [source content](#) that was edited to the style and standards of the LibreTexts platform.

CHAPTER OVERVIEW

8: Polymer Lattice Models

Polymer lattice models refer to models that represent chain configurations through the placement of a chain of connected beads onto a lattice. These models are particularly useful for describing the configurational entropy of a polymer and excluded volume effects. However, one can also explicitly enumerate how energetic interactions between beads influences the probability of observing a particular configuration. At a higher level, models can be used to describe protein folding and DNA hybridization.

[8.1: Entropy of Single Polymer Chain](#)

[8.2: Self-Avoiding Walks](#)

[8.3: Conformational Changes with Temperature](#)

[8.4: Flory–Huggins Model of Polymer Solutions](#)

[8.5: Polymer–Solvent Interactions](#)

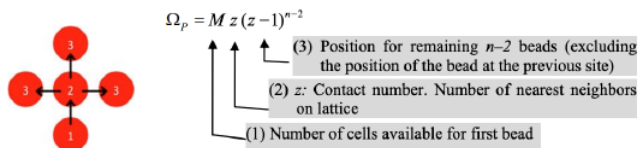
1. K. Dill and S. Bromberg, *Molecular Driving Forces: Statistical Thermodynamics in Biology, Chemistry, Physics, and Nanoscience*. (Taylor & Francis Group, New York, 2010); S. F. Sun, *Physical Chemistry of Macromolecules: Basic Principles and Issues, Array ed.* (J. Wiley, Hoboken, N.J., 2004), Ch. 4.

This page titled [8: Polymer Lattice Models](#) is shared under a [CC BY-NC-SA 4.0](#) license and was authored, remixed, and/or curated by [Andrei Tokmakoff](#) via [source content](#) that was edited to the style and standards of the LibreTexts platform.

8.1: Entropy of Single Polymer Chain

Entropy of Single Polymer Chain

Calculate the number of ways of placing a single homopolymer chain with n beads on lattice. Place beads by describing the number of ways of adding a bead to the end of a growing chain:



A random walk would correspond to the case where we allow the chain to walk back on itself. Then the expression is $\Omega_P = M z^{n-1}$

Note the mapping of terms in $\Omega_P = M z (z-1)^{n-2}$ onto $\Omega_P = \Omega_{trans} \Omega_{rot} \Omega_{conf}$.

$$\text{For } n \rightarrow \infty \quad M \gg N \quad \Omega_P \approx M (z-1)^{n-1}$$

$$\begin{aligned} S_p &= k_B \ln \Omega_P \\ &= k_B ((n-1) \ln(z-1) + \ln M) \end{aligned}$$

This expression assumes a dilute polymer solution, in which we neglect excluded volume, except for the preceding segment in the continuous chain.

This page titled [8.1: Entropy of Single Polymer Chain](#) is shared under a [CC BY-NC-SA 4.0](#) license and was authored, remixed, and/or curated by [Andrei Tokmakoff](#) via [source content](#) that was edited to the style and standards of the LibreTexts platform.

8.2: Self-Avoiding Walks

To account for excluded volumes, one can enumerate polymer configurations in which no two beads occupy the same site. Such configurations are called **self-avoiding walks** (SAWs). Theoretically it is predicted that the number of configurations for a random walk on a cubic lattice should scale with the number of beads as $\Omega_p(n) \propto z^n n^{\gamma-1}$, where γ is a constant which is equal to 1 for a random walk. By explicitly evaluating self-avoiding walks (SAWs) on a cubic lattice it can be shown that

$$\Omega_p(n) = 0.2\alpha^n n^{\gamma-1}$$

where $\alpha = 4.68$ and $\gamma = 1.16$, and the chain entropy is

$$S_p(n) = k_B [n \ln \alpha + (\gamma - 1) \ln n - 1.6].$$

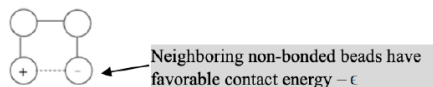
Comparing this expression with our first result $\Omega_P = Mz(z-1)^{n-2}$ we note that in the limit of a random walk on a cubic lattice, $\alpha=z=6$, when we exclude only the back step for placing the next bead atop the preceding one $\alpha = (z-1) = 5$, and the numerically determined value is $\alpha = 4.68$.

2. C. Vanderzande, Lattice Models of Polymers (Cambridge University Press, Cambridge, UK, 1998).

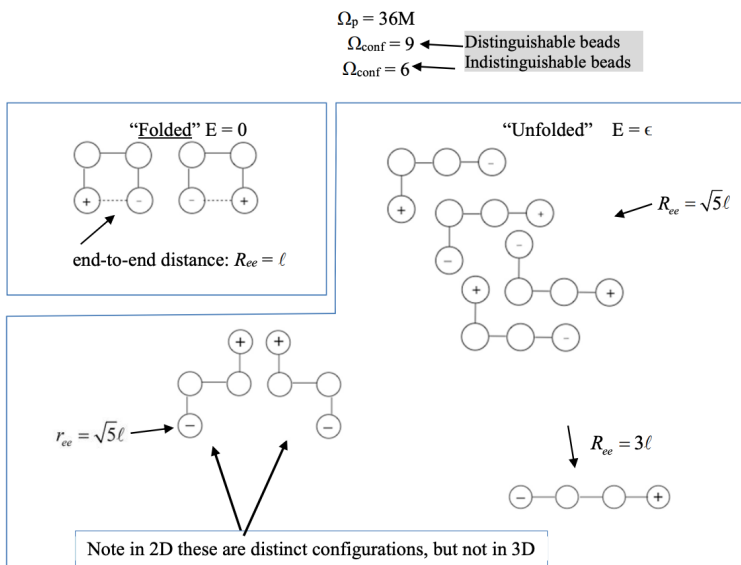
This page titled [8.2: Self-Avoiding Walks](#) is shared under a [CC BY-NC-SA 4.0](#) license and was authored, remixed, and/or curated by [Andrei Tokmakoff](#) via [source content](#) that was edited to the style and standards of the LibreTexts platform.

8.3: Conformational Changes with Temperature

Four bead polymer on a two-dimensional lattice

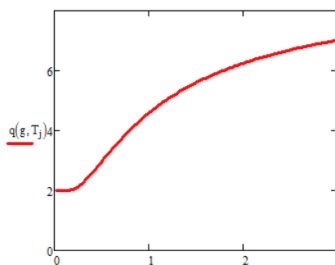


Place polymer on lattice $z = 4$ $n = 4$ in 2D (with distinguishable end beads):



Configurational Partition Function

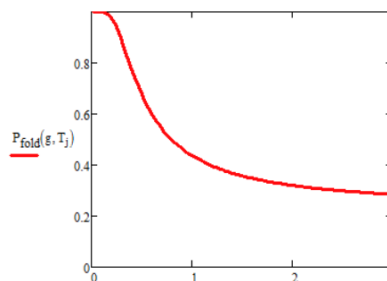
Number of thermally accessible microstates.



$$\begin{aligned}
 Q &= (q_{conf})^N \\
 q_{conf} &= \underbrace{\sum_{i \text{ states}=1}^9 e^{-E_i/kT}}_{\text{sum over microstates}} \\
 &= \underbrace{\sum_{j \text{ levels}=1}^2 g_j e^{-E_j/kT}}_{\text{sum over energy levels}} \\
 &= 2 + 7e^{-\epsilon/kT}
 \end{aligned}$$

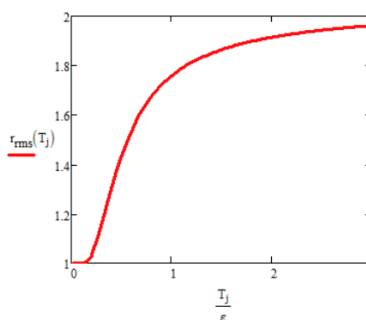
Probability of Being "Folded"

Fraction of molecules in the folded state



$$P_{fold} = \frac{g_{fold}e^{-E_{fold}/kT}}{q_{conf}} = \frac{2}{2 + 7e^{-\epsilon/kT}}$$

Mean End-to-End Distance



$$\begin{aligned} \langle r_{ee} \rangle &= \frac{\sum_{i=1}^9 r_i e^{-E_i/kT}}{q_{conf}} \\ &= \frac{(1)(2) + (\sqrt{5})6e^{-\epsilon/kT} + 3e^{-\epsilon/kT}}{q_{conf}} \\ &= \frac{2 + (6\sqrt{5} + 3)e^{-\epsilon/kT}}{q_{conf}} \end{aligned}$$

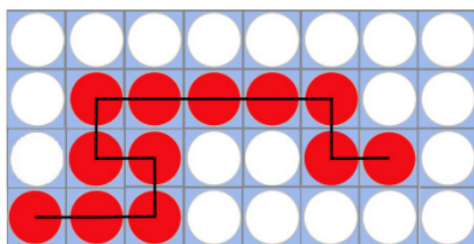
Also, we can access other thermodynamic quantities:

$$F = -k_B T \ln Q \quad U = \langle E \rangle = k_B T^2 \left(\frac{\partial \ln Q}{\partial T} \right)_{V,N}$$

$$S = - \left(\frac{\partial F}{\partial T} \right)_{V,N} = k_B \ln Q + k_B T \left(\frac{\partial \ln Q}{\partial T} \right)_{V,N}$$

This page titled [8.3: Conformational Changes with Temperature](#) is shared under a [CC BY-NC-SA 4.0](#) license and was authored, remixed, and/or curated by [Andrei Tokmakoff](#) via [source content](#) that was edited to the style and standards of the LibreTexts platform.

8.4: Flory–Huggins Model of Polymer Solutions



Let's begin by defining the variables for the lattice:

- M : total number of lattice cells
- N_P : number of polymer molecules
- n : number of beads per polymer
- N_S : number of solvent cells
- nN_P = total number of polymer beads

The total number of lattice sites is then composed of the fraction of sites occupied by polymer beads and the remaining sites, which we consider occupied by solvent:

$$M = nN_P + N_S$$

Volume fractions of solvent and polymer:

$$\phi_S = \frac{N_S}{M} \quad \phi_P = \frac{nN_P}{M} \quad \phi_S + \phi_P = 1$$

The mole fraction of polymer:

$$x_P = \frac{N_P}{N_S + N_P}$$

x_P is small even if the volume fraction is high.

Excluded Volume for Single Polymer Chain

Generally, excluded volume is difficult to account for if you don't want to elaborate configurations explicitly, as in self-avoiding walks. However, there is a mean field approach we can use to account for excluded volume.

A better estimate for chain configurations that partially accounts for excluded volume:

$$\Omega_p = M \left[z \left(\frac{M-1}{M} \right) \right] \left[(z-1) \left(\frac{M-2}{M} \right) \right] \dots \left[(z-1) \left(\frac{M-n+1}{M} \right) \right]$$

↑ 1st bead
↑ 3rd bead
↑ nth bead

Second bead on reduced lattice space counting only fraction of empty cells

Large n :

$$\Omega_P \approx \frac{(z-1)^{n-1}}{M} \frac{M!}{(M-n)!}$$

Entropy of Multiple Polymer Chains

For N_P chains, we count growth of chains by adding beads one at a time to all growing chains simultaneously.

1) First bead. The number of ways for placing the 1st bead for all chains:

$$v^{(1)} = M(M-1)(M-2)\dots(M-(N_P-1)) = \frac{M!}{(M-N_P)!}$$

\uparrow \uparrow \uparrow
 1st bead 1st bead 1st bead
 1st chain 2nd chain N_P th chain

2) Place the second bead on all chains. We assume the solution is dilute and neglect collisions between chains.

$$v^{(2)} = \left[z \left(\frac{M-N_P}{M} \right) \right] \left[z \left(\frac{M-N_P-1}{M} \right) \right] \dots \left[z \left(\frac{M-2N_P+1}{M} \right) \right]$$

\uparrow
 Ways of placing 2nd bead on 1st chain with a volume reduced by the number of beads present from the 1st beads. Volume fraction excluded: $(M-N_P)/M$

$$= \frac{(z)^{N_P} (M-N_P)!}{M (M-2N_P)!}$$

3) For placing the n^{th} bead on N_P growing chains. Here we neglect collisions between site i and sites $> (i+4)$, which is the smallest separation that one can clash on a cubic lattice.

$$V^{(n)} = \left(\frac{z-1}{M} \right)^{N_P(N-1)} \frac{(M-N_P)!}{(M-n \cdot N_P)!}$$

4) Total number of configurations of N_P chains with n beads:

$$\Omega_P = \frac{v^{(1)} v^{(n)}}{N_P!} \leftarrow \text{indistinguishability of polymer chains}$$

$$\Omega_P = \left(\frac{z-1}{M} \right)^{N_P(n-1)} \frac{M!}{(M-nN_P)! N_P!}$$

\uparrow
 $N_S!$

Entropy of Polymer Solution

Entropy of polymer/solvent mixture:

$$S_{\text{mix}} = k_B \ln \Omega_P$$

Calculate entropy of mixing:

$$\Delta S_{\text{mix}} = S_{\text{mix}} - S_{\text{solvent}}^0 - S_{\text{polymer}}^0$$

\uparrow \uparrow
 pure solvent pure polymer

$$S_{\text{solvent}}^0 = 0 \text{ since } \Omega_{\text{solvent}} = 1$$

The pure polymer has many possible entangled configurations Ω_P^0 , and therefore a lot of configurational entropy: S_{polymer}^0 . But we can calculate Ω_P^0 just by using the formula for Ω_P with the number of cells set to the number of polymer beads $M = nN_P$.

$$\Omega_P^0 = \left(\frac{z-1}{N_P \cdot n} \right)^{N_P(n-1)} \frac{(N_P \cdot n)!}{N_P!}$$

$$\frac{\Omega_P}{\Omega_P^0} = \left(\frac{N_P \cdot n}{M} \right)^{N_P(n-1)} \frac{M!}{N_S! (N_P \cdot n)!} \quad (8.4.1)$$

Since $\Delta S_{\text{mix}} = k_B \ln \frac{\Omega_P}{\Omega_P^0}$

$$\begin{aligned} \Delta S_{\text{mix}} &= -k_B N_S \ln \left(\frac{N_S}{M} \right) - k_B N_P \ln \left(\frac{N_P \cdot n}{M} \right) \\ &= -M k_B \left(\phi_S \ln \phi_S + \frac{\phi_P}{n} \ln \phi_P \right) \end{aligned}$$

where the volume fractions are:

$$\phi_S = \frac{N_S}{M} \quad \phi_P = \frac{nN_P}{M} = 1 - \phi_S$$

Note for $n = 1$, we have original lattice model of fluid.

This page titled [8.4: Flory–Huggins Model of Polymer Solutions](#) is shared under a [CC BY-NC-SA 4.0](#) license and was authored, remixed, and/or curated by [Andrei Tokmakoff](#) via [source content](#) that was edited to the style and standards of the LibreTexts platform.

8.5: Polymer–Solvent Interactions

- Use same strategy as lattice model of a fluid.
- Considering polymer (P) and solvent (S) cells:

$$U = m_{SS}\omega_{SS} + m_{PP}\omega_{PP} + m_{SP}\omega_{SP}$$

ω_{ij} = interaction energy between cells i and j
 m_{ij} = Number of contacts between i and j cells

- Number of solvent cell contacts:

$$zN_S = 2m_{SS} + m_{SP}$$

- Number of polymer cell contacts:

$$\approx (z-2) \cdot N_p \cdot n \approx z \cdot N_p n = 2m_{PP} + m_{SP}$$

\uparrow each bead connects to 2 other beads

- Mean field approximation: Substitute the average number of solvent/polymer contacts.

$$m_{SP} \approx \frac{zN_S N_p \cdot n}{M} = \langle m_{SP} \rangle$$

$$U_{\text{mix}} = k_B T \left\{ \frac{z\omega_{SS}}{2k_B T} N_S + \frac{z\omega_{PP}}{2k_B T} N_p n + \chi_{SP} \frac{N_S N_p}{M} n \right\}$$

$$\chi_{SP} = \frac{z}{k_B T} \left(\omega_{SP} - \frac{\omega_{SS} + \omega_{PP}}{2} \right) \text{ solvent-polymer bead exchange parameter}$$

$$\vdots$$

$$F_{\text{mix}} = N_S k_B T \ln \phi_S + N_p k_B T \ln \phi_P + \frac{z}{2} (\omega_{SS} N_S + \omega_{PP} N_p) + \chi_{SP} \frac{N_S N_p n}{M}$$

- Polymers expand in good solvents, collapse in bad solvents, retain Gaussian random coil behavior in neutral solvents (θ solvents).

Good solvents	$\chi < 0.5$	$\sqrt{\langle r^2 \rangle} \sim N^{3/5} \sim R_0 N^{3/5}$
Bad solvents (collapse)	$\chi > 0.5$	$R \sim R_0 N^{1/3}$
Theta solvents	$\chi = 0.5$	$\sqrt{\langle r^2 \rangle} \sim \frac{2N\ell^2}{3} = R_0$

This page titled [8.5: Polymer–Solvent Interactions](#) is shared under a [CC BY-NC-SA 4.0](#) license and was authored, remixed, and/or curated by [Andrei Tokmakoff](#) via [source content](#) that was edited to the style and standards of the LibreTexts platform.

CHAPTER OVERVIEW

9: Macromolecular Mechanics

An alternative approach to describing macromolecular conformation that applied both to equilibrium and non-equilibrium phenomena uses a mechanical description of the forces acting on the chain. Of course, forces are present everywhere in biology. Near equilibrium these exist as local fluctuating forces that induce thermally driven excursions from the free-energy minimum, and biological systems use non-equilibrium force generating processes derived from external energy sources (such as ATP) in numerous processes such as those in transport and signaling. For instance, the directed motion of molecular motors along actin and microtubules, or the allosteric transmembrane communication of a ligand binding event in GPCRs.

Our focus in this section is on how externally applied forces influence macromolecular conformation, and the experiments that allow careful application and measurement of forces on single macromolecules. These are being performed to understand mechanical properties and stress/strain relationships. They can also be unique reporters of biological function involving the strained molecules.

Single Molecule Force Application Experiments

	Force Range (pN)	Displacement (nm)	Loading Rate (pN/sec)	
Optical Tweezers:	0.1-100 pN	0.1-10 ⁵	5-10	Near Equilibrium
AFM:	10-10 ⁴	0.5-10 ⁴	100-1000	Non-equilibrium!
Stretching under flow:	0.1-1000 pN	10-10 ⁵	1-100	Steady state force
MD simulations:	Arb.	<10 nm	10 ⁵ -10 ⁷ !	

Remember $k_B T$: 4.1 pN nm

[9.1: Force and Work](#)

[9.2: Worm-like Chain](#)

[9.3: Polymer Elasticity and Force–Extension Behavior](#)

This page titled [9: Macromolecular Mechanics](#) is shared under a [CC BY-NC-SA 4.0](#) license and was authored, remixed, and/or curated by [Andrei Tokmakoff](#) via [source content](#) that was edited to the style and standards of the LibreTexts platform.

9.1: Force and Work

Here we will focus on the stretching and extension behavior of macromolecules. The work done on the system by an external force to extend a chain is

$$w = - \int \vec{f}_{ext} \cdot d\vec{x}$$

Work (w) is a scalar, while force (\vec{f}) and displacement (\vec{x}) are vectors. On extension, the external force is negative, leading to a positive value of w , meaning work was done on the system. Classical mechanics tells us that the force is the negative gradient of the potential one is stretching against ($\vec{f} = -\partial U/\partial x$), but we will have to work with free energy and the potential of mean force since the configurational entropy of the chain is important. Since the change in free energy for a process is related to the reversible work needed for that process, we can relate the force along a reversible path to the free energy through

$$\vec{f}_{rev} = - \left(\frac{\partial G}{\partial x} \right)_{p,T,N}$$

This describes the reversible process under which the system always remains at equilibrium, although certainly it is uncomfortable relating equilibrium properties (G) to nonequilibrium ones such as pulling a protein apart. For an arbitrary process, $\Delta G \leq w$.

Jarzynski Equality

A formal relationship between the free energy difference between two states and the work required to move the system from initial to final state has been proposed. The Jarzynski equality states

$$e^{-\Delta G/kT} = \langle e^{w/k_B T_{in}} \rangle_{path}$$

Here one averages the Boltzmann-weighted work in the quantity at right over all possible paths connecting the initial and final states, setting T to the initial temperature (T_{in}), and one obtains the Boltzmann weighted exponential in the free energy. This holds for irreversible processes! Further, since one can show that $\langle e^{-w/k_B T} \rangle \geq e^{-(w)/k_B T}$, we see that the average work done to move the system between two states is related to the free energy through $\langle w \rangle \geq \Delta G$. This reinforces what we know about the macroscopic nature of thermodynamics, but puts an interesting twist on it: Although the average work done to change the system will equal or exceed the free energy difference, for any one microscopic trajectory, the work may be less than the free energy difference. This has been verified by single molecule force/extension experiments.

Statistical Mechanics of Work

Let's relate work and the action of a force to changes in statistical thermodynamic variables.¹ The internal energy is

$$U = \langle E \rangle = \sum_j P_j E_j$$

and therefore, the change in energy in a thermodynamic process is

$$dU = d\langle E \rangle = \sum_j E_j dP_j + \sum_j P_j dE_j$$

Note the close relationship between this expression and the First Law:

$$dU = \delta w + \delta q$$

We can draw parallels between the two terms in these expressions:

$$\begin{aligned} \delta q_{rev} = T dS & \longleftrightarrow \sum_j E_j dP_j \\ \delta w \cong p dV \text{ or } f dx & \longleftrightarrow \sum_j P_j dE_j \end{aligned}$$

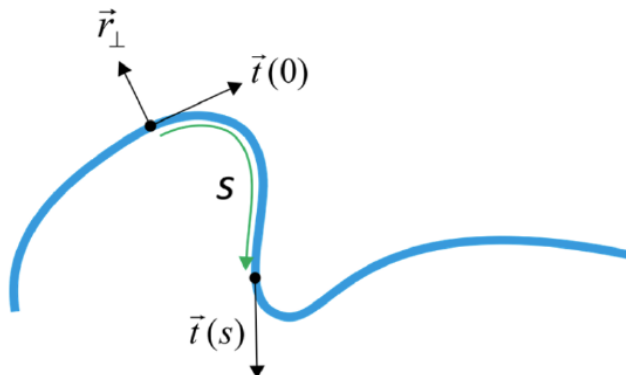
Heat is related to the ability to change populations of energetically different states, whereas work is related to the ability to change the energy levels with an external force.

1. T. L. Hill, An Introduction to Statistical Thermodynamics. (Addison-Wesley, Reading, MA, 1960), pp. 11–13, 66–77.

This page titled [9.1: Force and Work](#) is shared under a [CC BY-NC-SA 4.0](#) license and was authored, remixed, and/or curated by [Andrei Tokmakoff](#) via [source content](#) that was edited to the style and standards of the LibreTexts platform.

9.2: Worm-like Chain

The **worm-like chain** (WLC) is perhaps the most commonly encountered models of a polymer chain when describing the mechanics and the thermodynamics of macromolecules. This model describes the behavior of a thin flexible rod, and is particularly useful for describing stiff chains with weak curvature, such as double stranded DNA. Its behavior is only dependent on two parameters that describe the rod: κ_b its **bending stiffness**, and L_C , the **contour length**.



Let's define the variables in this WLC model:

- s The distance separating two points along the contour of the rod
- \vec{r}_\perp Normal unit vector
- $\vec{t} = \frac{\partial \vec{r}_\perp}{\partial s}$ Tangent vector
- $\frac{\partial \vec{t}}{\partial s}$ Curvature of chain
- $= \frac{1}{R}$ is inverse of local radius of curvature

The worm-like chain is characterized by:

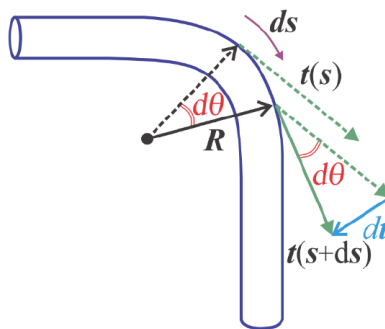
- **Persistence length**, which is defined in terms of tangent vector correlation function:

$$g(s) = \langle \vec{t}(0) \cdot \vec{t}(s) \rangle = \exp[-|s|/\ell_p] \quad (9.2.1)$$

- **Bending energy**: The energy it takes to bend the tangent vectors of a segment of length s can be expressed as

$$U_b = \frac{1}{2} \kappa_b \int_0^L ds \left(\frac{\partial \vec{t}}{\partial s} \right)^2 \quad (9.2.2)$$

Bending Energy



Let's evaluate the bending energy of the WLC, making some simplifying assumptions, useful for fairly rigid rods. If we consider short distances over which the curvature is small, then $\theta \approx s/R$ and

$$\frac{\partial \vec{t}}{\partial s} \approx \frac{d\theta}{ds} = \frac{1}{R} \quad (9.2.3)$$

Then we can express the bending energy in terms of an angle:

$$U_b \approx \frac{1}{2s} \kappa_b \theta^2 \quad (9.2.4)$$

Note the similarity of this expression to the energy needed to displace a particle bound in a harmonic potential with force constant k : $U = \frac{1}{2}kx^2$. The bending energy can be used to obtain thermodynamic averages. For instance, we can calculate the variance for the tangent vector angles as a function of s (spherical coordinates):

$$\langle \theta^2(s) \rangle = \frac{1}{Q_{bend}} \int_0^{2\pi} d\phi \int_0^\pi d\theta \sin\theta \theta^2 e^{-U_b(\theta)/k_B T} \quad (9.2.5)$$

$$= \frac{2s k_B T}{\kappa_b} \quad (9.2.6)$$

Here we have used $\sin\theta \approx \theta$. The partition function for the bending of the rod is:

$$Q_{bend} = \int_0^{2\pi} d\phi \int_0^\pi d\theta \sin\theta e^{-U_b(\theta)/k_B T}$$

Persistence Length

To describe the persistence length of the WLC, we recognize that Equation 9.2.1 can be written as $g(s) = \langle \cos\theta(s) \rangle$ and expand this for small θ :

$$\begin{aligned} g(s) &= \langle \cos\theta(s) \rangle \\ &= \left\langle 1 - \frac{\theta^2(s)}{2} + \dots \right\rangle \\ &\approx 1 - \frac{1}{2} \langle \theta^2(s) \rangle \end{aligned}$$

and from Equation 9.2.3 we can write:

$$g(s) \approx 1 - \frac{s k_B T}{\kappa_b}$$

If we compare this to an expansion of the exponential in Equation 9.2.1

$$g(s) = e^{-|s|/\ell_p} \approx 1 - \frac{|s|}{\ell_p}$$

we obtain an expression for the persistence length of the worm-like chain

$$\ell_p = \frac{\kappa_b}{k_B T}$$

End-to-End Distance

The end-to-end distance for the WLC is obtained by integrating the tangent vector over one contour length:

$$\vec{R} = \int_0^{L_C} ds \vec{t}(s)$$

So the variance in the end-to-end distance is determined from the tangent vector autocorrelation function, which we take to have an exponential form:

$$\begin{aligned}
 \langle R^2 \rangle &= \langle R \cdot R \rangle \\
 &= \int_0^{L_C} ds \int_0^{L_C} ds' \langle t(s)t(s') \rangle \\
 &= \int_0^{L_C} ds \int_0^{L_C} ds' e^{-(s-s')/\ell_p} \\
 \langle R^2 \rangle &= 2\ell_p L_C - 2\ell_p^2 \left(1 - e^{-L_C/\ell_p}\right)
 \end{aligned}$$

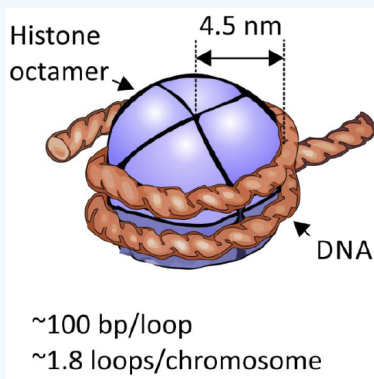
Let's examine this expression in two limits:

rigid: $\ell_p \gg L_C \quad \langle R^2 \rangle \approx L_C^2$

flexible: $\ell_p \ll L_C \quad \langle R^2 \rangle \approx 2L_C\ell_p \rightarrow n_e\ell_e^2 \rightarrow \therefore 2\ell_p = \ell_e$

✓ Example 9.2.1: DNA Bending in Nucleosomes

What energy is required to wrap DNA around the histone octamer in the nucleosome? Double stranded DNA is a stiff polymer with a persistence length of $\ell_p \approx 50$ nm, but the nucleosome has a radius of ~ 4.5 nm.



Solution

From ℓ_p and $k_B T = 4.1$ pN nm, we can determine the bending rigidity using:

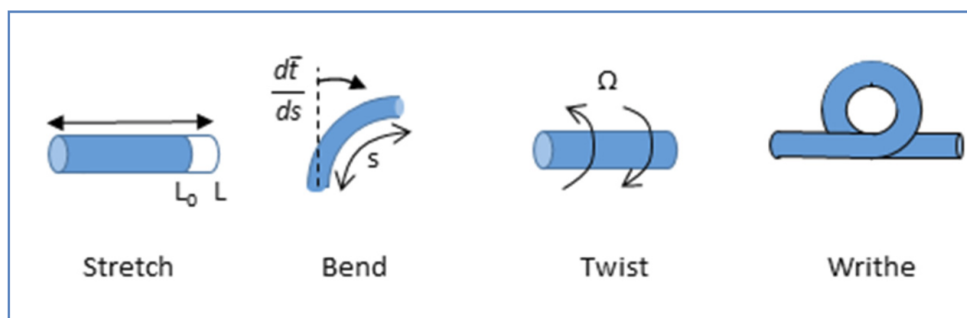
$$\kappa_b = \ell_p k_B T = (50 \text{ nm})(4.1 \text{ pN nm}) = 205 \text{ pN nm}^2$$

Then the energy required to bend dsDNA into one full loop is

$$\begin{aligned}
 U_b &\cong \frac{\kappa_b \theta^2}{2s} \approx \frac{\kappa_b (2\pi)^2}{2(2\pi R)} = \frac{\pi \kappa_b}{R} \\
 &= \frac{\pi(205 \text{ pN nm}^2)}{4.5 \text{ nm}} = 143 \text{ pN nm} \\
 &= 35 k_B T = 15 \text{ kcal (mol loops)}^{-1} \\
 &\quad \text{or } 0.15 \text{ kcal basepair}^{-1}
 \end{aligned}$$

Continuum Mechanics of a Thin Rod¹

The worm-like chain is a model derived from the continuum mechanics of a thin rod. In addition to bending, a thin rod is subject to other distortions: stretch, twist, and write.



Let's summarize the energies required for these deformations:

Deformation variables:

- s : Position along contour of rod
- L_0 : Unperturbed length of rod
- \vec{t} : Tangent vector.
- $d\vec{t}/ds$: curvature
- Ω : Local twist

The energy for distorting the rod is

$$U = U_{st} + U_b + U_{tw}$$

In the harmonic approximation for the restoring force, we can write these contributions as

$$U = \frac{1}{2} \int_{L_0}^L \kappa_{st} s ds + \frac{1}{2} \int_{L_0}^L \kappa_b \left(\frac{d\vec{t}}{ds} \right)^2 ds + \frac{1}{2} \int_{L_0}^L \kappa_{tw} \Omega^2 ds$$

The force constants, with representative values for dsDNA, are:

Stretching: $\kappa_{st} = \kappa_{st-entropic} + \kappa_{st-enthalpic}$

$$\kappa_{st-entropic} \approx 3k_B T / \ell_p L_c$$

Bending: κ_b

$$\kappa_b \approx 205 \text{ pN nm}^2$$

Twisting: κ_{tw}

$$\kappa_{tw} \approx (86 \text{ nm}) k_B T = 353 \text{ pN nm}^2$$

Writhe

An additional distortion in thin rods is **writhe**, which refers to coupled twisting and coiling, and is an important factor in DNA supercoiling. Twisting of a rod can induce in-plane looping of the rod, for instance as encountered with trying to coil a garden hose. The writhe number W of a rod refers to the number of complete loops made by the rod. The writhe can be positive or negative depending on whether the rod crosses over itself from right-to-left or left-to-right. The twist number T is the number of $\Omega = 2\pi$ rotations of the rod, and can also be positive or negative.



The linking number $L = T + W$ is conserved in B-form DNA, so that twist can be converted into writhe and vice-versa. Since DNA in cells is naturally negatively supercoiled in nucleosomes, topoisomerases are used to change of linking number by breaking and

reforming the phosphodiester backbone after relaxing the twist. Negatively supercoiled DNA can be converted into circular DNA by local bubbling (unwinding into single strands).

1. D. H. Boal, *Mechanics of the Cell*, 2nd ed. (Cambridge University Press, Cambridge, UK, 2012).

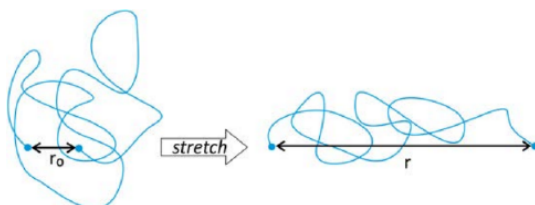
This page titled [9.2: Worm-like Chain](#) is shared under a [CC BY-NC-SA 4.0](#) license and was authored, remixed, and/or curated by [Andrei Tokmakoff](#) via [source content](#) that was edited to the style and standards of the LibreTexts platform.

9.3: Polymer Elasticity and Force–Extension Behavior

The Entropic Spring

To extend a polymer requires work. We calculate the reversible work to extend the macromolecule from the difference in free energy of the chain held between the initial and final state. This is naturally related to the free energy of the system as a function of polymer end-to-end distance:

$$w_{stretch} = F(r) - F(r_0) = - \int_{r_0}^r \vec{f}_{rev} \cdot d\vec{r}$$



For an ideal chain, the free energy depends only on the entropy of the chain: $F = -TS$. There are fewer configurational states available to the chain as you stretch to larger extension. The number of configurational states available to the system can be obtained by calculating the conformational partition function, Q_{conf} . For stretching in one-dimension, the Helmholtz free energy is:

$$\begin{aligned} dF &= -pdV - SdT + f \cdot dx \\ &= -k_B T \ln Q_{conf} \\ S_{conf} &= k_B \ln Q_{conf} \\ f &= - \left(\frac{\partial F}{\partial x} \right)_{V,T,N} = -k_B T \frac{\partial \ln Q_{conf}}{\partial x} = -T \frac{\partial S_{conf}}{\partial x} \end{aligned} \quad (9.3.1)$$

When you increase the end-to-end distance, the number of configurational states available to the system decreases. This requires an increasingly high force as the extension approaches the contour length. Note that more force is needed to stretch the chain at higher temperature.

Since this is a freely joined chain and all microstates have the same energy, we can equate the conformational partition function of a chain at a particular extension x with the probability density for the end-to-end distances of that chain

$$Q_{conf} \rightarrow P_{fjc}(r)$$

Although we are holding the ends of the chain at a fixed and stretching with the ends restrained along one direction (x), the probability distribution function takes the three-dimensional form to properly account for all chain configurations: $P_{conf}(r) = P_0 e^{-\beta^2 r^2}$ with $\beta^2 = 3k_B T / 2n\ell^2$ and $P_0 = \beta^3 / \pi^{3/2}$ is a constant. Then

$$\ln P_{conf}(r) = -\beta^2 r^2 + \ln P_0$$

The force needed to extend the chain can be calculated from eq. (9.3.1) after substituting $r^2 = x^2 + y^2 + z^2$, which gives

$$f = -2\beta^2 k_B T x = -\kappa_{st} x$$

So we have a linear relationship between force and displacement, which is classic Hooke's Law spring with a force constant κ_{st} given by

$$\kappa_{st} = \frac{3k_B T}{n\ell^2} = \frac{3k_B T}{\langle r^2 \rangle_0}$$

Here $\langle r^2 \rangle_0$ refers to the mean square end-to-end distance for the FJC in the absence of any applied forces. Remember: $\langle r^2 \rangle_0 = n\ell^2 = \ell L_C$. In the case that all of the restoring force is due to entropy, then we call this an entropic spring κ_{ES} .

$$\kappa_{ES} = \frac{T}{2} \left(\frac{\partial^2 S}{\partial x^2} \right)_{N,V,T}$$

This works for small forces, while the force is reversible. Notice that κ_{ES} increases with temperature -- as should be expected for entropic restoring forces.

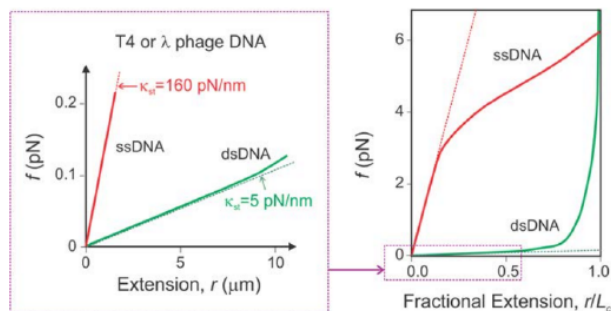
Example: Stretching DNA¹

At low force:

$$\text{dsDNA} \rightarrow \kappa_{st} = 5 \text{ pN/nm}$$

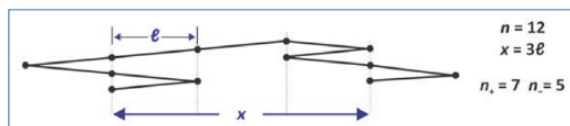
$$\text{ssDNA} \rightarrow \kappa_{st} = 160 \text{ pN/nm} \rightarrow \text{more entropy/more force}$$

At higher extension you asymptotically approach the contour length.



Force/Extension of a Random Walk Polymer

Let's derive force extension behavior for a random walk polymer in one dimension. The end-to-end distance is r , the segment length is ℓ , and the total number of segments is n .



For any given r , the number of configurations available to the polymer is:

$$\Omega = \frac{n!}{n_+!n_-!}$$

This follows from recognizing that the extension of a random walk chain in one dimension is related to the difference between the number of segments that step in the positive direction, n_+ , and those that step in the negative direction, n_- . The total number of steps is $n = n_+ + n_-$. Also, the end-to-end distance can be expressed as

$$r = (n_+ - n_-)\ell = (2n_+ - n)\ell = (n - 2n_-)\ell \quad (9.3.2)$$

$$n_{\pm} = \frac{1}{2} \left(n \pm \frac{r}{\ell} \right) \quad \frac{\partial n_{\pm}}{\partial r} = \pm \frac{1}{2\ell}$$

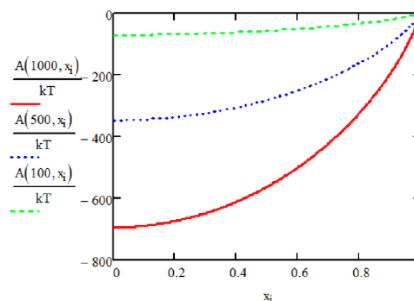
Then we can calculate the free energy of the random walk chain that results from the entropy of the chain, i.e., the degeneracy of configurational states at any extension. This looks like an entropy of mixing calculation:

$$\begin{aligned} F &= -k_B T \ln \Omega \\ &= -k_B T (n \ln n - n_+ \ln n_+ - n_- \ln n_-) \\ &= nk_B T (\phi_+ \ln \phi_+ + \phi_- \ln \phi_-) \end{aligned}$$

$$\phi_{\pm} = \frac{n_{\pm}}{n} = \frac{1}{2}(1 \pm x)$$

Here the fractional end-to-end extension of the chain is

$$x = \frac{r}{L_C} \tag{9.3.3}$$



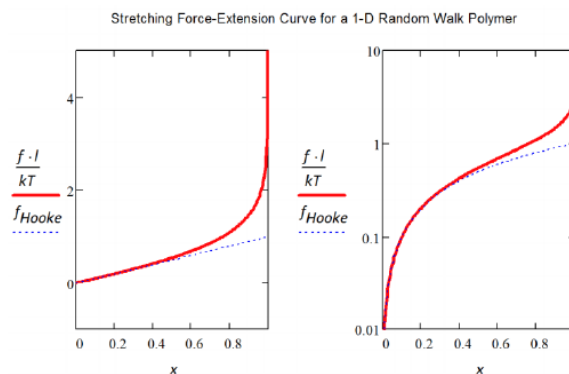
Next we can calculate the force needed to extend the polymer as a function of r :

$$f = -\frac{\partial F}{\partial r} \rightarrow \frac{\partial F}{\partial \phi_{\pm}} \frac{\partial \phi_{\pm}}{\partial r} \quad \frac{\partial \phi_{\pm}}{\partial r} = \pm \frac{1}{2L_C}$$

Using eq. (9.3.2)

$$\begin{aligned} f &= -nk_B T (\ln \phi_+ - \ln \phi_-) \left(\frac{1}{2L_C} \right) \\ &= -\frac{nk_B T}{2L_C} \ln \left(\frac{1+x}{1-x} \right) \\ &= -\frac{k_B T}{\ell} \frac{1}{2} \ln \left(\frac{1+x}{1-x} \right) \\ f &= -\frac{k_B T}{\ell} \tanh^{-1}(x) \end{aligned} \tag{9.3.4}$$

where I used the relationship: $\ln \left(\frac{1+x}{1-x} \right) = 2 \tanh^{-1}(x)$. Note, here the forces are scaled in units of $k_B T / \ell$. For small forces $x \ll 1$, $\tanh^{-1}(x) \approx x$ and eq. (9.3.4) gives $f \approx \frac{k_B T}{\ell L_C} r$. This gives Hooke's Law behavior with the entropic force constant expected for a 1D chain. For a 3D chain, we would expect: $f \approx \frac{3k_B T}{\ell L_C} r$. The spring constant scales with dimensionality.



The relationship between position, force, and the partition function

Now let's do this a little more carefully. From classical statistical mechanics, the partition function is

$$Q = \int \int dr^{3N} dp^{3N} \exp(-H/k_B T)$$

Where H is the Hamiltonian for the system. The average value for the position of a particle described by the Hamiltonian is

$$\langle x \rangle = \frac{1}{Q} \int \int dr^3 dp^3 x \exp(-H/k_B T)$$

If the Hamiltonian takes the form

$$H = -f \cdot x$$

Then

$$\langle x \rangle = \frac{k_B T}{Q} \left(\frac{\partial Q}{\partial f} \right)_{V,T,N} = k_B T \left(\frac{\partial \ln Q}{\partial f} \right)_{V,T,N}$$

This describes the average extension of a chain if a force is applied to the ends.

Force/Extension Behavior for a Freely Jointed Chain

Making use of the expressions above and $Q = q^N$

$$q_{conf} = \int \int dr^3 dp^3 e^{-U/k_B T} e^{\vec{f} \cdot \vec{r}/k_B T} \quad \langle r \rangle = N k_B T \left(\frac{\partial \ln q_{conf}}{\partial f} \right)_{U,r,n}$$

Here we also inserted a general Hamiltonian which accounts for the internal chain interaction potential and the force ex the chain: $H = U - \vec{f} \cdot \vec{r}$. For N freely jointed chains with n segments, we set $U \rightarrow 0$, and focus on force exerted on every segment of the chain.

$$\vec{f} \cdot \vec{r} = \sum_{i=1}^n \vec{f} \cdot \vec{\ell}_i = f \ell \sum_{i=1}^n \cos \theta_i$$

Treating the segments as independent and integrating over all θ , we find that

$$q_{conf}(f) = \frac{2\pi \sinh \varphi}{\varphi}$$

$$\langle r \rangle = n \ell \left[\coth \varphi - \frac{1}{\varphi} \right] \quad (9.3.5)$$

where the unitless force parameter is

$$\varphi = \frac{f \ell}{k_B T} \quad (9.3.6)$$

As before, the magnitude of force is expressed relative to $k_B T / \ell$. Note this calculation is for the average extension that results from a fixed force. If we want the force needed for a given average extension, then we need to invert the expression. Note, the functional form of the force-extension curve in eq. is different than what we found for the 1D random walk in eq. (9.3.4). We do not expect the same form for these problems, since our random walk example was on a square lattice, and the FJC propagates radially in all directions.

Derivation

For a single polymer chain:

$$q = \int \int dr^3 dp^3 e^{U/k_B T} e^{-f \cdot r/k_B T}$$

$$P(r) = \frac{1}{q} e^{-U/k_B T} e^{f \cdot r/k_B T}$$

$$\langle r \rangle = \frac{k_B T}{q} \left(\frac{\partial \ln q}{\partial f} \right)_u$$

In the case of the Freely Jointed Chain, set $U \rightarrow 0$.

$$\vec{f} \cdot \vec{r} = \vec{f} \cdot \sum_{i=1}^n \vec{\ell}_i = f \ell \sum_{i=1}^n \cos \theta_i$$

Decoupled segments:

$$\begin{aligned}
 q &\approx \int dr^3 \exp\left(\sum_i \frac{f\ell}{k_B T} \cos \theta_i\right) \\
 &= \left(\int_0^{2\pi} \int_0^\pi \exp[\varphi \cos \theta] \sin \theta d\theta d\phi\right)^n \\
 &= \left(\frac{2\pi \sinh(\varphi)}{\varphi}\right)^n \\
 \langle r \rangle &= k_B T \frac{\partial}{\partial f} \ln q \\
 &= nk_B T \frac{\partial}{\partial f} \left[\ln \left\{ \frac{2\pi \sinh(\varphi)}{\varphi} \right\} \right] \quad \coth(x) = \frac{e^x + e^{-x}}{e^x - e^{-x}} \\
 \langle r \rangle &= n\ell [\coth(\varphi) - \varphi^{-1}] \\
 \text{or } \langle x \rangle &= \coth(\varphi) - \varphi^{-1} \quad \text{The average fractional extension: } \langle x \rangle = \langle r \rangle / L_C
 \end{aligned}$$

Now let's look at the behavior of the expression for $\langle x \rangle$ -- also known as the Langevin function.

$$\langle r \rangle = n\ell [\coth(\varphi) - \varphi^{-1}] \quad (9.3.7)$$

Looking at limits:

- Weak force ($\varphi \ll 1$): $f \ll k_B T / \ell$

Inserting and truncating the expansion: $\coth \varphi = \frac{1}{\varphi} + \frac{1}{3}\varphi - \frac{1}{45}\varphi^3 + \frac{2}{945}\varphi^5 + \dots$, we get

$$\begin{aligned}
 \langle x \rangle &= \frac{\langle r \rangle}{L_C} \approx \frac{1}{3}\varphi \\
 \langle r \rangle &\approx \frac{1}{3} \frac{n\ell^2}{k_B T} f \\
 \text{or } f &= \frac{3k_B T}{n\ell^2} \langle r \rangle = \kappa_{ES} \langle r \rangle
 \end{aligned}$$

Note that this limit has the expected linear relationship between force and displacement, which is governed by the entropic spring constant.

- Strong force ($\varphi \gg 1$). $f \gg k_B T / \ell$ Taking the limit $\coth(x) \rightarrow 1$.

$$\langle r \rangle \simeq n\ell \left[1 - \frac{1}{\varphi} \right] \leftarrow \lim_{f \rightarrow \infty} = \lim_{\alpha \rightarrow \infty} = L_C \text{ Contour length}$$

$$\text{Or } f = \frac{k_B T}{\ell} \frac{1}{1 - \langle x \rangle} \text{ where } \langle x \rangle = \frac{\langle r \rangle}{L_C}$$

For strong force limit, the force extension behavior scales as, $x \sim 1 - f^{-1}$.

So, what is the work required to extend the chain?

At small forces, we can integrate over the linear force-extension behavior. Under those conditions, to extend from r to $r + \Delta r$, we have

$$w_{rev} = \int_0^{\Delta r} \kappa_{ES} r dr = \frac{3k_B T}{2n\ell^2} \Delta r^2$$

Force/Extension of Worm-like Chain

For the [worm-like chain model](#), we found that the variance in the end-to-end distance was

$$\langle r^2 \rangle = 2\ell_p L_C - 2\ell_p^2 (1 - e^{-L_C/\ell_p}) \quad (9.3.8)$$

where L_C is the contour length, and the persistence length was related to the bending force constant as $\ell_p = \frac{\kappa_b}{k_B T}$. The limiting behavior for eq. (9.3.8) is:

$$\begin{array}{ll} \text{rigid:} & \ell_p \gg L_C \quad \langle r^2 \rangle \propto L_C^2 \\ \text{flexible:} & \ell_p \ll L_C \quad \langle r^2 \rangle \sim 2L_C \ell_p \quad \therefore \text{for WLC} \\ & = n_e \ell_e^2 \quad (2\ell_p = \ell_e) \end{array}$$

Following a similar approach to the FJC above, it is not possible to find an exact solution for the force-extension behavior of the WLC, but it is possible to show the force extension behavior in the rigid and flexible limits.

Setting $2\ell_p = \ell_e$, $\varphi = f\ell_e/k_B T$, and using the fractional extension $\langle x \rangle = \frac{\langle r \rangle}{L_C}$:

1. Weak force ($\varphi \ll 1$) Expected Hooke's Law behavior

$$f\ell_e \ll k_B T \quad f = \frac{3k_B T}{\ell_e L_C} \rightarrow \frac{f\ell_e}{k_B T} = 3\langle x \rangle$$

For weak force limit, the force extension behavior scales as, $x \sim f$.

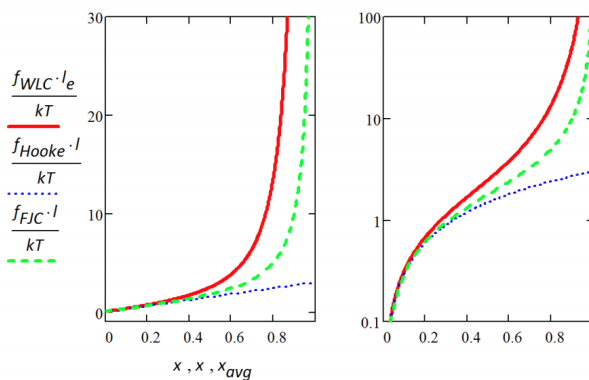
2. Strong force ($\varphi \gg 1$)

$$f\ell_e \gg k_B T \quad \langle r \rangle = L_C \left(1 - \frac{1}{2\sqrt{\varphi}} \right) \rightarrow \frac{f\ell_e}{k_B T} = \frac{1}{4(1 - \langle x \rangle)^2}$$

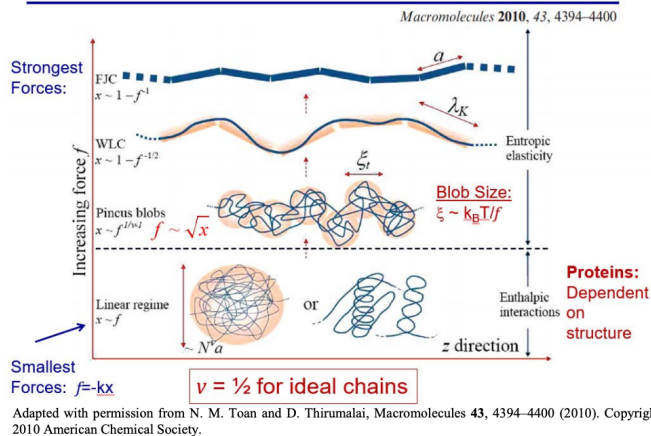
For strong force limit, the force extension behavior scales as, $x \sim 1 - f^{-1/2}$.

An approximate expression for the combined result (from Bustamante):

$$\frac{f\ell_p}{k_B T} = \frac{1}{4(1 - \langle x \rangle)^2} - \frac{1}{4} + \langle x \rangle \quad (9.3.9)$$



Stretching regimes



1. A. M. van Oijen and J. J. Loparo, Single-molecule studies of the replisome, Annu. Rev. Biophys. 39, 429–448 (2010).

This page titled 9.3: Polymer Elasticity and Force–Extension Behavior is shared under a CC BY-NC-SA 4.0 license and was authored, remixed, and/or curated by Andrei Tokmakoff via source content that was edited to the style and standards of the LibreTexts platform.

SECTION OVERVIEW

3: Diffusion

10: Diffusion

10.1: Continuum Diffusion

10.2: Solving the Diffusion Equation

10.3: Steady-State Solutions

11: Brownian Motion

11.1: Random Walk and Diffusion

11.2: Markov Chain and Stochastic Processes

11.3: Fluorescence Correlation Spectroscopy

11.4: Orientational Diffusion

12: Diffusion in a Potential

12.1: Diffusion with Drift

12.2: Biased Random Walk

12.3: Diffusion in a Potential

13: Friction and the Langevin Equation

13.1: Langevin Equation

13.2: Brownian Dynamics

Thumbnail: This is a simulation of the Brownian motion of a big particle (dust particle) that collides with a large set of smaller particles (molecules of a gas) which move with different velocities in different random directions. (CC BY-SA 3.0; Lookang via [Wikipedia](#))

This page titled [3: Diffusion](#) is shared under a [CC BY-NC-SA 4.0](#) license and was authored, remixed, and/or curated by [Andrei Tokmakoff](#) via [source content](#) that was edited to the style and standards of the LibreTexts platform.

CHAPTER OVERVIEW

10: Diffusion

[10.1: Continuum Diffusion](#)

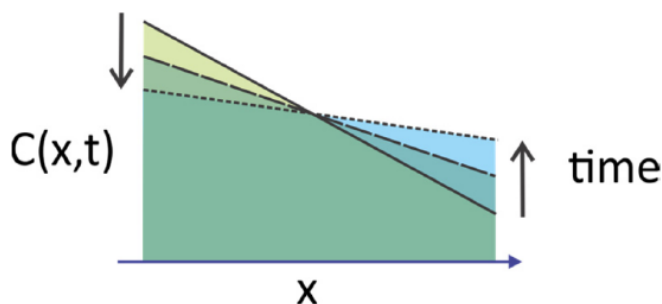
[10.2: Solving the Diffusion Equation](#)

[10.3: Steady-State Solutions](#)

This page titled [10: Diffusion](#) is shared under a [CC BY-NC-SA 4.0](#) license and was authored, remixed, and/or curated by [Andrei Tokmakoff](#) via [source content](#) that was edited to the style and standards of the LibreTexts platform.

10.1: Continuum Diffusion

We are now going to start a new set of topics that involve the dynamics of molecular transport. A significant fraction of how molecules move spatially in biophysics is described macroscopically by “diffusion” and microscopically through its counterpart “Brownian motion”. Diffusion refers to the phenomenon by which concentration and temperature gradients spontaneously disappear with time, and the properties of the system become spatially uniform. As such, diffusion refers to the transport of mass and energy in a nonequilibrium system that leads toward equilibrium. Brownian motion is also a spontaneous process observed in equilibrium and non-equilibrium systems. It refers to the random motion of molecules in fluids that arises from thermal fluctuations of the environment that rapidly randomize the velocity of particles. Much of the molecular transport in biophysics over nanometer distances arises from diffusion.



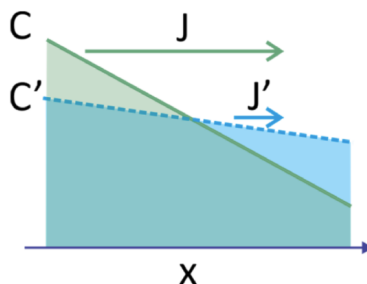
This can be contrasted with directed motion, which requires the input of energy and is crucial for transporting cargo to targets over micron-scale distances. Here we will start by describing diffusion in continuum systems, and in the next section show how this is related to the Brownian motion of discrete particles.

Fick's First Law

We will describe the time evolution of spatially varying concentration distributions $C(x, t)$ as they evolve toward equilibrium. These are formalized in two laws that were described by Adolf Fick (1855).¹ Fick's first law is the “common sense law” that is in line with everyone's physical intuition. Molecules on average will tend to diffuse from regions of higher concentration to regions of lower concentration. Therefore we say that the flux of molecules through a surface, J , is proportional to the concentration gradient across that surface.

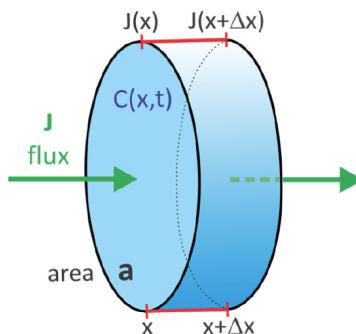
$$J = -D \frac{\partial C}{\partial x} \quad (10.1.1)$$

J is more accurately called a flux density, since it has units of concentration or number density per unit area and time. The proportionality constant between flux density J ($\text{mol m}^{-2} \text{s}^{-1}$) and concentration gradient (mol m^{-4}) which sets the timescale for the process is the diffusion constant D ($\text{m}^2 \text{s}^{-1}$). The negative sign assures that the flux points in the direction of decreasing concentration. This relationship follows naturally, when we look at the two concentration gradients in the figure. Both C and C' have a negative gradient that will lead to a flux in the positive direction. C will give a bigger flux than C' because there is more probability for flow to right. The gradient disappears and the concentration distribution becomes constant and time invariant at equilibrium. Note, in a general sense $\partial C / \partial x$ can be considered the leading term in an expansion of C in x .



Fick's Second Law

Fick's second law extends the first law by adding an additional constraint based on the conservation of mass. Consider diffusive transport along x in a pipe with cross-sectional area a , and the change in the total number of particles within a disk of thickness Δx over a time period Δt .



If we take this disk to be thin enough that the concentration is a constant at any moment in time, then the total number of particles in the slab at that time is obtained from the concentration times the volume:

$$N = aC(t)\Delta x$$

Within the time interval Δt the concentration can change and therefore the total number of particles within the disk changes by an amount

$$\Delta N = a\{C(t + \Delta t) - C(t)\}\Delta x$$

Now, the change in the number of particles is also dependent on the fluxes of molecules at the two surfaces of the disk. The number of molecules passing into one surface of the disk is $-aJ\Delta t$, and therefore the net change in the number of molecules during Δt is obtained from the difference of fluxes between the left and right surfaces of the disk:

$$\Delta N = -aJ(x + \Delta x) - J(x)\Delta t$$

Setting these two calculations of ΔN equal to each other, we see that the flux and concentration gradients for the disk are related as

$$\{C(t + \Delta t) - C(t)\}\Delta x = -\{J(x + \Delta x) - J(x)\}\Delta t$$

or rewriting this in differential form

$$\frac{\partial C}{\partial t} = -\frac{\partial J}{\partial x} \quad (10.1.2)$$

This important relationship is known as a continuity expression. Substituting eq. (10.1.1) into this expression leads to **Fick's Second Law**

$$\frac{\partial C}{\partial t} = D\frac{\partial^2 C}{\partial x^2} \quad (10.1.3)$$

This is the diffusion equation in one dimension, and in three dimensions:²

$$\frac{\partial C}{\partial t} = D\nabla^2 C \quad (10.1.4)$$

Equation (10.1.4) can be used to solve diffusive transport problems in a variety of problems, choosing the appropriate coordinate system and applying the specific boundary conditions for the problem of interest.

Diffusion from a Point Source

As our first example of how concentration distributions evolve diffusively, we consider the time-dependent concentration profile when the concentration is initially all localized to one point in space, $x = 0$. The initial condition is

$$C(x, t = 0) = C_0\delta(x)$$

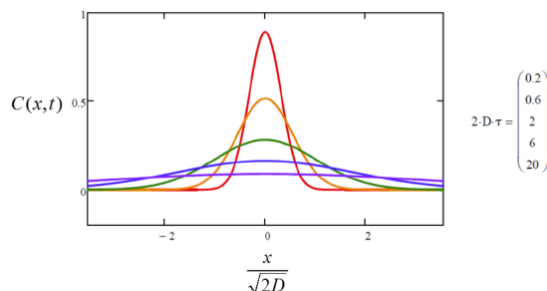
and the solution to eq. (10.1.3) is

$$C(x, t) = \frac{C_0}{\sqrt{4\pi Dt}} e^{-x^2/4Dt} \quad (10.1.5)$$

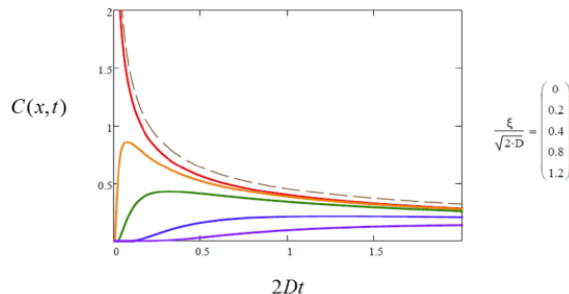
The concentration profile has a Gaussian form which is centered on the origin, $\langle x \rangle = 0$, with the mean square displacement broadening with time as:

$$\langle x^2 \rangle = 2Dt$$

$$\langle x^2 \rangle = 2Dt$$



Diffusive transport has no preferred direction. Concentration profiles spread evenly in the positive and negative direction, and the highest concentration observed will always be at the origin and have a value $C_{max} = C_0/\sqrt{4\pi Dt}$. Viewing time-dependent concentrations in space reveal that they reach a peak at $t_{max} = x^2/2D$, before decaying at $t^{-1/2}$ (dashed line below).



When we solve for 3D diffusion from a point source:

$$C(x, y, z, t = 0) = C_0 \delta(x) \delta(y) \delta(z)$$

If we have an isotropic medium in which D is identical for diffusion in the x, y, and z dimensions,

$$C(x, y, z, t) = \frac{C_0}{(4\pi Dt)^{3/2}} e^{-r^2/4Dt} \quad (10.1.6)$$

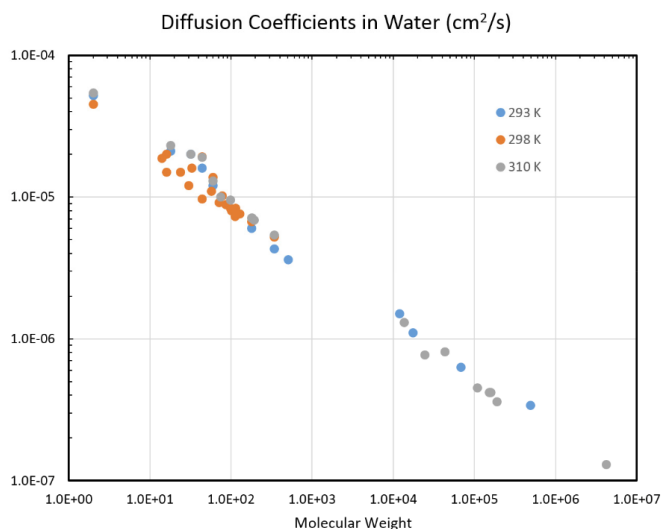
where $r^2 = x^2 + y^2 + z^2$. Calculating the mean square displacement from

$$\begin{aligned} \langle r^2 \rangle &= \frac{\int_0^\infty dr r^2 C(r, t)}{\int_0^\infty dr C(r, t)} \\ &= 6Dt \end{aligned}$$

or in d dimensions, $\langle r^2 \rangle = d(2Dt)$.

Diffusion Constants

Typical diffusion constants for biologically relevant molecules in water are shown in the graph below, varying from small molecules such as O_2 and glucose in the upper left to proteins and viruses in the lower right.



- For a typical globular protein, typically diffusion coefficients are:

$$\text{in water } D \sim 10^{-10} \text{ m}^2/\text{s}$$

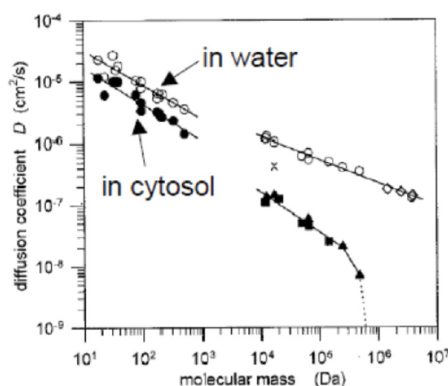
$$\text{in cells } D \sim 10^{-12} \text{ m}^2/\text{s}$$

$$\text{in lipids } D \sim 10^{-14} \text{ m}^2/\text{s}$$

$$\langle r^2 \rangle^{1/2} = 1 \mu\text{m}, \quad t \sim 0.4 \text{ sec in cells}$$

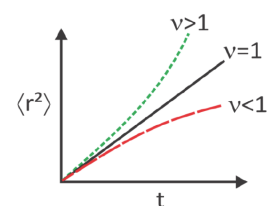
$$= 10 \mu\text{m}, \quad t \sim 40 \text{ sec in cells}$$

- Ions in water at room temperature usually have a diffusion coefficient of 0.6×10^{-5} to 2×10^{-5} cm²/s.
- Lipids:
 - Self-diffusion 10^{-12} m²/s
 - Tracer molecules in lipid bilayers $1-10 \times 10^{-12}$ m²/s



Anomalous Diffusion

The characteristic of simple diffusive behavior is the linear relationship between the mean square displacement and time. Deviation from this behavior is known as anomalous diffusion, and is characterized by a scaling relationship $\langle r^2 \rangle \sim t^\nu$. We refer to $\nu < 1$ as sub-diffusive behavior and $\nu > 1$ as super-diffusive. Diffusion in crowded environments can result in sub-diffusion.³



Thermodynamic Perspective on Diffusion

Thermodynamically, we can consider the driving force for diffusion as a gradient in the free energy or chemical potential of the system. From this perspective, in the absence of any other interactions, the driving force for reaching uniform spatial concentration is the **entropy of mixing**. For a mixture with mole fraction x_A , we showed

$$\begin{aligned}\Delta S_{mix} &= -Nk_B(x_A \ln x_A + x_B \ln x_B) & x_B = 1 - x_A \\ &\approx -N_A k_B \ln x_A & \text{for } x_A \ll 1\end{aligned}$$

We then use $\Delta F = -T\Delta S$ to calculate the chemical potential:

$$\begin{aligned}\mu_A &= \left(\frac{\partial F}{\partial N_A} \right)_{V,T} \\ \mu_a &\approx k_B T \ln x_A\end{aligned}$$

We see that a concentration gradient, means that the mole fraction and therefore chemical potential is different for two positions in the system. At equilibrium $\mu_A(r_1) = \mu_A(r_2)$, which occurs when $x_A(r_1) = x_A(r_2)$.

Thermodynamics does not tell you about rate, only the direction of spontaneous change(although occasionally diffusion is discussed in terms of a time-dependent “entropyproduction”). The diffusion constant is the proportionality constant between gradients in concentration or chemical potential and the time-dependent flux of particles. The flux density described in Fick’s first law can be related to μ_i , the chemical potential for species i :

$$J_i = \frac{-D_i C_i}{k_B T} \frac{\partial \mu_i}{\partial r_i}$$

-
1. A. Fick, Ueber diffusion, Ann. Phys. 170, 59–86 (1855).
 2. This equation assumes that D is a constant, but if it is a function of space: $C = \nabla(D\nabla C)$. In three dimensions, Fick’s First Law and the continuity expression are: $J(r, t) = vC(r, t) - D\nabla C(r, t)$ and $dC(r, t)/dt = -\nabla \cdot J(r, t)$ where v is the velocity of the fluid. These expressions emphasize that flux density and velocity are vectors, whereas concentration field is a scalar.
 3. J. A. Dix and A. S. Verkman, Crowding effects on diffusion in solutions and cells, Annu. Rev. Biophys. 37, 247–263 (2008).

This page titled [10.1: Continuum Diffusion](#) is shared under a [CC BY-NC-SA 4.0](#) license and was authored, remixed, and/or curated by [Andrei Tokmakoff](#) via [source content](#) that was edited to the style and standards of the LibreTexts platform.

10.2: Solving the Diffusion Equation

Solutions to the diffusion equation, such as eq. (10.1.5) and (10.1.6), are commonly solved with the use of Fourier transforms. If we define the transformation from real space to reciprocal space as

$$\tilde{C}(k, t) = \int_{-\infty}^{\infty} C(x) e^{ikx} dx$$

one can express the diffusion equation in 1D as

$$\frac{d\tilde{C}(k, t)}{dt} = -Dk^2 \tilde{C}(k, t) \quad (10.2.1)$$

[More generally one finds that the Fourier transform of a linear differential equation in x can be expressed in polynomial form: $\mathcal{F}(\partial^n f / \partial x^n) = (ik)^n \tilde{f}(k)$. This manipulation converts a partial differential equation into an ordinary one, which has the straightforward solution $\tilde{C}(k, t) = \tilde{C}(k, 0) \exp(-Dk^2 t)$. We do need to express the boundary conditions in reciprocal space, but then, this solution can be transformed back to obtain the real space solution using $C(x, t) = (2\pi)^{-1} \int_{-\infty}^{\infty} \tilde{C}(k, t) e^{-ikx} dx$.

Since eq. (10.2.1) is a linear differential equation, sums of solutions to the diffusion equation are also solutions. We can use this superposition principle to solve problems for complex initial conditions. Similarly, when the diffusion constant is independent of x and t , the general solution to the diffusion equation can also be expressed as a Fourier series. If we separate the time and space variables, so that the form of the solution is $C(x, t) = X(x)T(t)$ we find that we can write

$$\frac{1}{DT} \frac{\partial T}{\partial t} = \frac{1}{x} \frac{\partial^2 x}{\partial x^2} = -\alpha^2$$

Where α is a constant. Then $T = e^{-\alpha^2 Dt}$ and $x = A \cos \alpha x + B \sin \alpha x$. This leads to the general form:

$$C(x, t) = \sum_{n=0}^{\infty} (A_n \cos \alpha_n x + B_n \sin \alpha_n x) e^{-\alpha_n^2 Dt} \quad (10.2.2)$$

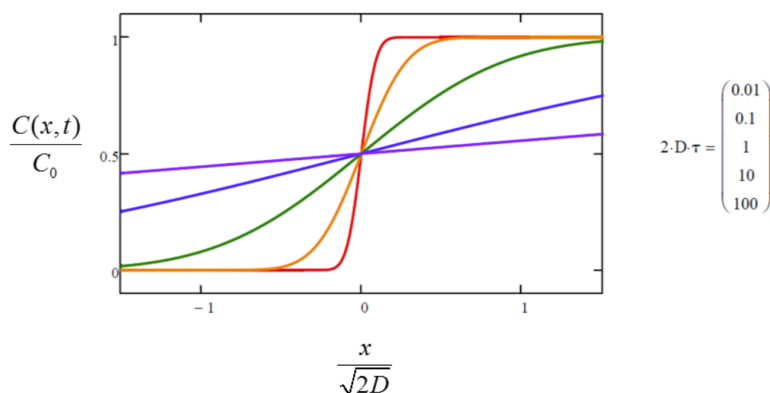
Here A_n and B_n are constants determined by the boundary conditions.

Examples

Diffusion across boundary

At time $t = 0$, the concentration is uniform at a value C_0 for $x \geq 0$, and zero for $x < 0$, similar to removing a barrier between two homogeneous media. Using the superposition principle, the solution is obtained by integrating the point source solution, eq. (10.1.5), over all initial point sources $\delta(x - x_0)$ such that $x_0 = 0 \rightarrow \infty$. Defining $y^2 = (x - x_0)^2 / 4Dt$,

$$C(x, t) = \frac{C_0}{\sqrt{\pi}} \int_{-\infty}^{\infty} \frac{(x - x_0)}{\sqrt{4Dt}} dy e^{-y^2} = \frac{C_0}{2} \operatorname{erfc} \left(\frac{-(x - x_0)}{\sqrt{4Dt}} \right)$$

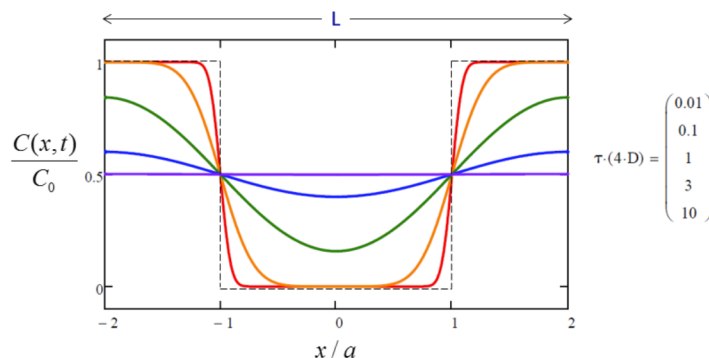


Diffusion into "hole"

A concentration "hole" of width $2a$ is inserted into a box of length $2L$ with an initial concentration of C_0 . Let's take $L = 2a$. Concentration profile solution:

$$C(x, t) = C_0 \left[\left(\frac{L-a}{L} \right) - \sum_{n=1}^{\infty} A_n \cos(\alpha_n x) e^{-\alpha_n^2 D t} \right]$$

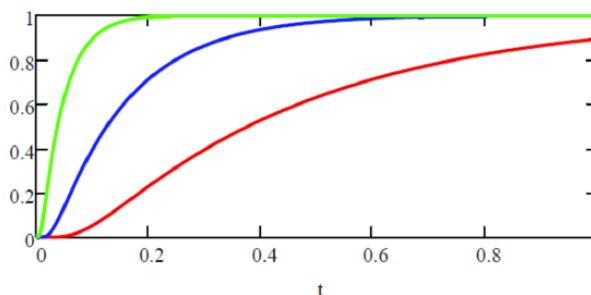
$$A_n = \frac{2 \sin(\alpha_n a)}{n\pi} \quad \alpha_n = \frac{n\pi}{L}$$



- **Fluorescence Recovery after Photobleaching (FRAP):** We can use this solution to describe the diffusion of fluorescently labeled molecules into a photobleached spot. Usually observe the increase of fluorescence with time from this spot. We integrate concentration over initial hole:

$$\begin{aligned} N_{FRAP}(t) &= \int_{-a}^{+a} C(x, t) dx \\ &= C_0 \left[\frac{2a}{L}(L-1) - L \sum_{n=1}^{\infty} A_n^2 e^{-\alpha_n^2 D t} \right] \end{aligned}$$

$D = 1, 3, 10$



Reflecting and Absorbing Boundary Conditions

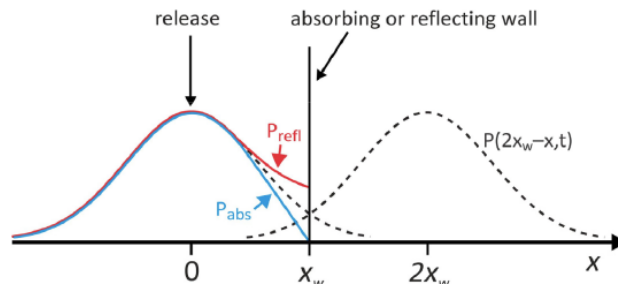
We will be interested in describing the time-dependent probability distribution for the case in which particles are released at $x=0$, subject to encountering an impenetrable wall at $x=x_w$, which can either absorb or reflect particles.

Consider the case of a reflecting wall, where the boundary condition requires that the flux at x_w is zero. This boundary condition and the resulting pile-up near the wall can be described by making use of the fact that any $P(x > x_w, t)$ can be reflected about x_w , which is equivalent to removing the boundary and adding a second source term to $P(x, t)$ for particles released at $x = 2x_w$

$$P_{refl}(x, t) = P(x, t) + P(2x_w - x, t) \quad (x < x_w)$$

This is also known as a wrap-around solution, since any component with any population from $P(x, t)$ that passes the position of the wall is reflected about x_w . Similarly, an absorbing wall, $P(x = x_w, t) = 0$, means that we remove any population that reached x_w , which is obtained from the difference of the two mirrored probability distributions:

$$P_{abs}(x, t) = P(x, t) - P(2x_w - x, t) \quad (x < x_w)$$



This page titled [10.2: Solving the Diffusion Equation](#) is shared under a [CC BY-NC-SA 4.0](#) license and was authored, remixed, and/or curated by [Andrei Tokmakoff](#) via [source content](#) that was edited to the style and standards of the LibreTexts platform.

10.3: Steady-State Solutions

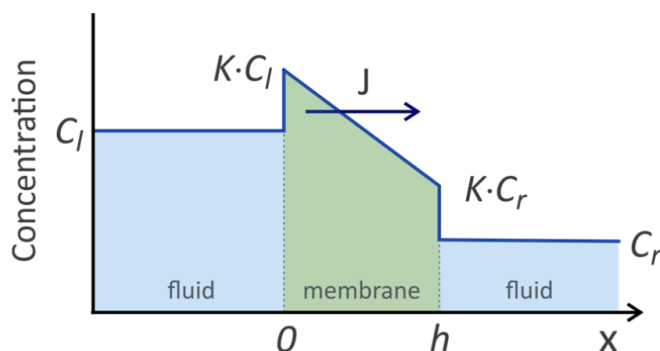
Steady state solutions can be applied when the concentration gradient may vary in space but does not change with time, $\partial C / \partial t = 0$. Under those conditions, the diffusion eq. (10.1.4) simplifies to Laplace's equation

$$\nabla^2 C = 0 \quad (10.3.1)$$

For certain conditions this can be integrated directly by applying the proper boundary conditions, and then the steady state flux at a target position is obtained from [Fick's first law](#), Equation 10.1.1.

Diffusion through a Membrane¹

The steady-state solution to the diffusion equation in one dimension can be used to describe the diffusion of a small molecule through a cell plasma membrane that resists the diffusion of the molecule.



In this model, the membrane thickness is h , and the concentrations of the diffusing small molecule in the fluid on left and right side of membrane are C_l and C_r . Within the membrane resists diffusion of the small molecule, which is reflected in the small molecule's [partition coefficient](#) between membrane and fluid:

$$K_p = \frac{C_{\text{membrane}}}{C_{\text{fluid}}}$$

K_p can vary between 10^3 and 10^{-7} depending on the nature of the small molecules and membrane composition.

For the steady-state diffusion equation $\partial^2 C / \partial x^2 = 0$, solutions take the form $C(x) = A_1 x + A_2$. Applying boundary conditions for the concentration of small molecule in the membrane at the two boundaries, we find

$$A_1 = \frac{K_p(C_r - C_l)}{h} \quad A_2 = K_p C_l$$

Then we can write the transmembrane flux density of the small molecule across the membrane as

$$J = -D_{\text{mol}} \frac{\partial C}{\partial x} = \frac{K_p D_{\text{mol}}}{h} (C_l - C_r) = \frac{K_p D_{\text{mol}} \Delta C}{h}$$

The membrane permeability is equivalent to the volume of small molecule solution that diffuses across a given area of the membrane per unit time, and is defined as

$$P_m \equiv \frac{J}{\Delta C} = \frac{K_p D_{\text{mol}}}{h} (m s^{-1}) \quad (10.3.2)$$

The membrane resistance to flow is $R = 1/P_m$, and the rate of transport across the membrane is $dn/dt = J A$, where A is area.

This linear relationship in eq. (10.3.2) between P_m and K_p , also known as the **Overton relation**, has been verified for thousands of molecules. For small molecules with molecular weight < 50 , P_m can vary from 10^1 to $10^{-6} \text{ cm s}^{-1}$. It varies considerably even for water across different membrane systems, but its typical value for a phospholipid vesicle is $10^{-3} \text{ cm s}^{-1}$. Some of the highest values ($> 50 \text{ cm s}^{-1}$) are observed for O_2 . Cations such as Na^+ and K^+ have permeabilities of $\sim 5 \times 10^{-14} \text{ cm s}^{-1}$, and small peptides have values of 10^{-9} – $10^{-6} \text{ cm s}^{-1}$.

Diffusion to Capture

What is the flux of a diffusing species onto a spherical surface from a solution with a bulk concentration C_0 ? This problem appears often for diffusion limited reaction rates. To find this, we calculate the steady-state radial concentration profile $C(r)$ around a perfectly absorbing sphere with radius a , i.e. $C(a) = 0$. At steady state, we solve eq. (10.3.1) by taking the diffusion to depend only on the radial coordinate r and not the angular ones.

$$\frac{1}{r^2} \frac{\partial}{\partial r} \left(r^2 \frac{\partial C}{\partial r} \right) = 0$$

Let's look for the simplest solution. We begin by assuming that the quantity in parenthesis is a constant and integrate twice to give

$$C(r) = -\frac{A_1}{r} + A_2 \quad (10.3.3)$$

Where A_1 and A_2 are constants of integration. Now, using the boundary conditions $C(a) = 0$ and $C(\infty) = C_0$ we find:

$$C(r) = C_0 \left(1 - \frac{a}{r} \right)$$

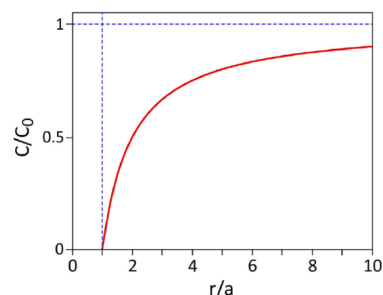
Next, we use this expression to calculate the flux of molecules incident on the surface of the sphere ($r = a$).

$$J(a) = -D \frac{\partial C}{\partial r} \Big|_{r=a} = -\frac{DC_0}{a} \quad (10.3.4)$$

Here J is the flux density in units of (molecules area⁻¹ sec⁻¹) or [(mol/L) area⁻¹ sec⁻¹]. The sign of the flux density is negative reflecting that it is a vector quantity directed toward $r = 0$. We then calculate the rate of collisions of molecules with the sphere (the flux, j) by multiplying the magnitude of J by the surface area of the sphere ($A = 4\pi a^2$):

$$j = JA = 4\pi DaC_0$$

This shows that the rate constant, which expresses the proportionality between rate of collisions and concentration is $k = 4\pi Da$.



Probability of Capture

In an extension of this problem useful to ligand binding simulations, we can ask what the probability is that a molecule released near an absorbing sphere will reach the sphere rather than diffuse away?

Suppose a particle is released near a spherical absorber of radius a at a point $r = b$. What is the probability that the particle will be absorbed at $r = a$ rather than wandering off beyond an outer perimeter at $r = c$?

To solve this problem we solve for the steady-state flux at the surfaces a and c subject to the boundary conditions $C(a) = 0$, $C(b) = C_0$, and $C(c) = 0$. That is, the inner and outer surfaces are perfectly absorbing, but the concentration has a maximum value $C(b) = C_0$ at $r = b$.

We separate the problem into two zones, a -to- b and b -to- c , and apply the general solution eq. (10.3.3) to these zones with the appropriate boundary conditions to yield:

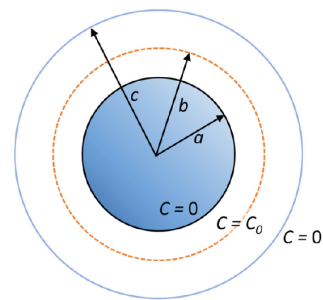
$$C(r) = \frac{C_0}{(1 - a/b)} \left(1 - \frac{a}{r} \right) \quad a \leq r \leq b$$

$$C(r) = \frac{C_0}{(c/b - 1)} \left(1 - \frac{a}{r} \right) \quad b \leq r \leq c$$

Then the radial flux density is:

$$J_r(r) = -\frac{DC_0}{(1 - a/b)} \frac{a}{r^2} \quad a \leq r \leq b$$

$$J_r(r) = \frac{DC_0}{(c/b - 1)} \frac{c}{r^2} \quad b \leq r \leq c$$



Calculating the areas of the two absorbing surfaces and multiplying the flux densities by the areas gives the flux. The flux from the spherical shell source to the inner absorber is

$$j_{in} = 4\pi DC_0 \frac{a}{(1 - a/b)}$$

and the flux from the spherical shell source to the outer absorber is

$$j_{out} = 4\pi DC_0 \frac{c}{(c/b - 1)}$$

We obtain the probability that a particle released at $r = b$ and absorbed at $r = a$ from the ratio

$$P_{capture} = \frac{j_{in}}{j_{in} + j_{out}} = \frac{a(c - b)}{b(c - a)}$$

In the limit $c \rightarrow \infty$, this probability is just a/b . This is the probability of capture for the sphere of radius a immersed in an infinite medium. Note that this probability decreases only inversely with the radial distance b^{-1} , rather than the surface area of the sphere.

-
1. A. Walter and J. Gutknecht, Permeability of small nonelectrolytes through lipid bilayer membranes, *J. Membr.Biol.* 90, 207–217 (1986).

Readings

- H. C. Berg, *Random Walks in Biology*. (Princeton University Press, Princeton, N.J., 1993).
- K. Dill and S. Bromberg, *Molecular Driving Forces: Statistical Thermodynamics in Biology, Chemistry, Physics, and Nanoscience*. (Taylor & Francis Group, New York, 2010).

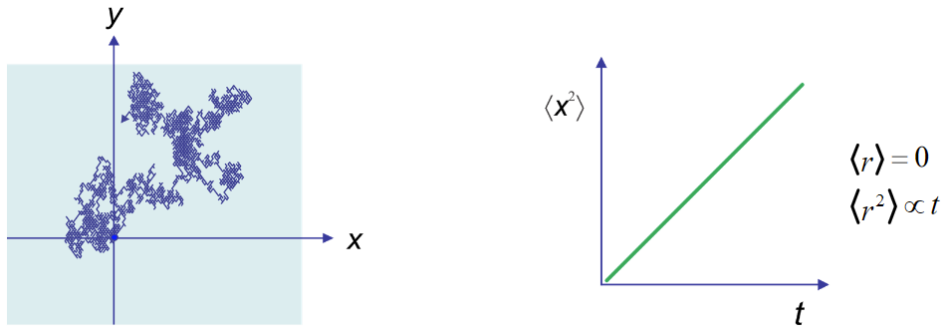
This page titled [10.3: Steady-State Solutions](#) is shared under a [CC BY-NC-SA 4.0](#) license and was authored, remixed, and/or curated by [Andrei Tokmakoff](#) via [source content](#) that was edited to the style and standards of the LibreTexts platform.

CHAPTER OVERVIEW

11: Brownian Motion

Brownian motion refers to the random motions of small particles under thermal excitation in solution first described by Robert Brown (1827),¹ who with his microscope observed the random, jittery spatial motion of pollen grains in water. This phenomenon is intrinsically linked with diffusion. Diffusion is the macroscopic realization of the Brownian motion of molecules within concentration gradients. The theoretical basis for this relationship was described by Einstein in 1905,² and Jean Perrin³ provided the detailed experiments that confirmed his predictions.

Since the motion of any one particle is unique, the Brownian motion must be described statistically. We observe that the mean-squared displacement of a particle averaged over many measurements grows linearly with time, just as with diffusion.

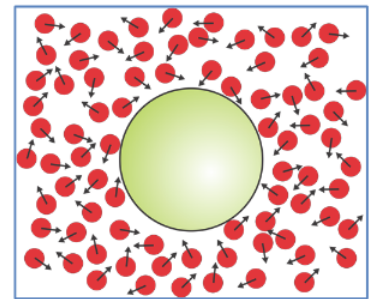


The proportionality factor between mean-squared displacement and time is the diffusion constant in Fick's Second Law. As for diffusion, the proportionality factor depends on dimensionality. In 1D, if $\langle x^2(t) \rangle / t = 2D$ then in 3D $\langle r^2(t) \rangle / t = 6D$, where D is the diffusion constant.

Brownian motion is a property of molecules at thermal equilibrium. It applies to a larger particle (i.e., a protein) experiencing an imbalance of many microscopic forces exerted by many much small molecules of the surroundings (i.e., water). The thermal agitation originates by partitioning the kinetic energy of the system on average as $k_B T / 2$ per degree of freedom. Free diffusion implies motion which is only limited by kinetic energy.

Brownian motion applies to a specific range of forces and masses where thermal energy ($k_B T(300 \text{ K}) = 4.1 \text{ pN nm}$) can have a significant influence on a particle. Let's look at the average translational kinetic energy:

$$\left\langle \frac{mv_x^2}{2} \right\rangle = \frac{1}{2} k_B T$$



For a $\sim 10 \text{ kDa}$ protein with mass $\sim 10^{-23} \text{ kg}$, the root mean squared velocity due to thermal energy is $v_{rms} = \langle v_x^2 \rangle^{1/2} = 20 \text{ m/s}$. For water at 300 K, $D \sim 10^{-5} \text{ cm}^2/\text{s}$. The same protein has a net displacement in one second of $x_{rms} = \langle x^2 \rangle^{1/2} = \sqrt{2Dt} \approx 50 \mu\text{m}$. The large difference in these values indicates the large number of randomizing collisions that this particle experiences during one second of evolution: $(v_{rms} \cdot 1 \text{ sec}) / x_{rms} \approx 4 \times 10^5$. For the protein, the velocities and displacements are a dominant force on the molecular scale. In comparison, a 1 kg mass with $k_B T$ of energy will have $v_{rms} \sim 10^{-11} \text{ m/s}$, and an equally insignificant displacement!

Ergodic Hypothesis

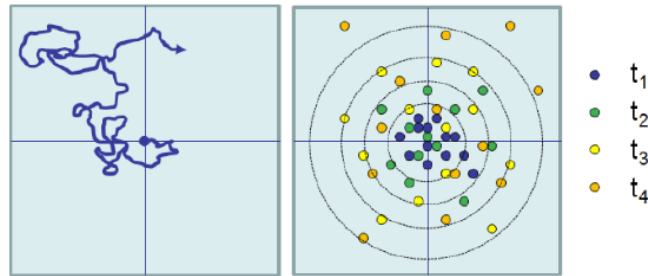
A system is known as ergodic when time average and ensemble averages for a time-dependent variable are equal.

$$\text{Ensemble average: } \langle x \rangle = \frac{1}{N} \sum_i x_i = \int P(x) x dx$$

$$\text{Time-average: } \overline{x(t)} = \lim_{T \rightarrow \infty} \frac{1}{T} \int_0^T x(t) dt$$

In practice, the time average can be calculated using a single particle trajectory by averaging over the displacement observed for all time intervals within the trajectory such that $t=(t_{\text{final}}- t_{\text{initial}})$.

In the case of Brownian motion and diffusion: $\langle |r(t) - r_0|^2 \rangle = \overline{|r(t) - r_0|^2}$.



[11.1: Random Walk and Diffusion](#)

[11.2: Markov Chain and Stochastic Processes](#)

[11.3: Fluorescence Correlation Spectroscopy](#)

[11.4: Orientational Diffusion](#)

-
1. R. Brown, "On the Particles Contained in the Pollen of Plants; and On the General Existence of Active Molecules in Organic and Inorganic Bodies" in *The Miscellaneous Botanical Works of Robert Brown*, edited by J. J. Bennett (R. Hardwicke, London, 1866), Vol. 1, pp. 463-486.
 2. A. Einstein, Über die von der molekularkinetischen Theorie der Wärme geforderte Bewegung von in ruhenden Flüssigkeiten suspendierten Teilchen, *Ann. Phys.* 322, 549–560 (1905).
 3. J. Perrin, *Brownian Movement and Molecular Reality*. (Taylor and Francis, London, 1910).
-

This page titled [11: Brownian Motion](#) is shared under a [CC BY-NC-SA 4.0](#) license and was authored, remixed, and/or curated by [Andrei Tokmakoff](#) via [source content](#) that was edited to the style and standards of the LibreTexts platform.

11.1: Random Walk and Diffusion

We want to describe the correspondence between a microscopic picture for the random walk of particles and macroscopic diffusion of particle concentration gradients. We will describe the statistics for the location of a random walker in one dimension (x), which is allowed to step a distance Δx to the right (+) or left (-) during each time interval Δt . At each time point a step must be taken left or right, and steps to left and right are equally probable.

Let's begin by describing where the system is at after taking n steps qualitatively. We can relate the position of the system to where it was before taking a step by writing:

$$x(n) = x(n-1) \pm \Delta x$$

This expression can be averaged over many steps:

$$\begin{aligned} \langle x(n) \rangle &= \langle x(n-1) \pm \Delta x \rangle \\ &= \langle x(n-1) \rangle = \langle x(n-2) \rangle = \dots = \langle x(0) \rangle \end{aligned}$$

Since there is equal probability of moving left or right with each step, the $\pm \Delta x$ term averages to zero, and $\langle x \rangle$ does not change with time. The most probable position for any time will always be the starting point.

Now consider the variance in the displacement:

$$\begin{aligned} \langle x^2(n) \rangle &= \langle x^2(n-1) \pm 2\Delta x x(n-1) + (\Delta x)^2 \rangle \\ &= \langle x^2(n-1) \rangle + (\Delta x)^2 \end{aligned}$$

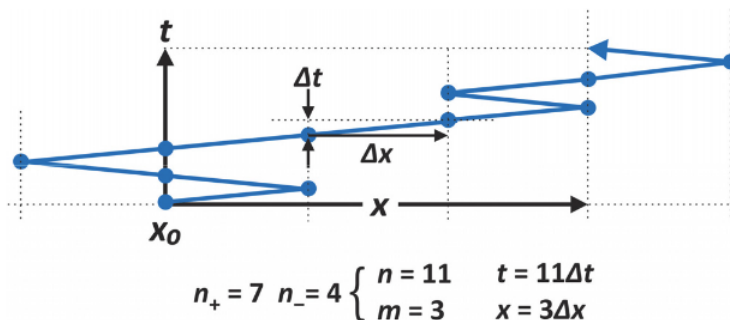
In the first line, the middle term averages to zero, and the variance gains a factor of Δx^2 . Repeating this process for each successive step back shows that the mean square displacement grows linearly in the number of steps.

$$\begin{aligned} \langle x^2(0) \rangle &= 0 \\ \langle x^2(1) \rangle &= (\delta x)^2 \\ \langle x^2(2) \rangle &= 2(\delta x)^2 \\ &\vdots \\ \langle x^2(n) \rangle &= n(\Delta x)^2 \end{aligned} \tag{11.1.1}$$

Qualitatively, these arguments indicate that the statistics of a random walker should have the same mean and variance as the concentration distribution for diffusion of particles from an initial position.

Random Walk Step Distribution Function

Now let's look at this a little more carefully and describe the probability distribution for the position of particles after n steps, which we equate with the number of possible random walk trajectories that can lead to a particular displacement. What is the probability of starting at $x_0 = 0$ and reaching point x after n jumps separated by the time interval Δt ?



Similar to our discussion of the random walk polymer, we can express the displacement of a random jumper to the total number of jumps in the positive direction n_+ and in the negative direction n_- . If we make n total jumps, then

$$n = n_+ + n_- \quad \longrightarrow \quad t = n\Delta t$$

The total number of steps n is also our proxy for the length of time for a given trajectory, t . The distance between the initial and final position is related to the difference in + and – steps:

$$m = n_+ - n_- \quad \longrightarrow \quad x = m\Delta x$$

Here m is our proxy for the total displacement x . Note from these definitions we can express n_+ and n_- as

$$n_{\pm} = \frac{n \pm m}{2} \quad (11.1.2)$$

The number of different ways of making n jumps with the constraint of n_+ positive and n_- negative jumps is

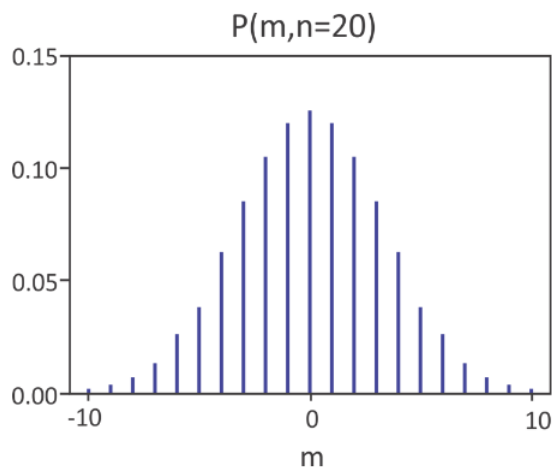
$$\Omega = \frac{n!}{n_+!n_-!}$$

The probability of observing a particular sequence of n “+” and “–” jumps is $P(n) = (P_+)^{n_+} (P_-)^{n_-} = (1/2)^n$.

The total number of trajectories that are possible with n equally probably “+” and “–” jumps is 2^n , so the probability that any one sequence of n steps will end up at position m is given by $\Omega/2^n$ or

$$\begin{aligned} P(m, n) &= \left(\frac{1}{2}\right)^n \frac{n!}{n_+!n_-!} \\ &= \left(\frac{1}{2}\right)^n \frac{n!}{\frac{n+m}{2}! \frac{n-m}{2}!} \end{aligned}$$

This is the binomial probability distribution function. Looking at the example below for twenty steps, we see $\langle m \rangle = 0$ and for a discrete probability distribution which has a Gaussian envelope.



For very large n , the distribution function becomes continuous. To see this, let's apply Stirling's approximation, $n! \approx (n/e)^n \sqrt{2\pi n}$, and after a bit of manipulation we find¹

$$P(m, n) = \sqrt{\frac{2}{\pi n}} e^{-m^2/2n} \quad (11.1.3)$$

Note, this distribution has an envelope that follows a normal Gaussian distribution for a continuous variable where the variance σ^2 is proportional to the number of steps n .

To express this with a time variable, we instead insert $n = t/\Delta t$ and $m = x/\Delta x$ in eq. (11.1.3) to obtain the discrete probability distribution function:

$$P(x, t) = \sqrt{\frac{\Delta t}{2\pi t}} \exp\left[-\frac{\Delta t x^2}{2t(\Delta x)^2}\right]$$

Note that we can re-write this discrete probability distribution similar to the continuum diffusion solution

$$P(x, t) = \sqrt{\frac{(\Delta x)^2}{4\pi Dt}} e^{-x^2/4Dt} \quad (11.1.4)$$

if we equate the variance and diffusion constant as

$$D = \frac{(\Delta x)^2}{2\Delta t}$$

Equation (11.1.4) is slightly different because P is a unitless probability for finding the particle between x and $x+\Delta x$, rather than a continuous probability density ρ with units of m^{-1} : $\rho(x,t) dx = P(x,t)$. Even so, eq. (11.1.4) suggests that the time-dependent probability distribution function for the random walk obeys a diffusion equation

$$\frac{\partial P}{\partial t} = \Delta x D \frac{\partial^2 P}{\partial x^2} \quad \text{or} \quad \frac{\partial \rho}{\partial t} = D \frac{\partial^2 \rho}{\partial x^2} \quad (11.1.5)$$

Three-Dimensional Random Walk

We can extend this treatment to diffusion from a point source in three dimensions, by using a random walk of n steps of length Δx on a 3D cubic lattice. The steps are divided into those taken in the x , y , and z directions:

$$n = n_x + n_y + n_z$$

and distance of the walker from the origin is obtained from the net displacement along the x , y , and z axes:

$$r = (x^2 + y^2 + z^2)^{1/2} = m\Delta x$$

$$m = \sqrt{m_x^2 + m_y^2 + m_z^2}$$

For each time-interval the walker takes a step choosing the positive or negative direction along the x , y , and z axes with equal probability. Since each dimension is independent of the others

$$P(r, n) = P(m_x, n_x)P(m_y, n_y)P(m_z, n_z)$$

Looking at the radial displacement from the origin, we find

$$\sigma_x^2 + \sigma_y^2 + \sigma_z^2 = \sigma_r^2$$

where

$$\sigma_x^2 = \frac{(\Delta x)^2 t}{\Delta t} \rightarrow 2D_x t$$

but since each dimension is equally probable $\sigma_r^2 = 3\sigma_x^2$. Then using eq. (11.1.3)

$$P(r, t) = \left(\frac{3\Delta x^2}{2\pi\sigma_r^2}\right)^{3/2} e^{-3r^2/2\sigma_r^2}$$

where $\sigma_r^2 = 6Dt$.

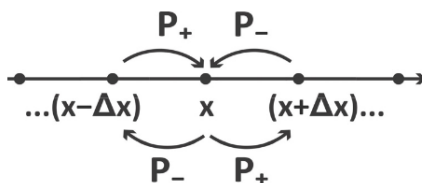
1. M. Daune, Molecular Biophysics: Structures in Motion. (Oxford University Press, New York, 1999), Ch. 7.

This page titled [11.1: Random Walk and Diffusion](#) is shared under a [CC BY-NC-SA 4.0](#) license and was authored, remixed, and/or curated by [Andrei Tokmakoff](#) via [source content](#) that was edited to the style and standards of the LibreTexts platform.

11.2: Markov Chain and Stochastic Processes

Working again with the same problem in one dimension, let's try and write an equation of motion for the **random walk probability distribution**: $P(x, t)$.

- This is an example of a stochastic process, in which the evolution of a system in time and space has a random variable that needs to be treated statistically.
- As above, the movement of a walker only depends on the position where it is at, and not on any preceding steps. When the system has no memory of where it was earlier, we call it a **Markovian system**.
- Generally speaking, there are many flavors of a stochastic problem in which you describe the probability of being at a position x at time t , and these can be categorized by whether x and t are treated as continuous or discrete variables. The class of problem we are discussing with discrete x and t points is known as a **Markov Chain**. The case where space is treated discretely and time continuously results in a **Master Equation**, whereas a Langevin equation or Fokker–Planck equation describes the case of continuous x and t .
- To describe the walker's time-dependence, we relate the probability distribution at one point in time, $P(x, t + \Delta t)$, to the probability distribution for the preceding time step, $P(x, t)$ in terms of the probabilities of a walker making a step to the right (P_+) or to the left (P_-) during the interval Δt . Note, when $P_+ \neq P_-$, there is a **stepping bias** in the system. If $P_+ + P_- < 1$, there is a resistance to stepping either as a result of an energy barrier or excluded volume on the chain.
- In addition to the loss of probability by stepping away from x to the left or right, we need to account for the steps from adjacent sites that end at x .



Then the probability of observing the particle at position x during the interval Δt is:

$$\begin{aligned} P(x, t + \Delta t) &= P(x, t) - P_+ \cdot P(x, t) - P_- \cdot P(x, t) + P_+ \cdot P(x - \Delta x, t) + P_- \cdot P(x + \Delta x, t) \\ &= (1 - P_+ - P_-) \cdot P(x, t) + P_+ \cdot P(x - \Delta x, t) + P_- \cdot P(x + \Delta x, t) \\ &= P(x, t) + P_+ [P(x - \Delta x, t) - P(x, t)] + P_- [P(x + \Delta x, t) - P(x, t)] \end{aligned}$$

and the net change probability is

$$P(x, t + \Delta t) - P(x, t) = P_+ [P(x - \Delta x, t) - P(x, t)] + P_- [P(x + \Delta x, t) - P(x, t)]$$

We can cast this as a time-derivative if we divide the change of probability by the time-step Δt :

$$\begin{aligned} \frac{\partial P}{\partial t} &= \frac{P(x, t + \Delta t) - P(x, t)}{\Delta t} \\ &= P_+ [P(x - \Delta x, t) - P(x, t)] + P_- [P(x + \Delta x, t) - P(x, t)] \\ &= P_+ \Delta P_- (x, t) + P_- \Delta P_+ (x, t) \end{aligned} \tag{11.2.1}$$

Where $P_{\pm} = P_{\pm} / \Delta t$ is the right and left stepping rate, and $\Delta P_{\pm}(x, t) = P(x \pm \Delta x, t) - P(x, t)$

We would like to show that this random walk model results in a diffusion equation for the probability density $\rho(x, t)$ we deduced in Equation (11.1.5). To simplify, we assume that the left and right stepping probabilities $P_+ = P_- = \frac{1}{2}$, and substitute

$$P(x, t) = \rho(x, t) dx$$

into Equation (11.2.1):

$$\frac{\partial \rho}{\partial t} = P [\rho(x - \Delta x, t) - 2\rho(x, t) + \rho(x + \Delta x, t)]$$

where $P = 1/2 \Delta t$. We then expand these probability density terms in x as

$$\rho(x, t) = \rho(0, t) + \frac{\partial \rho}{\partial x} x + \frac{1}{2} \frac{\partial^2 \rho}{\partial x^2} x^2$$

and find that the probability density follows a diffusion equation

$$\frac{\partial \rho}{\partial t} = D \frac{\partial^2 \rho}{\partial x^2}$$

where $D = \Delta x^2 / 2\Delta t$.

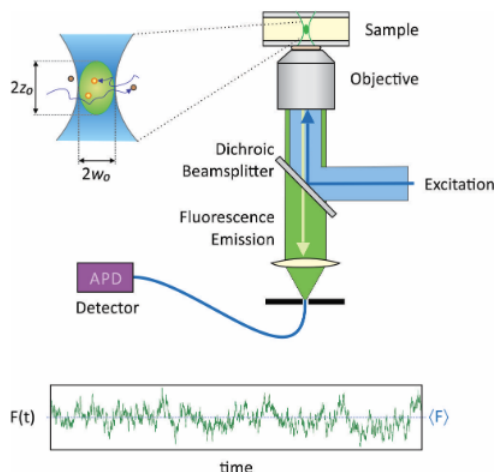
Reading Materials

- A. Nitzan, *Chemical Dynamics in Condensed Phases: Relaxation, Transfer and Reactions in Condensed Molecular Systems*. (Oxford University Press, New York, 2006).

This page titled [11.2: Markov Chain and Stochastic Processes](#) is shared under a [CC BY-NC-SA 4.0](#) license and was authored, remixed, and/or curated by [Andrei Tokmakoff](#) via [source content](#) that was edited to the style and standards of the LibreTexts platform.

11.3: Fluorescence Correlation Spectroscopy

Fluorescence correlation spectroscopy (FCS) allows one to measure diffusive properties of fluorescent molecules, and is closely related to FRAP. Instead of measuring time-dependent concentration profiles and modeling the kinetics as continuum diffusion, FCS follows the steady state fluctuations in number density of a very dilute fluorescent probe molecule in the small volume observed in a confocal microscope. We measure the fluctuating changes in fluorescence intensity emitted from probe molecules as they diffuse into and out of the focal volume.



- Average concentration of sample: $C_0 = <10^{-9} \text{ M} - 10^{-7} \text{ M}>$.
- This corresponds to an average of ~ 0.1 -100 molecules in the focal volume, although this number varies with diffusion into and out of the volume.
- The fluctuating fluorescence trajectory is proportional to the time-dependent number density or concentration:

$$F(t) \propto C(t)$$

- How big are the fluctuations? For a Gaussian random process, we expect $\frac{\delta N_{rms}}{N} \sim \frac{1}{\sqrt{N}}$
- The observed concentration at any point in time can be expressed as time-dependent fluctuations about an average value: $C(t) = \bar{C} + \delta C(t)$.

To describe the experimental observable, we model the time-dependence of $\delta C(t)$ from the diffusion equation:

$$\frac{\partial \delta C}{\partial t} = D \nabla^2 \delta C$$

$$\langle \delta C(r, 0) \delta C(r', t) \rangle = \frac{C_0}{(4\pi Dt)^{3/2}} e^{-(r-r')^2/4Dt}$$

The concentration fluctuations can be related to the fluorescence intensity fluctuations as

$$F(t) = AW(r)C(r, t)$$

$W(r)$: Spatial optical profile of excitation and detection

A : Other experimental excitation and detection parameters

Calculate FCS correlation function for fluorescence intensity fluctuations. $F(t) = \langle F \rangle - \delta F(t)$

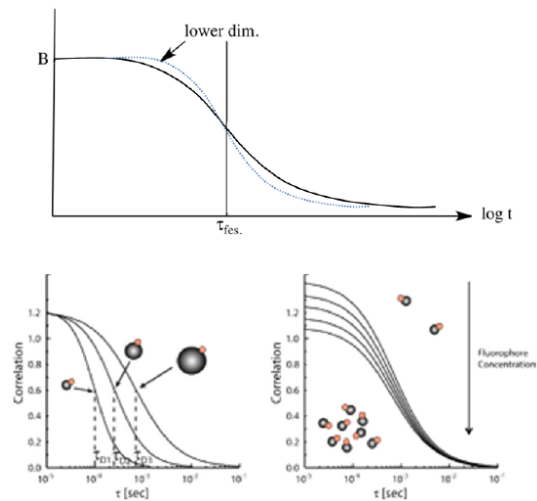
$$G(t) = \frac{\langle \delta F(0) \delta F(t) \rangle}{\langle \delta F \rangle^2}$$

For the case of a Gaussian beam with a waist size w_0 :

$$G(t) \sim \frac{B}{1 + t/\tau_{FCS}}$$

Where the amplitude is $B = 4\pi A^2 I_0^2 \overline{\delta C_0^2} w_0^2$, and the correlation time is related to the diffusion constant by:

$$\tau_{FCS} = \frac{w_0^2}{4D}$$



Readings

- P. Schwille and E. Haustein, "Fluorescence Correlation Spectroscopy: An Introduction to its Concepts and Applications" in Biophysics Textbook Online.

This page titled [11.3: Fluorescence Correlation Spectroscopy](#) is shared under a [CC BY-NC-SA 4.0](#) license and was authored, remixed, and/or curated by [Andrei Tokmakoff](#) via [source content](#) that was edited to the style and standards of the LibreTexts platform.

11.4: Orientational Diffusion

The concepts we developed for translation diffusion and Brownian motion are readily extended to rotational diffusion. For continuum diffusion, if one often assumes that one can separate the particle probability density into a radial and angular part: $P(r, \theta, \phi) = P(r)P(\theta, \phi)$. Then one also separate the diffusion equation into two parts for which the orientational diffusion follows a small-angle diffusion equation

$$\frac{\partial P(\Omega, t)}{\partial t} = D_{or} \nabla^2 P(\Omega, t) \quad (11.4.1)$$

where Ω refers to the spherical coordinates (θ, φ) . D_{or} is the **orientational diffusion constant** with units of $\text{rad}^2 \text{ s}^{-1}$. Microscopically, one can consider orientational diffusion as a random walk on the surface of a sphere, with steps being small angular displacements in θ and φ . Equation 11.4.1 allows us to obtain the time-dependent probability distribution function $P(\Omega, t|\Omega_0)$ that describes the distribution of directions Ω at time t , given that the vector had the orientation Ω_0 at time $t = 0$. This can be expressed as an expansion in spherical harmonics

$$P(\Omega, t|\Omega_0) = \sum_{\ell=0}^{\infty} \sum_{m=-\ell}^{\ell} c_{\ell}^m(t) [Y_{\ell}^m(\Omega_0)]^* Y_{\ell}^m(\Omega)$$

The expansion coefficients are given by

$$c_{\ell}^m(t) = \exp[-\ell(\ell+1)D_{or}t]$$

Readings

- H. C. Berg, Random Walks in Biology. (Princeton University Press, Princeton, N.J., 1993).
- R. Phillips, J. Kondev, J. Theriot and H. Garcia, Physical Biology of the Cell, 2nd ed. (Taylor & Francis Group, New York, 2012).

This page titled [11.4: Orientational Diffusion](#) is shared under a [CC BY-NC-SA 4.0](#) license and was authored, remixed, and/or curated by [Andrei Tokmakoff](#) via [source content](#) that was edited to the style and standards of the LibreTexts platform.

CHAPTER OVERVIEW

12: Diffusion in a Potential

In this section, we extend the concepts of diffusion and Brownian motion into a regime where the time-evolution is not entirely random, but includes a driving force. We will refer to this class of problems as diffusion in a potential, although it is also referred to as diffusion with drift, diffusion in a velocity or force field, or diffusion in the presence of an external force. We will see that these problems can be related to a biased random walk or to motion of a Brownian particle subject to an internal or external potential. Our discussion below will be confined to problems involving diffusion in one dimension.

The common theme is that we account for transport of particles through a surface in terms of two sources of flux, the diffusive flux and an additional driven contribution that arises from a potential, field, or external force experienced by the particle:

$$J = J_{diff} + J_U \quad (12.1)$$

Here we label the second flux component with U to signify potential. This may be a result of an external force acting on a diffusing system (for instance, electrophoresis and sedimentation), or the bias that results from interactions between diffusing particles. In mass transport through fluid flow the second term is known as the advective flux, $J_U \rightarrow J_{adv}$.

[12.1: Diffusion with Drift](#)

[12.2: Biased Random Walk](#)

[12.3: Diffusion in a Potential](#)

This page titled [12: Diffusion in a Potential](#) is shared under a [CC BY-NC-SA 4.0](#) license and was authored, remixed, and/or curated by [Andrei Tokmakoff](#) via [source content](#) that was edited to the style and standards of the LibreTexts platform.

12.1: Diffusion with Drift

If diffusion occurs within a moving fluid, the time-dependent concentration profiles will be influenced by the local velocity of the fluid, or drift velocity v_x . The net advective flux density for the concentration passing through an area per unit time is then

$$J_{adv} = v_x C \quad (12.1.1)$$

So that the total flux according to eq. (12.1) is

$$J = -D \frac{\partial C}{\partial x} + v_x C \quad (12.1.2)$$

Now using the continuity expression $\partial C / \partial t = -\partial J / \partial x$, and assuming a constant drift velocity the diffusion coefficient is¹

$$\frac{\partial C}{\partial t} = D \frac{\partial^2 C}{\partial x^2} - v_x \frac{\partial C}{\partial x} \quad (12.1.3)$$

This equation is the same as the normal diffusion equation in the inertial frame of reference. If we shift to a frame moving at v_x , we can define the relative displacement

$$\bar{x} = x - v_x t$$

Remember, C is a function of x and t , and expressing eq. (12.1.2) in terms of \bar{x} via the chain rule, we find that we can recast it as the simple diffusion equation:

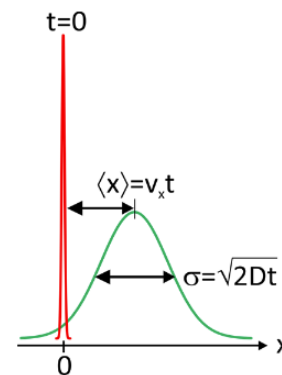
$$\frac{\partial C}{\partial t} = D \frac{\partial^2 C}{\partial \bar{x}^2}$$

Then the solution for diffusion from a point source becomes

$$C(\bar{x}, t) = \frac{1}{\sqrt{4\pi Dt}} e^{-\bar{x}^2/4Dt}$$

$$C(x, t) = \frac{1}{\sqrt{4\pi Dt}} e^{-(x-v_x t)^2/4Dt}$$

So the peak of the distribution moves as $\langle x \rangle = v_x t$ and the width grows as $\sigma = [(\overline{x^2}) - (\langle x \rangle)^2]^{1/2} = (2Dt)^{1/2}$.



Let's consider the relative magnitude of the diffusive and drift velocity contributions to the motion of a protein in water. A typical diffusion constant is $10^{-6} \text{ cm}^2/\text{s}$, meaning that the root mean square displacement in a one microsecond time period is 14 nm. If we compare this with the typical velocity of blood in capillaries, $v = 0.3 \text{ mm/s}$, in the same microsecond the same protein is pushed $\langle x \rangle = 0.3 \text{ nm}$. For this example, diffusion dominates the transport process on the nanometer scale, however, with the increase of time scale and transport distance, the drift term will grow in significance due to the $t^{1/2}$ scaling of diffusive transport.

Péclet Number

The Péclet number P_e is a unitless number used in continuum hydrodynamics to characterize the relative importance of diffusive transport and advective transport processes. Language note:

- Convection: internal currents within fluid
- Advection: mass transport due to convection

We characterize this with a ratio of the rates or equivalently the characteristic time scale for transport with these processes:

$$P_e = \frac{\text{advective flux}(J_{adv})}{\text{diffusive flux}(J_{diff})} \approx \frac{\text{diffusion timescale}(t_{diff})}{\text{advection timescale}(t_{adv})}$$

Limits

- $P_e \ll 1$ Diffusion dominated. In this limit, diffusive transport spreads the concentration profile symmetrically about the maximum as illustrated above.

- $P_e \gg 1$ Flow dominated. Effectively no spreading to concentration; it is just carried along with the flow.

If we define a characteristic transport length d and the flow velocity v , then

$$t_{adv} \approx \frac{d}{v}$$

Given a diffusion constant D , the diffusive time-scale is taken to be

$$t_{diff} \approx \frac{d^2}{D}$$

So That

$$P_e = \frac{vd}{D}$$

1. In three dimensions: $\mathbf{J}(\mathbf{r}, t) = -D\overline{\Delta}C(\mathbf{r}, t) + \mathbf{v}C(\mathbf{r}, t)$ and $\dot{C} = \nabla \cdot (D\overline{\nabla}C) - \nabla \cdot (\mathbf{v}C)$.

This page titled [12.1: Diffusion with Drift](#) is shared under a [CC BY-NC-SA 4.0](#) license and was authored, remixed, and/or curated by [Andrei Tokmakoff](#) via [source content](#) that was edited to the style and standards of the LibreTexts platform.

12.2: Biased Random Walk

The diffusion with drift equation can be obtained from a biased random walk problem. To illustrate, we extend the earlier description of a walker on a 1D lattice that can step left or right by an amount distance Δx for every time interval Δt . However, in this case there is unequal probability of stepping right (+) or left (-) during Δt : $P_+ \neq P_-$. Probabilistically speaking, the change in position for a given time interval can be expressed as

$$\begin{aligned}\langle x(t + \Delta t) \rangle &= \langle x(t) + \Delta x P_+ - \Delta x P_- \rangle \\ &= \langle x(t) \rangle + \Delta x (P_+ - P_-)\end{aligned}\quad (12.2.1)$$

We see that the average position of random walkers depends on the difference in left and right stepping rates. To help link stepping with time, we define rate constants for stepping left or right,

$$k_{\pm} = \frac{P_{\pm}}{\Delta t}\quad (12.2.2)$$

with $k_+ \neq k_-$. Then Equation 12.2.1 can be written as

$$\begin{aligned}\langle x(t + \Delta t) \rangle &= \langle x(t) \rangle + (k_+ - k_-)\Delta t \Delta x \\ &= \langle x(t) \rangle + v_x \Delta t\end{aligned}\quad (12.2.3)$$

where the drift velocity is related to the difference in hopping rates

$$v_x = (k_+ - k_-)\Delta x$$

Expressing Equation 12.2.3 as the result of many steps says that the mean of the position distribution behaves like traditional linear motion: $\langle x(t) \rangle = x_0 + v_x t$.

What about the variance in the distribution? Calculating the mean-square value of x from Equation 12.2.1 gives

$$\begin{aligned}\langle x^2(t + \Delta t) \rangle &= \langle x^2(t) \pm 2\Delta x \Delta t k_{\pm} x(t) + (k_+ + k_-)^2 \Delta x^2 \Delta t^2 \rangle \\ &= \langle x^2(t) \rangle + 2v_x \Delta t \langle x(t) \rangle + (k_+ + k_-)\Delta x^2 \Delta t\end{aligned}\quad (12.2.4)$$

where we used $(k_+ + k_-)\Delta t = 1$.

Using this to calculate the variance in x :

$$\sigma^2(t) = (k_+ + k_-)\Delta x^2 t\quad (12.2.5)$$

and then comparing with $\langle x^2 \rangle^{1/2} = 2Dt$, leads to the conclusion that the breadth of the distribution σ spreads as it would in the absence of a drift velocity, and the diffusion coefficient for this biased random walk is given by

$$D = \frac{1}{2}(k_+ + k_-)\Delta x^2$$

When the left and right stepping rates are the same, we recover our earlier result $2D = \Delta x^2/\Delta t$.

This page titled [12.2: Biased Random Walk](#) is shared under a [CC BY-NC-SA 4.0](#) license and was authored, remixed, and/or curated by [Andrei Tokmakoff](#) via [source content](#) that was edited to the style and standards of the LibreTexts platform.

12.3: Diffusion in a Potential

Fokker–Planck Equation

Diffusion with drift or diffusion in a velocity field is closely related to diffusion of a particle under the influence of an external force f or potential U .

$$f(x) = -\frac{\partial U}{\partial x}$$

When random forces on a particle dominate the inertial ones, we can equate the drift velocity and external force through the friction coefficient

$$\begin{aligned} m\ddot{x} &= f_d + f_r(t) + f_{ext} \\ f_d &= -\zeta v_x \\ f_{ext} &= \zeta v_x \\ f &= \zeta v_x \end{aligned} \quad (12.3.1)$$

and therefore the contribution of the force or potential to the total flux is

$$J_U = v_x C = \frac{f}{\zeta} C = -\frac{C}{\zeta} \frac{\partial U}{\partial x} \quad (12.3.2)$$

The Fokker–Planck equation refers to stochastic equations of motion for the continuous probability density $\rho(x, t)$ with units of m^{-1} . The corresponding continuity expression for the probability density is

$$\frac{\partial \rho}{\partial t} = -\frac{\partial j}{\partial x}$$

where j is the flux, or probability current, with units of s^{-1} , rather than the flux density we used for continuum diffusion J ($\text{m}^{-2} \text{s}^{-1}$). If the concentration flux is instead expressed in terms of a probability density eq. (12.1.3) becomes

$$j = -D \frac{\partial \rho}{\partial x} + \frac{f(x)}{\zeta} \rho \quad (12.3.3)$$

and the continuity expression is used to obtain the time-evolution of the probability density:

$$\frac{\partial \rho}{\partial t} = D \frac{\partial^2 \rho}{\partial x^2} - \frac{\partial}{\partial x} \left[\frac{f(x)}{\zeta} \rho \right] \quad (12.3.4)$$

This is known as a Fokker–Planck equation.

Smoluchowski Equation

Similarly, we can express diffusion in the presence of an internal interaction potential $U(x)$ using eq. (12.3.2) and the Einstein relation

$$\zeta = \frac{k_B T}{D} \quad (12.3.5)$$

Then the total flux with contributions from the diffusive flux and potential flux can be written as

$$J = -D \frac{\partial C}{\partial x} - \frac{DC}{k_B T} \left(\frac{\partial U}{\partial x} \right) \quad (12.3.6)$$

and the corresponding diffusion equation is

$$\frac{\partial C}{\partial t} = D \left[\frac{\partial^2 C}{\partial x^2} - \frac{\partial}{\partial x} \left[\frac{C}{k_B T} \left(\frac{\partial U}{\partial x} \right) \right] \right] \quad (12.3.7)$$

This is known as the Smoluchowski Equation.

Linear Potential

For the case of a linear external potential, we can write the potential in terms of a constant external force $U = -f_{ext}x$. This makes eq. (12.3.7) identical to eq. (12.1.3), if we use eqs. (12.3.1) and (12.3.5) to define the drift velocity as

$$v_x = \frac{f_{ext}D}{k_B T} \equiv \underset{sim}{f} D$$

$$J = -D \frac{\partial C}{\partial x} + fDC$$

Here I defined $\underset{\sim}{f}$ as the constant external force expressed in units of $k_B T$.

The probability distribution that describes the position of particles released at x_0 after a time t is

$$P(x, t) = \frac{1}{\sqrt{4\pi Dt}} \exp \left[-\frac{(x - x_0 - \underset{\sim}{f}Dt)^2}{4Dt} \right]$$

As expected, the mean position of the diffusing particle is given by $\langle x(t) \rangle = x_0 + v_x t$.

To make use of this, let's calculate the time it takes a monovalent ion to diffuse freely across the width of a membrane (d) under the influence of a linear electrostatic potential of $\Phi = 0.3V$. With $U = e\Phi$

$$t = \frac{d}{v_x} = \frac{k_B T d}{f_{ext} D} = \frac{k_B T d^2}{e\Phi D}$$

Using $d = 4 \text{ nm}$, $D = 10^{-5} \text{ cm}^2/\text{s}$, and $e = 1.6 \times 10^{-19} \text{ C}$, we obtain $t = 1.4 \text{ ns}$.

Steady-State Solutions

For steady-state solutions to the Fokker–Planck or Smoluchowski equations, we can make use of a commonly used mathematical manipulation. As an example, let's work with eq. (12.3.3), re-writing it as

$$j = -D \left[\frac{\partial \rho}{\partial x} - \frac{\rho}{k_B T} \left(\frac{\partial U}{\partial x} \right) \right] \quad (12.3.8)$$

We can rewrite the quantity in brackets as:

$$e^{-U(x)/k_B T} \frac{d}{dx} \left[\rho e^{U(x)/k_B T} \right]$$

Separating variables, we obtain

$$-\frac{j}{D} e^{U(x)/k_B T} dx = d(\rho e^{U(x)/k_B T})$$

This is an expression that can be manipulated in various ways and integrated over different boundary conditions.¹ For instance, recognizing that j is a constant under steady state conditions, and integrating from x to a boundary b :

$$\begin{aligned} -\frac{j}{D} \int_x^b e^{U(x)/k_B T} dx &= \int_x^b d(\rho e^{U(x)/k_B T}) \\ &= \rho(b) e^{U(b)/k_B T} - \rho(x) e^{U(x)/k_B T} \end{aligned}$$

This leads one to an important expression for the steady state flux in the diffusive limit:

$$j = \frac{-D [\rho(b) e^{U(b)/k_B T} - \rho(x) e^{U(x)/k_B T}]}{\int_x^b e^{U(x)/k_B T} dx}$$

The boundary chosen depends on the problem, for instance b is set to infinity in diffusion to capture problems or set as a fixed boundary for first-passage time problems.

For problems involving an absorbing boundary condition, $\rho(b) = 0$, and we can solve for the probability density as

$$\rho(x) = \frac{j}{D} e^{-U(x)/k_B T} \left[\int_x^b e^{U(x')/k_B T} dx' \right]$$

If we integrate both sides of this expression over the entire space, the left hand side is just unity, so we can express the steady-state flux as

$$j = D^{-1} \left[\int_0^b e^{-U(x)/k_B T} \left[\int_x^b e^{U(x')/k_B T} dx' \right] dx \right]^{-1}$$

1. The general three-dimensional expression is $\mathbf{J}(\mathbf{r}, t) = -D e^{-U(\mathbf{r})/k_B T} \nabla \cdot [e^{U(\mathbf{r})/k_B T} \rho(\mathbf{r}, t)]$.

This page titled [12.3: Diffusion in a Potential](#) is shared under a [CC BY-NC-SA 4.0](#) license and was authored, remixed, and/or curated by [Andrei Tokmakoff](#) via [source content](#) that was edited to the style and standards of the LibreTexts platform.

CHAPTER OVERVIEW

13: Friction and the Langevin Equation

Now let's relate the phenomena of Brownian motion and diffusion to the concept of friction, i.e., the resistance to movement that the particle in the fluid experiences. These concepts were developed by Einstein in the case of microscopic motion under thermal excitation, and macroscopically by George Stokes who was the father of hydrodynamic theory.

[13.1: Langevin Equation](#)

[13.2: Brownian Dynamics](#)

This page titled [13: Friction and the Langevin Equation](#) is shared under a [CC BY-NC-SA 4.0](#) license and was authored, remixed, and/or curated by [Andrei Tokmakoff](#) via [source content](#) that was edited to the style and standards of the LibreTexts platform.

13.1: Langevin Equation

Consider the forces acting on a particle as we pull it through a fluid. We pull the particle with an external force f_{ext} , which is opposed by a drag force from the fluid, f_d . The drag or damping acts as resistance to motion of the particle, which results from trying to move the fluid out of the way.

$$f_d = -\zeta v \quad \zeta(\text{kg/s}) \quad (13.1.1)$$

A drag force requires movement, so it is proportional to the velocity of the particle $v = dx/dt = \dot{x}$ and the friction coefficient ζ is the proportionality constant that describes the magnitude of the damping. Newton's second law relates the acceleration of this particle is to the sum of these forces:

$$ma = f_d + f_{ext}$$

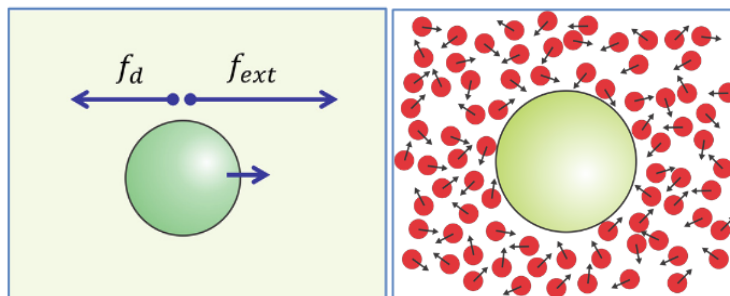


Figure 13.1.1

Now microscopically, we also recognize that there are time-dependent random forces that the molecules of the fluid exert on a molecule (f_r). So that the specific molecular details of solute–solvent collisions can be averaged over, it is useful to think about a nanoscale solute in water (e.g., biological macromolecules) with dimensions large enough that its position is simultaneously influenced by many solvent molecules, but is also light enough that the constant interactions with the solvent leave an unbalanced force acting on the solute at any moment in time:

$$\bar{f}_r(t) = -\sum_i \bar{f}_i(t)$$

Then Newton's second law is

$$ma = f_d + f_{ext} + f_r(t)$$

The drag force is present regardless of whether an external force is present, so in the absence of external forces ($f_{ext} = 0$) the equation of motion governing the spontaneous fluctuations of this solute is determined from the forces due to drag and the random fluctuations:

$$ma = f_d + f_r(t) \quad (13.1.2)$$

$$m\ddot{x} + \zeta\dot{x} - f_r(t) = 0 \quad (13.1.3)$$

This equation of motion is the **Langevin equation**. An equation of motion such as this that includes a time-dependent random force is known as “**stochastic**”.

Inserting a random process into a deterministic equation means that we need to use a statistical approach to solve this equation. We will be looking to describe the average and root-mean-squared position of the particle. First, what can we say about the random force? Although there may be momentary imbalances, on average the perturbations from the solvent on a larger particle will average to zero at equilibrium:

$$\langle f_r(t) \rangle = 0 \quad (13.1.4)$$

Equation 13.1.2 seems to imply that the drag force and the random force are independent, but in fact they originate in the same molecular forces. If the molecule of interest is a protein that experiences the fluctuations of many rapidly moving solvent molecules, then the averaged forces due to random fluctuations and the drag forces are related. The **fluctuation–dissipation**

theorem is the general relationship that relates the friction to the correlation function for the random force. In the Markovian limit this is

$$\langle f_r(t)f_r(t') \rangle = 2\zeta k_B T \delta(t-t') \quad (13.1.5)$$

or

$$\zeta = \frac{\langle f_r^2 \rangle}{2k_B T}$$

Markovian indicates that no correlation exists between the random force for $|t-t'| > 0$. More generally, we can recover the friction coefficient from the integral over the correlation function for the random force

$$\zeta = \frac{1}{2k_B T} \int_{-\infty}^{+\infty} dt \langle f_R(0)f_R(t) \rangle$$

To describe the time evolution of the position of our protein molecule, we would like to obtain an expression for mean-square displacement $\langle x^2(t) \rangle$. The position of the molecule can be described by integrating over its time-dependent velocity: $x(t) = \int_0^t dt' \dot{x}(t')$, so we can express the mean-square displacement in terms of the velocity autocorrelation function

$$\langle x^2(t) \rangle = \int_0^t dt' \int_0^t dt'' \langle \dot{x}(t')\dot{x}(t'') \rangle \quad (13.1.6)$$

Our approach to obtaining $\langle x^2(t) \rangle$ starts by multiplying eq. (13.1.2) by x and then ensemble averaging.

$$m \langle x \frac{d}{dt} \dot{x} \rangle + \zeta \langle x \dot{x} \rangle - \langle x f_r(t) \rangle = 0 \quad (13.1.7)$$

From eq. (13.1.3), the last term is zero, and from the chain rule we know

$$\frac{d}{dt} \langle x \dot{x} \rangle = x \frac{d}{dt} \dot{x} + \frac{dx}{dt} \dot{x} \quad (13.1.8)$$

Therefore, we can write eq. (13.1.6) as

$$m \left(\frac{d}{dt} \langle x \dot{x} \rangle - \langle \dot{x} \dot{x} \rangle \right) + \zeta \langle x \dot{x} \rangle = 0 \quad (13.1.9)$$

Further, the equipartition theorem states that for each translational degree of freedom the kinetic energy is partitioned as

$$\frac{1}{2} m \langle \dot{x}^2 \rangle = \frac{k_B T}{2} \quad (13.1.10)$$

So,

$$m \frac{d}{dt} \langle x \dot{x} \rangle + \zeta \langle x \dot{x} \rangle = k_B T \quad (13.1.11)$$

Here we are describing motion in 1D, but when fluctuations and displacement are included for 3D motion, then we switch $x \rightarrow r$ and $k_B T \rightarrow 3k_B T$. Integrating eq. (13.1.10) twice with respect to time, and using the initial condition $x(0) = 0$, we obtain

$$\langle x^2 \rangle = \frac{2k_B T}{\zeta} \left\{ t + \frac{m}{\zeta} \left[\exp\left(-\frac{\zeta}{m} t\right) - 1 \right] \right\} \quad (13.1.12)$$

in 3D:

$$\langle r^2 \rangle = \frac{6k_B T}{\zeta} \left\{ t + \frac{m}{\zeta} \left[\exp\left(-\frac{\zeta}{m} t\right) - 1 \right] \right\}$$

To investigate eq. (13.1.11), let's consider two limiting cases. We see that m/ζ has units of time, and so we define the relaxation time

$$\tau_C = m/\zeta \quad (13.1.13)$$

and investigate time scale short and long compared to τ_C :

1) For $t \ll \tau_C$, we can expand the exponential in eq. (11) and retain the first three terms, which leads to

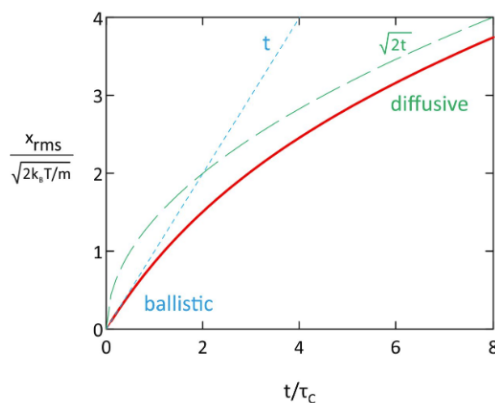
$$\langle x^2 \rangle \approx \frac{k_B T}{m} t^2 = \langle v^2 \rangle t^2 \quad (\text{short time: inertial}) \quad (13.1.14)$$

2) For $t \gg \tau_C$, eq. (11) is dominated by the leading term:

$$\langle x^2 \rangle = \frac{2k_B T}{\zeta} t \quad (\text{long time: diffusive}) \quad (13.1.15)$$

In the diffusive limit the behavior of the molecule is governed entirely by the fluid, and its mass does not matter. The diffusive limit in a stochastic equation of motion is equivalent to setting $m \rightarrow 0$.

We see that τ_C is a time-scale separating motion in the inertial and diffusive limits. It is a correlation time for the randomization of the velocity of the particle due to the random fluctuations of the environment.



For very little friction or short time, the particle moves with traditional deterministic motion $x_{\text{rms}} = v_{\text{rms}} t$, where root-mean-square displacement $x_{\text{rms}} = \langle x^2 \rangle^{1/2}$ and v_{rms} comes from the average translational kinetic energy of the particle. For high-friction or long times, we see diffusive behavior with $x_{\text{rms}} \sim t^{1/2}$. Furthermore, by comparing eq. (13.1.14) to our earlier continuum result, $\langle x^2 \rangle = 2Dt$, we see that the diffusion constant can be related to the friction coefficient by

$$D = \frac{k_B T}{\zeta} \quad (\text{in 1D}) \quad (13.1.16)$$

This is the Einstein formula. For 3D problems, we replace $k_B T$ with $3k_B T$ in the expressions above and find $D_{3D} = 3k_B T / \zeta$.

$$\tau_C = \frac{m}{\zeta} = \frac{mD}{k_B T} \quad (\text{in 1D})$$

How long does it take to approach the diffusive regime? Very fast. Consider a 100 kDa protein with $R = 3$ nm in water at $T = 300$ K, we find a characteristic correlation time for randomizing velocities of $\tau_C = 3 \times 10^{-12}$ s, which corresponds to a distance of about 10^{-2} nm before the onset of diffusive behavior.

We can find other relationships. Noting the relationship of $\langle x^2 \rangle$ to the velocity autocorrelation function in eq. (13.1.5), we find that the particle velocity is described by

$$\langle v_x(0)v_x(t) \rangle = \langle v_x^2 \rangle e^{-\zeta t/m} = \langle v_x^2 \rangle e^{-t/\tau_C} \quad v_x = \dot{x}$$

which can be integrated over time to obtain the diffusion constant.

$$\int_0^\infty \langle v_x(0)v_x(t) \rangle dt = \frac{k_B T}{\zeta} = D \quad (13.1.17)$$

This expression is the Green–Kubo relationship. This is a practical way of analyzing molecular trajectories in simulations or using particle-tracking experiments to quantify diffusion constants or friction coefficients.

This page titled [13.1: Langevin Equation](#) is shared under a [CC BY-NC-SA 4.0](#) license and was authored, remixed, and/or curated by [Andrei Tokmakoff](#) via [source content](#) that was edited to the style and standards of the LibreTexts platform.

13.2: Brownian Dynamics

The Langevin equation for the motion of a Brownian particle can be modified to account for an additional external force, in addition to the drag force and random force. From Newton's Second Law:

$$m\ddot{x} = f_d + f_r(t) + f_{ext}(t)$$

where the added force is obtained from the gradient of the potential it experiences:

$$f_{ext} = -\frac{\partial U}{\partial x} \quad (13.2.1)$$

With the fluctuation-dissipation relation $\langle f_r(t)f_r(t') \rangle = 2\zeta k_B T \delta(t-t')$, the Langevin equation becomes

$$m\ddot{x} + (\partial U / \partial x) + \zeta \dot{x} - \sqrt{2\zeta k_B T} R(t) = 0 \quad (13.2.2)$$

Here $R(t)$ refers to a Gaussian distributed sequence of random numbers with $\langle R(t) \rangle = 0$ and $\langle R(t)R(t') \rangle = \delta(t-t')$.

Brownian dynamics simulations are performed using this equation of motion in the diffusion-dominated, or strong friction limit $|m\ddot{x}| \ll |\zeta \dot{x}|$. Then, we can neglect inertial motion, and set the acceleration of the particle to zero to obtain an expression for the velocity of the particle

$$\dot{x}(t) = \frac{\partial U}{\partial x} - \sqrt{2k_B T / \zeta} R(t)$$

We then integrate this equation of motion in the presence of random perturbations to determine the dynamics $x(t)$.

Readings

1. R. Zwanzig, Nonequilibrium Statistical Mechanics. (Oxford University Press, New York, 2001).
2. B. J. Berne and R. Pecora, Dynamic Light Scattering: With Applications to Chemistry, Biology, and Physics. (Wiley, New York, 1976).

This page titled [13.2: Brownian Dynamics](#) is shared under a [CC BY-NC-SA 4.0](#) license and was authored, remixed, and/or curated by [Andrei Tokmakoff](#) via [source content](#) that was edited to the style and standards of the LibreTexts platform.

SECTION OVERVIEW

4: Transport

14: Hydrodynamics

14.1: Newtonian Fluids

14.2: Stokes' Law

14.3: Laminar and Turbulent Flow

15: Passive Transport

15.1: Dimensionality Reduction

15.2: Facilitated Diffusion

15.3: Search Times in Facilitated Diffusion

16: Targeted Diffusion

16.1: Diffusion to Capture

16.2: Diffusion to Capture with Interactions

16.3: Mean First Passage Time

17: Directed and Active Transport

17.1: Motor Proteins

17.2: Passive vs Active Transport

17.3: Brownian Ratchet

17.4: Polymerization Ratchet and Translocation Ratchet

This page titled [4: Transport](#) is shared under a [CC BY-NC-SA 4.0](#) license and was authored, remixed, and/or curated by [Andrei Tokmakoff](#) via [source content](#) that was edited to the style and standards of the LibreTexts platform.

CHAPTER OVERVIEW

14: Hydrodynamics

- Diffusion equations, random walks, and the Langevin equation are useful for describing transport driven by random thermal forces under equilibrium conditions or not far from equilibrium (the linear response regime).
- Fluid Dynamics and hydrodynamics refer to continuum approaches that allows us to describe non-equilibrium conditions for transport in fluids. Hydrodynamics describes flow and transport of objects through a fluid experiencing resistance or friction.

[14.1: Newtonian Fluids](#)

[14.2: Stokes' Law](#)

[14.3: Laminar and Turbulent Flow](#)

This page titled [14: Hydrodynamics](#) is shared under a [CC BY-NC-SA 4.0](#) license and was authored, remixed, and/or curated by [Andrei Tokmakoff](#) via [source content](#) that was edited to the style and standards of the LibreTexts platform.

14.1: Newtonian Fluids

- Fluids described through continuum mechanics.
 - Stress: Force applied to an object. Stress is force applied over a surface area, a . Force has normal (z) and parallel components (x).
 - The stress can be decomposed it into the normal component perpendicular to the surface \vec{f}_z/a , and the shear stress parallel to the surface \vec{f}_x/a .
 - Strain: The deformation (change in dimension) of object as a result of the stress.
- Solids
 - A solid is considered Newtonian if its behavior follows a linear relationship between elastic stress and strain, i.e. Hooke's Law.
 - Solids are stiff and will return to their original configuration when stressed, but can't deform far (without rupture).
- Fluids
 - Fluids cannot support a strain and remain at equilibrium. Conservation of momentum dictates that application of a force will induce a flow.
 - Fluids resist flow (viscous flow).
 - Newtonian fluids follow a linear relation between shear stress and the strain rate.

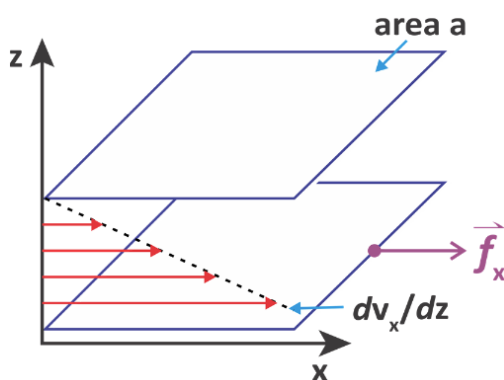
Viscosity

Viscosity measures the resistance to shear forces. A fluid is placed between two plates of area a separated along z , and one plate is moved relative to the other by applying a shear force along x . At contact, the velocity of the fluid at the interface with either plate is equal to the velocity of the plate as a result of intermolecular interactions: $\vec{v}_x(z=0) = 0$. This is known as the no-slip boundary condition. The movement of one plate with respect to the other sets up a velocity gradient along z . This velocity gradient is equal to the strain rate.

The relationship between the shear velocity gradient and the force is

$$\vec{f}_x = a\eta \frac{d\vec{v}_x}{dz}$$

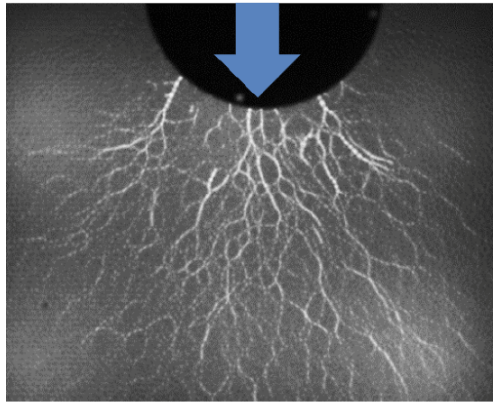
where η , the dynamic viscosity ($\text{kg m}^{-1} \text{s}^{-1}$), is the proportionality factor. For water at 25°C , the dynamic viscosity is $\eta = 8.9 \times 10^{-3} \text{ Pa s}$.



Stresses in a Dense Particle Fluid

A normal stress is a pressure (force per unit area), and these forces are transmitted through a fluid as a result of the conservation of momentum in an incompressible medium. This force transduction also means that a stress applied in one direction can induce a strain in another, i.e. a stress tensor is needed to describe the proportionality between the stress and strain vectors.

In an anisotropic particulate system, force transmission from one region of the fluid to another results from "force chains" involving steaming motion of particles that repel each other. These force chains are not simply unidirectional, but also branch into networks that bypass unaffected regions of the system.



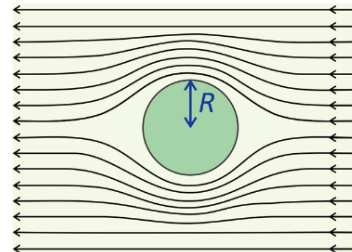
Adapted from National Science Foundation, “Granular Materials”, June 15, 2012. Copyright 2012 National Science Foundation.
<https://www.youtube.com/watch?v=R7g6wdmYB78>

This page titled [14.1: Newtonian Fluids](#) is shared under a [CC BY-NC-SA 4.0](#) license and was authored, remixed, and/or curated by [Andrei Tokmakoff](#) via [source content](#) that was edited to the style and standards of the LibreTexts platform.

14.2: Stokes' Law

How is a fluid's macroscopic resistance to flow related to microscopic friction originating in random forces between the fluid's molecules? In discussing the Langevin equation, we noted that the friction coefficient ζ was the proportionality constant between the drag force experienced by an object and its velocity through the fluid: $f_d = -\zeta v$. Since this drag force is equal and opposite to the stress exerted on an object as it moves through a fluid, there is a relationship of the drag force to the fluid viscosity. Specifically, we can show that Einstein's friction coefficient ζ is related to the dynamic viscosity of the fluid η , as well as other factors describing the size and shape of the object (but not its mass).

This connection is possible as a result of George Stokes' description of the fluid velocity field around a sphere moving through a viscous fluid at a constant velocity. He considered a sphere of radius R moving through a fluid with laminar flow: that in which the fluid exhibits smooth parallel velocity profiles without lateral mixing. Under those conditions, and no-slip boundary conditions, one finds that the drag force on a sphere is



$$f_d = 6\pi\eta R_h v$$

and viscous force per unit area is entirely uniform across the surface of the sphere. This gives us Stokes' Law

$$\zeta = 6\pi\eta R_h \quad (14.2.1)$$

Here R_h is referred to as the hydrodynamic radius of the sphere, the radius at which one can apply the no-slip boundary condition, but which on a molecular scale may include water that is strongly bound to the molecule. Combining eq. (1) with the Einstein formula for diffusion coefficient, $D = k_B T / \zeta$ gives the Stokes–Einstein relationship for the translation diffusion constant of a sphere¹

$$D_{trans} = \frac{k_B T}{6\pi\eta R_h} \quad (14.2.2)$$

One can obtain a similar a Stokes–Einstein relationship for orientational diffusion of a sphere in a viscous fluid. Relating the orientational diffusion constant and the drag force that arises from resistance to shear, one obtains

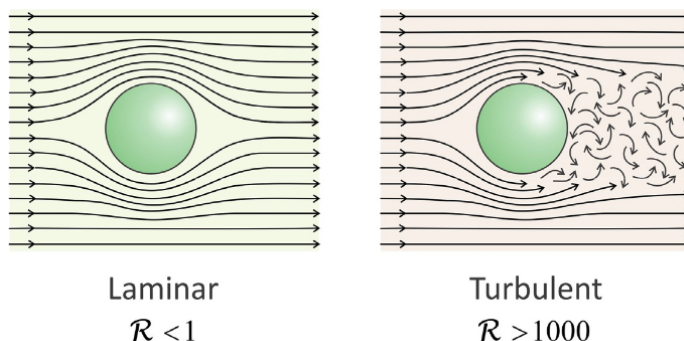
$$D_{rot} = \frac{k_B T}{6V_h \eta}$$

1. B. J. Berne and R. Pecora, Dynamic Light Scattering: With Applications to Chemistry, Biology, and Physics. (Wiley, New York, 1976), pp. 78, 91.

This page titled [14.2: Stokes' Law](#) is shared under a [CC BY-NC-SA 4.0](#) license and was authored, remixed, and/or curated by [Andrei Tokmakoff](#) via [source content](#) that was edited to the style and standards of the LibreTexts platform.

14.3: Laminar and Turbulent Flow

- Laminar flow: Fluid travels in smooth parallel lines without lateral mixing.
- Turbulent flow: Flow velocity field is unstable, with vortices that dissipate kinetic energy of fluid more rapidly than laminar regime.



Reynolds Number

The Reynolds number is a dimensionless number used to indicate whether flow conditions are in the laminar or turbulent regimes. It indicates whether the motion of a particle in a fluid is dominated by inertial or viscous forces.¹

$$\mathcal{R} = \frac{\text{inertial forces}}{\text{viscous forces}}$$

When $\mathcal{R} > 1$, the particle moves freely, experiencing only weak resistance to its motion by the fluid. If $\mathcal{R} < 1$, it is dominated by the resistance and internal forces of the fluid. For the latter case, we can consider the limit $m \rightarrow 0$ in eq. **Error! Reference source not found.**, and find that the velocity of the particle is proportional to the random fluctuations: $v(t) = f_r(t)/\zeta$.

We can also express the Reynolds number in other forms:

- In terms of the fluid velocity flow properties: $\mathcal{R} = \frac{v\rho(d\bar{v}/dz)}{\eta(d^2\bar{v}/dz^2)}$
- In terms of the Langevin variables: $\mathcal{R} = f_{in}/f_d$.

Hydrodynamically, for a sphere of radius r moving through a fluid with dynamic viscosity η and density ρ at velocity v ,

$$\mathcal{R} = \frac{rv\rho}{\eta}$$

Consider for an object with radius 1 cm moving at 10 cm/s through water: $\mathcal{R} = 10^3$. Now compare to a protein with radius 1 nm moving at 10 m/s: $\mathcal{R} = 10^{-2}$.

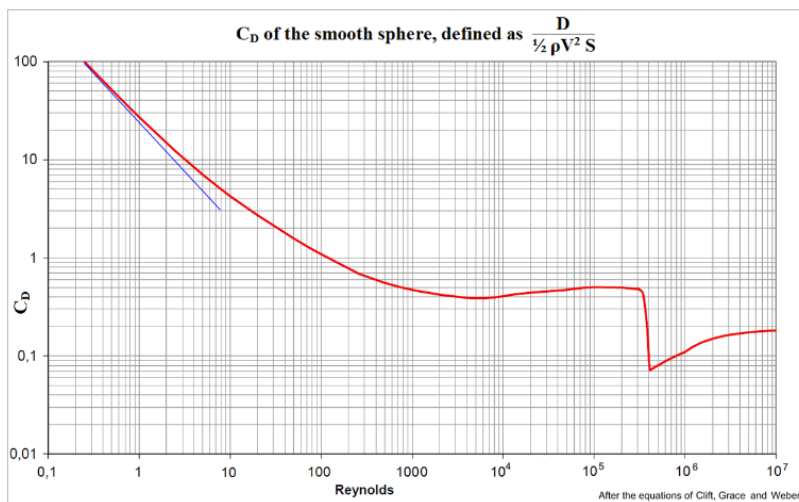
Drag Force in Hydrodynamics

The drag force on an object is determined by the force required to displace the fluid against the direction of flow. A sphere, rod, or cube with the same mass and surface area will respond differently to flow. Empirically, the drag force on an object can be expressed as

$$f_d = \left[\frac{1}{2} \rho C_d v^2 \right] a$$

This expression takes the form of a pressure (term in brackets) exerted on the cross-sectional area of the object along the direction of flow, a . C_d is the drag coefficient, a dimensionless proportionality constant that depends on the shape of the object. In the case of a sphere of radius r : $a = \pi r^2$ in the turbulent flow regime ($\mathcal{R} > 1000$) $C_d = 0.44-0.47$. Determination of C_d is somewhat empirical since it depends on \mathcal{R} and the type of flow around the sphere.

The drag coefficient for a sphere in the viscous/laminar/Stokes flow regimes ($\mathcal{R} < 1$) is $C_d = 24/\mathcal{R}$. This comes from using the Stokes Law for the drag force on a sphere $f_d = 6\pi\eta vr$ and the Reynolds number $\mathcal{R} = \rho vd/\eta$.



Shape	Drag Coefficient
Sphere	0.47
Half-sphere	0.42
Cone	0.50
Cube	1.05
Angled Cube	0.80
Long Cylinder	0.82
Short Cylinder	1.15
Streamlined Body	0.04
Streamlined Half-body	0.09

Measured Drag Coefficients

Reprinted with permission from [Bernard de Go Mars](#), [Drag coefficient of a sphere as a function of Reynolds number](#), [CC BY-SA 3.0](#).

1. E. M. Purcell, Life at low Reynolds number, Am. J. Phys. 45, 3–11 (1977).

This page titled [14.3: Laminar and Turbulent Flow](#) is shared under a [CC BY-NC-SA 4.0](#) license and was authored, remixed, and/or curated by [Andrei Tokmakoff](#) via [source content](#) that was edited to the style and standards of the LibreTexts platform.

CHAPTER OVERVIEW

15: Passive Transport

Passive transport is often synonymous with diffusion, where thermal energy is the only source of motion.

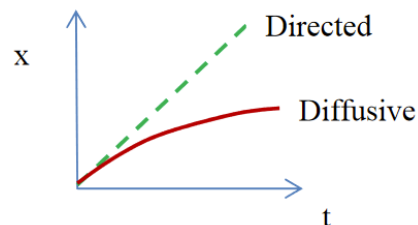
$$\langle r(t) \rangle = 0 \qquad \langle r^2(t) \rangle^{1/2} = \sqrt{6Dt} \qquad r_{rms} \propto \sqrt{t}$$

In biological systems, diffusive transport may work on a short scale, but it is not effective for long-range transport. Consider:

$$\langle r^2 \rangle^{1/2} \text{ for small protein moving in water}$$

$$\sim 10 \text{ nm} \rightarrow 10^{-7} \text{ s}$$

$$\sim 10 \text{ } \mu\text{m} \rightarrow 10^{-1} \text{ s}$$



Active transport refers to directed motion:

$$\langle r(t) \rangle = \langle v \rangle t \qquad r \propto t$$

This requires an input of energy into the system, however, we must still deal with random thermal fluctuations.

How do you speed up transport?

We will discuss these possibilities:

- Reduce dimensionality: Facilitated diffusion
- Free energy (chemical potential) gradient: Diffusion in a potential
- Directional: Requires input of energy, which drives the switching between two conformational states of the moving particle tied to translation.

[15.1: Dimensionality Reduction](#)

[15.2: Facilitated Diffusion](#)

[15.3: Search Times in Facilitated Diffusion](#)

This page titled [15: Passive Transport](#) is shared under a [CC BY-NC-SA 4.0](#) license and was authored, remixed, and/or curated by [Andrei Tokmakoff](#) via [source content](#) that was edited to the style and standards of the LibreTexts platform.

15.1: Dimensionality Reduction

One approach that does not require energy input works by recognizing that displacement is faster in systems with reduced dimensionality. Let's think about the time it takes to diffusively encounter a small fixed target in a large volume, and how this depends on the dimensionality of the search. We will look at the mean first passage time to find a small target with radius b centered in a spherical volume with radius R , where $R \gg b$. If the molecules are initially uniformly distributed within the volume the average time it takes for them to encounter the target (i.e., MFPT) is¹

$$\langle \tau_{3D} \rangle \simeq \frac{R^2}{3D_3} \left(\frac{R}{b} \right) \quad R \gg b$$

$$\langle \tau_{2D} \rangle \simeq \frac{R^2}{2D_2} \ln \left(\frac{R}{b} \right) \quad R \gg b$$

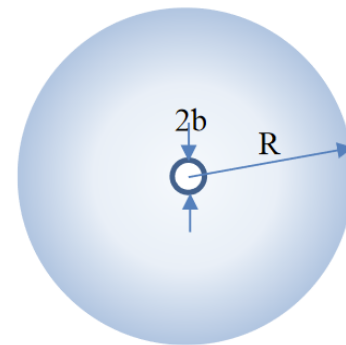
$$\langle \tau_{1D} \rangle \simeq \frac{R^2}{3D_1}$$

Here D_n is the diffusion constants in n dimensions (cm^2/sec). If we assume that the magnitude of D does not vary much with n , the leading terms in these expressions are about equal, and the big differences are in the last factor

$$\left(\frac{R}{b} \right) > \ln \left(\frac{R}{b} \right) \gg 1$$

$$\langle \tau_{3D} \rangle > \langle \tau_{2D} \rangle \gg \langle \tau_{1D} \rangle$$

Based on the volume that needs searching, there can be a tremendous advantage to lowering the dimensionality.



-
1. O. G. Berg and P. H. von Hippel, Diffusion-controlled macromolecular interactions, *Annu. Rev. Biophys. Biophys. Chem.* 14, 131-158 (1985); H. C. Berg and E. M. Purcell, Physics of chemoreception, *Biophys. J.* 20, 193-219 (1977).

This page titled [15.1: Dimensionality Reduction](#) is shared under a [CC BY-NC-SA 4.0](#) license and was authored, remixed, and/or curated by [Andrei Tokmakoff](#) via [source content](#) that was edited to the style and standards of the LibreTexts platform.

15.2: Facilitated Diffusion

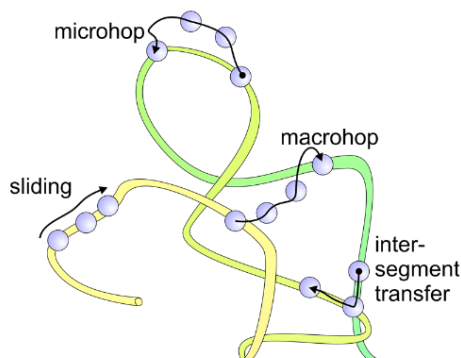
Facilitated diffusion is a type of dimensionality reduction that has been used to describe the motion of transcription factors and regulatory proteins looking for their binding target on DNA.¹

E. coli Lac Repressor

Experiments by Riggs et al. showed that *E. coli* Lac repressor finds its binding site about one hundred times faster than expected by 3D diffusion.² They measured $k_a = 7 \times 10^9 \text{ M}^{-1} \text{ s}^{-1}$, which is 100–1000 times faster than typical rates. The calculated diffusion-limited association rate from the Smoluchowski equation is $k_a \approx 10^8 \text{ M}^{-1} \text{ s}^{-1}$ using estimated values of $D \approx 5 \times 10^{-7} \text{ cm}^2 \text{ s}^{-1}$ and $R \approx 5 \times 10^{-8} \text{ cm}$. Berg and von Hippel theoretically described the possible ways in which nonspecific binding to DNA enabled more efficient one-dimensional motion coupled to three-dimensional transport.³

Many Possibilities for Locating Targets Diffusively: Coupled 1D+3D Diffusion

1. Sliding (1D diffusion along chain as a result of nonspecific interaction)
2. Microhop (local translocation with free diffusion)
3. Macrohop (...to distal segment via free diffusion)
4. Intersegmental transfer at crossing—varies with DNA dynamics

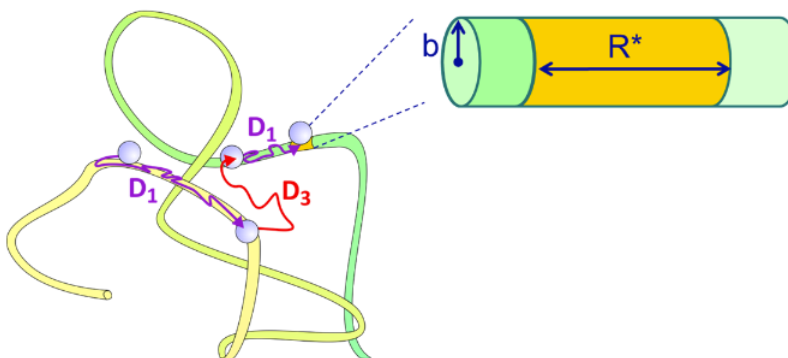


Consider Coupled Sliding and Diffusion: The Steady-State Solution

The transcription factor diffuses in 1D along DNA with the objective of locating a specific binding site. The association of the protein and DNA at all points is governed by a nonspecific interaction. Sliding requires a balance of nonspecific attractive forces that are not too strong (or the protein will not move) or too weak (or it will not stay bound). The nonspecific interaction is governed by an equilibrium constant and exchange rates between the bound and free forms:

$$F \xrightleftharpoons[k_d]{k_a} B \qquad K = \frac{k_a}{k_d} = \frac{\bar{\tau}_{1D}}{\bar{\tau}_{3D}}$$

We can also think of this equilibrium constant in terms of the average times spent diffusing in 1D or 3D. The protein stays bound for a period of time dictated by the dissociation rate k_d . It can then diffuse in 3D until reaching a contact with DNA again, at a point which may be short range in distance but widely separated in sequence.



The target for the transcription factor search can be much larger than the physical size of the binding sequence. Since the 1D sliding is the efficient route to finding the binding site, the target size is effectively covered by the mean 1D diffusion length of the protein, that is, the average distance over which the protein will diffuse in 1D before it dissociates. Since one can express the average time that a protein remains bound as $\bar{\tau}_{1D} = k_d^{-1}$, the target will have DNA contour length of

$$R^* = \left(\frac{4D_1}{k_d} \right)^{1/2}$$

If the DNA is treated as an infinitely long cylinder with radius b , and the protein is considered to have a uniform probability of nonspecifically associating with the entire surface of the DNA, then one can solve for the steady-state solution for the diffusion equation, assuming a completely absorbing target. The rate constant for specific binding to the target has been determined as

$$\eta = \frac{D_1 K'}{D_3 b}$$

where K' is the equilibrium constant for nonspecific binding per unit surface area of the cylinder ($M^{-1} \text{ cm}^{-2}$ or cm). We can express the equilibrium constant per base-pair as $K = 2\pi\ell b K'$, where ℓ is the length of a base pair along the contour of the DNA. The association rate will be given by the product of k_{bind} and the concentration of protein.

-
1. P. H. von Hippel and O. G. Berg, Facilitated target location in biological systems, *J. Biol. Chem.* 264 (2), 675–678 (1989).
 2. A. D. Riggs, S. Bourgeois and M. Cohn, The lac repressor-operator interaction, *J. Mol. Biol.* 53 (3), 401–417 (1970); Y. M. Wang, R. H. Austin and E. C. Cox, Single molecule measurements of repressor protein 1D diffusion on DNA, *Phys. Rev. Lett.* 97 (4), 048302 (2006).
 3. O. G. Berg, R. B. Winter and P. H. Von Hippel, Diffusion-driven mechanisms of protein translocation on nucleic acids. 1. Models and theory, *Biochemistry* 20 (24), 6929–6948 (1981).
-

This page titled [15.2: Facilitated Diffusion](#) is shared under a [CC BY-NC-SA 4.0](#) license and was authored, remixed, and/or curated by [Andrei Tokmakoff](#) via [source content](#) that was edited to the style and standards of the LibreTexts platform.

15.3: Search Times in Facilitated Diffusion

Consider a series of repetitive 1D and 3D diffusion cycles.¹ The search time for a protein to find its target is

$$t_s = \sum_{i=1}^k (\tau_{1D,i} + \tau_{3D,i})$$

where k is the number of cycles. If the genome has a length of M bases and the average number of bases scanned per cycle is \bar{n} , the average number of cycles $\bar{k} = M/\bar{n}$, and the average search time can be written as

$$\bar{t}_s = \frac{M}{\bar{n}} (\bar{\tau}_{1D,i} + \bar{\tau}_{3D,i}) \quad (15.3.1)$$

$\bar{\tau}$ is the mean search time during one cycle. If we assume that sliding occurs through normal 1D diffusion, then we expect that $\bar{n} \propto \sqrt{D_{1D}\bar{\tau}_{1D}}$, where the diffusion constant is expressed in units of bp^2/s . More accurately, it is found that if you executed a random walk with an exponentially weighted distribution of search times:

$$P(\tau_{1D}) = \bar{\tau}_{1D}^{-1} \exp(-\tau_{1D}/\bar{\tau}_{1D})$$

$$\bar{n} = \sqrt{4D_{1D}\bar{\tau}_{1D}}$$

$$\bar{t}_s = \frac{M}{\sqrt{4D_{1D}\bar{\tau}_{1D}}} (\bar{\tau}_{1D} + \bar{\tau}_{3D})$$

Let's calculate the optimal search time, t_{opt} . In the limits that $\bar{\tau}_1$ or $\bar{\tau}_3 \rightarrow 0$, you just have pure 1D or 3D diffusion, but this leads to suboptimal search times because a decrease in $\bar{\tau}_{1D}$ or $\bar{\tau}_{3D}$ leads to an increase in the other. To find the minimum search time we solve:

$$\frac{\partial \bar{t}_s}{\partial \tau_{1D}} = 0$$

and find that t_{opt} corresponds to the condition

$$\bar{\tau}_{1D} = \bar{\tau}_{3D}$$

Using this in eq. (15.3.1) we have

$$t_{\text{opt}} = \frac{2M}{\bar{n}} \bar{\tau}_{3D} = M \sqrt{\frac{\bar{\tau}_{3D}}{D_{1D}}}$$

$$\bar{n}_{\text{opt}} = \sqrt{4D_{1D}\bar{\tau}_{3D}}$$

Now let's find out how much this 1D + 3D search process speeds up over the pure 1D or 3D search.

- **3D only:** $\bar{\tau}_{1D} \rightarrow 0 \quad \therefore \bar{n} \rightarrow \sim 1$ leading to

$$\bar{t}_{3D} = M\bar{\tau}_{3D}$$

Facilitated diffusion speeds up the search relative to pure 3D diffusion by a factor proportional to the average number of bases searched during the 1D sliding.

$$\frac{\bar{t}_{3D}}{(\bar{t}_s)_{\text{opt}}} = \frac{\bar{n}}{2}$$

- **1D only:** $\bar{\tau}_{3D} \rightarrow 0 \quad \therefore \bar{n} \rightarrow M$, and

$$\bar{t}_{1D} \approx \frac{M^2}{4D_{1D}}$$

$$\frac{\bar{\tau}_{1D}}{(\bar{t}_s)_{\text{opt}}} = \frac{M}{4} \sqrt{\frac{1}{D_{1D}\tau_{1D}}} = \frac{M}{\bar{n}}$$

Facilitated diffusion speeds up the search over pure 1D diffusion by a factor of M/\bar{n} .

Example: Bacterial Genome

$$M \approx 5 \times 10^6 \text{ bp}$$

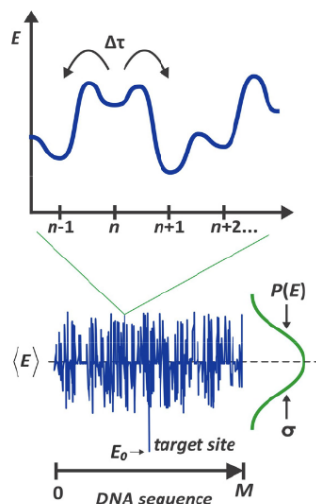
$$\bar{n} \approx 200 - 500 \text{ bp}$$

Optimal facilitated diffusion is $\sim 10^2$ faster than 3D

$\sim 10^4$ faster than 1D

Energetics of Diffusion

What determines the diffusion coefficient for sliding and $\bar{\tau}_1$? We need the non-specific protein interaction to be strong enough that it doesn't dissociate too rapidly, but also weak enough that it can slide rapidly. To analyze this, we use a model in which the protein is diffusing on a modulated energy landscape looking for a low energy binding site.



Model²

- Assume each sequence can have different interaction with the protein.
- Base pairs in binding patch contribute additively and independently to give a binding energy E_n for each site, n .
- Assume that the variation in the binding energies as a function of site follow Gaussian random statistics, characterized by the average binding energy $\langle E \rangle$ and the surface energy roughness σ .
- The protein will attempt to move to an adjacent site at a frequency $\nu = \Delta\tau^{-1}$. The rate of jumping is the probability that the attempt is successful times ν , and depends on the energy difference between adjacent sites, $\Delta E = E_{n\pm 1} - E_n$. The rate is ν if $\Delta E < 0$, and $\nu \cdot \exp[-\Delta E/k_B T]$ for $\Delta E > 0$.

Calculating the mean first passage time to reach a target site at a distance of L base pairs from the original position yields

$$\bar{\tau}_{1D} = L^2 \Delta\tau \left(1 + \frac{1}{2} \left(\frac{\sigma}{k_B T} \right)^2 \right)^{-1/2} e^{-7\sigma^2/4(k_B T)^2}$$

Which follows a diffusive form with a diffusion constant

$$D_{1D} = \frac{L^2}{2\bar{\tau}_{1D}} = \frac{1}{2\Delta\tau} \left(1 + \frac{1}{2} \left(\frac{\sigma}{k_B T} \right)^2 \right)^{1/2} e^{-7\sigma^2/4(k_B T)^2} \quad (15.3.2)$$

Using this to find conditions for the fastest search time:

$$t_{opt} = \frac{M}{2} \sqrt{\frac{\pi \bar{\tau}_{3D}}{4 D_{1D}}} \quad \bar{n}_{opt} = \sqrt{\frac{16}{\pi} D_{1D} \bar{\tau}_{3D}} \quad \bar{\tau}_{1D} = \bar{\tau}_{3D}$$

Speed vs Stability Paradox

Speed: Fast speed \rightarrow fast search in 1D. From eq. (15.3.2), we see that

$$D_{1D} \propto \exp\left[-\left(\frac{\sigma^2}{k_B T}\right)\right] \quad (15.3.3)$$

With this strong dependence on σ , effective sliding with proper \bar{n} requires

$$\sigma < 2k_B T$$

Stability: On the other hand, we need to remain stably bound for proper recognition and activity. To estimate we argue that we want the equilibrium probability of having the protein bound at the target site be $P_{eq} \approx 0.25$. If E_0 is minimum energy of the binding site, and the probability of occupying the binding site is the following. First we can estimate that

$$E_0 \approx -\sigma \sqrt{2 \log M}$$

which suggests that for adequate binding:

$$\sigma > 5k_B T$$

Proposed Two-State Sliding Mechanism

To account for these differences, a model has been proposed:

- While 1D sliding, protein is constantly switching between two states, the search and recognize conformations: $S \rightleftharpoons R$. S binds loosely and allows fast diffusion, whereas R interacts more strongly such that σ increases in the R state.
- These fast conformational transitions must have a rate faster than

$$> \frac{\bar{n}}{\bar{\tau}_{1D}} \sim 10^4 \text{ s}^{-1}$$

- Other Criteria:

$$\langle E_R \rangle < \langle E_S \rangle$$

$$\sigma_R > \sigma_S$$

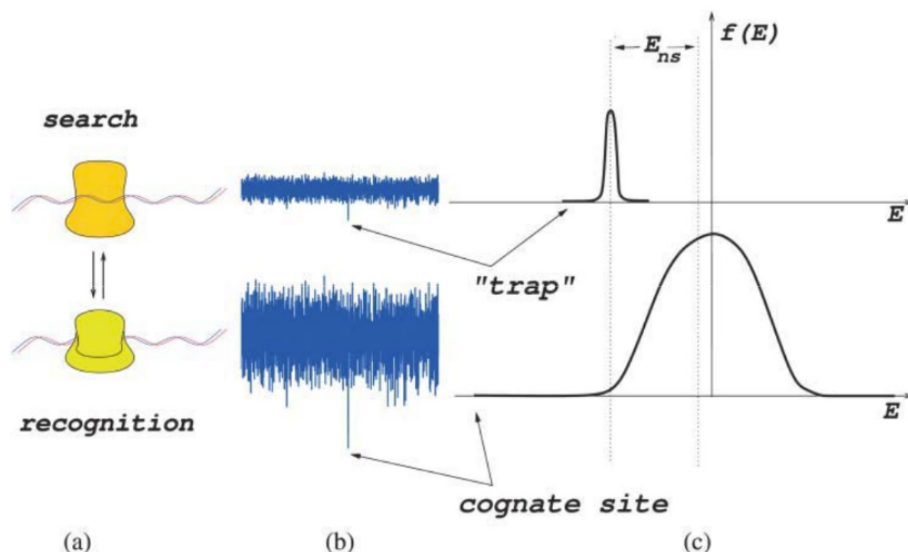


FIGURE 6 Cartoon demonstrating the two-mode search-and-fold mechanism. (Top) Search mode; (bottom) recognition mode. (a) Two conformations of the protein bound to DNA: partially unfolded (top) and fully folded (bottom). (b) The binding energy landscape experienced by the protein in the corresponding conformations. (c) The spectrum of the binding energy determining stability of the protein in the corresponding conformations.

Reprinted from M. Slutsky and L. A. Mirny, Kinetics of protein-DNA interaction: Facilitated target location in sequence-dependent potential, Biophys. J. 87 (6), 4021–4035 (2004), with permission from Elsevier.

Diffusion on rough energy landscape

The observation in eq. (15.3.3), relating the roughness of an energy landscape to an effective diffusion rate is quite general.³ If we are diffusing over a distance long enough that the corrugation of the energy landscape looks like Gaussian random noise with a standard deviation σ , we expect the effective diffusion coefficient to scale as

$$D_{eff} = D_0 \exp \left[- \left(\frac{\sigma^2}{k_B T} \right) \right] \quad (15.3.4)$$

where D_0 is the diffusion constant in the absence of the energy roughness.

Single-Molecule Experiments

To now there still is no definitive evidence for coupled 1D + 3D transport, although there is a lot of data now showing 1D sliding. These studies used flow to stretch DNA and followed the position of fluorescently labelled proteins as they diffused along the DNA.

Austin: Lac Repression follow up \rightarrow observed D_{1D} varies by many orders of magnitude.⁴

$$D_{1D} : 10^2 - 10^5 \text{ nm}^2/\text{s}$$

$$\bar{n} \approx 500 \text{ nm}$$

Blainey and Xie: hOGG1 DNA repair protein:⁵

$$\Delta G_{slide}^\ddagger \approx 0.5 \text{ kcal/mol} \approx k_B T$$

$$D_{1D} \sim 5 \times 10^6 \text{ bp}^2/\text{s}$$

$$\bar{n} \approx 440 \text{ bp}$$

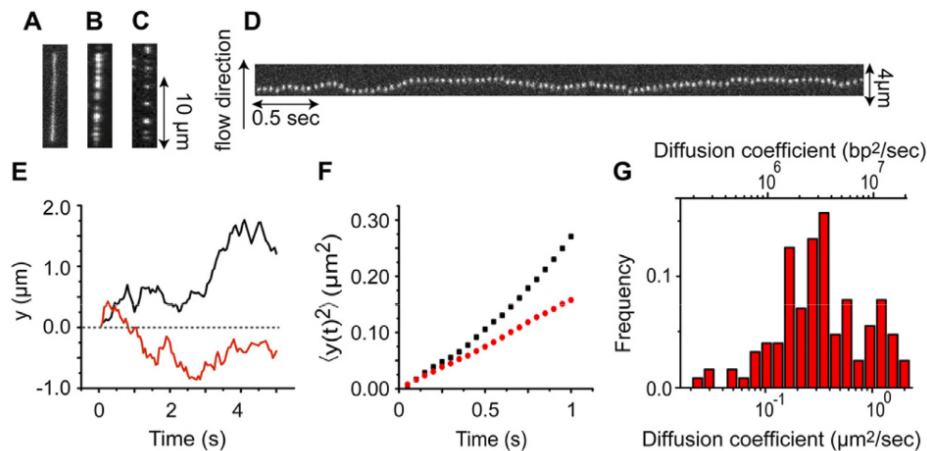


Figure 7. A) Kymograph of an individual fluorescently labeled p53 transcription factor moving along flow-stretched DNA. The x axis represents time and the flow is directed upward along the y-axis. B) Trajectories of two p53 proteins diffusing on λ -DNA. C) Mean square displacement (MSD) versus time of the same two trajectories. D) Histogram of the diffusion coefficient D of 162 individual p53 proteins. Figure reproduced with permission from

Reprinted from A. Tafvizi, F. Huang, J. S. Leith, A. R. Fersht, L. A. Mirny and A. M. van Oijen, Tumor Suppressor p53 Slides on DNA with Low Friction and High Stability, *Biophys. J.* 95 (1), L01–L03 (2008), with permission from Elsevier.

$$D_{1D} \quad 10^6 - 10^7 \text{ bp}^2/\text{s} \approx 10^{-1} - 10^0 \text{ } \mu\text{m}^2/\text{s}$$

1. (5)M. Slutsky and L. A. Mirny, Kinetics of protein-DNA interaction: Facilitated target location in sequence-dependent potential, *Biophys. J.* 87 (6), 4021–4035 (2004); A. Tafvizi, L. A. Mirny and A. M. van Oijen, Dancing on DNA: Kinetic aspects of search processes on DNA, *Chemphyschem* 12 (8), 1481–1489 (2011).
2. M. Slutsky and L. A. Mirny, Kinetics of protein-DNA interaction: Facilitated target location in sequence-dependent potential, *Biophys. J.* 87 (6), 4021–4035 (2004).
3. R. Zwanzig, Diffusion in a rough potential, *Proc. Natl. Acad. Sci. U. S. A.* 85 (7), 2029 (1988).
4. Y. M. Wang, R. H. Austin and E. C. Cox, Single molecule measurements of repressor protein 1D diffusion on DNA, *Phys. Rev. Lett.* 97 (4), 048302 (2006).
5. P. C. Blainey, A. M. van Oijen, A. Banerjee, G. L. Verdine and X. S. Xie, A base-excision DNA-repair protein finds intrahelical lesion bases by fast sliding in contact with DNA, *Proc. Natl. Acad. Sci. U. S. A.* 103 (15), 5752 (2006).

This page titled [15.3: Search Times in Facilitated Diffusion](#) is shared under a [CC BY-NC-SA 4.0](#) license and was authored, remixed, and/or curated by [Andrei Tokmakoff](#) via [source content](#) that was edited to the style and standards of the LibreTexts platform.

CHAPTER OVERVIEW

16: Targeted Diffusion

[16.1: Diffusion to Capture](#)

[16.2: Diffusion to Capture with Interactions](#)

[16.3: Mean First Passage Time](#)

This page titled [16: Targeted Diffusion](#) is shared under a [CC BY-NC-SA 4.0](#) license and was authored, remixed, and/or curated by [Andrei Tokmakoff](#) via [source content](#) that was edited to the style and standards of the LibreTexts platform.

16.1: Diffusion to Capture

In this section we will discuss the kinetics of association of a diffusing particle with a target. What is the rate at which a diffusing molecule reaches its target? These diffusion-to-capture problems show up in many contexts. For instance:

1. Molecule diffusing to fixed target(s). Binding of ligands to enzymes or receptors. Binding of transcription factors to DNA. Here the target may have complex topology or target configurations, but it is fixed relative to a diffusing small molecule ($D_{molec} \gg D_{target}$). The diffusion may occur in 1, 2, and/or 3 dimensions, depending on the problem.
2. Bimolecular Diffusive Encounter. Diffusion limited chemical reactions. How do two molecules diffuse into proximity and react? Reaction–diffusion equations.

We will consider two approaches to dealing with these problems:

1. **Steady-state solutions.** The general strategy is to determine the flux of molecules incident on the target from the steady state solution to the diffusion equation with an absorbing boundary condition at the target to account for loss of diffusing molecules once they reach the target. Then the concentration gradient at the target surface can be used to calculate a flux or rate of collisions.
2. **Mean-first passage time.** This is a time-dependent representation of the rate in which you calculate the average time that it takes for a diffusing object to first reach a target.

Diffusion to Capture by Sphere

What is the rate of encounter of a diffusing species with a spherical target? We can find a steady-state solution by determining the steady-state radial concentration profile $C(r)$. Assume that reaction is immediate on encounter at a radius a . This sets the boundary condition, $C(a) = 0$. We also know the bulk concentration $C_0 = C(\infty)$. From our earlier discussion, the steady state solution to this problem is

$$C(r) = C_0 \left(1 - \frac{a}{r}\right)$$

Next, to calculate the rate of collisions with the sphere, we first calculate the flux density of molecules incident on the surface of the sphere ($r = a$):

$$J(a) = -D \frac{\partial C}{\partial r} \Big|_{r=a} = -\frac{DC_0}{a} \quad (16.1.1)$$

J is expressed as (molec area⁻¹ sec⁻¹) or [(mol/L) area⁻¹ sec⁻¹]. We then calculate the flux, or rate of collisions of molecules with the sphere (molec sec⁻¹), by multiplying the flux density by the surface area of the sphere ($A = 4\pi a^2$):

$$\begin{aligned} j &= \frac{dN}{dt} = JA = \left(\frac{DC_0}{a}\right) (4\pi a^2) \\ &= 4\pi DaC_0 \\ &\equiv kC_0 \end{aligned}$$

We associate the constant or proportionality between rate of collisions and concentration with the pseudo first-order association rate constant, $k = 4\pi Da$, which is proportional to the rate of diffusion to the target and the size of the target.

React-Diffusion

The discussion above describes the rate of collisions of solutes with an absorbing sphere, which are applicable if the absorbing sphere is fixed. For problems involving the encounter between two species that are both diffusing in solution ($A + B \rightarrow X$), you can extend this treatment to the encounter of two types of particles A and B, which are characterized by two bulk concentrations C_A and C_B , two radii R_A and R_B , and two diffusion constants D_A and D_B .

To describe the rate of reaction, we need to calculate the total rate of collisions between A and B molecules. Rather than describing the diffusion of both A and B molecules, it is simpler to fix the frame of reference on B and recognize that we want to describe the diffusion of A with respect to B. In that case, the effective diffusion constant is

$$D = D_a + D_b$$

Furthermore, we expand our encounter radius to the sum of the radii of the two spheres ($R_{AB} = r_A + r_B$). The flux density of A molecules incident on a single B at an encounter radius of R_{AB} is given by eq. (1)

$$J_{a \rightarrow b} = \frac{DC_A}{R_{AB}}$$

Here J describes the number of molecules of A incident per unit area at a radius R_{AB} from B molecules per unit time, [molec A] [area of B]⁻¹ sec⁻¹. If we treat the motion of B to be uncorrelated with A, then the total rate of collisions between A and B can be obtained from the product of $J_{A \rightarrow B}$ with the area of a sphere of radius R_{AB} and the total concentration of B:

$$\begin{aligned} \frac{dN_{A \leftrightarrow B}}{dt} &= J_{A \rightarrow B} A_{AB} C_B \\ &= J_{A \rightarrow B} (4\pi R_{AB}^2) C_B \\ &= 4\pi D R_{AB} C_A C_B \end{aligned}$$

The same result is obtained if we begin with the flux density of B incident on A, $J_{B \rightarrow A}$, using the same encounter radius and diffusion constant. Now comparing this with expected second order rate law for a bimolecular reaction

$$\frac{dN_{A \leftrightarrow B}}{dt} = k_a C_A C_B$$

we see

$$k_a = 4\pi(D_A + D_B)R_{AB}$$

k_a is the rate constant for a diffusion limited reaction (association). It has units of cm³ s⁻¹, which can be converted to (L mol⁻¹ s⁻¹) by multiplying by Avagadro's number.

Reactive patches

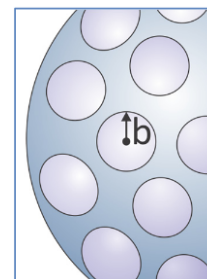
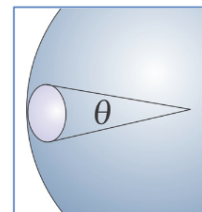
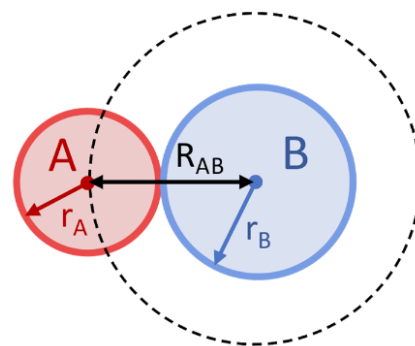
If you modify these expressions so that only part of the sphere is reactive, then similar results ensue, in which one recovers the same diffusion limited association rate ($k_{a,0}$) multiplied by an additional factor that depends on the geometry of the surface area that is active: $k_a = k_{a,0} \cdot [\text{constant}]$. For instance if we consider a small circular patch on a sphere that subtends a half angle θ , the geometric factor should scale as $\sin\theta$. For small θ , $\sin\theta \approx \theta$. If you have small patches on two spheres, which must diffusively encounter each other, the slowing of the association rate relative to the case with the fully accessible spherical surface area is

$$k_a / k_{a,0} = \theta_A \theta_B (\theta_A + \theta_B) / 8$$

For the association rate of molecules with a sphere of radius R covered with n absorbing spots of radius b:

$$k_a = k_{a,0} = \left(1 + \frac{\pi R}{nb}\right)^{-1}$$

Additional configurations are explored in Berg.



1. D. F. Calef and J. M. Deutch, Diffusion-controlled reactions, Annu. Rev. Phys. Chem. 34 (1), 493-524 (1983).

This page titled [16.1: Diffusion to Capture](#) is shared under a [CC BY-NC-SA 4.0](#) license and was authored, remixed, and/or curated by [Andrei Tokmakoff](#) via [source content](#) that was edited to the style and standards of the LibreTexts platform.

16.2: Diffusion to Capture with Interactions

What if the association is influenced by an additional potential for A-B interactions? Following our earlier discussion for diffusion in a potential, the potential U_{AB} results in an additional contribution to the flux:

$$J_U = -\frac{D_A C_A}{k_B T} \frac{\partial U_{AB}}{\partial r}$$

So the total flux of A incident on B from normal diffusion J_{diff} and the interaction potential J_U is

$$J_{A \rightarrow B} = -D_A \left[\frac{\partial C_A}{\partial r} + \frac{C_A}{k_B T} \frac{\partial U_{AB}}{\partial r} \right]$$

To solve this we make use of a mathematical manipulation commonly used in solving the Smoluchowski equation in which we rewrite the quantity in brackets as

$$J_{A \rightarrow B} = -D_A \left[e^{U_{AB}/k_B T} \frac{d [C_A e^{U_{AB}/k_B T}]}{dr} \right] \quad (16.2.1)$$

Substitute this into the expression for the rate of collisions of A with B:

$$\begin{aligned} \frac{dn_{A \rightarrow B}}{dt} &= A_B J_{A \rightarrow B} \\ &= 4\pi R_B^2 J_{A \rightarrow B} \end{aligned}$$

Separate variables and integrate from the surface of the sphere to $r = \infty$ using the boundary conditions: $C(R_B) = 0, C(\infty) = C_A$:

$$\left(\frac{dn_{A \rightarrow B}}{dt} \right) \underbrace{\int_{R_B}^{\infty} e^{U_{AB}/k_B T} \frac{dr}{r^2}}_{(R^*)^{-1}} = 4\pi D_A \underbrace{\int_0^{C_A} d [C_A e^{U_{AB}/k_B T}]}_{C_A} \quad (16.2.2)$$

Note that integral on the right is just the bulk concentration of A. The integral on the right has units of inverse distance, and we can write this in terms of the variable R^* :

$$(R^*)^{-1} = \int_{R_B}^{\infty} e^{U_{AB}/k_B T} r^{-2} dr$$

Note that when no potential is present, then $U_{AB} \rightarrow 0$, and $R^* = R_B$. Therefore R^* is an effective encounter distance which accounts for the added influence of the interaction potential, and we can express it in terms of f , a correction factor the normal encounter radius: $R^* = f R_B$. For attractive interactions $R^* > R_B$ and $f > 1$, and vice versa.¹

Returning to eq. (16.2.2), we see that the rate of collisions of A with B is

$$\frac{dn_{A \rightarrow B}}{dt} = 4\pi D_A R^* C_A$$

As before, if we account for the total number of collisions for two diffusing molecules A and B:

$$\begin{aligned} \frac{dn_{TOT}}{dt} &= J_{A \rightarrow B} A_{AB} C_B \\ &= k_a C_A C_B \\ k_a &= 4\pi (D_A + D_B) R_{AB}^* \\ R_{AB}^* &= R_A^* + R_B^* \end{aligned}$$

Example: Electrostatic potential²

Let's calculate the form of the where the interaction is the Coulomb potential.³

$$U_{AB}(r) = \frac{z_A z_B e^2}{4\pi\epsilon r} = k_B T \frac{\ell_B}{r}$$

where the Bjerrum length is $\ell_B = z_A z_B e^2 / (4\pi\epsilon k_B T)$. Then

$$\begin{aligned} (R_{AB}^*)^{-1} &= \int_{R_{AB}}^{\infty} e^{U_{AB}/k_B T} \frac{dr}{r^2} \\ &= \ell_B^{-1} [\exp(\ell_B/R_{AB}) - 1] \end{aligned}$$

and

$$R_{AB}^* = \ell_B (e^{\ell_B/R_{AB}} - 1)^{-1}$$

For $\ell_B \gg R_{AB}$, $R_{AB}^* \rightarrow R_{AB}$. For $\ell_B = R_{AB}$, $R_{AB}^* = 0.58R_{AB}$ if the charges have the same sign (repel), or $R_{AB}^* = 1.58R_{AB}$ if they are opposite charges (attract).

$$4\pi r^2 J_{A \rightarrow B} = \frac{4\pi D_A [C_A(\infty)e^{U_{AB}(\infty)/k_B T} - C_A(R_0)e^{U_{AB}(R_0)/k_B T}]}{\int_{R_0}^{\infty} r^{-2} e^{U_{AB}(r)/k_B T} dr}$$

$C_A(\infty)$ is the bulk concentration of A. For the perfectly absorbing sphere, the concentration of A at the boundary with B, $C_A(R_0)=0$. For a homogeneous solution we also assume that the interaction potential at long range $U_{AB}(\infty) = 0$.

1. A more general form for the flux, in which the boundary condition at the surface of the sphere $C_A(R_0)$ is non-zero, for instance when there is an additional chemical reaction on contact, is
2. See also J. I. Steinfeld, Chemical Kinetics and Dynamics, 2nd ed. (Prentice Hall, Upper Saddle River, N.J., 1998), 4.2-4.4.
3. See M. Vijayakumar, K.-Y. Wong, G. Schreiber, A. R. Fersht, A. Szabo and H.-X. Zhou, Electrostatic enhancement of diffusion-controlled protein-protein association: comparison of theory and experiment on barnase and barstar, J. Mol. Biol. 278 (5), 1015-1024 (1998).

This page titled [16.2: Diffusion to Capture with Interactions](#) is shared under a [CC BY-NC-SA 4.0](#) license and was authored, remixed, and/or curated by [Andrei Tokmakoff](#) via [source content](#) that was edited to the style and standards of the LibreTexts platform.

16.3: Mean First Passage Time

Another way of describing diffusion-to-target rates is in terms of first passage times. The mean first passage time (MFPT), $\langle \tau \rangle$, is the average time it takes for a diffusing particle to reach a target position for the first time. The inverse of $\langle \tau \rangle$ gives the rate of the corresponding diffusion-limited reaction. A first passage time approach is particularly relevant to problems in which a description the time-dependent averages hide intrinsically important behavior of outliers and rare events, particularly in the analysis of single molecule kinetics.

To describe first passage times, we begin by defining the reaction probability R and the survival probability S . R is a conditional probability function that describes the probability that a molecule starting at a point $x_0 = 0$ at time t_0 will reach a reaction boundary at $x = x_f$ for the first time after time t : $R(x_f, t | x_0, t_0)$. S is just the conditional probability that the molecule has *not* reached $x = b$ during that time interval: $S(x_f, t | x_0, t_0)$. Therefore

$$R + S = 1$$

Next, we define $F(\tau, x_f | x_0)$, the first passage probability density. $F(\tau)d\tau$ is the probability that a molecule passes through $x = x_f$ for the first time between times τ and $\tau + d\tau$. R , S , and F are only a function of time for a fixed position of the reaction boundary, i.e. they integrate over any spatial variations. To connect F with the survival probability, we recognize that the reaction probability can be obtained by integrating over all possible first passage times for time intervals $\tau < t$. Dropping space variables, recognizing that $(t - t_0) = \tau$, and setting $x_0 = 0$,

$$R(t) = \int_0^t F(\tau) d\tau$$

This relation implies that the first passage time distribution can be obtained by differentiating S

$$F(t) = \frac{\partial}{\partial t} R(t) = -\frac{\partial}{\partial t} S(t) \quad (16.3.1)$$

Then the MFPT is obtained by averaging over $F(t)$

$$\langle \tau \rangle = \int_0^\infty \tau F(\tau) d\tau \quad (16.3.2)$$

To evaluate these quantities for a particular problem, we seek to relate them to the time-dependent probability density, $P(x, t | x_0, t_0)$, which is an explicit function of time and space. The connection between P and F is not immediately obvious because evaluating P at $x = x_f$ without the proper boundary conditions includes trajectories that have passed through $x = x_f$ before returning there again later. The key to relating these is to recognize that the survival probability can be obtained by calculating a diffusion problem with an absorbing boundary condition at $x = x_f$ that does not allow the particle to escape: $P(x_f, t | x_0) = 0$. The resulting probability distribution $P_a(x, t | x_0, t_0)$ is not conserved but gradually loses probability density with time. Hence, we can see that the survival probability is an integral over the remaining probability density that describes particles that have not yet reached the boundary:

$$S(t) = \int_{-\infty}^{x_f} dx P_a(x, t) \quad (16.3.3)$$

The mean free passage time can be written as

$$\langle \tau \rangle = \int_{-\infty}^{x_f} dx \int_0^\infty dt P_a(x, t)$$

The next important realization is that the first passage time distribution is related to the flux of diffusing particles through x_f . Combining eq. (16.3.1) and (16.3.3) shows us

$$F(t) = - \int_{-\infty}^{x_f} dx \frac{\partial}{\partial t} P_a(x, t) \quad (16.3.4)$$

Next we make use of the continuity expression for the probability density

$$\frac{\partial P}{\partial t} = - \frac{\partial j}{\partial x}$$

j is a flux, or probability current, with units of s^{-1} , not the flux density we used for continuum diffusion J ($m^{-2} s^{-1}$). Then eq. (16.3.4) becomes

$$F(t) = \int_{-\infty}^{x_f} dx \frac{\partial}{\partial x} j_a(x, t) = j_a(x_f, t) \quad (16.3.5)$$

So the first passage time distribution is equal to the flux distribution for particles crossing the boundary at time t . Furthermore, from eq. (16.3.2), we see that the MFPT is just the inverse of the average flux of particles crossing the absorbing boundary:

$$\langle \tau \rangle = \frac{1}{\langle j_a(x_f) \rangle} \quad (16.3.6)$$

In chemical kinetics, $\langle j_a(x_f) \rangle$ is the rate constant from transition state theory.

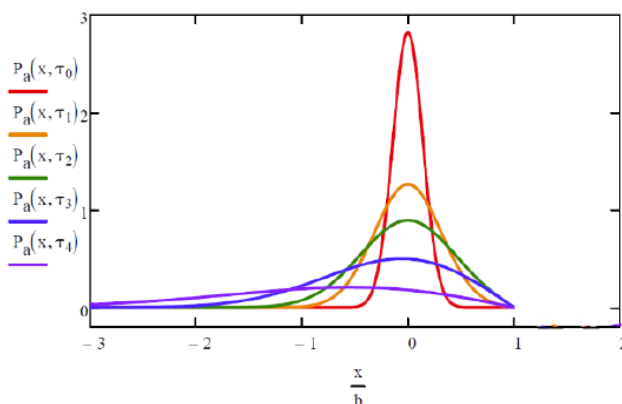
Calculating the First Passage Time Distribution

To calculate F one needs to solve a Fokker–Planck equation for the equivalent diffusion problem with an absorbing boundary condition. As an example, we can write these expressions explicitly for diffusion from a point source. This problem is solved using the Fourier transform method, applying absorbing boundary conditions at x_f to give

$$P_a(x, t) = P(x, t) - P(2x_f - x, t) \quad (x \leq x_f)$$

which is expressed in terms of the probability distribution in the absence of absorbing boundary conditions:

$$P(x, t) = (4\pi Dt)^{1/2} \exp \left[-\frac{(x - x_0)^2}{4Dt} \right]$$



The corresponding first passage time distribution is:

$$F(t) = \frac{x_f - x_0}{(4\pi Dt^3)^{1/2}} \exp \left[-\frac{(x - x_0)^2}{4Dt} \right]$$

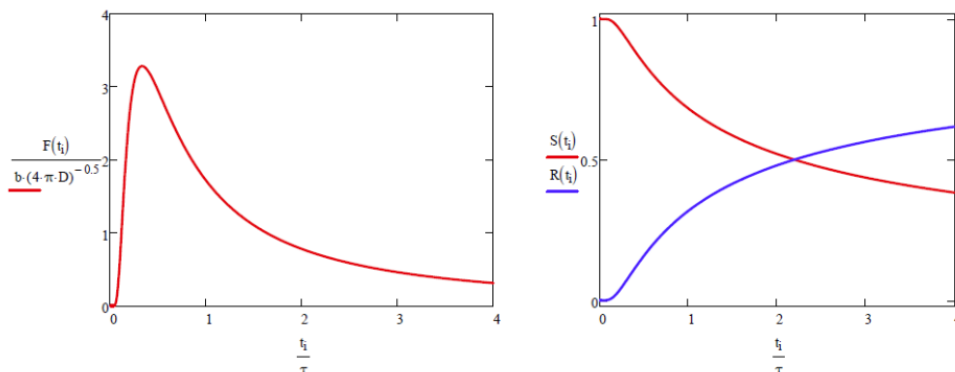
$F(t)$ decays in time as $t^{-3/2}$, leading to a long tail in the distribution. The mean of this distribution gives the MFPT

$$\langle \tau \rangle = x_f^2 / 2D$$

and the most probable passage time is $x_f^2 / 6D$. Also, we can use eq. (16.3.3) to obtain the survival probability

$$S(t) = \operatorname{erf} \left(\frac{x_f}{\sqrt{4Dt}} \right) = \operatorname{erf} \left(\sqrt{\frac{\langle \tau \rangle}{2t}} \right)$$

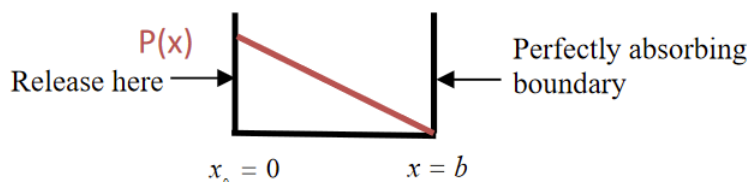
$S(t)$ depends on the distance of the target and the rms diffusion length over time t . At long times $S(t)$ decays as $t^{-1/2}$.



It is interesting to calculate the probability that the diffusing particle will reach x_f at any time. From eq. (16.3.4), we can see that this probability can be calculated from $\int_0^\infty F(\tau) d\tau$. For the current example, this integral over F gives unity, saying that a random walker in 1D will eventually reach every point on a line. Equivalently, it is guaranteed to return to the origin at some point in time. This observation holds in 1D and 2D, but not 3D.

Calculating the MFPT From Steady-State Flux

From eq. (16.3.6) we see that it is also possible to calculate the MFPT by solving for the flux at an absorbing boundary in a steady state calculation. As a simple example, consider the problem of releasing a particle on the left side of a box, $P(x, 0) = \delta(x, x_0)$, and placing the reaction boundary at the other side of the box $x = b$. We solve the steady-state diffusion equation $\partial^2 P_a / \partial x^2 = 0$ with an absorbing boundary at $x = b$, i.e., $P(b, t) = 0$. This problem is equivalent to absorbing every diffusing particle that reaches the right side and immediately releasing it again on the left side.



The steady-state solution is

$$P_a(x) = \frac{2}{b} \left(1 - \frac{x}{b}\right)$$

Then, we can calculate the flux of diffusing particles at $x=b$:

$$j(b) = -D \frac{\partial P}{\partial x} \Big|_{x=b} = \frac{2D}{b^2}$$

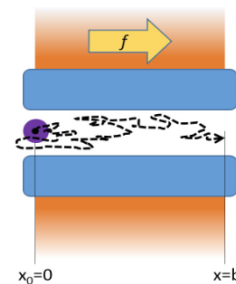
and from the inverse we obtain the MFPT:

$$\langle \tau \rangle = \frac{1}{j(b)} = \left(\frac{b^2}{2D} \right)$$

MFPT in a Potential

To extend this further, let's examine a similar 1D problem in which a particle is released at $x_0 = 0$, and diffuses in x toward a reaction boundary at $x = b$, but this time under the influence of a potential $U(x)$. We will calculate the MFPT for arrival at the boundary. Such a problem could be used to calculate the diffusion of an ion through an ion channel under the influence of the transmembrane electrochemical potential.

From our earlier discussion of diffusion in a potential, the steady state flux is



$$j = \frac{-D [P(b)e^{U(b)/k_B T} - P(x)e^{U(x)/k_B T}]}{\int_x^b e^{U(x')/k_B T} dx'}$$

Applying the absorbing boundary condition, $P(b) = 0$, the steady state probability density is

$$P_a(x) = \frac{j}{D} e^{-U(x)/k_B T} \int_x^b e^{U(x')/k_B T} dx' \quad (16.3.7)$$

Now integrating both sides over the entire box, the left side is unity, so we obtain an expression for the flux

$$\frac{1}{j} = \frac{1}{D} \int_0^b e^{-U(x)/k_B T} \left[\int_x^b e^{U(x')/k_B T} / k_B T dx' \right] dx \quad (16.3.8)$$

But j^{-1} is just the MFPT, so this expression gives us $\langle \tau \rangle$. Note that if we set U to be a constant in eq. (16.3.8), that we recover the expressions for $\langle \tau \rangle$, j , and P_a in the preceding example.

Diffusion in a linear potential

For the case of a linear external potential, we can write the potential in terms of a constant external force $U = -fx$. Solving this with the steady state solution, we substitute U into eq. (16.3.8) and obtain

$$\langle \tau \rangle = \frac{1}{j} = \frac{1}{Df^2} \left[e^{-fb} - 1 + fb \right] \quad (16.3.9)$$

where $f = f/k_B T$ is the force expressed in units of thermal energy. Substituting into eq. (16.3.7) gives the steady state probability density

$$P(x) = \frac{f \left(1 - e^{-f(b-x)} \right)}{e^{-fb} - 1 + fb}$$

Now let's compare these results from calculations using the first passage time distribution. This requires solving the diffusion equation in the presence of the external potential. In the case of a linear potential, we can solve this by expressing the constant force as a drift velocity

$$v_x = \frac{f}{\zeta} = \frac{fD}{k_B T} = fD$$

Then the solution is obtained from our earlier example of diffusion with drift:

$$P(x, t) = -\frac{1}{\sqrt{4\pi Dt}} \exp \left[-\frac{(x - fDt)^2}{4Dt} \right]$$

The corresponding first passage time distribution is

$$F(t) = \frac{b}{\sqrt{4\pi Dt^3}} \exp \left[-\frac{(b - fDt)^2}{4Dt} \right]$$

and the MFPT is given by eq. (16.3.9).

1. A. Nitzan, Chemical Dynamics in Condensed Phases: Relaxation, Transfer and Reactions in Condensed Molecular Systems. (Oxford University Press, New York, 2006); S. Iyer-Biswas and A. Zilman, First-Passage Processes in Cellular Biology, Adv. Chem. Phys. 160, 261–306 (2016).
2. H. C. Berg, Random Walks in Biology. (Princeton University Press, Princeton, N.J., 1993).

This page titled [16.3: Mean First Passage Time](#) is shared under a [CC BY-NC-SA 4.0](#) license and was authored, remixed, and/or curated by [Andrei Tokmakoff](#) via [source content](#) that was edited to the style and standards of the LibreTexts platform.

CHAPTER OVERVIEW

17: Directed and Active Transport

[17.1: Motor Proteins](#)

[17.2: Passive vs Active Transport](#)

[17.3: Brownian Ratchet](#)

[17.4: Polymerization Ratchet and Translocation Ratchet](#)

This page titled [17: Directed and Active Transport](#) is shared under a [CC BY-NC-SA 4.0](#) license and was authored, remixed, and/or curated by [Andrei Tokmakoff](#) via [source content](#) that was edited to the style and standards of the LibreTexts platform.

17.1: Motor Proteins

Many proteins act as molecular motors using an energy source to move themselves or cargo in space. They create directed motion by coupling energy use to conformational change.

Motor Classes

Translational

- Cytoskeletal motors that step along filaments (actin, microtubules)
- Helicase translation along DNA

Rotary

- ATP synthase
- Flagellar motors

Polymerization

- Cell motility

Translocation

- DNA packaging in viral capsids
- Transport of polypeptides across membranes

Translational Motors

Processivity

- Some motors stay on fixed track for numerous cycles
- Others bind/unbind often—mixing stepping and diffusion

Cytoskeletal motors

- Used to move vesicles and displace one filament relative to another
- Move along filaments—tracks have polarity (\pm)
- Steps of fixed size

Classes

- Dynein moves on Microtubules (+ \rightarrow -)
- Kinesin Microtubules (mostly - \rightarrow +)
- Myosin Actin

Molecular Motors

We can make a number of observations about common properties of translational and rotational motor proteins.

Molecular motors are cyclical

- They are “processive” involving discrete stepping motion
- Multiple cycles lead to directional linear or rotary motion

Molecular motors require an external energy source

- Commonly this energy comes from ATP hydrolysis
 - ~ 50 kJ/mol or ~ 20 kBT or ~ 80 pN/nm
 - ATP consumption correlated with stepping
- Or from proton transfer across a transmembrane proton gradient

Protein motion is strongly influenced by thermal fluctuations and Brownian motion

- Molecular motors work at energies close to $k_B T$
- Short range motions are diffusive—dominated by collisions
- Inertial motion does not apply

This page titled [17.1: Motor Proteins](#) is shared under a [CC BY-NC-SA 4.0](#) license and was authored, remixed, and/or curated by [Andrei Tokmakoff](#) via [source content](#) that was edited to the style and standards of the LibreTexts platform.

17.2: Passive vs Active Transport

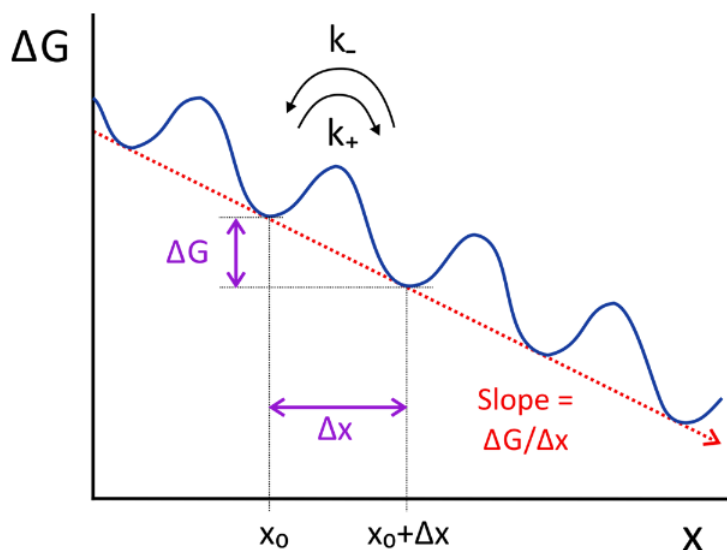
Directed motion of molecules in a statistically deterministic manner (i.e., $\bar{x}(t) = \bar{v}t$) in a thermally fluctuating environment cannot happen spontaneously. It requires a free energy source, which may come from chemical bonds, charge transfer, and electrochemical gradients. From one perspective, displacing a particle requires work, and the force behind this work originates in free energy gradients along the direction of propagation

$$w = - \int_{path} f dx \quad f_{rev} = \frac{\partial G}{\partial x}$$

An example of this is steady-state diffusion driven by a spatial difference in chemical potential, for instance the diffusion of ions through a membrane channel driven by a transmembrane potential. This problem is one of passive transport. Although an active input of energy was required to generate the transmembrane potential and the net motion of the ion is directional, the ion itself is a passive participant in this process. Such processes can be modeled as diffusion within a potential.

Active transport refers to the direct input of energy into the driving the moving object in a directional manner. At a molecular scale, even with this input of energy, fluctuations and Brownian motion remain very important.

Even so, there are multiple ways in which to conceive of directed motion. Step-wise processive motion can also be viewed as a series of states along a free energy or chemical potential gradient. Consider this energy landscape:



Under steady state conditions, detailed balance dictates that the ratio of rates for passing forward or reverse over a barrier is dictated by the free energy difference between the initial and final states:

$$\frac{k_+}{k_-} = e^{-\Delta G/k_B T}$$

and thus the active driving force for this downhill process is

$$f \approx - \frac{\Delta G}{\Delta x} = \frac{k_B T}{\Delta x} \ln \frac{k_+}{k_-}$$

This perspective is intimately linked with a biased random walk model when we remember that

$$\frac{k_+}{k_-} = \frac{P_+}{P_-}$$

If our free energy is the combination of a chemical process (ΔG_0) and an external force, then we can write

$$\frac{k_+}{k_-} = \exp[-(\Delta G_0 + f\Delta x)/k_B T]$$

Feynman's Brownian Ratchet

Feynman used a thought experiment to show you cannot get work from thermal noise.¹ Assume you want to use the thermal kinetic energy from the molecules in a gas, and decide to use the collisions of these molecules with a vane to rotate an axle. The direction of rotation will be based on the velocity of the molecules hitting the vane, so to assure that this rotation proceeds only one way, we use a ratchet with a pawl and spring to catch the ratchet when it advances in one direction.

This is the concept of rectified Brownian motion.

At a microscopic level, this reasoning does not hold, because the energy used to rotate the ratchet must be enough to lift the pawl against the force of the spring. If we match the thermal energy of gas $T = \frac{1}{2}m\langle v_x^2 \rangle$ to the energy needed to raise the pawl $U = \frac{1}{2}\kappa x^2$ we find that the pawl will also be undergoing fluctuations in x with similar statistics to the bombardment of the vane $\kappa = \sqrt{mk_B T / \langle x^2 \rangle}$. Therefore, the ratchet will instead thermally diffuse back and forth as a random walk. Further, Feynman showed that if you imbedded the vane and ratchet in reservoirs of temperature T_1 and T_2 , respectively, then the ratchet will advance as desired if $T_1 > T_2$, but will move in reverse if $T_1 < T_2$. Thus, one cannot extract useful work from thermal fluctuations alone. You need some input of energy—any source of free energy.

1. http://www.feynmanlectures.caltech.edu/I_46.html

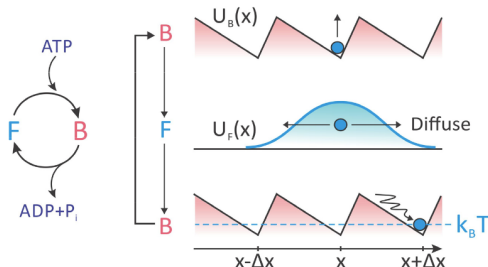
This page titled [17.2: Passive vs Active Transport](#) is shared under a [CC BY-NC-SA 4.0](#) license and was authored, remixed, and/or curated by [Andrei Tokmakoff](#) via [source content](#) that was edited to the style and standards of the LibreTexts platform.

17.3: Brownian Ratchet

The **Brownian ratchet** refers to a class of models for directed transport using **Brownian motion** that is rectified through the input of energy. For a diffusing particle, the energy is used to switch between two states that differ in their diffusive transport processes. This behavior results in biased diffusion. It is broadly applied for processive molecular motors stepping between discrete states, and it therefore particularly useful for understanding translational and rotational motor proteins.

One common observation we find is that directed motion requires the object to switch between two states that are coupled to its motion, and for which the exchange is driven by input energy. Switching between states results in biased diffusion. The interpretation of real systems within the context of this model can vary. Some people consider this cycle as deterministic, whereas others consider it quite random and noisy, however, in either case, Brownian motion is exploited to an advantage in moving the particle.

We will consider an example relevant to the ATP-fueled stepping of cytoskeletal motors along a filament. The motor cycles between two states: (1) a bound state (B), for which the protein binds to a particular site on the filament upon itself binding ATP, and (2) a free state (F) for which the protein freely diffuses along the filament upon ATP hydrolysis and release of ADP + P_i. The bound state is described by a periodic, spatially asymmetric energy profile $U_B(x)$, for which the protein localizes to a particular energy minimum along the filament. Key characteristics of this potential are a series of sites separated by a barrier $\Delta U > k_B T$, and an asymmetry in each well that biases the system toward a local minimum in the direction of travel. In the free state, there are no barriers to motion and the protein diffuses freely. When the free protein binds another ATP, it returns to $U_B(x)$ and relaxes to the nearest energy minimum.



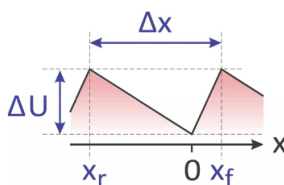
Let's investigate the factors governing the motion of the particle in this Brownian ratchet, using the perspective of a biased random walk. The important parameters for our model are:

- The distance between adjacent binding sites is Δx .
- The position of the forward barrier relative to the binding site is x_f . A barrier for reverse diffusion is at $-x_r$, so that

$$x_f + x_r = \Delta x \tag{17.3.1}$$

The asymmetry of U_B is described by

$$\alpha = (x_f - x_r) / \Delta x \tag{17.3.2}$$



- The average time that a ratchet stays free or bound are τ_F and τ_B . Therefore, the average time per bind/release cycle is

$$\Delta t = \tau_F + \tau_B$$

- We define a diffusion length ℓ which is dependent on the time that the protein is free

$$\ell_0(\tau_F) = \sqrt{4D\tau_F}$$

Conditions For Efficient Transport

Let's consider the conditions to maximize the velocity of the Brownian ratchet.

1. While in F : the optimal period to be diffusing freely is governed by two opposing concerns. We want the particle to be free long enough to diffuse past the forward barrier, but not so long that it diffused past the reverse barrier. Thus we would like the diffusion length to lie between the distances to these barriers:

$$\ell_0 = \sqrt{4D\tau_F}$$

$$x_r > \ell_0 > x_f$$

Using the average value as a target:

$$\ell_0 \approx \frac{x_r + x_f}{2} = \frac{\Delta x}{2}$$

$$\tau_F \approx \frac{\Delta x^2}{16D}$$

2. While in B : After the binding ATP, we would like the particle to stay with ATP bound long enough to relax to the minimum of the asymmetric energy landscape. Competing with this consideration, we do not want it to stay bound any longer than necessary if speed is the issue.

We can calculate the time needed to relax from the barrier at x , forward to the potential minimum, if we know the drift velocity v_d of this particle under the influence of the potential.

$$\tau_B \approx x_r / v_d$$

The drift velocity is related to the force on the particle through the friction coefficient, $v_d = f / \zeta$, and we can obtain the magnitude of the force from the slope of the potential:

$$|f| = \frac{\Delta U}{x_r}$$

So the drift velocity is $v_d = \frac{fD}{k_B T} = \frac{\Delta U D}{x_r k_B T}$ and the optimal bound time is

$$\tau_B \approx \frac{x_r^2 k_B T}{\Delta U D}$$

Now let's look at this a bit more carefully. We can now calculate the probability of diffusing forward over the barrier during the free interval by integrating over the fraction of the population that has diffused beyond x_f during τ_f . Using the diffusive probability distribution with $x_0 \rightarrow 0$,

$$P_+ = \frac{1}{\sqrt{4\pi D\tau_f}} \int_{x_f}^{\infty} e^{-x^2/4D\tau_f} dx$$

$$= \frac{1}{2} \operatorname{erfc}\left(\frac{x_f}{\ell_0}\right)$$

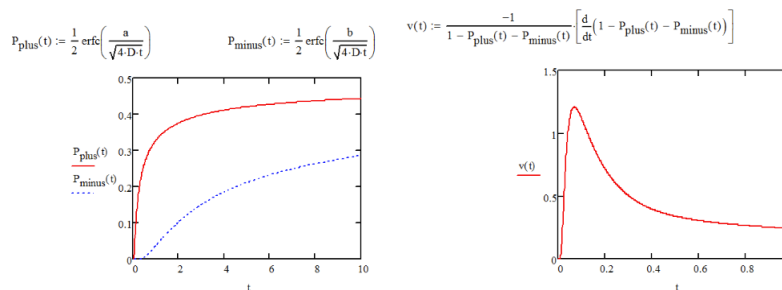
Similarly, the probability for diffusing backward over the barrier at $x = -x_r$ is

$$P_- = \frac{1}{2} \operatorname{erfc}\left(\frac{x_r}{\ell_0}\right)$$

Now we can determine the average velocity of the protein by calculating the average displacement in a given time step. The average displacement is the difference in probability for taking a forward versus a reverse step, times the step size. This displacement occurs during the time interval Δt . Therefore,

$$\nu = \frac{\Delta x}{\Delta t} (P_+ - P_-) = \frac{\Delta x}{2\Delta t} \left[\operatorname{erfc}\left(\frac{x_r}{\ell_0}\right) - \operatorname{erfc}\left(\frac{x_f}{\ell_0}\right) \right]$$

It is clear from this expression that the velocity is zero when the asymmetry of the potential is zero. For asymmetric potentials, P_+ and P_- are dependent on τ_f , with one rising in time faster than the other. As a result, the velocity, which depends on the difference of these reaches a maximum in the vicinity of $\tau_f = x_f^2/D$.



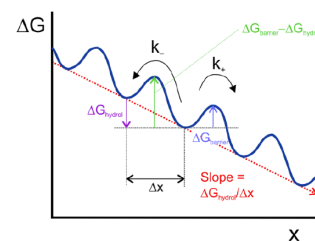
So how does the ATP hydrolysis influence the free energy gradient? Here free energy gradient is

$$\frac{\Delta G_{\text{Hyd.}}}{\Delta x}$$

$$k_+ = A_+ e^{-(\Delta G_{\text{barrier}} - \Delta G_{\text{hydrolysis}})/kT}$$

$$k_- = A_- e^{-(\Delta G_{\text{barrier}})/kT}$$

$$\nu = (k_+ - k_-) \Delta x$$

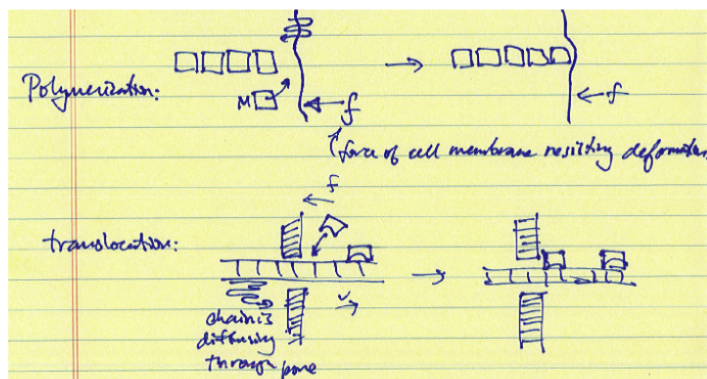


K. Dill and S. Bromberg, *Molecular Driving Forces: Statistical Thermodynamics in Biology, Chemistry, Physics, and Nanoscience*. (Taylor & Francis Group, New York, 2010); R. Phillips, J. Kondev, J. Theriot and H. Garcia, *Physical Biology of the Cell*, 2nd ed. (Taylor & Francis Group, New York, 2012).

This page titled 17.3: Brownian Ratchet is shared under a CC BY-NC-SA 4.0 license and was authored, remixed, and/or curated by Andrei Tokmakoff via source content that was edited to the style and standards of the LibreTexts platform.

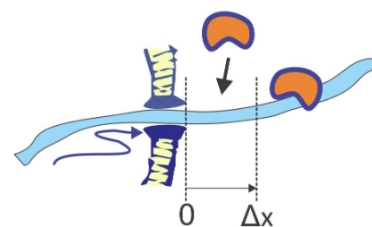
17.4: Polymerization Ratchet and Translocation Ratchet

Polymerization and translocation ratchets refer to processes that result in directional displacements of a polymer or oligomer chain rather than a specific protein. The models for these ratchets also involve rectified Brownian motion, in which a binding unit is added to a diffusing chain to bias the diffusive motion in a desired direction. Once the displacement reaches a certain diffusion length, a monomer or binding protein can add to the chain, locking in the forward diffusion of the chain. In this case, it is the binding or attachment of protein units that consumes energy, typically in the form of ATP or GTP hydrolysis.



Translocation Ratchet¹

Protein translocation across cell membranes is a ubiquitous process for transporting polypeptide chains across bacterial and organelle membranes through channels with the help of chaperone proteins on the inner side of the membrane. The translocation ratchet refers to a model in which the transport of the chain occurs through Brownian motion which is rectified by the binding of proteins to the chain on one side of the pore as it is displaced. Once the chain diffuses through the pore for a distance Δx , a protein can bind to the chain, stopping backward diffusion. At each step, energy is required to drive the binding of the chaperone protein.



The translocation ratchet refers to a continuum model for the diffusion of the chain. It is possible to map this diffusion problem onto a Smoluchowski equation, but it would be hard to solve for the probability density. It is easier if we are just interested in describing the average velocity of the chain under steady state conditions, we can solve for the steady-state chain flux across the pore:

$$J(x) = -D \left(\frac{\partial P}{\partial x} + \frac{f}{k_B T} P \right) \quad (17.4.1)$$

where f is the force acting against the chain displacement. Steady state behavior corresponds to $\partial P / \partial t = 0$, so from the continuity equation

$$\frac{\partial P}{\partial t} = -\frac{\partial J}{\partial x}$$

we know that $\partial J / \partial x = 0$. Therefore J is a constant. To find P , we want to solve

$$\frac{\partial P}{\partial x} + \frac{f}{k_B T} P + \frac{J}{D} = 0$$

for which the general solution is $P = A_1 e^{-fx/k_B T} + A_2$. We find the integration constants using the boundary condition $P(\Delta x, t) = 0$, which reflects that a protein will immediately and irreversibly bind once the diffusing chain reaches an extension Δx . (No back-stepping is allowed.) And we use the conservation statement:

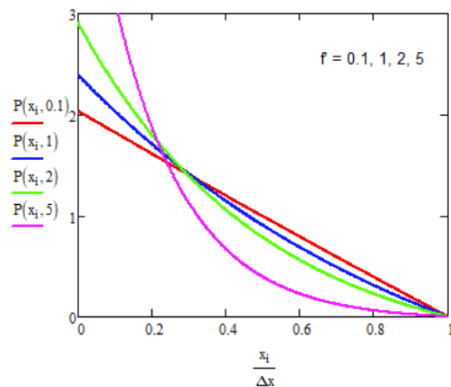
$$\int_0^{\Delta x} dx P(x) = 1$$

which says that a protein must be bound within the interval 0 to Δx . The steady-state probability distribution with these two boundary conditions is

$$P(x) = \frac{\tilde{f} \left[\exp\left(\tilde{f}(1 - x/\Delta x)\right) - 1 \right]}{\Delta x \left(1 + \tilde{f} - e^{\tilde{f}} \right)} \quad (17.4.2)$$

$$\tilde{f} = \frac{f \Delta x}{k_B T}$$

\tilde{f} is a dimensionless constant that expresses the load force in units of $k_B T$ opposing ratchet displacement by Δx .

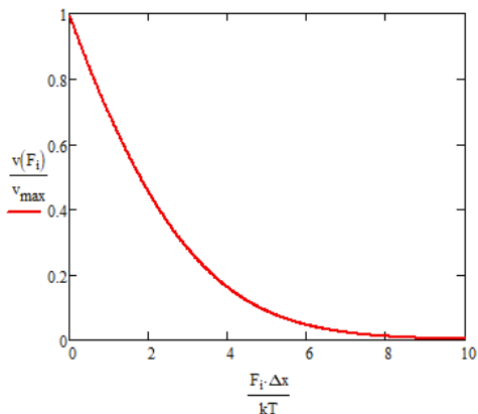


Substituting eq. (17.4.2) into eq. (17.4.1) allows us to solve for J.

$$J(x) = \frac{-D \tilde{f}^2}{\Delta x^2 \left(1 + \tilde{f} - e^{\tilde{f}} \right)} \left(1 - 2 \exp \left[\tilde{f} \left(\frac{x}{\Delta x} - 1 \right) \right] \right)$$

Now, the average velocity can be determined from $\langle \nu \rangle = J \Delta x$. Evaluating the flux at $x = \Delta x$:

$$\langle \nu \rangle = \frac{2D}{\Delta x} \left[\frac{\tilde{f}^2/2}{e^{\tilde{f}} - \tilde{f} - 1} \right]$$



Now look at low force limit $\tilde{f} \rightarrow 0$. Expand $e^{\tilde{f}} = 1 + \tilde{f} + \tilde{f}^2/2$:

$$\langle \nu \rangle \rightarrow \frac{2D}{\Delta x} = v_{max}$$

Note that this is the maximum velocity for ideal ratchet, and it follows the expected behavior for pure diffusive motion.

Now consider probability of the protein binding is governed by equilibrium between free and bound forms:

$$F \xrightleftharpoons[k_d]{k_a} B \quad K = \frac{k_a}{k_d} = \frac{\tau_B}{\tau_F}$$

Here k_a refers to the effecting quasi-first-order rate constant for binding at a chaperone concentration [chap]: $k_a = k'_a[\text{chap}]$.

Fast kinetics approximation

$$\langle \nu \rangle = \frac{2D}{\Delta x} \left[\frac{\frac{f^2/2}{e^{\tilde{f}} - 1}}{1 - K(e^{\tilde{f}} - 1)} - \tilde{f} \right]$$

$$\langle \nu \rangle_{max} = \frac{2D}{\Delta x} \left(\frac{1}{1 + 2K} \right)$$

Stall Load

$$f_0 = \frac{k_B T}{\Delta x} \ln \left(1 + \frac{1}{K} \right)$$

-
1. C. S. Peskin, G. M. Odell and G. F. Oster, Cellular motions and thermal fluctuations: the Brownian ratchet, Biophys. J. 65 (1), 316–324 (1993).
-

17.4: Polymerization Ratchet and Translocation Ratchet is shared under a [not declared](#) license and was authored, remixed, and/or curated by LibreTexts.

SECTION OVERVIEW

5: Cooperativity

18: Cooperativity

18.1: Helix–Coil Transition

18.2: Two-State Thermodynamics

19: Self-Assembly

19.1: Micelle Formation

19.2: Classical Nucleation Theory

19.3: Why Are Micelles Uniform in Size?

19.4: Shape of Self-Assembled Amphiphiles

This page titled [5: Cooperativity](#) is shared under a [CC BY-NC-SA 4.0](#) license and was authored, remixed, and/or curated by [Andrei Tokmakoff](#) via [source content](#) that was edited to the style and standards of the LibreTexts platform.

CHAPTER OVERVIEW

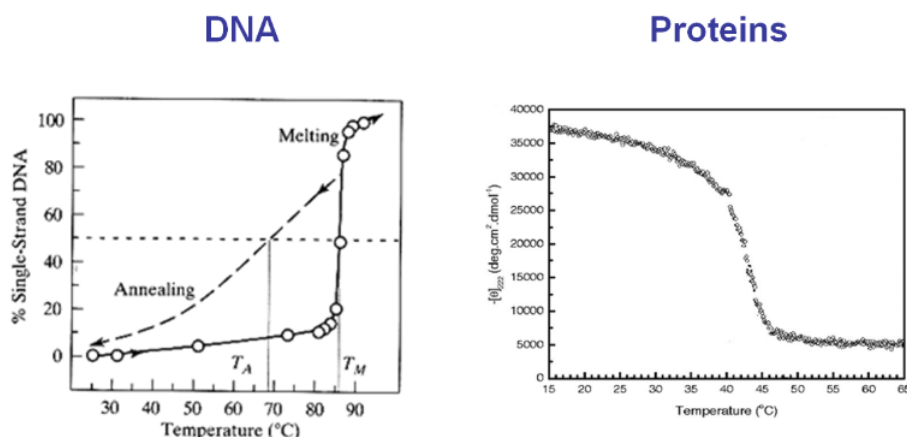
18: Cooperativity

It is often observed in molecular biology that nanoscale structures with sophisticated architectures assemble spontaneously, without the input of external energy. The behavior is therefore governed by physical principles that we can describe with thermodynamics and statistical mechanics. Examples include:

- Protein and RNA folding
- DNA hybridization
- Assembly of protein complexes and viral capsids
- Micelle and vesicle formation

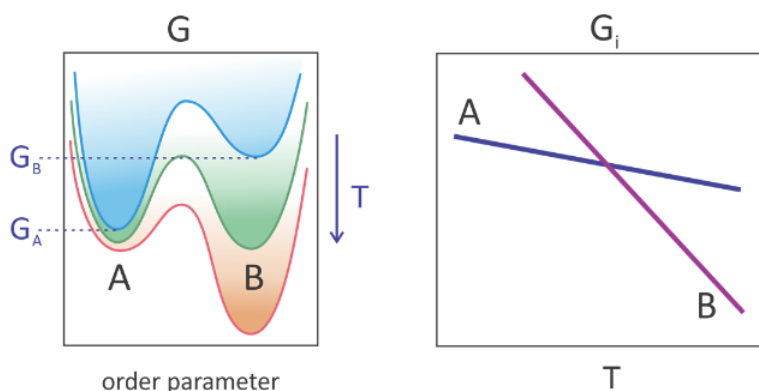
Although each of these processes has distinct characteristics, they can be broadly described as self-assembly processes.

A characteristic of self-assembly is that it appears thermodynamically and kinetically as a simple “two-state transition”, even if thousands of atomic degrees of freedom are involved. That is, as one changes thermodynamic control variables such as temperature, one experimentally observes an assembled state and a disassembled state, but rarely an intermediate, partially assembled state. Furthermore, small changes in these thermodynamic variables can lead to dramatic changes, i.e., melting of DNA or proteins over a few degrees. This binary or switch-like behavior is very different from the smoothly varying unfolding curves we derived for simple lattice models of polymers.



Phase transitions and phase equilibria are related phenomena described by the presence (or coexistence) of two states. These manifest themselves as a large change in the macroscopic properties of the system with only small changes in temperature or other thermodynamic variables. Heating liquid water from 99 °C to 101 °C has a profound effect on the density, which a 2° change at 25 °C would not have.

Such a “first-order” phase transition arises from a discontinuity in the free energy as a function of an intensive thermodynamic variable.¹ The thermodynamic description of two-state behavior governing a phase transition is illustrated below for the equilibrium between phases A and B. The free-energy profile is plotted as a function of an order parameter, a variable that distinguishes the physical characteristics relevant to the change of phase. For instance for a liquid–gas-phase transition, the volume or density are order parameters that change dramatically. As the temperature is increased the free energy of each state, characterized by its free energy minimum (G_i), decreases smoothly and continuously. However, state B decreases more rapidly than state A. While state A is the global free-energy minimum at low temperatures, state B is at high temperature. The phases are at equilibrium with each other at the temperature where $G_A = G_B$.



The presence of a phase transition is dependent on all molecules of the system changing state together, or cooperatively. In a first-order phase transition, this change is infinitely sharp or discontinuous, but the helix–coil transition and related cooperative phenomena can be continuous. Cooperativity is a term that can refer both to macroscopic phenomena and to a molecular scale. We use it to refer to many degrees of freedom changing concertedly. The size or number of particles or molecules participating in a cooperative process is the cooperative unit. In the case of a liquid–gas-phase transition, the cooperative unit is the macroscopic sample, whereas for protein folding it may involve most of the molecule.

What underlies cooperativity? We find that the free energy of the system is not simply additive in the parts. The energy of a particular configurational state depends on the configuration of its neighbors. For instance, the presence of one contact or molecular interaction increases or decreases the propensity for a second contact or interaction. We refer to this as positive or negative cooperativity. Beyond self-assembly, cooperativity plays a role in the binding of multiple ligands and allostery. Here we want to discuss the basic concepts relevant to cooperativity and its relationship to two-state behavior.

Based on observations we have previously made in other contexts, we can expect that cooperative behavior must involve competing thermodynamic effects. Structure is formed at the expense of a large loss of entropy, but the numerous favorable contacts that are formed lower the enthalpy even more. The free-energy change may be small, but this results from two opposing effects of large magnitude and opposite sign (H vs. TS). A small tweak in temperature can completely change the system.

[18.1: Helix–Coil Transition](#)

[18.2: Two-State Thermodynamics](#)

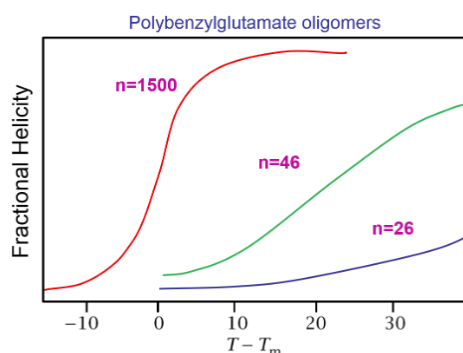
1. A first order transition is described as a discontinuity in $\partial G/\partial S$ or $\partial G/\partial V$. A second order transition is one in which two phases merge into one at a critical point and is described by a discontinuity in the heat capacity or expansivity/compressibility of the system ($\partial S/\partial T$, $\partial S/\partial P$, $\partial V/\partial T$, or $\partial V/\partial P$).

This page titled [18: Cooperativity](#) is shared under a [CC BY-NC-SA 4.0](#) license and was authored, remixed, and/or curated by [Andrei Tokmakoff](#) via [source content](#) that was edited to the style and standards of the LibreTexts platform.

18.1: Helix–Coil Transition

Cooperativity plays an important role in the description of the helix–coil transition, which refers to the reversible transition of macromolecules between coil and extended helical structures. This phenomenon was observed by Paul Doty in the 1950s for the conversion of polypeptides between a coil and α -helical form,² and for the melting and hybridization of DNA.³ Bruno Zimm developed a statistical theory with J. Bragg that described the helix–coil transition, which forms the basis of our discussion.⁴

One of the observations that motivated this work is shown in the figure below. The fraction of helical structure observed in the polypeptide poly-benzylglutamate showed a temperature-dependent melting behavior in which the steepness of the transition increased with polymer chain length. This length dependence indicates a higher probability of forming helices when more residues are present, and that the linkages do not act independently. This suggests a two-step mechanism. The rate-limiting step of forming an α helix is the nucleation of a single hydrogen bonded residue $i \rightarrow i + 4$ loop. Once this occurs, the addition of further hydrogen bonds to extend this helix is much easier and occurs in rapid succession.



Adapted from B. H. Zimm, P. Doty and K. Iso, Proc. Natl. Acad. Sci. U. S. A. **45**, 1601-1607 (1959). Copyright 1959 PNAS.

To model this behavior, we imagine that the polypeptide consists of a chain of segments that can take on two configurations, H or C .

Symbol	Name	Effect
H	Helix	Decreases entropy but also lowers enthalpy
C	Coil	Raises entropy

To specify the state of a conformation through a sequence, i.e.,

... $HCHHHHCCCCHHH$...

Remember to not take this too literally, and be flexible in the interpretation of your model. Although this model was derived with an α -helix formation in polypeptides in mind, in a more general sense H and C do not necessarily refer explicitly to residues of a sequence, but just for independently interacting regions.

If there are n segments, these can be divided into n_H helical and n_C coil segments.

$$n_H + n_C = n$$

The segments need not correspond directly to amino acids, but structurally and energetically distinct regions. Our goal will be to calculate the fractional helicity of this system θ_H as a function of temperature, by calculating the conformational partition function, q_{conf} , by an explicit summation over i microstates, Boltzmann weighed by the microstate energy E_i :

$$q_{\text{conf}}(n) = \sum_{i \text{ config.}} e^{-E_i/k_B T} \quad (18.1.1)$$

Non-cooperative Model

We start our analysis by discussing a non-cooperative model. We assume:

- Each segment can switch conformation between H and C independently of the others.
- The formation of H from C lowers the configurational energy by $\Delta\varepsilon$. $\Delta\varepsilon = E_H - E_C$ is a free-energy change per residue, where $\Delta\varepsilon < 0$. We will take the coil state to be the reference energy $E_C = 0$.

- Therefore the energy of the system is determined from the number of H residues present, not the specific sequence of H and C segments.

$$E_i = E(n_H) = n_H \Delta\varepsilon$$

Then, we can calculate q_{conf} using $g(n, n_H)$, the degeneracy of distinguishable states for a polymer of length n with n_H helical segments. The conformational partition function is obtained by

$$q_{\text{conf}}(n) = \sum_{n_H=0}^n g(n, n_H) e^{-n_H \Delta\varepsilon / k_B T} \quad (18.1.2)$$

In evaluating the partition functions in helix–coil transition models, it is particularly useful to define a “statistical weight” for the helical configuration. It describes the influence of having an H on the probability of observing a particular configuration at $k_B T$:

$$s = e^{-\Delta\varepsilon / k_B T} \quad (18.1.3)$$

For the present model, we can think of s as an equilibrium constant for the process of adding a helical residue to a sequence:

$$s = \frac{P(n_H + 1)}{P(n_H)}$$

This equilibrium constant is related to the free energy change for adding a helical residue to the growing chain. Then we can write eq. (18.1.2) as

$$q_{\text{conf}}(n) = \sum_{n_H=0}^n g(n, n_H) s^{n_H}$$

Since there are only two possible configurations (H and C), the degeneracy of configurations with n_H helical segments in a chain of length n is given by the binomial coefficients:

$$g(n, n_H) = \frac{n!}{n_H! n_C!} = \binom{n}{n_H} \quad (18.1.4)$$

since $n_C = n - n_H$. Then using the binomial theorem, we obtain

$$q_{\text{conf}}(n) = (1 + s)^n \quad (18.1.5)$$

Also, the probability of a chain with n segments having n_H helical linkages is

$$P(n, n_H) = \frac{g(n, n_H) e^{-E(n_H) / k_B T}}{q_{\text{conf}}} = \binom{n}{n_H} \frac{s^{n_H}}{(1 + s)^n} \quad (18.1.6)$$

✓ Example: $n = 4$

The conformations available are shown here.

q	No. of Helices	Sequences	Microstate Count
q_0	0 H	$CCCC$	1
q_1	1 H	$HCCC$	4
		$CHCC$	
		$CCHC$	
		$CCCH$	
q_2	2 H	$HHCC$	6
		$CHHC$	
		$CCHH$	
		$HCHC$	
		$CHCH$	
		$HCCH$	
q_3	3 H	$CHHH$	4
		$HCHH$	
		$HHCH$	
		$HHHC$	
q_4	4 H	$HHHH$	1

The molecular conformational partition function is

$$\begin{aligned}
 q_{\text{conf}} &= \overbrace{1}^{\text{all } C} + \overbrace{4e^{-\Delta\varepsilon/k_{BT}}}^{\text{one } H} + \overbrace{6e^{-2\Delta\varepsilon/k_{BT}}}^{\text{two } H} + 4e^{-3\Delta\varepsilon/k_{BT}} + e^{-4\Delta\varepsilon/k_{BT}} \\
 &= 1 + 4s + 6s^2 + 4s^3 + s^4 \\
 &= (1+s)^4
 \end{aligned}$$

The last step follows from Pascal's Rule for binomial coefficients. From eq. (18.1.6), the probability of having two helical residues in a four-residue sequence is:

$$P(4, 2) = \frac{6s^2}{(1+s)^4}$$

To relate this to an observable quantity, we define the fractional helicity, the average fraction of residues that are in the H form.

$$\theta_H = \frac{\langle n_H \rangle}{n} \quad (18.1.7)$$

$$\langle n_H \rangle = \sum_{n_H=0}^n n_H P(n, n_H) \quad (18.1.8)$$

Using this amazing little identity, which we derive below,

$$\langle n_H \rangle = \frac{s}{q} \frac{\partial q}{\partial s} \quad (18.1.9)$$

You can use eq. (18.1.5) to show:

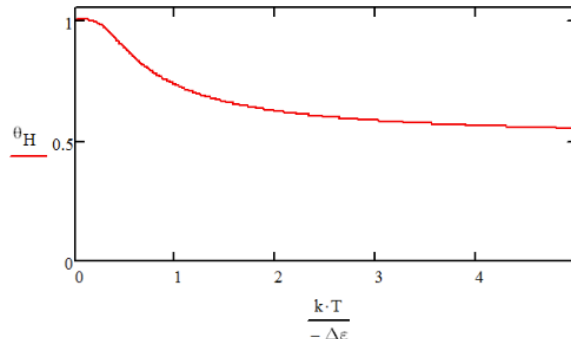
$$\langle n_H \rangle = \frac{ns}{1+s} \quad (18.1.10)$$

and

$$\theta_H = \frac{s}{1+s} \quad (18.1.11)$$

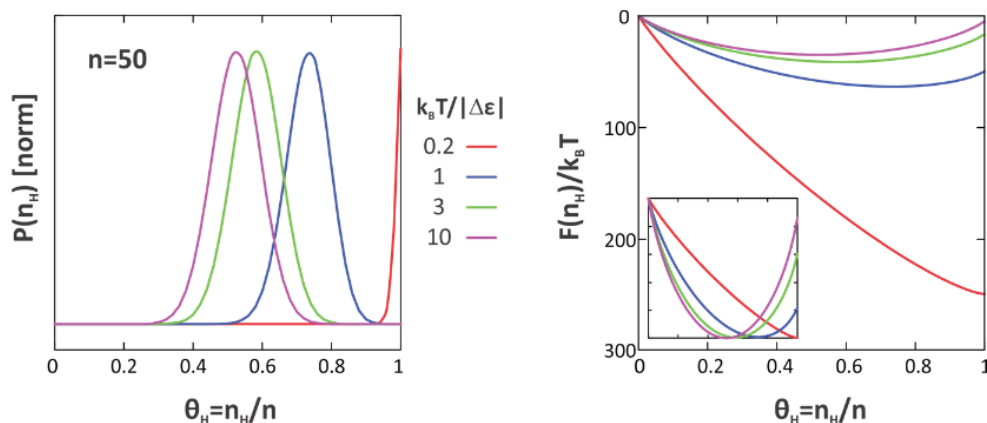
This takes the same form as one would expect for the simple chemical equilibrium of an $C \rightleftharpoons H$ molecular reaction. If we define the equilibrium constant $K_{HC} = [H]/[C]$, then the fraction of molecules in the H state is $\theta_H = [H]/([C] + [H]) = K_{HC}/(1 + K_{HC})$. In this limit $s = K_{HC}$.

Below we plot eq. (18.1.11), choosing $\Delta\epsilon$ to be independent of temperature. θ_H is a smooth and slowly varying function of T and does not show cooperative behavior. Its high temperature limit is $\theta_H = 0.5$, reflecting the fact that in the absence of barriers, the H and C configurations are equally probable for every residue.



We can look a bit deeper at what is happening with the structures present by plotting the probability distribution function for finding n_H helical segments within a chain of length n , eq. (18.1.6), and the associated energy landscape (a potential of mean force):

$$F(n, n_H) = -Nk_B T \ln [P(n, n_H)] \approx -Nk_B T \ln [g(n, n_H) s^{n_H}]$$



The maximum probability and free-energy minimum is located at full helix content at the lowest temperature, and gradually shifts toward $n_H/n = 0.5$ with increasing temperature. The probability density appears Gaussian, and the corresponding free energy appears parabolic. Using similar methods to that described above, we can show that the variance in this distribution scales as $n^{-1/2}$. The presence of a single shifting minimum is referred to as a transition in a one-state system, rather than two-state behavior expected for phase transitions. Here n_H is the order parameter that characterizes the extent of folding of the helix.

Where does eq. (18.1.9) come from? For the moment, we will drop the “conf” and “ H ” subscripts, mainly to write things more compactly, but also to emphasize the generality of this method to all polynomial expansions. Using eq. (18.1.2), $q = \sum_n g s^n$, and recognizing that g is not a function of s :

$$\begin{aligned} \frac{\partial q}{\partial s} &= \sum_n n g s^{n-1} \\ &= \frac{1}{s} \sum_n n g s^n \end{aligned}$$

From eq. (18.1.6), $P_n = g s^n / q$, we can write this in terms of the helical segment probability

$$\frac{1}{q} \frac{\partial q}{\partial s} = \frac{1}{s} \sum_n n P_n \quad (18.1.12)$$

Comparing eq. (18.1.13) with eq. (18.1.12), $\langle n \rangle = \sum_n n P_n$, we see that

$$\frac{s}{q} \frac{\partial q}{\partial s} = \langle n \rangle \quad \text{or} \quad \frac{\partial \ln q}{\partial \ln s} = \langle n \rangle \quad (18.1.13)$$

This method of obtaining averages from derivatives of a polynomial appears regularly in statistical mechanics.⁵

Cooperative Zimm–Bragg Model

Let's modify the model to add an element of cooperativity to the segments in the chain. In order to form a helix, you need to nucleate a helical turn and then adding adjacent helical segments is easier. The probability of forming a turn is relatively low, meaning the free energy barrier for nucleation of one H in a sequence of C is relatively high: $\Delta G_{nuc} > 0$. However the free-energy change per residue for forming H from C within a helical stretch, ΔG_{HC} , stabilizes the growing helix. Based on these free energies, we define statistical weights:

$$s = e^{-\Delta G_{HC}/k_B T}$$

$$\sigma = e^{-\Delta G_{nuc}/k_B T}$$

s and σ are also known as the Zimm–Bragg parameters. Here, s is the statistical weight to add one helical segment to an existing continuous sequence (or stretch) of H , which we interpret as an equilibrium constant:

$$s = \frac{[\dots CHHHHCC \dots]}{[\dots CHHHCCC \dots]} = \frac{P_H(n_H + 1)}{P_H(n_H)}$$

σ is the statistical weight for each stretch of H . This is purely to reflect the probability of forming a new helical segment within a stretch of C . The energy benefit of making the helical form is additional:

$$\sigma s = \frac{[\dots CCCHCC \dots]}{[\dots CCCCCC \dots]} = \frac{P_H(\nu_H + 1)}{P_H(\nu_H)}$$

ν_H is the number of helical stretch segments in a chain. Note that the formation of the first helical segment has a contribution from both the nucleation barrier (σ) and the formation of the first stabilizing interaction (s). The statistical weight for a particular microstate is then $e^{-E_i/k_B T} = s^{n_H} \sigma^{\nu_H}$. Since ΔG_{nuc} will be large and positive, $\sigma \ll 1$. Also, we take $s > 1$, and the presence of cooperativity will mainly hinge on $\sigma \ll s$.

✓ Example

A 35 segment chain has $2^{35} = 3.4 \times 10^{10}$ possible configurations. This particular microstate has fifteen helical segments ($n_H = 16$) partitioned into three helical stretches ($\nu_H = 3$):



We ignore all C 's since the C state is the ground state and their statistical weight is 1.

$$e^{-E_i/k_B T} = s^{n_H} \sigma^{\nu_H} = s^{16} \sigma^3$$

Now the partition function involves a sum over all possible helical segments and stretches:

$$q_{\text{conf}}(n) = \sum_{n_H=0}^n \sum_{\nu_H=0}^{\nu_{\text{max}}} g(n, n_H, \nu_H) s^{n_H} \sigma^{\nu_H} \quad (18.1.14)$$

Since the all-coil state ($n_H = 0$) is the reference state, it contributes a value of 1 to the partition function (the leading term in the summation). Therefore, the probability of observing the all-coil state is

$$P(n, n_H = 0) = q_{\text{conf}}^{-1} \quad (18.1.15)$$

From eq. (18.1.15), the mean number of helical residues is

$$\langle n_H \rangle = \frac{1}{q_{\text{conf}}} \sum_{n_H=0}^n \sum_{\nu_H=0}^{\nu_{\text{max}}} n_H g(n, n_H, \nu_H) s^{n_H} \sigma^{\nu_H}$$

In these equations, ν_{max} refers to the maximum number of helical stretches for a given n_H , $n_H/2$ for even n_H and $(n_H/2) + 1$ for odd n_H .

Zipper model

As a next step, we examine what happens with the simplifying assumption that one helical stretch is allowed. This is the single stretch approximation or the zipper model, in which conversion to a helix proceeds quickly once a single turn has been nucleated. This is reasonable for short chains in which two stretches are unlikely due to steric constraints. For the single stretch case, we only need to account for $\nu_H = 0$ and 1. For $\nu_H = 0$ the system is all coil ($n_H = 0$) and there is only one microstate to count, $g(n, 0, 0) = 1$. For a single helical stretch we need to account for the number of ways of positioning a single helical stretch of n_H residues on a chain of length n : $g(n, n_H, 1) = n - n_H + 1$. Then the partition function, eq. (18.1.15), is

$$q_{\text{zip}}(n) = 1 + \sigma \sum_{n_H=1}^n (n - n_H + 1) s^{n_H} \quad (18.1.16)$$

We can evaluate these sums using the relations

$$\sum_{n_H=1}^n \frac{s^{n_H}}{s-1} = \frac{s^{n+1} - s}{(s-1)^2}$$

$$\sum_{n_H=1}^n n_H s^{n_H} = \frac{s}{(s-1)^2} [n s^{n+1} - (n+1) s^n + 1]$$

which leads to

$$q_{\text{zip}}(n) = 1 + \frac{\sigma s^2}{(s-1)^2} \left(s^n + \frac{n}{s} - (n+1) \right)$$

Following the general expression in eq. (18.1.6), and counting the degeneracy of ways to place a stretch of n_H segments, the probability distribution of helical segments is

$$P_H(n, n_H) = \frac{(n - n_H + 1) \sigma s^{n_H}}{q_{\text{conf}}} \quad 1 \leq n_H \leq n \quad (18.1.17)$$

This expression does not apply to the case $n_H = 0$, for which we turn to eq. (18.1.16). The helical fraction is obtained from $\theta_H = \frac{s}{n} (\partial \ln q_{\text{zip}} / \partial s)$:

$$\theta_H = \frac{\sigma s}{(s-1)^3} \left(\frac{n s^{n+2} - (n+2) s^{n+1} + (n+2) s - n}{n \{ 1 + (\sigma s / (s-1)^2) (s^{n+1} + n - (n+1) s) \}} \right)$$

Multiple stretches

Expressions for the full partition function of chains with length n , eq. (18.1.15), can be evaluated for one-dimensional models that account for nearest neighbor interactions (Ising model) using an approach based on a statistical weight matrix, \mathbf{M} . You can show that the Zimm–Bragg partition function can be written as a product of matrices of the form

$$q_{\text{conf}}(n) = \begin{pmatrix} 1 & 0 \end{pmatrix} \mathbf{M}^n \begin{pmatrix} 1 \\ 1 \end{pmatrix}$$

$$\mathbf{M} = \begin{pmatrix} 1 & \sigma s \\ 1 & s \end{pmatrix}$$

Each matrix represents possible configurations of two adjoining partners, and \mathbf{M} raised to the n th power gives all configurations for a chain of length n . This form also indicates that we can obtain a closed form for q_{conf} from the eigenvalues of \mathbf{M} raised to the n th power. If \mathbf{T} is the transformation that diagonalizes \mathbf{M} , $\mathbf{A} = \mathbf{T}^{-1} \mathbf{M} \mathbf{T}$, then $\mathbf{M}^n = \mathbf{T} \mathbf{A}^n \mathbf{T}^{-1}$. This approach allows us to write

$$q_{\text{conf}} = \tilde{\lambda}^{-1} (\lambda_+^{n+1} (1 - \lambda_-) - \lambda_-^{n+1} (1 - \lambda_+))$$

with

$$\lambda_{\pm} = \frac{1}{2} \left((1-s) \pm \tilde{\lambda} \right)$$

$$\tilde{\lambda} = \lambda_+ - \lambda_- = ((1-s)^2 + 4\sigma s)^{-1/2}$$

and the fractional helicity is obtained from

$$\theta_H = \frac{\langle n_H \rangle}{n} = \frac{s}{n} \frac{\partial \ln q_{\text{conf}}}{\partial s} \quad (18.1.18)$$

Simplifying these expressions for the limit of long chains ($n \rightarrow \infty, \lambda_+^{n+1} \gg \lambda_-^{n+1}$), one finds

$$q_{\text{conf}} \approx \left(\frac{1 + s + \lambda}{2} \right)^n$$

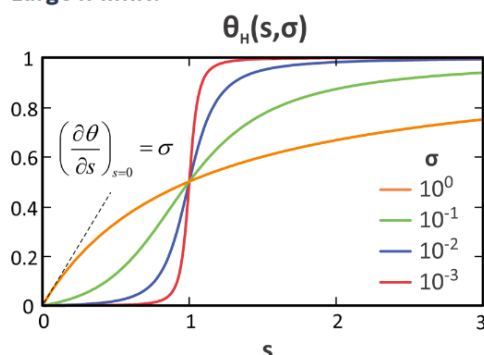
and

$$\theta_H = s \left(\frac{1 + \frac{1}{\lambda}(s-1+2\sigma)}{1 + s + \lambda} \right) \quad (18.1.19)$$

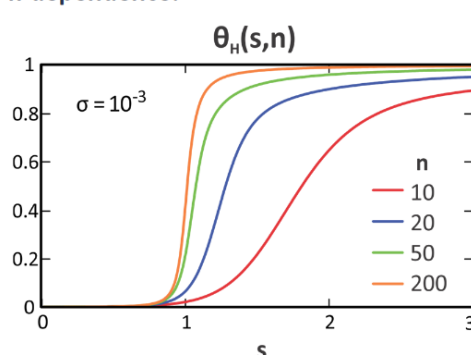
Note that when you set $\sigma = 1$, you recover the noncooperative expression, eq. (18.1.11). When $s \rightarrow 1$, $\theta_H \rightarrow 0.5$.

Below, we examine the transition behavior in the large n limit from eq. (18.1.20) as a function of the cooperativity parameter σ . We note that a sharp transition between an ensemble that is mostly coil to one that is mostly helix occurs near $s = 1$, the point where these states exist with equal probability. When the $C \rightleftharpoons H$ equilibrium shifts slightly to favor H (s slightly greater than 1), most of the sample quickly converts to helical form. When the equilibrium shifts slightly toward C , most of the sample follows. As σ decreases, the steepness of this transition grows as $(d\theta/ds)_{s=1} = 1/4\sigma^{1/2}$. Therefore, we conclude that highly cooperative transitions will have $s \approx 1$ and $\sigma \ll s$. In practice for polypeptides, we find that σ/s lies between 5×10^{-3} and 5×10^{-5} .

Large n limit:



n dependence:



Next, we explore the chain-length dependence for finite chains. We find that the cooperativity of this transition, observed through the steepness of the curve at $\theta_H = 0.5$ increases with n . We also observe that the observed midpoint ($\theta_H = 0.5$) lies at $s > 1$, where the single linkage equilibrium favors the H form. This reflects the constraints on the length of helical stretches available a given chain.

Temperature Dependence

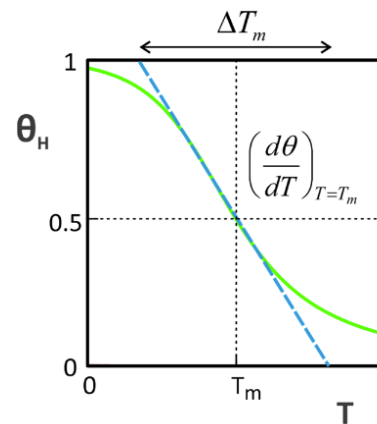
Now let's describe the temperature dependence of the cooperative model. The helix-coil transition shows a cooperative melting transition, where heating the sample a few degrees causes a dramatic change from a sample that is primarily in the C form to one that is primarily H . Multiple temperature-dependent factors make this a bit difficult to deal with analytically, therefore we focus on the behavior at the melting temperature T_m , which we define as the point where $\theta_H(T_m) = 0.5$.

Look at the slope of θ at T_m . From chain rule:

$$\frac{d\theta}{dT} = \frac{d\theta}{ds} \cdot \frac{ds}{dT} = \frac{d\theta}{ds} \cdot s \frac{d \ln s}{dT}$$

Since we interpret s as an equilibrium constant for the addition of one helical residue to a stretch, we can write a van't Hoff relation

$$\frac{d \ln s}{dT} = \frac{\Delta H_{HC}^0}{k_B T^2}$$



Note that this relation assumes that ΔH_0 is independent of temperature, which generally is a concern, but we will not worry too much since we are just evaluating this at T_M . Next we focus our discussion on the high n limit. From the Zimm–Bragg model:

$$\left(\frac{d\theta}{ds}\right)_{s=1} = \frac{1}{4\sigma^{1/2}}$$

Then, we set $s(T_m) = 1$, and combine these results to give the slope of the melting curve at T_m :

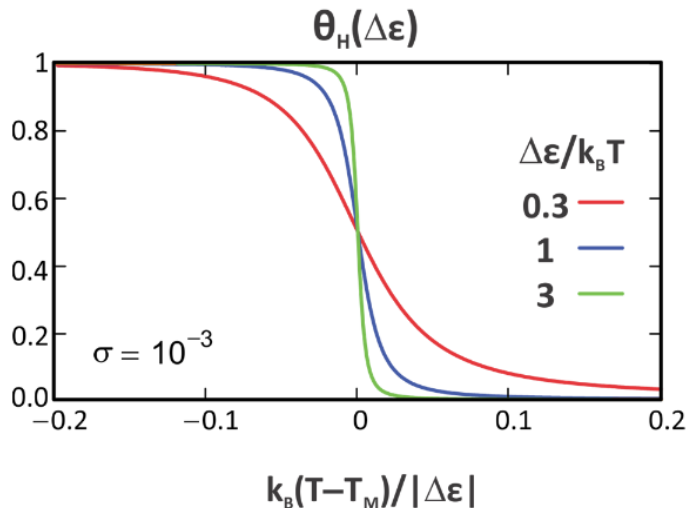
$$\left(\frac{d\theta}{dT}\right)_{T=T_m} = \frac{\Delta H_{HC}^0}{4\sigma^{1/2}k_B T_m^2}$$

The slope of θ at T_m has units of inverse temperature, so we can also express this as a transition width: $\Delta T_m = (d\theta/dT)_{T_m}^{-1}$.

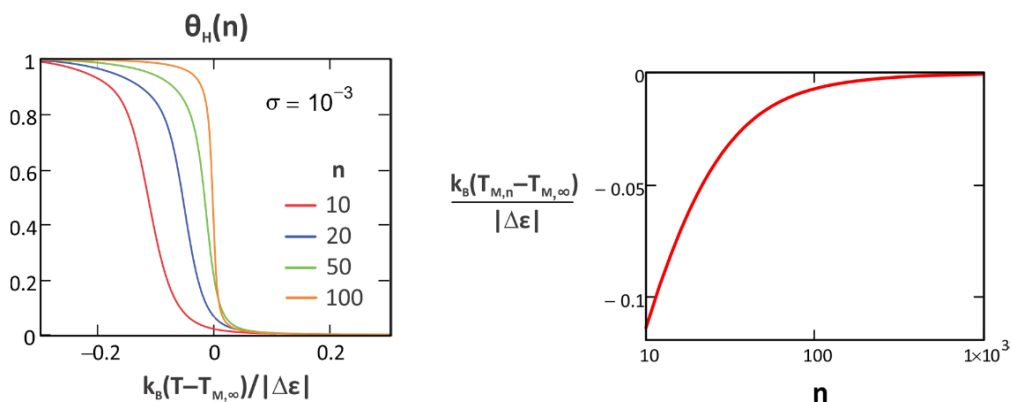
Keep in mind this van't Hoff analysis comes with some real limitations when applied to experimental data. It does not account for the finite size of the system, which we have seen shifts $s(T_m)$ to be > 1 , and the knowledge of parameters at T_m does not necessarily translate to other temperatures. To the extent that you can apply the assumptions, the van't Hoff expression can also be used to predict the helical fraction as a function of temperature in the vicinity of T_M using

$$\ln s = \frac{\Delta H_{HC}^0}{k_B} \left(\frac{1}{T_M} - \frac{1}{T} \right) \quad (18.1.20)$$

and assuming that σ is independent of temperature.



Below we show the length dependence of the melting temperature. As the length of the chain approaches infinite, the helix/coil transition becomes a step function in temperature. This trend matches the expectations for a phase transition: in the thermodynamic limit, the infinite system, will show discontinuous behavior. For finite lengths, the melting temperature T_m is lower than that for the infinite chain ($T_{m,\infty}$), but approaches this value for $n > 300$.



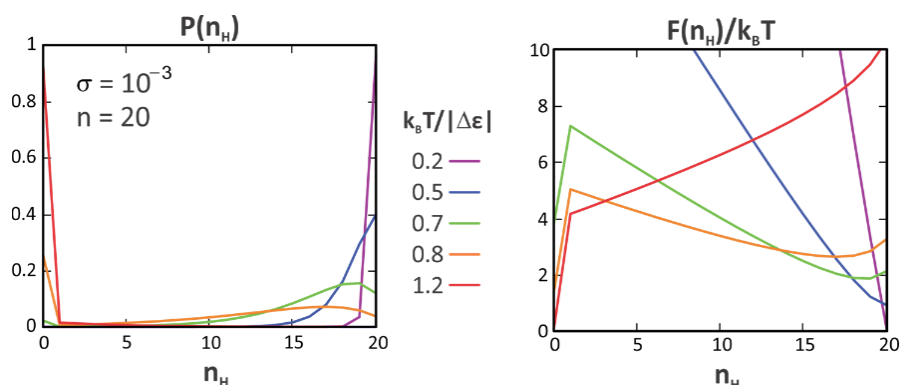
Calorimetric parameters for polypeptide chains

Side-chain only has a small effect on the helix-coil propagation parameter:

Sample	ΔH_{HC}^0 (mol^{-1} residue $^{-1}$)	σ	Other
Alanine-rich peptides, Ac-Y(AEAAKA)8F-NH ₂ , Ac-(AAKAA)kY-NH ₂	-0.95 to -1.3kcal	0.002	
Poly(L-lysine), Poly(L-glutamate)	-1.1kcal	0.0025	
Poly-alanine	-0.95kcal	0.003	$s(0^\circ\text{C}) = 1.35$
Alanine oligomers	-0.85kcal		$\Delta S^0 = 3\text{cal mol}^{-1}\text{K}^{-1}$ residue $^{-1}$
Various homopolypeptides	$\sim 4\text{kJ}$		$\Delta C_P = -32\text{J mol}^{-1}\text{K}^{-1}$ residue $^{-1}$

Free-Energy Landscape

Finally, we investigate the free-energy landscape for the Zimm-Bragg model of the helix-coil transition. The figure below shows the helical probability distribution and corresponding energy landscape for different values of the reduced temperature $k_B T / \Delta \epsilon$ for a chain length of $n = 40$ and $\sigma = 10^{-3}$. Note that $P(n_H)$ is calculated from eq. (18.1.18) for all but the all-coil state, which comes from eq. (18.1.16).



The cooperative model shows two-state behavior. At low temperature and high temperature, the system is almost entirely in the all-helix or all-coil configuration, respectively; however, at intermediate temperatures, the distribution of helical configurations can be very broad. The least probable configuration is a chain with only one helical segment.

This behavior looks much closer to the two-state behavior expected from phase-transition behavior. The free energy has minima for $n_H = 0$ and for $n_H > 1$, and the free energy difference between these states shifts with temperature to favor one or the other minimum.

1. C. R. Cantor and P. R. Schimmel, Biophysical Chemistry Part III: The Behavior of Biological Macromolecules. (W. H. Freeman, San Francisco, 1980), Ch. 20; D. Poland and H. A. Scheraga, Theory of Helix-Coil Transitions in Biopolymers. (Academic Press, New York, 1970).

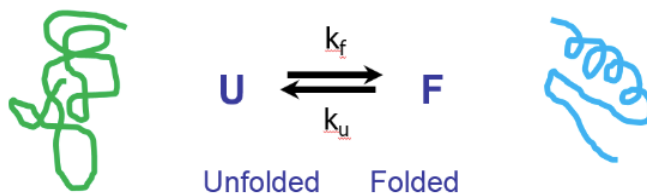
2. P. Doty, A. M. Holtzer, J. H. Bradbury and E. R. Blout, POLYPEPTIDES. II. THE CONFIGURATION OF POLYMERS OF γ -BENZYL-L-GLUTAMATE IN Solution, J. Am. Chem. Soc. 76 (17), 4493-4494 (1954); P. Doty and J. T. Yang, POLYPEPTIDES. VII. POLY- γ -BENZYL-L-GLUTAMATE: THE HELIX-COIL TRANSITION IN Solution, J. Am. Chem. Soc. 78 (2), 498-500 (1956).

3. J. Marmur and P. Doty, Heterogeneity in Deoxyribonucleic Acids: I. Dependence on Composition of the Configurational Stability of Deoxyribonucleic Acids, *Nature* 183 (4673), 1427-1429 (1959).
4. B. H. Zimm and J. K. Bragg, Theory of the phase transition between helix and random coil in polypeptide chains, *J. Chem. Phys.* 31, 526-535 (1959).
5. K. Dill and S. Bromberg, *Molecular Driving Forces: Statistical Thermodynamics in Biology, Chemistry, Physics, and Nanoscience*. (Taylor & Francis Group, New York, 2010), Appendix C p. 705.

This page titled [18.1: Helix–Coil Transition](#) is shared under a [CC BY-NC-SA 4.0](#) license and was authored, remixed, and/or curated by [Andrei Tokmakoff](#) via [source content](#) that was edited to the style and standards of the LibreTexts platform.

18.2: Two-State Thermodynamics

Here we describe the basic thermodynamics of two-state systems, which are commonly used for processes such as protein folding, binding, and DNA hybridization. Working with the example of protein folding analyzed through the temperature-dependent folded protein content.



$$K = \frac{k_f}{k_u} = \frac{[F]}{[U]} = \frac{\phi_F}{1 - \phi_F}$$

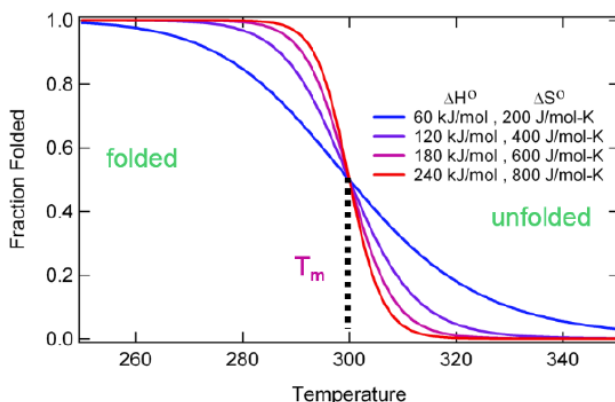
where ϕ_F is the fraction of protein that is folded, and the fraction that is unfolded is $(1 - \phi_F)$.

$$\phi_F = \frac{K}{K + 1}$$

$$K = e^{-\Delta G^0 / RT}$$

$$\phi_F = \frac{1}{1 + e^{-\Delta G^0 / RT}} = \frac{1}{1 + e^{\Delta H^0 / RT} e^{-\Delta S^0 / R}}$$

Define the melting temperature T_m as the temperature at which $\phi_F = 0.5$. Then at T_m , $\Delta G^0 = 0$ or $T_m = \Delta H^0 / \Delta S^0$. Characteristic melting curves for $T_m = 300$ K are below:



We can analyze the slope of curve at T_m using a van't Hoff analysis:

$$\frac{d\phi_F}{dT} = \frac{d\phi_F}{dK} \cdot \frac{dK}{dT} = \frac{d\phi_F}{dK} \cdot K \frac{d \ln K}{dT}$$

$$\frac{d \ln K}{dT} = \frac{\Delta H^0}{RT^2}$$

$$\frac{d\phi_F}{dK} = K^{-2} (1 + K)^{-2}$$

$$\left(\frac{d\phi_F}{dT} \right)_{T=T_m} = \frac{\Delta H^0}{4RT_m^2} \quad \text{since } K = 1 \text{ at } T_m$$

This analysis assumes that there is no temperature dependence to ΔH , although we know well that it does from our earlier discussion of hydrophobicity. A more realistic two-state model will allow for a change in heat capacity between the U and F states that describes the temperature dependence of the enthalpy and entropy.

$$\Delta G^0(T) = \Delta H^0(T_m) - T\Delta S^0(T_m) + \Delta C_p \left[T - T_m - T \ln \frac{T}{T_m} \right]$$

This page titled [18.2: Two-State Thermodynamics](#) is shared under a [CC BY-NC-SA 4.0](#) license and was authored, remixed, and/or curated by [Andrei Tokmakoff](#) via [source content](#) that was edited to the style and standards of the LibreTexts platform.

CHAPTER OVERVIEW

19: Self-Assembly

Cooperative self-assembly refers to the the spontaneous formation of sophisticated structures from many molecular units. Generally, we think of this as involving many molecules (cooperative units), although single- and bi-molecular problems can be wrapped into this description, as in the helix–coil transition. Examples include:

- Peptides and proteins
 - Protein folding, binding, and association
 - Amyloid fibrilization
 - Assembly of multi-protein complexes
 - Viral capsid self-assembly
- Nucleic acids
 - DNA hybridization, DNA origami
 - Folding and association of RNA structures: pseudoknots, ribozymes
- Lipids
 - Bilayer structures
 - Micelle formation

Although molecular structures also assemble with the input of energy, the emphasis here is on spontaneous self-assembly in the absence of external input.

[19.1: Micelle Formation](#)

[19.2: Classical Nucleation Theory](#)

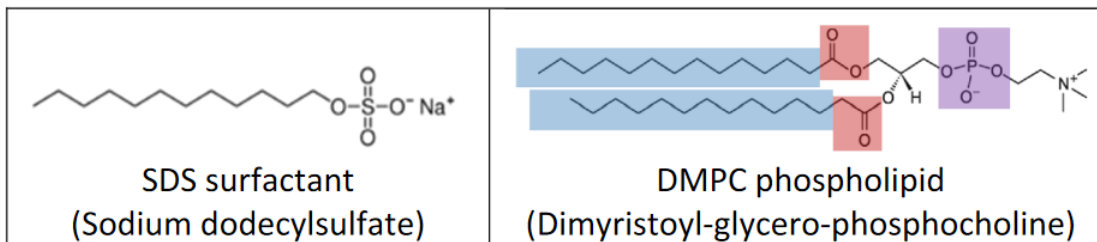
[19.3: Why Are Micelles Uniform in Size?](#)

[19.4: Shape of Self-Assembled Amphiphiles](#)

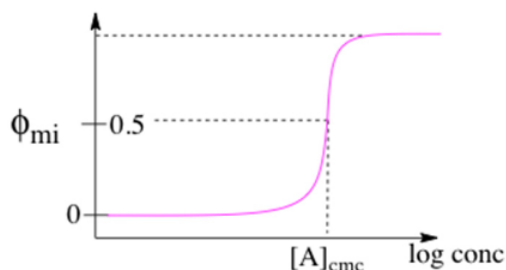
This page titled [19: Self-Assembly](#) is shared under a [CC BY-NC-SA 4.0](#) license and was authored, remixed, and/or curated by [Andrei Tokmakoff](#) via [source content](#) that was edited to the style and standards of the LibreTexts platform.

19.1: Micelle Formation

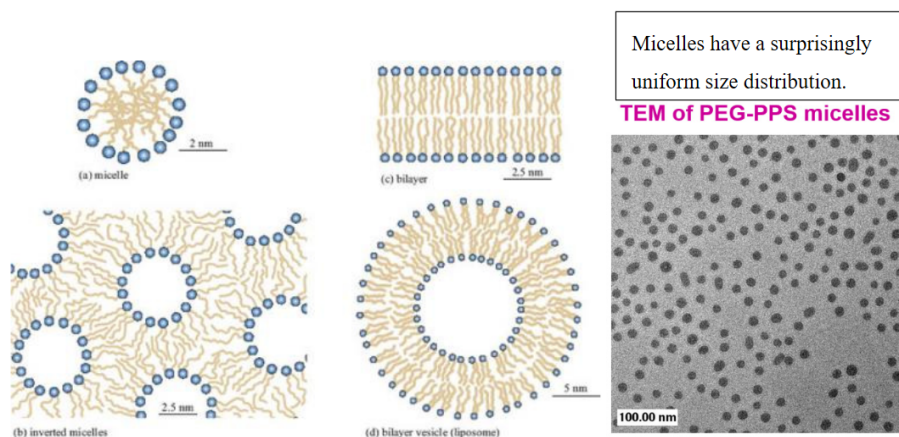
In particular, we will focus on micellar structures formed from a single species of amphiphilic molecule in aqueous solution. These are typically lipids or surfactants that have a charged or polar head group linked to one or more long hydrocarbon chains.



Such amphiphiles assemble into a variety of structures, the result of which depends critically on the concentration, composition, and temperature of the system. For SDS surfactant, micelles are favored. These condense hydrophobic chains into a fluid like core and present the charged head groups to the water. The formation of micelles is observed above a **critical micelle concentration** (CMC).



As the surfactant is dissolved, the solution is primarily monomeric at low concentration, but micelles involving 30–100 molecules suddenly appear for concentrations greater than the CMC.



Reprinted from <http://swartz-lab.epfl.ch/page-20594-en.html>.

To begin investigating this phenomenon, we can start by simplifying the equilibrium to a two-state form:



K_n is the equilibrium constant for assembling a micelle with n amphiphiles from solution. n is called the **aggregation number**.

$$K_n = \frac{[A_n]}{[A]^n} = e^{-\Delta G_m^0 \text{ micelle} / k_B T} \quad (19.1.2)$$

The total number of A molecules present is the sum of the free monomers and those monomers present in micelles:

$$CTOT = [A] + n[A_n]. \quad (19.1.3)$$

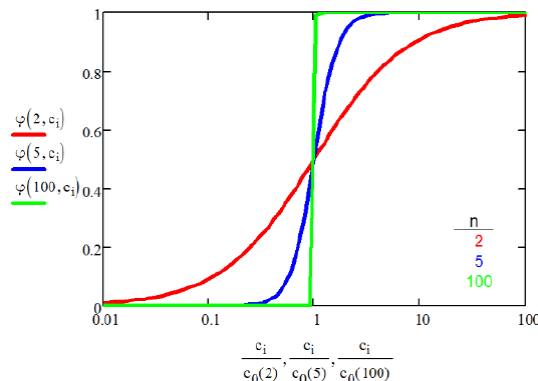
The fraction of monomers present in micelles:

$$\phi_{mi} = \frac{n[A_n]}{CTOT} = \frac{n[A_n]}{[A] + n[A_n]} = \frac{nK_n[A]^{n-1}}{1 + nK_n[A]^{n-1}} \quad (19.1.4)$$

This function has an inflection point at the CMC, for which the steepness of the transition increases with n . Setting $\phi_{mi} = 0.5$, we obtain the CMC (c_0) as

$$c_0 = [A]_{cmc} = \frac{1}{(nK_n)^{1/n-1}} \quad (19.1.5)$$

Function steepens with aggregation number n :



Thus for large n , and cooperative micelle formation:

$$\Delta G_{micelle}^0 = -RT \ln c_0 \quad (19.1.6)$$

Note the similarity of Equation 19.1.2 to the results for fractional helicity in the helix-coil transition:

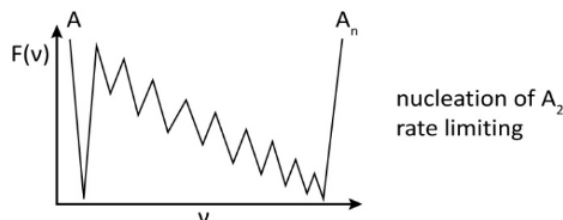
$$\frac{s^n}{1 + s^n} \quad (19.1.7)$$

This similarity indicates that a cooperative model exists for micelle formation in which the aggregation number reflects the number of cooperative units in the process. Cooperativity can be obtained from models that require surmounting a high nucleation barrier before rapidly adding many more molecules to reach the micelle composition. The simplest description of such a process would proceed in a step-wise growth form (a zipper model) for n copies of monomer A assembling into a single micelle A_n .



$$K_n = \prod_{i=1}^{n-1} K_i \quad K_i = \frac{k_f(i \rightarrow i+1)}{k_r(i+1 \rightarrow i)} \quad (19.1.9)$$

Examples of how the energy landscape looks as a function of oligomerization number v are shown below. However, if you remove the short-range correlation, overall we expect the shape of the energy landscape to still be two-state depending on the nucleation mechanism.



This picture is overly simple though, since it is not a one-dimensional chain problem. Rather, we expect that there are equilibria connecting all possible aggregation number clusters to form larger aggregates. A more appropriate description of the free energy barrier for nucleating a micelle is similar to classical nucleation theory for forming a liquid droplet from vapor.

D. H. Boal, *Mechanics of the Cell*, 2nd ed. (Cambridge University Press, Cambridge, UK, 2012), p. 250.

This page titled [19.1: Micelle Formation](#) is shared under a [CC BY-NC-SA 4.0](#) license and was authored, remixed, and/or curated by [Andrei Tokmakoff](#) via [source content](#) that was edited to the style and standards of the LibreTexts platform.

19.2: Classical Nucleation Theory

Let's summarize the thermodynamic theory for the nucleation of a liquid droplet by the association of molecules from the vapor. The free energy for forming a droplet out of n molecules (which we refer to as monomers) has two contributions: a surface energy term that describes the energy needed to make droplet interface and a volume term that describes the cohesive energy of the monomers.

$$\Delta G_n = \gamma a - \Delta \epsilon V \quad (19.2.1)$$

Note the similarity to our discussion of the [hydrophobic effect](#), where γ was just the surface tension of water. $\Delta \epsilon$ is the bulk cohesive energy—a positive number. Since this is a homogeneous cluster, we expect the cluster volume V to be proportional to n and, for a spherical droplet, the surface area a to be proportional to $V^{2/3}$ and thus $n^{2/3}$ (remember our discussion of hydrophobic collapse). To write this in terms of monomer units, we can express the total area in terms of the average surface area per molecule in the droplet:

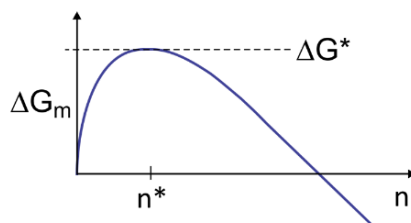
$$\alpha = a/n \quad (19.2.2)$$

and as the monomer volume V_0 . Then the free energy is

$$\Delta G_n = \gamma \alpha n^{2/3} - \Delta \epsilon V_0 n \quad (19.2.3)$$

and the chemical potential of the droplet as

$$\begin{aligned} \Delta \mu_n &= \frac{\partial \Delta G_m}{\partial n} \\ &= \frac{2}{3} \gamma_0 \alpha n^{-1/3} + \Delta \epsilon V_0 \end{aligned}$$



These competing effects result in a maximum in ΔG versus n , which is known as the **critical nucleation cluster size** n^* . The free energy at n^* is positive and called the nucleation barrier ΔG^* . We find n^* by setting Equation ??? equal to zero:

$$n^* = \left(\frac{2\gamma_0 \alpha}{3\Delta \epsilon V_0} \right)^3 \quad (19.2.4)$$

and substituting into Equation 19.2.3

$$G^* = \frac{4}{27} \frac{(\gamma_0 \alpha)^3}{(\Delta \epsilon V_0)^2} \quad (19.2.5)$$

For nucleation of a liquid droplet from vapor, if fewer than n^* monomers associate, there is not enough cohesive energy to allow the growth of a droplet and the nucleus will dissociate. If more than n^* monomers associate, the droplet is still unstable, but the direction of spontaneous change will increase the size of the droplet and a liquid phase will grow from the nucleus. The process of micelle formation requires a balance of attractive and repulsive forces that stabilize an aggregate, which can depend on surface and volume terms. Thus the $\Delta G_{\text{micelle}}$ has a similar form, but the signs of different factors may be positive or negative.

P. S. Richard, Nucleation: theory and applications to protein solutions and colloidal suspensions, *J. Phys.: Condens. Matter* 19 (3), 033101 (2007).

This page titled [19.2: Classical Nucleation Theory](#) is shared under a [CC BY-NC-SA 4.0](#) license and was authored, remixed, and/or curated by [Andrei Tokmakoff](#) via [source content](#) that was edited to the style and standards of the LibreTexts platform.

19.3: Why Are Micelles Uniform in Size?

Micelles are formed by amphiphiles that want to bury hydrophobic chains and expose charged head groups to water. Since a cavity must be formed for the micelle, the resulting surface tension of the cavity (the hydrophobic effect) results in the system trying to minimize its surface area, and thereby the number of molecules in the micelle. At the same time, the electrostatic repulsion between headgroups results in driving force to increase the surface area per headgroup. These competing effects result in an optimal micelle size.

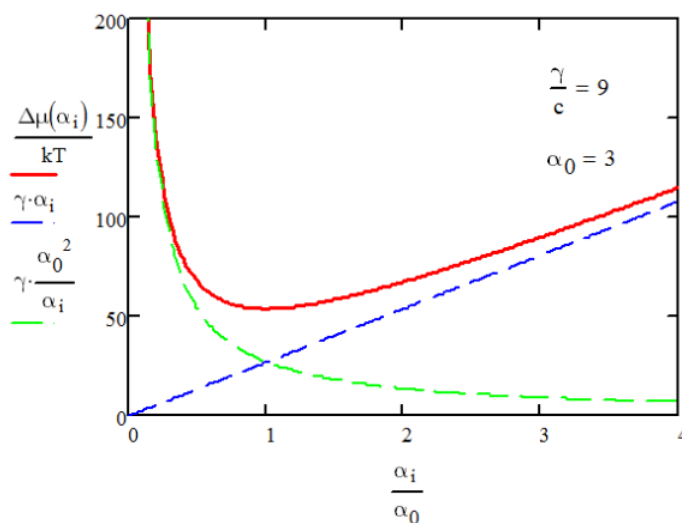
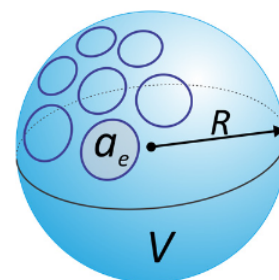
We start by defining the chemical potential $\Delta\mu_n$, which is the free energy per mole of amphiphilic molecule A to assemble a micelle with n molecules. Instead of using n , we will try to express the size of the micelle in terms of its surface area a and assume that it is spherical. Then, the free energy for forming a cavity for the micelle grows as γa , where γ is the surface tension. The surface area is expressed as an average surface area spanned by the charged headgroup of a monomer unit:

$$a_e = a/n \quad (19.3.1)$$

The repulsion term is hard to predict and depends on many variables. There are the electrostatic repulsions between head groups, but there is also the entropic penalty for forming the micelle that depends on size. As an approximation, we anticipate that the free energy should be inversely proportional to surface area. Then the free energy for forming a micelle with n molecules is

$$\begin{aligned} \Delta G_n &= \gamma a + \frac{x}{a} \\ &= \gamma n a_e + \frac{x}{n a_e} \end{aligned}$$

where x is a constant.



Solving for $\Delta\mu = \partial\Delta G / \partial n$, differentiating it with respect to a_e , and setting to zero, we find the optimal micelle size, a_0 , is

$$a_0 = \sqrt{\frac{x}{\gamma n^2}} \quad (19.3.2)$$

Solving for x and substituting in eq. (4), we obtain the chemical potential as:

$$\Delta\mu = \frac{\gamma}{a_e} (a_e^2 + a_0^2) = 2\gamma a_0 + \frac{\gamma}{a_e} (a_e - a_0)^2 \quad (19.3.3)$$

It has a parabolic shape with a minimum at a_0 .

Next, we can obtain the probability distribution for the micelle size as a function of head group surface area and aggregation number

$$P_n = \exp(-n\Delta\mu/k_B T) \quad (19.3.4)$$

$$P_n(a_e) \exp\left(-\frac{n\gamma(a_e - a_0)^2}{a_e k_B T}\right) \quad (19.3.5)$$

The relative populations of micelles are distributed in a Gaussian distribution about a_0 . The distribution of sizes has a standard deviation (or polydispersity) given by

$$\sigma = \sqrt{\frac{n a_e k_B T}{2\gamma}} \quad (19.3.6)$$

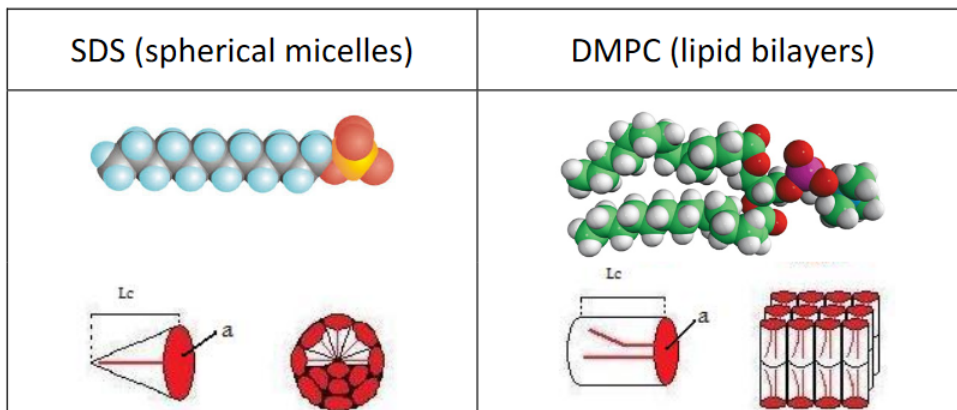
From $a = 4\pi r^2 = n a_e$, we predict that the breadth of the micelle size distribution will scale linearly in the micelle radius, and as the square root of temperature and molecule number.

K. Dill and S. Bromberg, *Molecular Driving Forces: Statistical Thermodynamics in Biology, Chemistry, Physics, and Nanoscience*. (Taylor & Francis Group, New York, 2010); J. N. Israelachvili, *Intermolecular and Surface Forces*, 3rd ed. (Academic Press, Burlington, MA, 2011), Ch. 20.

This page titled [19.3: Why Are Micelles Uniform in Size?](#) is shared under a [CC BY-NC-SA 4.0](#) license and was authored, remixed, and/or curated by [Andrei Tokmakoff](#) via [source content](#) that was edited to the style and standards of the LibreTexts platform.

19.4: Shape of Self-Assembled Amphiphiles

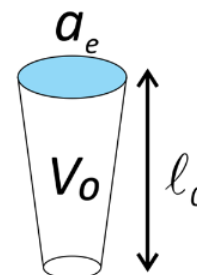
Empirically it is observed that certain features of the molecular structure of amphiphilic molecules and surfactants are correlated with the shape of the larger structures that they self-assemble into. For instance, single long hydrocarbon tails with a sulfo- group (like SDS) tend to aggregate into spherical micelles, whereas phospholipids with two hydrocarbon chains (like DMPC) prefer to form bilayers. Since structure formation is largely governed by the hydrophobic effect, condensing the hydrophobic tails and driving the charged groups to a water interfaces, this leads to the conclusion that the volume and packing of the hydrophobic tail plays a key role in shape. While the molecular volume and the head group size and charge are fixed, the fluid nature of the hydrocarbon chain allows the molecule to pack into different configurations.



This structural variability is captured by the packing parameter:

$$p = \frac{V_0}{a_e \ell_0}$$

where V_0 and ℓ_0 are the volume and length of the hydrocarbon chain, and a_e is the average surface area per charged head group. V_0/ℓ_0 is relatively constant at $\sim 0.2 \text{ nm}^2$, but the shape of the chain may vary from extended (cylindrical) to compact (conical), which will favor a particular packing.



	$10^0\text{-}10^1 \text{ nm}$	$10^1\text{-}10^4 \text{ nm}$	$10^1\text{-}10^5 \text{ nm}$	$10^0\text{-}10^2 \text{ nm}$
$p = v/a_0l$	$p < 1/3$	$1/3 < p < 1/2$	$1/2 < p < 1$	$p \sim 1$
aggregates	sphere	cylinder	vesicle	bilayer

Reprinted with permission from Z. Chu, C. A. Dreiss and Y. Feng, Chem. Soc. Rev. **42** (17), 7174-7203 (2013). Copyright 2013 Royal Society of Chemistry.

Empirically it is found that systems with $p < 1/3$ typically form micelles, for cylindrical structures for $1/3 < p < 1/2$, and for bilayer structures for $1/2 < p < 1$. Simple geometric arguments can be made to rationalize this observation. Taking a spherical aggregate with radius R and aggregation number n as an example, we expect the ratio of the volume to the surface area to be

$$\frac{V}{A} = \frac{nV_0}{na_e} = \frac{R}{3} \rightarrow V_0 = \frac{a_e R}{3} \quad (19.4.1)$$

Substituting into the packing parameter:

$$p = \frac{V_0}{a_e \ell_0} = \frac{R}{3\ell_0} \quad (19.4.2)$$

Now, even though the exact conformation of the hydrocarbon chain is not known, the length of the hydrocarbon tail will not be longer than the radius of the micelle, i.e., $\ell_0 \geq R$. Therefore

$$\therefore p \leq \frac{1}{3} \quad (\text{spheres}) \quad (19.4.3)$$

Similar arguments can be used to explain why extended lipid bilayers have $p \approx 1$ and cylinders for $p \approx \frac{1}{2}$. In a more general sense, we note that the packing parameter is related to the curvature of the aggregate surface. As p decreases below one, the aggregate forms an increasingly curved surface. (Thus vesicles are expected to have $\frac{1}{2} < p < 1$). It is also possible to have $p > 1$. In this case, the curvature also increases with increasing p , although the sign of the curvature inverts (from convex to concave). Such conditions result in inverted structures, such as reverse micelles in which water is confined in a spherical pool in contact with the charged headgroups, and the hydrocarbon tails are project outward into a hydrophobic solvent.

Readings

J. N. Israelachvili, *Intermolecular and Surface Forces*, 3rd ed. (Academic Press, Burlington, MA, 2011).

This page titled [19.4: Shape of Self-Assembled Amphiphiles](#) is shared under a [CC BY-NC-SA 4.0](#) license and was authored, remixed, and/or curated by [Andrei Tokmakoff](#) via [source content](#) that was edited to the style and standards of the LibreTexts platform.

SECTION OVERVIEW

6: Dynamics and Kinetics

20: Protein Folding

20.1: Models for Simulating Folding

20.2: Perspectives on Protein Folding Dynamics

21: Binding and Association

21.1: Thermodynamics and Biomolecular Reactions

21.2: Statistical Thermodynamics of Biomolecular Reactions

21.3: DNA Hybridization

21.4: Biomolecular Kinetics

21.5: Diffusion-Limited Reactions

21.6: Protein Recognition and Binding

21.7: Forces Guiding Binding

21.8: Specificity in Recognition and Binding

22: Biophysical Reaction Dynamics

22.1: Concepts and Definitions

22.2: Computing Dynamics

22.3: Representations of Dynamics

22.4: Analyzing Trajectories

22.5: Time-Correlation Functions

23: Barrier Crossing and Activated Processes

23.1: Transition State Theory

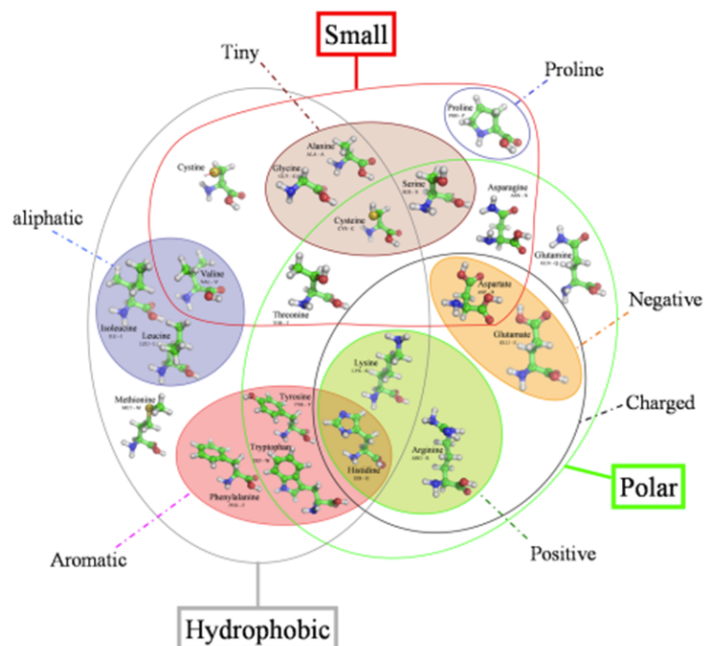
23.2: Kramers' Theory

This page titled [6: Dynamics and Kinetics](#) is shared under a [CC BY-NC-SA 4.0](#) license and was authored, remixed, and/or curated by [Andrei Tokmakoff](#) via [source content](#) that was edited to the style and standards of the LibreTexts platform.

CHAPTER OVERVIEW

20: Protein Folding

- Composed of 50–500 amino acids linked in 1D sequence by the polypeptide backbone
- The amino acid physical and chemical properties of the 20 amino acids dictate an intricate and functional 3D structure.
- Folded structure is energetic ground state (Anfinsen)



Reprinted from http://swift.cmbi.ru.nl/teach/Wageningen/IMAGE/aa_venn_diagram.png

Many proteins spontaneously refold into native form *in vitro* with high fidelity and high speed.

Different approaches to studying this phenomenon:

- How does the primary sequence encode the 3D structure?
- Can you predict the 3D fold from a primary sequence?
- Design a polypeptide chain that folds into a known structure.
- What is the mechanism by which a disordered chain rapidly adopts its native structure?

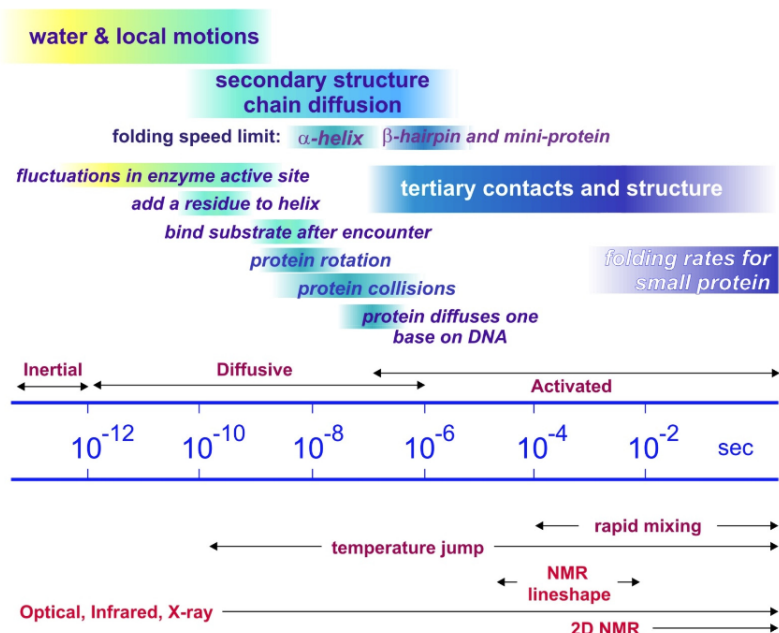
Our emphasis here is mechanistic. What drives this process? The physical properties of the connected pendant chains interacting cooperatively give rise to the structure.

It is said that the primary sequence dictates the three-dimensional structure, but this is not the whole story, and it emphasizes a certain perspective. Certainly we need water, and defined thermodynamic conditions in temperature, pH, and ionic strength. In a sense the protein is the framework and the solvent is the glue. Folded proteins may not be as structured from crystal structures, as one is led to believe.

Kinetics and Dynamics

Observed protein folding time scales span decades. Observations for protein folding typically measured in ms, seconds, and minutes. This is the time scale for activated folding across a free-energy barrier. The intrinsic time scale for the underlying

diffusive processes that allow conformations to evolve and local contacts to be formed through free diffusion is ps to μ s. The folding of small secondary structure happens on 0.1–1 μ s for helices and \sim 1–10 μ s for hairpins. The fastest folding mini-proteins (20–30 residues) is \sim 1 μ s.



Cooperativity

What drives this? Some hints:

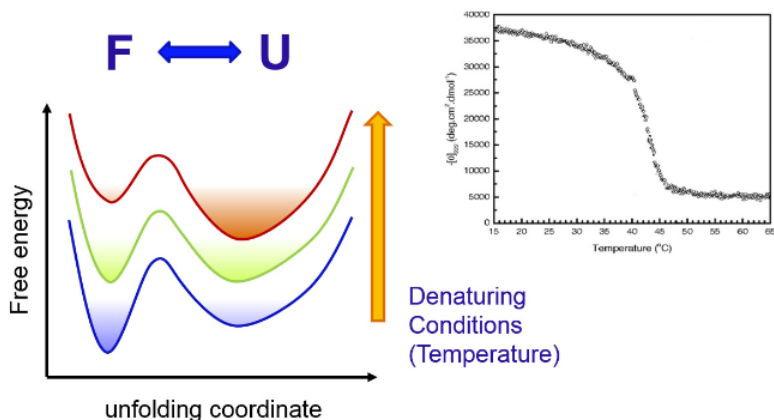
Levinthal's paradox¹

The folded configuration cannot be found through a purely random search process.

- Assume: 3 states/amino acid linkage \times 100 linkages
- $3^{100} = 5 \times 10^{47}$ states \times Sample 10⁻¹³sec/state
- 10²⁷ years to sample

Two-state thermodynamics

To all appearances, the system (often) behaves as if there are only two thermodynamic states.



Entropy/Enthalpy

ΔG is a delicate balance of two large opposing energy contributions ΔH and $T\Delta S$.

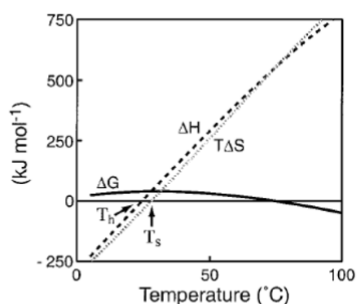
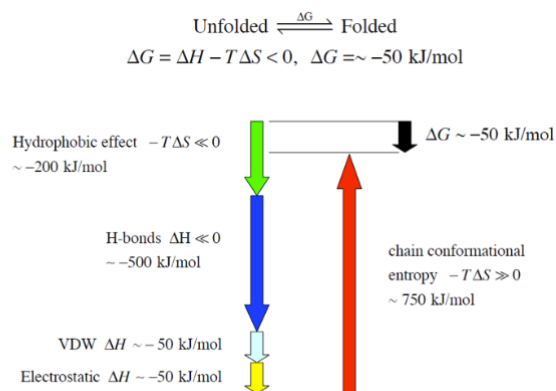


Figure 3. Protein unfolding free energy, $\Delta G = G_u - G_f$, entropy, ΔS , and enthalpy, ΔH , versus temperature. For proteins, $T_s \approx T_h$. Data on myoglobin from Makhatadze, G. I. and Privalov, P. L. *Biophys. Chem.* 1994, 51, 291.



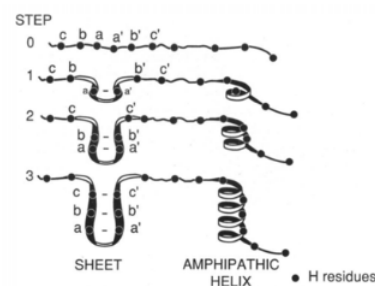
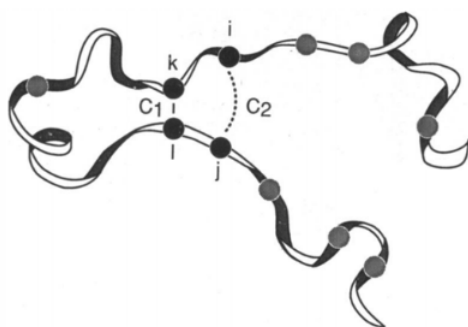
Reprinted with permission from N. T. Southall, K. A. Dill and A. D. J. Haymet, *J. Phys. Chem. B* 106, 521-533 (2002). Copyright 2002 American Chemical Society.

Reprinted from James Chou (2008).
<http://cmcd.hms.harvard.edu/activiti...1/lecture7.pdf>.

Cooperativity underlies these observations

Probability of forming one contact is higher if another contact is formed.

- Zipping
- Hydrophobic collapse



Reprinted from K. A. Dill, K. M. Fiebig and H. S. Chan, *Proc. Natl. Acad. Sci. U. S. A.* 90,1942-1946 (1993). Copyright 1993 PNAS.

Protein Folding Conceptual Pictures

Traditional pictures rooted in classical thermodynamics and reaction kinetics.

- Postulate particular sequence of events.
- Focus on importance of a certain physical effect.

1. **Framework or kinetic zipper**
2. **Hydrophobic collapse**
3. **Nucleation-condensation**

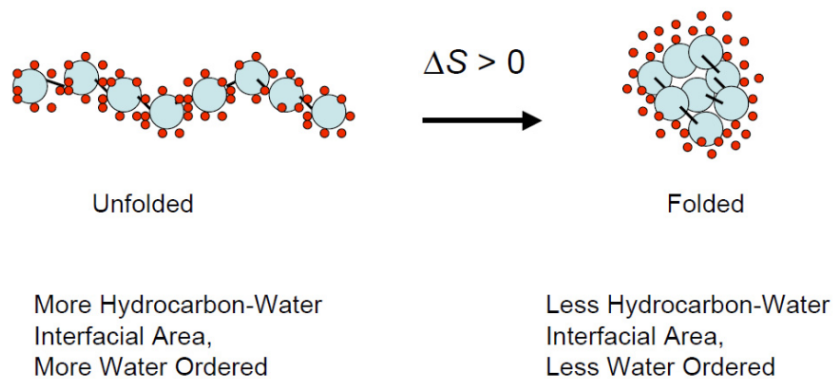
Framework/Kinetic Zipper Model

- Observation from peptides: secondary structures fold rapidly following nucleation.
- Secondary structure formation precedes tertiary organization.
- Emphasis:
 - Hierarchy and pathway
 - Focus on backbone, secondary structure

Hydrophobic Collapse

- Observation: protein structure has hydrophobic residues buried in center and hydrophilic groups near surface.
- An extended chain rapidly collapses to bury hydrophobic groups and thereby speeds search for native contacts.
- Collapsed state: molten globule
- Secondary and tertiary structure form together following collapse.

U \longleftrightarrow **Molten Globule** \longleftrightarrow **F**



Nucleation–Condensation

Nucleation of tertiary native contacts is important first step, and structure condenses around that.

Some observations so far:

- Importance of collective coordinates
- Big challenge: We don't know much about the unfolded state.

1. C. Levinthal, Are there pathways for protein folding?, J. Chim. Phys. Phys.-Chim. Biol. 65, 44-45 (1968).

[20.1: Models for Simulating Folding](#)

[20.2: Perspectives on Protein Folding Dynamics](#)

This page titled [20: Protein Folding](#) is shared under a [CC BY-NC-SA 4.0](#) license and was authored, remixed, and/or curated by [Andrei Tokmakoff](#) via [source content](#) that was edited to the style and standards of the LibreTexts platform.

20.1: Models for Simulating Folding

Our study of folding mechanism and the statistical mechanical relationship between structure and stability have been guided by models. Of these, simple reductionist models guided the conceptual development from the statistical mechanics side, since full atom simulations were initially intractable. We will focus on the simple models.

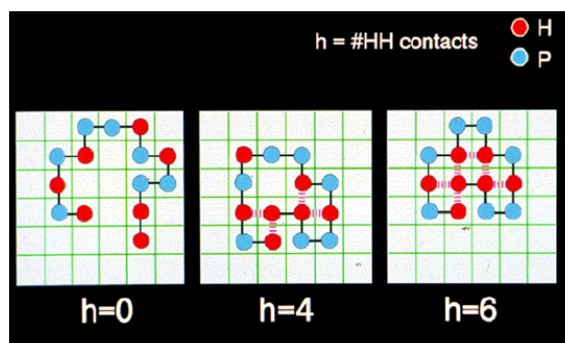
- Reductionist Model
 - Lattice Models
 - Gō Models
 - Coarse Grained
- Atomistic
 - Force fields



*Increasing level
of molecular detail*

HP Model¹

- Chain of beads. Self-avoiding walk on square lattice.
- 2 types of beads: Hydrophobic (H) and polar (P).
- H-H contacts are energetically favorable to H-P contacts. more H → collapse to compact state, but many collapsed structures more P → well-solvated, doesn't fold ~1:1 H:P optimal
- Can be used for folding mechanism using Monte Carlo.



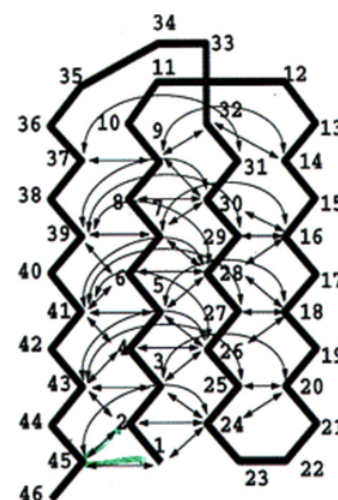
Coarse-Grained Models²

Hierarchy of various models that reduce protein structure to a set of interacting beads.

Gō Models³

Gō models and Gō-like models refer to a class of coarse-grained models in which formation of structure is driven by a minimalist interaction potential that drives the system to its native structure. The folded state must be known

- Coarse grained
 - Original: one bead per AA
 - “Off-lattice model”
- Native-state biasing potential
 - Multiple forces in single interaction potential
 - Need to know folded structure
 - Increased simulation speed
 - Doesn't do well metastable intermediates or non-native contacts



1. K. F. Lau and K. A. Dill, A lattice statistical mechanics model of the conformational and sequence spaces of proteins, *Macromolecules* 22, 3986-3997 (1989).
2. V. Tozzini, Coarse-grained models for proteins, *Curr. Opin. Struct. Biol.* 15, 144-150 (2005).
3. Y. Ueda, H. Taketomi and N. Gō, Studies on protein folding, unfolding, and fluctuations by computer simulation. II. A. Three-dimensional lattice model of lysozyme, *Biopolymers* 17, 1531-1548 (1978).

This page titled [20.1: Models for Simulating Folding](#) is shared under a [CC BY-NC-SA 4.0](#) license and was authored, remixed, and/or curated by [Andrei Tokmakoff](#) via [source content](#) that was edited to the style and standards of the LibreTexts platform.

20.2: Perspectives on Protein Folding Dynamics

These models have helped drive theoretical developments that provide alternate perspectives on how proteins fold:

State Perspective

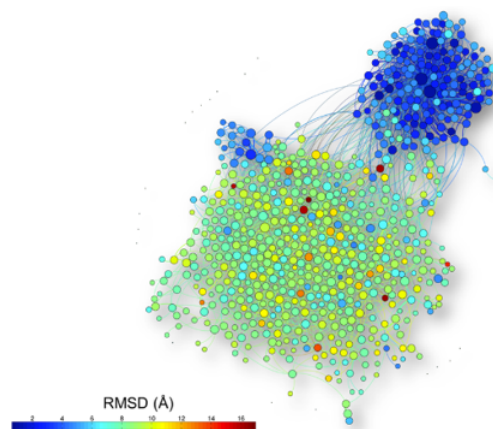
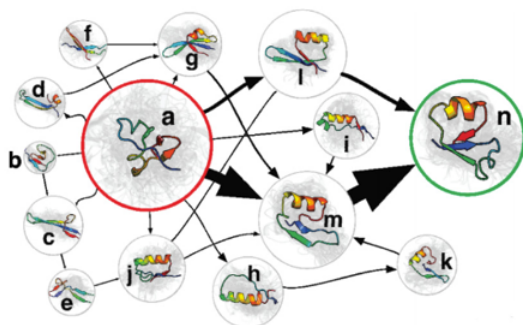
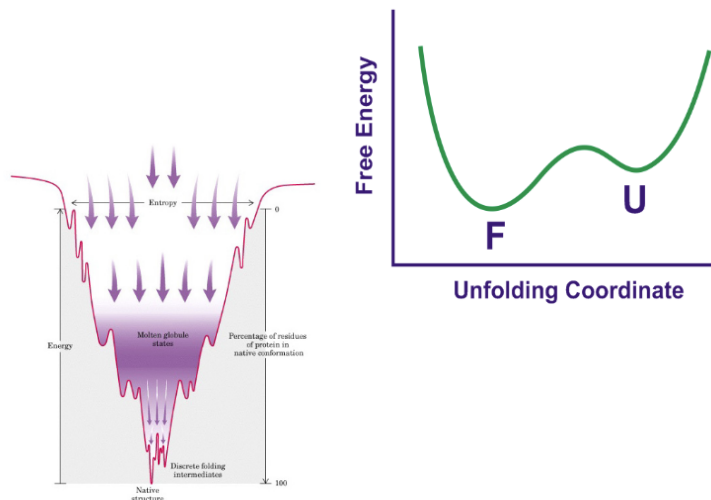
- Interchange between states with defined configurations
- What are the states, barriers and reaction coordinates?

Statistical Perspective

- Change in global variables
- Configurational entropy

Networks

- Characterize conformational variation and network of connectivity between them.



	Reprinted with permission from V. A. Voelz, G. R. Bowman, K. Beauchamp and V. S. Pande, <i>J. Am. Chem. Soc.</i> 132, 1526-1528 (2010). Copyright 2010 American Chemical Society.		Reprinted with permission from C. R. Baiz, Y.-S. Lin, C. S. Peng, K. A. Beauchamp, V. A. Voelz, V. S. Pande and A. Tokmakoff, <i>Biophys. J.</i> 106, 1359-1370 (2014). Copyright Elsevier 2014.
--	---	--	--

The statistical perspective is important. The standard ways of talking about folding is in terms of activated processes, in which we describe states that have defined structures, and which exchange across barriers along a reaction coordinate. And the emphasis is on molecularly interpreting these states. There is nothing formally wrong with that except that it is an unsatisfying way of treating problems where one has entropic barriers.

Folding Funnels and Configurational Entropy

Helps with entropic barriers¹

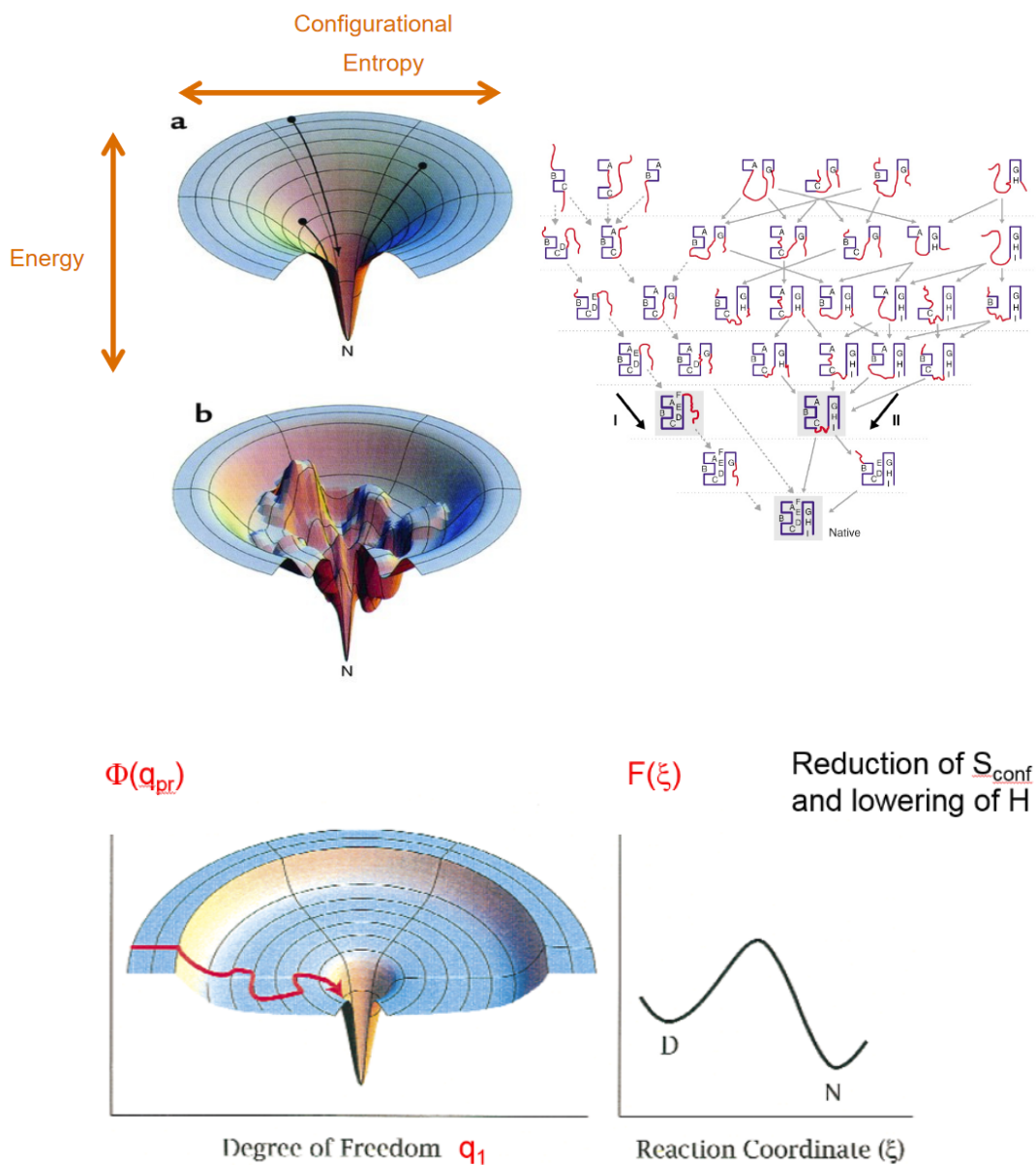


Fig. 5. (A) Energy landscape vs. (B) reaction diagram. A landscape is a free energy F_{micro} of each individual chain conformation vs. the many microscopic degrees of freedom. A reaction diagram is a free energy F_{macro} of an ensemble of molecules, and includes the chain conformational entropy. Here F_{macro} is a function of a single variable, ξ , such as a reaction coordinate. The reaction coordinate is usually not known for protein folding. The red arrow on the landscape indicates a possible micropath, an individual folding trajectory. In this case, the micropath never involves an uphill step, and yet the reaction diagram has a free energy barrier. The barrier is due to the slow entropic search of many different chains seeking the entry to the central steep funnel.

Reprinted with permission from K. A. Dill, Protein Sci. 8, 1166-1180 (1999). John Wiley and Sons 1999.

Transition State vs Ensemble Kinetics

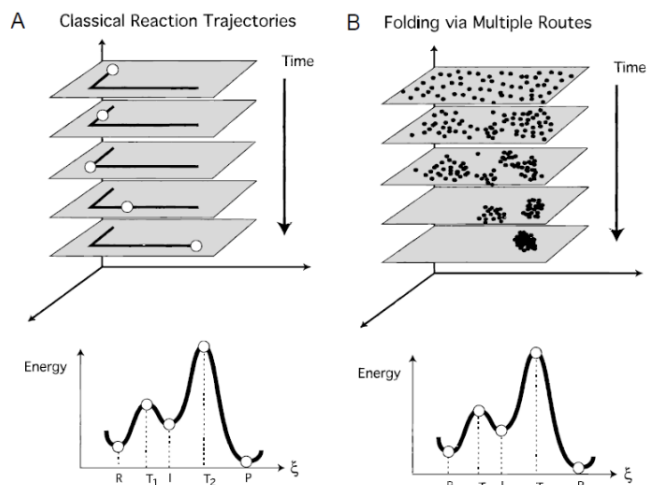


Fig. 8. A: For chemical reactions (energies $\gg kT$), the macrostates on reaction coordinate diagrams correspond to the time series of microstates on the energy landscape. B: For folding processes (energies per interaction $\approx kT$), the observed macrostates may not uniquely specify the time series of microstates on the energy landscape.

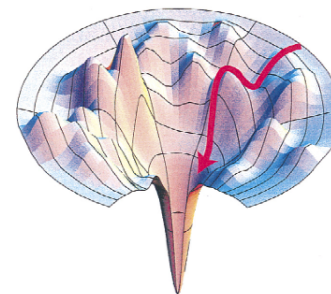


Fig. 9. An uphill micropath (red line) is surrounded by more favorable routes that do not involve uphill steps to reach the native state.

Reprinted with permission from K. A. Dill, *Protein Sci.* 8, 1166-1180 (1999). John Wiley and Sons 1999.

1. K. A. Dill, *Polymer principles and protein folding*, *Protein Sci.* 8, 1166-1180 (1999).

This page titled [20.2: Perspectives on Protein Folding Dynamics](#) is shared under a [CC BY-NC-SA 4.0](#) license and was authored, remixed, and/or curated by [Andrei Tokmakoff](#) via [source content](#) that was edited to the style and standards of the LibreTexts platform.

CHAPTER OVERVIEW

21: Binding and Association

Molecular associations are at the heart of biological processes. Specific functional interactions are present at every level of cellular activity. Some of the most important:

1) Proteins Interacting with Small Molecules and Ions

- Enzyme/substrate interactions and catalysis
- Ligand/receptor binding
- Chemical energy transduction (for instance ATP)
- Signaling (for instance neurotransmitters, cAMP)
- Drug or inhibitor binding
- Antibody binding antigen
- Small molecule and ion transport
 - $Mb + O_2 \rightarrow MbO_2$
 - Ion channels and transporters

2) Protein–Protein Interactions

- Signaling and regulation networks
- Receptors binding to ligands activate receptors
 - GPCRs bind agonist/hormone for transmembrane signal transduction
- Assembly and function of multi-protein complexes
 - Replication machinery in replisome consists of multiple proteins including DNA polymerase, DNA ligase, topoisomerase, helicase
 - Kinetochore orchestrate interactions of chromatin and the motor proteins that separate sister chromatids during cell division

3) Protein–Nucleic Acid Interactions

- All steps in the central dogma
- Transcription factor binding
- DNA repair machinery
- Ribozymes

In all of these examples, the common thread is a macromolecule, which typically executes a conformational change during the interaction process. Conformational flexibility and entropy changes during binding play an important role in describing these processes.

[21.1: Thermodynamics and Biomolecular Reactions](#)

[21.2: Statistical Thermodynamics of Biomolecular Reactions](#)

[21.3: DNA Hybridization](#)

[21.4: Biomolecular Kinetics](#)

[21.5: Diffusion-Limited Reactions](#)

[21.6: Protein Recognition and Binding](#)

[21.7: Forces Guiding Binding](#)

[21.8: Specificity in Recognition and Binding](#)

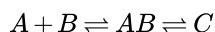
This page titled [21: Binding and Association](#) is shared under a [CC BY-NC-SA 4.0](#) license and was authored, remixed, and/or curated by [Andrei Tokmakoff](#) via [source content](#) that was edited to the style and standards of the LibreTexts platform.

21.1: Thermodynamics and Biomolecular Reactions

To begin, we recognize that binding and association processes are bimolecular reactions. Let's describe the basics of this process. The simplest kinetic scheme for bimolecular association is



A and B could be any two molecules that interact chemically or physically to result in a final bound state; for instance, an enzyme and its substrate, a ligand and receptor, or two specifically interacting proteins. From a mechanistic point of view, it is helpful to add an intermediate step:



Here AB refers to transient encounter complex, which may be a metastable kinetic intermediate or a transition state. Then the initial step in this scheme reflects the rates of two molecules diffusing into proximity of their mutual target sites (including proper alignments). The second step is recognition and binding. It reflects the detailed chemical process needed to form specific contacts, execute conformational rearrangements, or perform activated chemical reactions. We separate these steps here to build a conceptual perspective, but in practice these processes may be intimately intertwined.

Equilibrium Constant

Let's start by reviewing the basic thermodynamics of bimolecular reactions, such as reaction scheme (21.1.1). The thermodynamics is described in terms of the chemical potential for the molecular species in the system ($i = A, B, C$)

$$\mu_i = \left(\frac{\partial G}{\partial N_i} \right)_{p, T, \{N_j, j \neq i\}}$$

where N_i is the number of molecules of species i . The dependence of the chemical potential on the concentration can be expressed as

$$\mu_i = \mu_i^0 + RT \ln \frac{c_i}{c^0} \quad (21.1.2)$$

c_i is the concentration of reactant i in mol L^{-1} , and the standard state concentration is $c^0 = 1 \text{ mol L}^{-1}$. So the molar reaction free energy for scheme (1) is

$$\begin{aligned} \Delta \bar{G} &= \sum_i v_i \mu_i \\ &= \mu_C - \mu_A - \mu_B, \\ &= \Delta \bar{G}^0 + RT \ln K \end{aligned}$$

v_i is the stoichiometric coefficient for component i . K is the reaction quotient

$$K = \frac{(c_C/c^0)}{(c_A/c^0)(c_B/c^0)} \quad (21.1.3)$$

At equilibrium, $\Delta \bar{G} = 0$, so

$$\Delta \bar{G}^0 = -RT \ln K_a \quad (21.1.4)$$

where the association constant K_a is the value of the reaction quotient under equilibrium conditions. Dropping c^0 , with the understanding that we must express concentration in M units:

$$K_a = \frac{c_C}{c_A c_B} \quad (21.1.5)$$

Since it is defined as a standard state quantity, K_a is a fundamental constant independent of concentration and pressure or volume, and is only dependent on temperature. The inverse of K_a is K_d the equilibrium constant for the C dissociation reaction $C \rightleftharpoons A + B$.

Concentration and Fraction Bound

Experimentally one controls the total mass $m_{TOT} = m_C + m_A + m_B$, or concentration

$$c_{TOT} = c_C + c_A + c_B \quad (21.1.6)$$

The composition of system can be described by the fraction of concentration due to species i as

$$\theta_i = \frac{c_i}{c_{TOT}}$$

$$\theta_A + \theta_B + \theta_C = 1$$

We can readily relate K_a to θ_i , but it is practical to set some specific constraint on the composition here. If we constrain the A:B composition to be 1:1, which is enforced either by initially mixing equal mole fractions of A and B, or by preparing the system initially with pure C, then

$$K_a = \frac{4\theta_C}{(1 - \theta_C)^2 c_{TOT}} \quad (\theta_A = \theta_B)$$

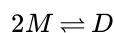
$$= \frac{(1 - 2\theta_A)}{\theta_A^2 c_{TOT}}$$

This expression might be used for mixing equimolar solutions of binding partners, such as complementary DNA oligonucleotides. Using eq. (21.1.6) (with $c_A=c_B$) and (21.1.7) here, we can obtain the composition as a function of total concentration fraction as a function of the total concentration

$$\theta_C = \left(1 + \frac{2}{K_a c_{TOT}}\right) - \sqrt{\left(1 + \frac{2}{K_a c_{TOT}}\right)^2 - 1} \quad (21.1.7)$$

$$\theta_A = \frac{1}{2}(1 - \theta_C)$$

In the case where $A=B$, applicable to homodimerization or hybridization of self-complementary oligonucleotides, we rewrite scheme (21.1.1) as the association of monomers to form a dimer



and find:

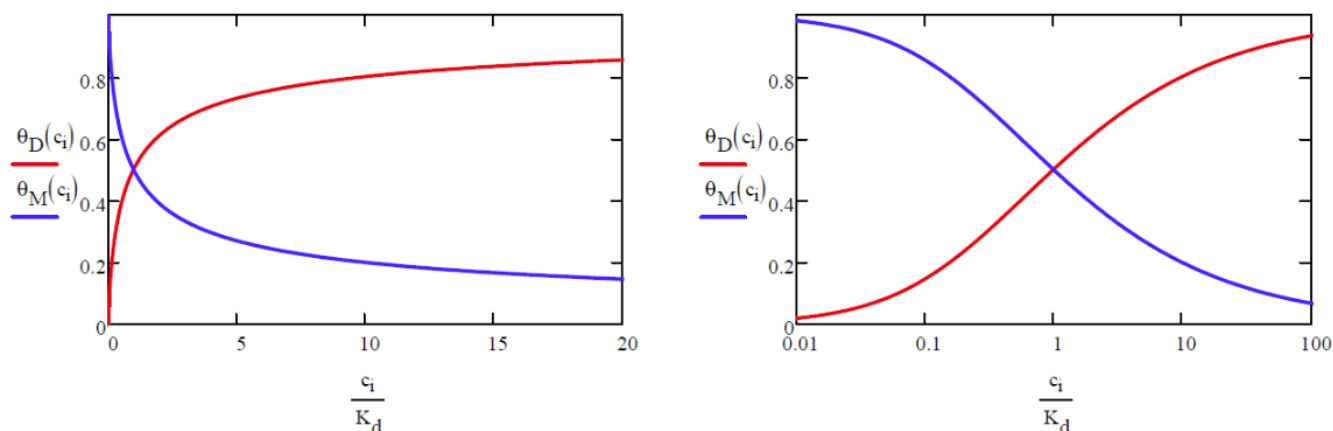
$$K_a = \theta_D / 2(1 - \theta_D)^2 c_{TOT}$$

$$K_a = (1 - \theta_M) / 2\theta_M^2 c_{TOT}$$

$$\theta_D = 1 + \frac{1}{4c_{TOT}K_a} (1 - \sqrt{1 + 8c_{TOT}K_a}) \quad (21.1.8)$$

$$\theta_M = 1 - \theta_D \quad (21.1.9)$$

These expressions for the fraction of monomer and dimer, and the corresponding concentrations of monomer and dimer are shown below. An increase in the total concentration results in a shift of the equilibrium toward the dimer state. Note that $c_{TOT} = (9K_a)^{-1} = K_d/9$ at $\theta_M = \theta_D = 0.5$,



For ligand receptor binding, ligand concentration will typically be much greater than that of the receptor, and we are commonly interested in fraction of receptors that have a ligand bound, θ_{bound} . Re-writing our association reaction as



we write the fraction bound as

$$\begin{aligned} \theta_{bound} &= \frac{c_{LR}}{c_R + c_{LR}} \\ &= \frac{c_L K_a}{1 + c_L K_a} \end{aligned}$$

This is equivalent to a **Langmuir absorption isotherm**.

Temperature Dependence

The temperature dependence of K_a is governed by eq. (21.1.4) and the fundamental relation

$$\Delta G^0(T) = \Delta H^0(T) - T\Delta S^0(T) \quad (21.1.11)$$

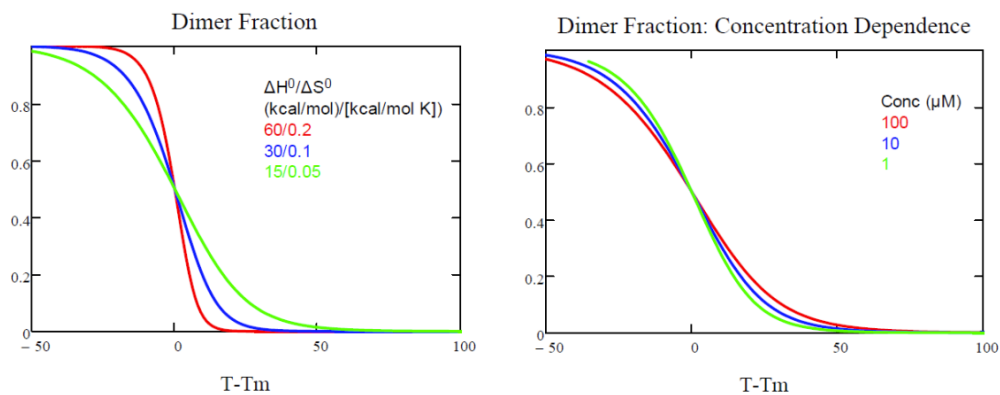
Under the assumption that ΔH^0 and ΔS^0 are temperature independent, we find

$$K_a(T) = \exp \left[-\frac{\Delta H_a^0}{RT} + \frac{\Delta S_a^0}{R} \right] \quad (21.1.12)$$

This allows us to describe the temperature-dependent composition of a system using the expressions above for θ_i . While eq. (12) allows you to predict a melting curve for a given set of thermodynamic parameters, it is more difficult to use it to extract those parameters from experiments because it only relates the value of K_d at one temperature to another.

Temperature is often used to thermally dissociate or melt dsDNA or proteins, and the analysis of these experiments requires that we define a reference temperature. In the case of DNA melting, the most common and readily accessible reference temperature is the melting temperature T_m defined as the point where the mole fractions of ssDNA (monomer) and dsDNA (dimer) are equal, $\theta_M = \theta_D = 0.5$. This definition is practically motivated, since DNA melting curves typically have high and low temperature limits that correspond to pure dimer or pure monomer. Then T_m is commonly associated with the inflection point of the melting curve or the peak of the first derivative of the melting curve. From eq. (21.1.9), we see that the equilibrium constants for the association and dissociation reaction are given by the total concentration of DNA: $K_a(T_m) = K_d(T_m) - 1 = c_{tot}^{-1}$ and $\Delta G_d^0(T_m) = -RT_m \ln c_{tot}$. Furthermore, eq. (21.1.12) implies $T_m = \Delta H^0 / \Delta S^0$.

The examples below show the dependence of melting curves on thermodynamic parameters, T_m , and concentration. These examples set a constant value of T_m ($\Delta H^0 / \Delta S^0$). The concentration dependence is plotted for $\Delta H^0 = 15 \text{ kcal mol}^{-1}$ and $\Delta S^0 = 50 \text{ cal mol}^{-1} \text{ K}^{-1}$.



For conformational changes in macromolecules, it is expected that the enthalpy and entropy will be temperature dependent. Drawing from the definition of the heat capacity,

$$C_p = \left(\frac{\partial H}{\partial T} \right)_{N,P} = T \left(\frac{\partial S}{\partial T} \right)_{N,P}$$

we can describe the temperature dependence of ΔH^0 and ΔS^0 by integrating from a reference temperature T^0 to T . If ΔC_p is independent of temperature over a small enough temperature range, then we obtain a linear temperature dependence to the enthalpy and entropy of the form

$$\Delta H^0(T) = \Delta H^0(T_0) + \Delta C_p [T - T_0] \quad (21.1.13)$$

$$\Delta S^0(T) = \Delta S^0(T_0) + \Delta C_p \left(\frac{T}{T_0} \right) \quad (21.1.14)$$

These expressions allow us to relate values of ΔH^0 , ΔS^0 , and ΔG^0 at temperature T to its value at the reference temperature T^0 . From these expressions, we obtain a more accurate description of the temperature dependence of the equilibrium constant is

$$K_d(T) = \exp \left[-\frac{\Delta H_m^0}{RT} + \frac{\Delta S_m^0}{R} - \frac{C_p}{R} \left[1 - \frac{T_m}{T} - \ln \left(\frac{T}{T_m} \right) \right] \right] \quad (21.1.15)$$

where $\Delta H_m^0 = \Delta H^0(T_m)$ and $\Delta S_m^0 = \Delta S^0(T_m)$ are the enthalpy and entropy for the dissociation reaction evaluated at T_m .

This page titled [21.1: Thermodynamics and Biomolecular Reactions](#) is shared under a [CC BY-NC-SA 4.0](#) license and was authored, remixed, and/or curated by [Andrei Tokmakoff](#) via [source content](#) that was edited to the style and standards of the LibreTexts platform.

21.2: Statistical Thermodynamics of Biomolecular Reactions

Statistical mechanics can be used to calculate K_a on the basis of the partition function. The canonical partition function Q is related to the Helmholtz free energy through

$$F = -k_B T \ln Q \quad (21.2.1)$$

$$Q = \sum_{\alpha} e^{-E_{\alpha}/k_B T} \quad (21.2.2)$$

where the sum is over all microstates (a particular configuration of the molecular constituents to a macroscopic system), Boltzmann weighted by the energy of that microstate E_{α} . The chemical potential of molecular species i is given by

$$\mu_i = -k_B T \left(\frac{\partial \ln Q}{\partial N_i} \right)_{V, T, \{N_{j \neq i}\}} \quad (21.2.3)$$

We will assume that we can partition Q into contributions from different molecular components of a reacting system such that

$$Q = \prod_i Q_i \quad (21.2.4)$$

The ability to separate the partition function stems from the assumption that certain degrees of freedom are separable from each other. When two sub-systems are independent of one another, their free energies should add ($F_{\text{TOT}} = F_1 + F_2$) and therefore their partition functions are separable into products: $Q_{\text{TOT}} = Q_1 Q_2$. Generally this separability is a result of being able to write the Hamiltonian as $H_{\text{TOT}} = H_1 + H_2$, which results in the microstate energy being expressed as a sum of two independent parts: $E_{\alpha} = E_{\alpha,1} + E_{\alpha,2}$. In addition to separating the different molecular species, it is also very helpful to separate the translational and internal degrees of freedom for each species, $Q_i = Q_{i,\text{trans}} Q_{i,\text{int}}$. The entropy of mixing originates from the translational partition function, and therefore will be used to describe concentration dependence.

For N_i non-interacting, indistinguishable molecules, we can relate the canonical and molecular partition function q_i for component i as

$$Q_i = \frac{q_i^{N_i}}{N_i!} \quad (21.2.5)$$

and using Sterling's approximation we obtain the chemical potential,

$$\mu_i = -RT \ln \frac{q_i}{N_i} \quad (21.2.6)$$

Following the reasoning in eqs. (2)–(5), we can write the equilibrium constant as

$$K_a = \frac{N_C}{N_A N_B} = \frac{q_C}{q_A q_B} V \quad (21.2.7)$$

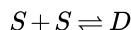
This expression reflects that the equilibrium constant is related to the stoichiometrically scaled ratio of molecular partition functions per unit volume $K_a = \prod_i (q_i/V)^{\nu_i}$. Then the standard binding free energy is determined by eq. (4).

This page titled [21.2: Statistical Thermodynamics of Biomolecular Reactions](#) is shared under a [CC BY-NC-SA 4.0](#) license and was authored, remixed, and/or curated by [Andrei Tokmakoff](#) via [source content](#) that was edited to the style and standards of the LibreTexts platform.

21.3: DNA Hybridization

To illustrate the use of statistical thermodynamics to describe binding, we discuss simple models for the hybridization or melting of DNA. These models are similar to our description of the helix–coil transition in their approach. These do not distinguish the different nucleobases, only considering nucleotides along a chain that are paired (bp) or free (f).

Consider the case of the pairing between self-complementary oligonucleotides.



S refers to any fully dissociated ssDNA and D to any dimer forms that involve two strands which have at least one base pair formed. We can then follow expressions for monomer–dimer equilibria above. The equilibrium constant for the association of single strands is

$$K_a = \frac{c_D}{c_S^2} \quad (21.3.1)$$

This equilibrium constant is determined by the concentration-dependent free-energy barrier for two strands to diffuse into contact and create the first base pair. If the total concentration of molecules present is either monomer or dimer, the form is

$$C_{TOT} = c_S + 2c_D \quad (21.3.2)$$

then the fraction of the DNA strands in the dimer form is

$$\theta_D = \frac{2c_D}{C_{tot}} \quad (21.3.3)$$

and eq. (10) leads to

$$\theta_D = 1 + (4K_a C_{tot})^{-1} - \sqrt{(1 + (4K_a C_{tot})^{-1})^2 - 1} \quad (21.3.4)$$

We see that at the total concentration, which results in a dimer fraction $\theta_D = 0.5$, the association constant is obtained from $K_a = (9C_{tot})^{-1}$. This is a traditional description of the thermodynamics of a monomer–dimer equilibrium.

We can calculate K_a from the molecular partition functions for the S and D states:

$$K_a = \frac{q_D}{q_S^2}$$

Different models for hybridization will vary in the form of these partition functions. For either state, we can separate the partition function into contributions from the conformational degrees of freedom relevant to the base-pairing and hybridization, and other degrees of freedom, $q_i = q_{i,conf} q_{i,ext}$. Assuming that the external degrees of freedom will be largely of an entropic nature, we neglect an explicit calculation and factor out the external degrees of freedom by defining the variable γ :

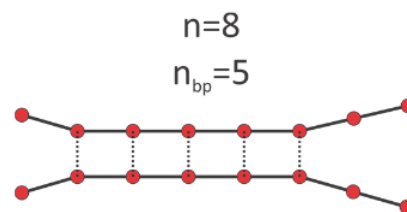
$$\gamma = \frac{q_{D,ext} C_{tot}}{q_{S,ext}^2} \quad (21.3.5)$$

then

$$\theta_D = 1 + \frac{q_{S,int}^2}{4\gamma q_{D,int}} - \sqrt{\left(1 + \frac{q_{S,int}^2}{4\gamma q_{D,int}}\right)^2 - 1} \quad (21.3.6)$$

Short Oligonucleotides: The Zipper Model

For short oligonucleotide hybridization, a common (and reasonable) approximation is the single stretch model, which assumed that base-pairing will only occur as a single continuous stretch of base pairs. This is reasonable for short oligomers ($n < 20$) where two distinct helical stretches separated by a bubble (loop) are unlikely given the persistence length of dsDNA. The zipper model refers to the single-stretch case with “perfect matching”, in which only pairing between the bases in precisely sequence-



aligned DNA strands is counted. As a result of these two approximations, the only dissociated base pairs observed in this model appear at the end of a chain (fraying).

The number of bases in a single strand is n and the number of bases that are paired is n_{bp} . For the dimer, we consider all configurations that have at least one base pair formed. The dimer partition function can be written as

$$\begin{aligned} q_{D,int}(n) &= \sigma \sum_{n_{bp}=1}^n g(n, n_{bp}) s^{n_{bp}} \\ &= \sigma \sum_{n_{bp}=1}^n (n - n_{bp} + 1) s^{n_{bp}} \end{aligned}$$

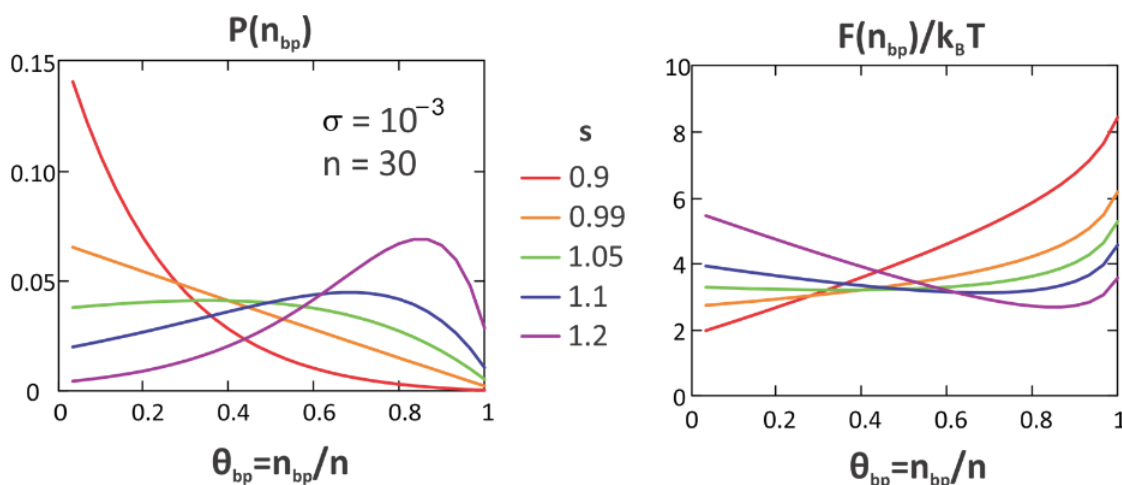
Here g is the number of ways of arranging n_{bp} continuous base pairs on a strand with length n ; σ is the statistical weight for nucleating the first base pair; and s is the statistical weight for forming a base pair next to an already-paired segment: $s = e^{-\Delta\varepsilon_{bp}/k_B T}$. Therefore, in the zipper model, the equilibrium constant in eq. (23) between ssDNA and dimers involving at least one intact base pair is: $K_{zip} = \sigma s$. In the case of homogeneous polynucleotide chains, in which sliding of registry between chains is allowed: $q_{D,int}(n) = \sigma \sum_{n_{bp}=1}^n (n - n_{bp} + 1)^2 s^{n_{bp}}$. The sum in eq. (27) can be evaluated exactly, giving

$$q_{D,int}(n) = \frac{\sigma s}{(s-1)^2} [s^{n+1} - (n+1)s + n] \quad (21.3.7)$$

In the case that $s > 1$ ($\Delta\varepsilon_{bp} < 0$) and $n \gg 1$, $q_{D,int} \rightarrow \sigma s^n$. Also, the probability distribution of helical segments is

$$P_{bp}(n, n_{bp}) = \frac{(n - n_{bp} + 1) \sigma s^{n_{bp}}}{q_{D,int}} \quad 1 \leq n_{bp} \leq n \quad (21.3.8)$$

The plot below shows illustrations of the probability density and associated energy landscape for a narrow range of s across the helix-coil transition. These figures illustrate a duplex state that always has a single free-energy minimum characterized by frayed configurations.



In addition to the fraction of molecules that associate to form a dimer, we must also consider the fraction of contacts that successfully form a base pair in the dimer state

$$\theta_{bp} = \frac{\langle n_{bp} \rangle}{n}$$

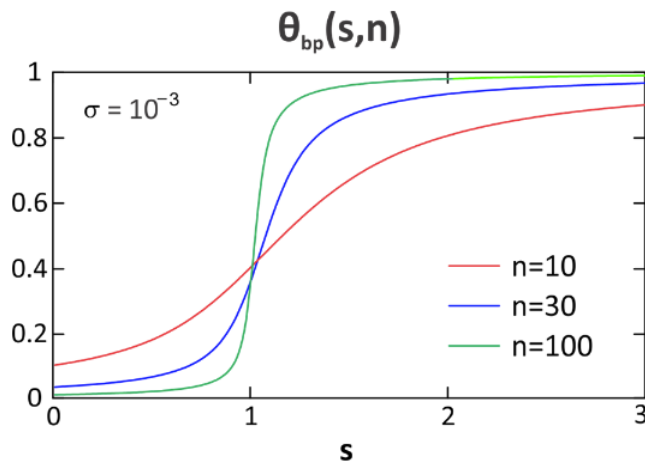
We can evaluate this using the identity

$$\langle n_H \rangle = \frac{s}{q} \frac{\partial q}{\partial s}$$

Using eq. (28) we have

$$\theta_{bp} = \frac{ns^{n+2} - (n+2)s^{n+1} + (n+2)s - n}{n(s-1)(s^{n+1} - s(n+1) + n)}$$

Similar to the helix-coil transition in polypeptides, θ_{bp} shows cooperative behavior with a transition centered at $s = 1$, which gets steeper with increasing n and decreasing σ .



Finally, we can write the total fraction of nucleobases that participate in a base pair as the product of the fraction of the DNA strands that are associated in a dimer form, and the average fraction of bases of the dimer that are paired.

$$\theta_{tot} = \theta_D \theta_{bp}$$

This page titled [21.3: DNA Hybridization](#) is shared under a [CC BY-NC-SA 4.0](#) license and was authored, remixed, and/or curated by [Andrei Tokmakoff](#) via [source content](#) that was edited to the style and standards of the LibreTexts platform.

21.4: Biomolecular Kinetics

Returning to our basic two-state scheme, we define the rate constants k_a and k_d for the association and dissociation reactions:



From detailed balance, which requires that the total flux for the forward and back reactions be equal under equilibrium conditions:

$$K_a = \frac{k_a}{k_d} \quad (21.4.2)$$

The units for K_a are M^{-1} , $M^{-1}s^{-1}$ for k_a , and s^{-1} for k_d .

For the case where we explicitly consider the AB encounter complex:



Schemes of this sort are referred to as reaction–diffusion problems. Note, this corresponds to the scheme used in Michaelis–Menten kinetics for enzyme catalysis, where AB is an enzyme–substrate complex prior to the catalytic step.

The kinetic equations corresponding to this scheme are often solved with the help of a steady-state approximation ($\partial[AB]/\partial t \approx 0$), leading to

$$\frac{d[C]}{dt} = k_a[A][B] - k_d[C] \quad (21.4.4)$$

$$k_a = \frac{k_1 k_2}{(k_{-1} + k_2)} \quad k_d = \frac{k_{-1} k_{-2}}{k_{-1} + k_2} \quad (21.4.5)$$

Let's look at the limiting scenarios:

1. Diffusion controlled reactions refer to the case when reaction or final association is immediate once A and B diffusively encounter one another, i.e., $k_2 \gg k_{-1}$. Then the observed rate of product formation $k_a \approx k_1$, and we can then equate k_1 with the diffusion-limited association rate we have already discussed.
2. Pre-Equilibrium. When the reaction is limited by the chemical step, an equilibrium is established by which A and B can associate and dissociate many times prior to reaction, and the AB complex establishes a pre-equilibrium with the unbound partners defined by a nonspecific association constant $K'_a = k_1/k_{-1}$. Then the observed association rate is $k_a = k_2 K'_a$.

What if both diffusion and reaction within encounter complex matter? That is the two rates $k_1 \approx k_2$.



Now all the rates matter. This can be solved in the same manner that we did for diffusion to capture by a sphere, but with boundary conditions that have finite concentration of reactive species at the critical radius. The steady-state solution gives:

$$k_{eff} = \frac{k_a k_{rxn}}{k_a + k_{rxn}}$$

$$k_{eff}^{-1} = k_a^{-1} + k_{rxn}^{-1}$$

k_{eff} is the effective rate of forming the product C. It depends on the association rate k_a (or k_1) and k_{rxn} is an effective forward reaction rate that depends on k_2 and k_{-1} .

Competing Factors in Diffusion–Reaction Processes

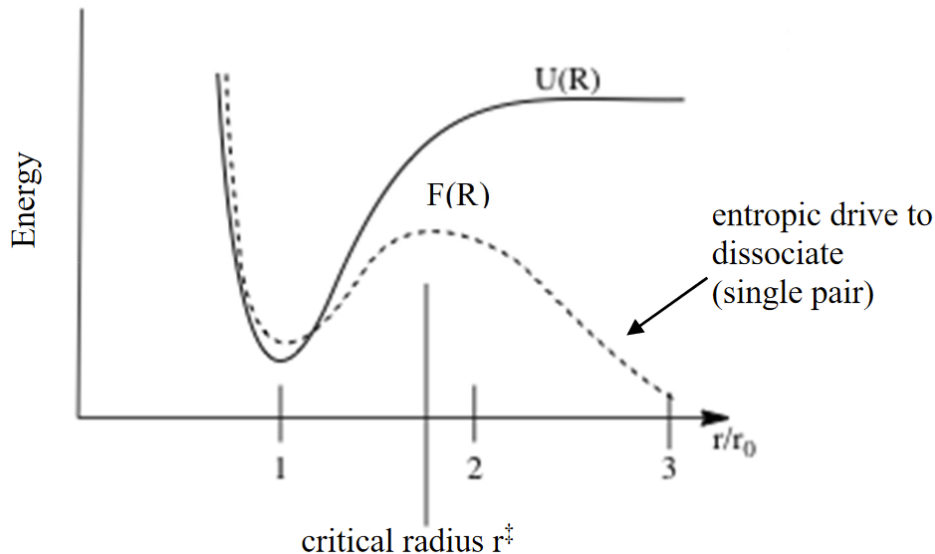
In diffusion–reaction processes, there are two competing factors that govern the outcome of the binding process. These are another manifestation of the familiar enthalpy–entropy compensation effects we have seen before. There is a competition between enthalpically favorable contacts in the bound state and the favorable entropy for the configurational space available to the unbound partners. Overall, there must be some favorable driving force for the interaction, which can be expressed in terms of a binding potential $U_{AB}(R)$ that favors the bound state. On the other hand, for any one molecule A, the translational configuration space available to the partner B will grow as R^2 .

We can put these concepts together in a simple model.¹ The probability of finding B at a distance R from A is

$$P(R)dR = Q^{-1} e^{-U(R)/kT} 4\pi R^2 dR \quad (21.4.7)$$

where Q is a normalization constant. Then we can define a free energy along the radial coordinate

$$\begin{aligned} F(R) &= -k_B T \ln P(R)dR \\ &= U(R) - k_B T \ln R^2 - \ln Q \end{aligned}$$



Here $F(R)$ applies to a single A-B pair, and therefore the free energy drops continuously as R increases. This corresponds to the infinitely dilute limit, under which circumstance the partners will never bind. However, in practice there is a finite volume and concentration for the two partners. We only need to know the distance to the nearest possible binding partner $\langle R_{AB} \rangle$. We can then put an upper bound on the radii sampled on this free energy surface. In the simplest approximation, we can determine a cut off radius in terms of the volume available to each B, which is the inverse of the B concentration: $\frac{4}{3}\pi r_c^3 = [B]^{-1}$. Then, the probability of finding the partners in the bound state is

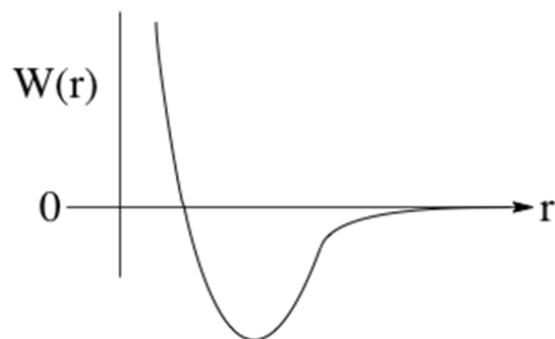
$$P_a = \frac{\int_0^{r^*} e^{-F(r)/k_B T} 4\pi r^2 dr}{\int_0^{r_c} e^{-F(r)/k_B T} 4\pi r^2 dr} \quad (21.4.8)$$

At a more molecular scale, the rates of molecular association can be related to diffusion on a potential of mean force. $g(r)$ is the radial distribution function that describes the radial variation of B density about A, and is related to the potential of mean force $W(r)$ through $g(r) = \exp[-W(r)/k_B T]$. Then the association rate obtained from the flux at a radius defined by the association barrier ($r = r^\ddagger$) is

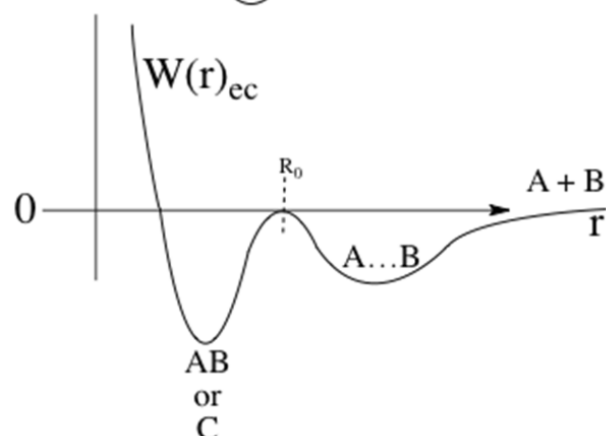
$$k_a^{-1} = \int_{r^\ddagger}^{\infty} dr [4\pi r^2 D(r) e^{-W(r)/k_B T}]^{-1} \quad (21.4.9)$$

Here $D(r)$ is the radial diffusion coefficient that describes the relative diffusion of A and B. The spatial dependence reflects the fact that at small r the molecules do not really diffuse independently of one another.

For weakly attractive:



or structural/large solutes
or encounter complex



1. D. A. Beard and H. Qian, *Chemical Biophysics; Quantitative Analysis of Cellular Systems*. (Cambridge University Press, Cambridge, UK, 2008).

This page titled [21.4: Biomolecular Kinetics](#) is shared under a [CC BY-NC-SA 4.0](#) license and was authored, remixed, and/or curated by [Andrei Tokmakoff](#) via [source content](#) that was edited to the style and standards of the LibreTexts platform.

21.5: Diffusion-Limited Reactions

Association Rate

The diffusion-limited association rate is typically approximated from the expression for the relative diffusion of A and B with an effective diffusion constant $D = D_A + D_B$ to within a critical encounter radius $R_0 = R_A + R_B$, as described earlier.

$$k_a = 4\pi R_0 f(D_A + D_B) \quad (21.5.1)$$

One can approximate association rates between two diffusing partners using the Stokes–Einstein expression: $D_A = k_B T / 6\pi\eta R_A$. For two identical spheres (i.e., dimerization) in water at $T = 300$ K, where $\eta \sim 1$ cP = $100 \text{ kg m}^{-1} \text{ s}^{-1}$,

$$k_a = \frac{8k_B T}{3\eta} = 6.6 \times 10^9 \text{ M}^{-1} \text{ s}^{-1} \quad (21.5.2)$$

Note that this model predicts that the association rate is not dependent on the size or mass of the object.

For bimolecular reactions, the diffusion may also include those orientational factors that bring two binding sites into proximity. Several studies have investigated these geometric effects.

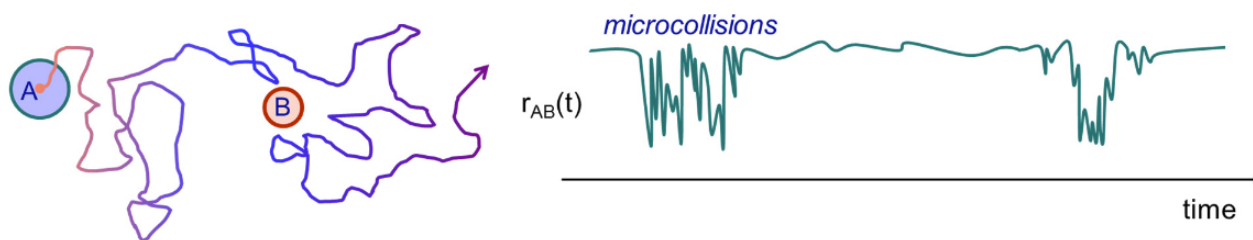
Example: Spheres with small binding patches

The combined probability that two binding patches are correctly oriented in both reference frames and that both are rotated into the correct azimuthal angle is:

$$P_r = \frac{1}{2}(1 - \cos \delta\theta_A) \frac{1}{2}(1 - \cos \delta\theta_B) \frac{\delta\varphi_{AB}}{\pi}$$

$$\approx \frac{1}{16\pi} \delta\theta_A^2 \delta\theta_B^2 \delta\varphi_{AB}$$

During diffusive encounter in dilute solution, once two partners collide but do not react, there is a high probability of re-colliding with the same partner before diffusing over a longer range to a new partner. Depending on concentration and the presence of interaction potentials, there may be 5–50 microcollisions with the same partner before encountering a new partner.



Diffusion-Limited Dissociation Rate

For the limit where associations are weak, k_1 and k_{-1} are fast and in equilibrium, and the dissociation is diffusion limited. Then we can calculate k_{-1}



Now we consider boundary conditions for flux moving away from a sphere such that

$$C_B(\infty) = 0$$

$$C_B(R_0) = \left(\frac{4}{3}\pi R_0^3\right)^{-1}$$

The boundary condition for concentration at the surface of the sphere is written so that the number density is one molecule per sphere.

The steady state distribution of B is found to be

$$C_B(r) = \frac{3}{4\pi R_0^2 r} \quad (21.5.4)$$

The dissociation flux at the surface is

$$J = -D_B \left(\frac{\partial C_B}{\partial r} \right)_{r=R_0} = \frac{3D_B}{4\pi R_0^4} \quad (21.5.5)$$

and the dissociation frequency is

$$\frac{J}{4\pi R_0^2} = \frac{3D_B}{R_0^2} \quad (21.5.6)$$

When we also consider the dissociative flux for the other partner in the association reaction,

$$k_{-1} = k_d = 3(D_A + D_B)R_0^{-2} \quad (21.5.7)$$

Written in a more general way for a system that may have an interaction potential

$$k_d = \frac{4\pi D e^{U(R_0)/kT}}{\frac{4}{3}\pi R_0^3 \int_{R_0}^{\infty} e^{U(r)/kT} r^{-2} dr} = 3DR^* R_0^{-3} \quad (21.5.8)$$

Note that equilibrium constants do not depend on D for diffusion-limited association/dissociation

$$K_D = \frac{k_D}{k_A} = \frac{3DR_0^{-2}}{4\pi R_0 D} = \frac{3}{4\pi R_0^3} \quad (21.5.9)$$

Note this is the inverse of the volume of a sphere.

-
1. D. Shoup, G. Lipari and A. Szabo, Diffusion-controlled bimolecular reaction rates. The effect of rotational diffusion and orientation constraints, *Biophys. J.* 36 (3), 697-714 (1981); D. Shoup and A. Szabo, Role of diffusion in ligand binding to macromolecules and cell-bound receptors, *Biophys. J.* 40 (1), 33-39 (1982).

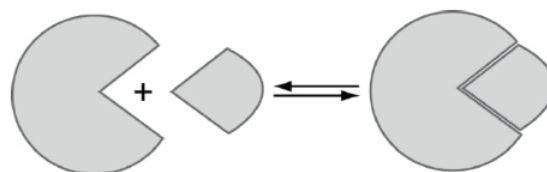
This page titled [21.5: Diffusion-Limited Reactions](#) is shared under a [CC BY-NC-SA 4.0](#) license and was authored, remixed, and/or curated by [Andrei Tokmakoff](#) via [source content](#) that was edited to the style and standards of the LibreTexts platform.

21.6: Protein Recognition and Binding

Enzyme/Substrate Binding

Lock-and-Key (Emil Fisher)

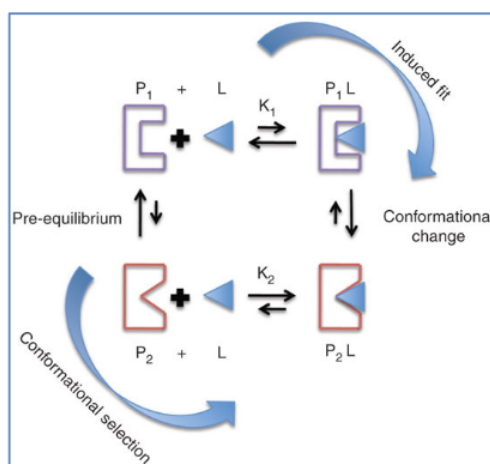
- Emphasizes shape complementarity
- Substrate typically rigid
- Concepts rooted in initial and final structure
- Does not directly address recognition



But protein-binding reactions typically involve conformational changes. Domain flexibility can give rise to dramatic increase in binding affinity. A significant conformational change/fluctuation may be needed to allow access to the binding pocket.

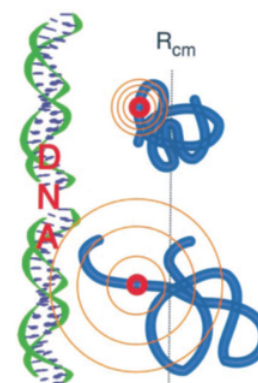
For binding a substrate, two models vary in the order of events for conformational change vs. binding event:

1. Induced fit (Daniel Koshland)
2. Conformational selection: Pre-existing equilibrium established during which enzyme explores a variety of conformations.



Protein-Protein Interactions

- Appreciation that structure is not the only variable
- Coupled folding and binding
 - Fold on contact
 - Fly-casting
- Both partners may be flexible

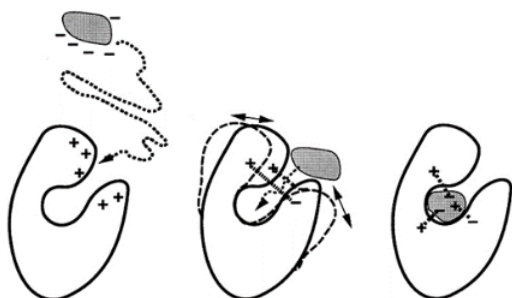


This page titled [21.6: Protein Recognition and Binding](#) is shared under a [CC BY-NC-SA 4.0](#) license and was authored, remixed, and/or curated by [Andrei Tokmakoff](#) via [source content](#) that was edited to the style and standards of the LibreTexts platform.

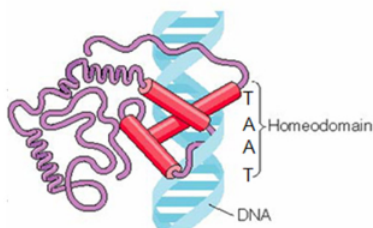
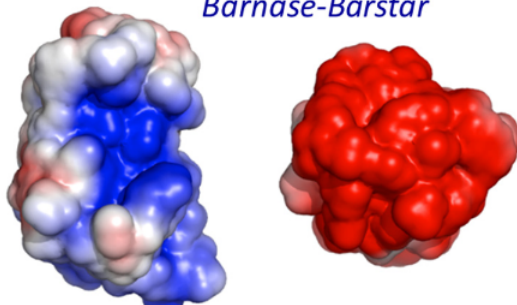
21.7: Forces Guiding Binding

Electrostatics

- Electrostatics play a role at long and short range
 - Long-range nonspecific interactions accelerate diffusive encounter
 - Short range guides specific contacts
- Electrostatic complementarity
- Electrostatic steering
- van der Waals, π - π stacking



Barnase-Barstar



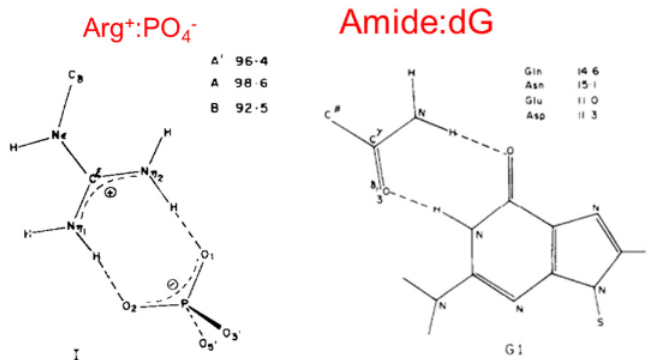
**Repressors: Helix-turn-helix
TAAT homeodomain**

Shape and Geometry

- Shape complementarity
- Orientational registry
- Folding
- Anchoring residues

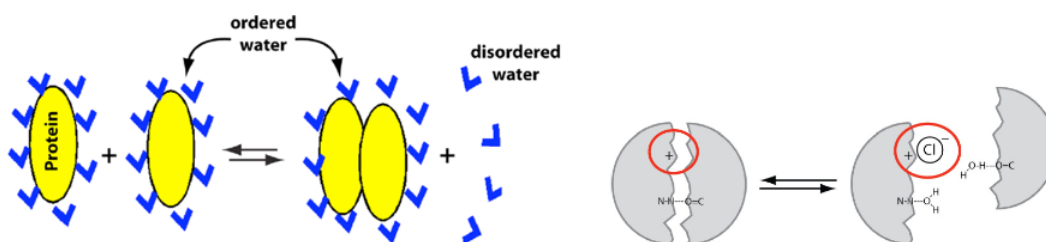
Hydrogen Bonding

- Short range
- Cross over from electrostatic to more charge transfer with strong HBs (like DNA, protein–DNA binding)
- Important in specificity



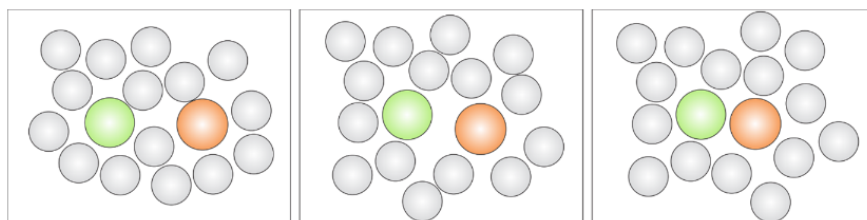
Solvation/Desolvation

- To bind, a ligand needs to desolvate the active site
- Bimolecular contacts will displace water
- Water often intimate binding participant (crystallographic waters)
- Hydrophobic patches
- Charge reconfiguration in electrolyte solutions at binding interface
- Electrostatic forces from water

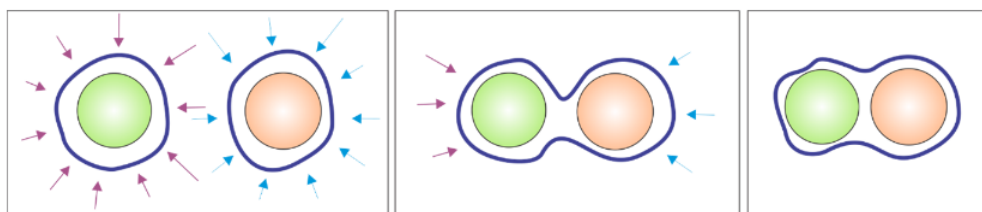


Depletion Forces

- Entropic effect
- Fluctuations that lead to an imbalance of forces that drives particles together
 - Crowding/Caging

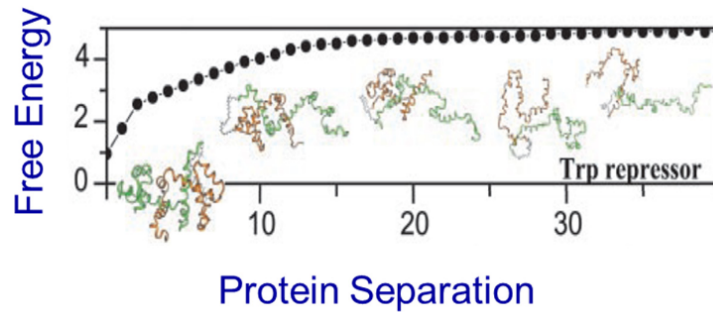


- Hydrophobicity
 - Dewetting and Interfacial Fluctuations



Folding/Conformational Change

- Disorder increases hydrodynamic volume
- Coupled folding and binding
 - Fly-casting mechanism
 - Partially unfolded partners
 - Long-range non-native interaction
 - Gradual decrease in free energy



This page titled [21.7: Forces Guiding Binding](#) is shared under a [CC BY-NC-SA 4.0](#) license and was authored, remixed, and/or curated by [Andrei Tokmakoff](#) via [source content](#) that was edited to the style and standards of the LibreTexts platform.

21.8: Specificity in Recognition and Binding

Specificity in Recognition

What determines the ability for a protein to recognize a specific target amongst many partners? To start, let's run a simple calculation. Take the case that a protein (transcription factor) has to recognize a string of n sequential nucleotides among a total of N bases in a dsDNA.

- Assume that each of the four bases (ATGC) is present with equal probability among the N bases, and that there are no enthalpic differences for binding to a particular base.
- Also, the recognition of a particular base is independent of the other bases in the sequence. (In practice this is a poor assumption).
- The probability of finding a particular n nucleotide sequence amongst all n nucleotide strings is

$$\left(\frac{1}{4}\right)^n \quad (21.8.1)$$

- For a particular n nucleotide sequence to be unique among a random sequence of N bases, we need

$$\left(\frac{1}{4}\right)^n \geq \frac{1}{N} \quad (21.8.2)$$

- Therefore we can say

$$n \geq \frac{\ln N}{\ln 4} \quad (21.8.3)$$

Example

For the case that you want to define a unique binding site among $N = 65\text{k}$ base pairs:

- A sequence of $n = \ln(65000)/\ln(4) \approx 8$ base pairs should statistically guarantee a unique binding site.
- $n = 9 \rightarrow 262$ kbp

This example illustrates that simple statistical considerations and the diversity of base combinations can provide a certain level of specificity in binding, but that other considerations are important for high fidelity binding. These considerations include the energetics of binding, the presence of multiple binding motifs for a base, and base-sequence specific binding motifs.

Energetics of Binding

We also need to think about the strength of interaction. Let's assume that the transcription factor has a nonspecific binding interaction with DNA that is weak, but a strong interaction for the target sequence. We quantify these through:

ΔG_1 : nonspecific binding

ΔG_2 : specific binding

Next, let's consider the degeneracy of possible binding sites:

g_n : number of nonspecific binding sites = $(N - n)$ or since $N \gg n$: $(N - n) \approx N$

g_s : number of sites that define the specific interaction: n

The probability of having a binding partner bound to a nonspecific sequence is

$$\begin{aligned} P_{\text{nonsp}} &= \frac{g_n e^{-\Delta G_1/kT}}{g_n e^{-\Delta G_1/kT} + g_s e^{-\Delta G_2/kT}} \\ &= \frac{(N - n) e^{-\Delta G_1/kT}}{(N - n) e^{-\Delta G_1/kT} + n e^{-\Delta G_2/kT}} \\ &= \frac{1}{1 + \frac{n}{N} e^{-\Delta G/kT}} \end{aligned}$$

where $\Delta G = \Delta G_2 - \Delta G_1$. We do not want to have a high probability of nonspecific binding, so let's minimize P_{nonsp} . Solving for ΔG , and recognizing $P_{\text{nonsp}} \ll 1$,

$$\Delta G \leq -k_B T \ln \left[\frac{N}{nP_{\text{nonsp}}} \right] \quad (21.8.4)$$

Suppose we want to have a probability of nonspecific binding to any region of DNA that is $P_{\text{nonsp}} \leq 1\%$. For $N = 10^6$ and $n = 10$, we find

$$\Delta G \approx -16k_B T \quad \text{or} \quad -1.6k_B T/\text{nucleotide} \quad (21.8.5)$$

for the probability that the partner being specifically bound with $P_{\text{sp}} > 99\%$.

Readings

1. G. Schreiber, G. Haran and H. X. Zhou, Fundamental aspects of protein–protein association kinetics, *Chem. Rev.* 109 (3), 839-860 (2009).
 2. D. Shoup, G. Lipari and A. Szabo, Diffusion-controlled bimolecular reaction rates. The effect of rotational diffusion and orientation constraints, *Biophys. J.* 36 (3), 697-714 (1981).
 3. D. Shoup and A. Szabo, Role of diffusion in ligand binding to macromolecules and cell-bound receptors, *Biophys. J.* 40 (1), 33-39 (1982).
-

This page titled [21.8: Specificity in Recognition and Binding](#) is shared under a [CC BY-NC-SA 4.0](#) license and was authored, remixed, and/or curated by [Andrei Tokmakoff](#) via [source content](#) that was edited to the style and standards of the LibreTexts platform.

CHAPTER OVERVIEW

22: Biophysical Reaction Dynamics

- [22.1: Concepts and Definitions](#)
- [22.2: Computing Dynamics](#)
- [22.3: Representations of Dynamics](#)
- [22.4: Analyzing Trajectories](#)
- [22.5: Time-Correlation Functions](#)

This page titled [22: Biophysical Reaction Dynamics](#) is shared under a [CC BY-NC-SA 4.0](#) license and was authored, remixed, and/or curated by [Andrei Tokmakoff](#) via [source content](#) that was edited to the style and standards of the LibreTexts platform.

22.1: Concepts and Definitions

Time-dependent problems in molecular biophysics: How do molecular systems change? How does a molecular system change its microscopic configuration? How are molecules transported? How does a system sample its thermodynamically accessible states?

Two types of descriptions of time-dependent processes:

1. **Kinetics:** Describes the rates of interconversion between states. This is typically measured by most experiments. It does not directly explain how processes happen, but it can be used to predict the time-dependent behavior of populations from a proposed mechanism.
2. **Dynamics:** A description of the time-evolving molecular structures involved in a process, with the objective of gaining insight into mechanism. At a molecular level, this information is typically more readily available from dynamical simulations of a model than from experiments.

There is no single way to describe biophysical kinetics and dynamics, so we will survey a few approaches. The emphasis here will be on the description and analysis of time-dependent phenomena, and not on the experimental or computational methods used to obtain the data.

Two common classes of problems:

1. **Barrier crossing or activated processes:** For a solution phase process, evolution between two or more states separated by a barrier whose energy is $\gg k_B T$. A description of “rare events” when the system rapidly jumps between states. Includes chemical reactions described by transition-state theory. \rightarrow We’ll look at two state problems.
2. **Diffusion processes:** Transport in the absence of significant enthalpic barriers. Many small barriers on the scale of $k_B T$ lead to “friction”, rapid randomization of momenta, and thereby diffusion.

Now let’s start with some basic definitions of terms we will use often:

Coordinates

Refers to many types of variables that are used to describe the structure or configuration of a system. For instance, this may refer to the positions of atoms in a MD simulation as a function of time $\{\mathbf{r}^N, t\}$, or these Cartesian variables might be transformed onto a set of internal coordinates (such as bond lengths, bond angles, and torsion angles), or these positions may be projected onto a different collective coordinate. Unlike our simple lattice models, the transformation from atomic to collective coordinate is complex when the objective is to calculate a partition function, since the atomic degrees of freedom are all correlated.

Collective coordinate

- A coordinate that reflects a sum/projection over multiple internal variables—from a high-dimensional space to a lower one.

Example: Solvent coordinate in electron transfer. In polar solvation, the position of the electron is governed by the stabilization by the configuration of solvent dipoles. An effective collective coordinate could be the difference in electrostatic potential between the donor and acceptor sites: $q \Phi_A - \Phi_D$.



Example: RMSD variation of structure with coordinates from a reference state.

$$RMSD = \sqrt{\frac{1}{n} \sum_{i=1}^n (\mathbf{r}_i - \mathbf{r}_i^0)^2} \quad (22.1.1)$$

where r is the position of an atom in an n atom molecule.

- Sometimes the term “order parameter” gets used to describe a collective coordinate. This term originated in the description of changes of symmetry at phase transitions, and is a more specific term than order parameter. While order parameters are collective variables, collective variables are not necessarily order parameters.

Reaction coordinate

- An internal variable that describes the forward progress of a reaction or process.
- Typically an abstract quantity, and not a simple configurational or geometrical coordinate. In making a connection to molecular structure, often the optimal reaction coordinate is not known or cannot be described, and so we talk about a “good reaction coordinate” as a collective variable that is a good approximate description of the progress of the reaction.

Energy Landscape

A structure is characterized by an energy of formation. There are many forms of energy that we will use, including free energy (G , A), internal energy or enthalpy (E , H), interaction potential (U , V), ... so we will have to be careful to define the energy for a problem. Most of the time, though, we are interested in free energy.

The energy landscape is used to express the relative stability of different states, the position and magnitude of barriers between states, and possible configurational entropy of certain states. It is closely related to the free energy of the system, and is often used synonymously with the potential of mean force. The energy landscape expresses how the energy of a system (typically, but it is not limited to, free energy) depends on one or more coordinates of the system. It is often used as a free energy analog of a potential energy surface. For many-particle systems, they can be presented as a reduced dimensional surface by projecting onto one or a few degrees of freedom of interest, by integrating over the remaining degrees of freedom.

“Energy landscapes” represent the free energy (or rather the negative of the logarithm of the probability) along a particular coordinate. Let’s remind ourselves of some definitions. The free energy of the system is calculated from .

$$A = -k_B T \ln Z \quad (22.1.2)$$

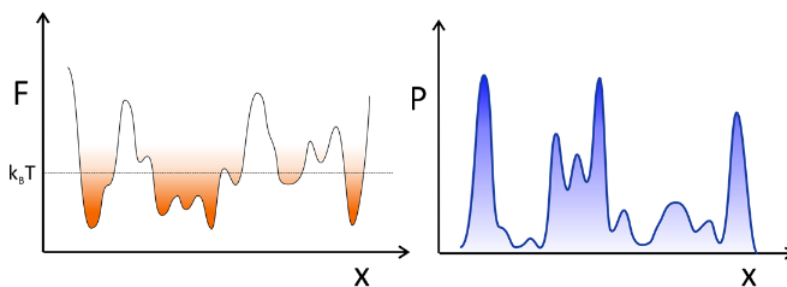
where Z is the partition function. The free energy is a number that reflects the thermally weighted number of microstates available to the system. The free energy determines the relative probability of occupying two states of the system:

$$\frac{P_A}{P_B} = e^{-(A_A - A_B)/k_B T} \quad (22.1.3)$$

The energy landscape is most closely related to a potential of mean force

$$F(x) = -k_B T \ln P(x) \quad (22.1.4)$$

$P(x)$ is the probability density that reflects the probability for observing the system at a position x . As such it is equivalent to decomposing the free energy as a function of the coordinate x . Whereas the partition function is evaluated by integrating a Boltzmann weighting over all degrees of freedom, $P(x)$ is obtained by integrating over all degrees of freedom except x .



States

We will use the term “state” in the thermodynamic sense: a distinguishable *minimum* or *basin* on free energy surface. States refer to a region of phase-space where you persist long compared to thermal fluctuations. The regions where there is a high probability of observing the system. One state is distinguished from another kinetically by a time-scale separation. The rate of evolving within a state is faster than the rate of transition between states.

Configuration

- Can refer to a distinct microstate or a structure that has been averaged over a local energy basin. You average over configurations (integrate over q) to get states (macrostates).

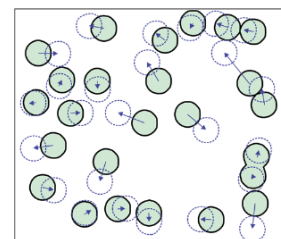
Transition State

- The transition state or transition–state ensemble, often labeled \ddagger , refers to those barrier configurations that have equal probability of making a transition forward or backward.
- It's not really a “state” by our definition, but a barrier or saddle point along a reaction coordinate.

This page titled [22.1: Concepts and Definitions](#) is shared under a [CC BY-NC-SA 4.0](#) license and was authored, remixed, and/or curated by [Andrei Tokmakoff](#) via [source content](#) that was edited to the style and standards of the LibreTexts platform.

22.2: Computing Dynamics

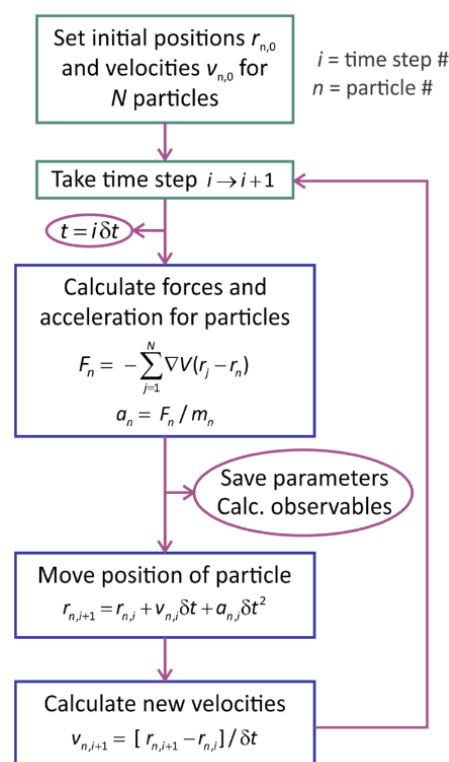
There are a number of ways of computationally modeling time-dependent processes in molecular biophysics. These methods integrate equations of motion for the molecular degrees of freedom evolving under a classical force-field interaction potential, a quantum mechanical Hamiltonian, or an energy landscape that could be phenomenological or atomistically detailed. Examples include using classical force fields to propagate Newton's equation of motion, integrating the Schrödinger equation, or integrating the Langevin equation on a potential of mean force. Since our interest is more on the description of computational or experimental data, this will just be a brief overview.



Classical Dynamics from a Potential (Force Field)

An overview of how to integrate Newton's equation of motion, leaving out many important details. This scheme, often used in MD simulations, is commonly called a Verlet integration.

- Set initial positions \mathbf{r} and velocities \mathbf{v} of particles. For equilibrium simulations, the velocities are chosen from a Maxwell-Boltzmann distribution.
- Take small successive steps in time δt , calculating the velocities and positions of the particles for the following time step.
 - At each time step calculate the forces on each particle by calculating the gradient of the potential with respect to \mathbf{r} : $\mathbf{F}(\mathbf{r}) = -\Delta V(\mathbf{r})$. The force is proportional to the acceleration $\mathbf{a} = \mathbf{F}/m$, where m is the mass of the particle.
 - Now propagate the position of each particle n in time from time step i to time step $i+1$ as $\mathbf{r}_{n,i+1} = \mathbf{r}_{n,i} + \mathbf{v}_{n,i} \delta t + \mathbf{a}_{n,i} \delta t^2$. This is a good point to save information for the system at a particular time.
 - Calculate the new velocity for each particle from $\mathbf{v}_{n,i+1} = [\mathbf{r}_{n,i+1} - \mathbf{r}_{n,i}] / \delta t$.
- Now, you can increment the time step and repeat step iteratively.



Langevin Dynamics

Building on our discussion of Brownian motion, the Langevin equation is an equation of motion for a particle acting under the influence of a fixed potential U , friction, and a time-dependent random force. Writing it in one dimension:

$$ma = f_{\text{potential}} + f_{\text{friction}} + f_{\text{random}}(t) \quad (22.2.1)$$

$$m \frac{\partial^2 x}{\partial t^2} = -\frac{\partial U}{\partial x} - \zeta \frac{\partial x}{\partial t} + f_r(t) \quad (22.2.2)$$

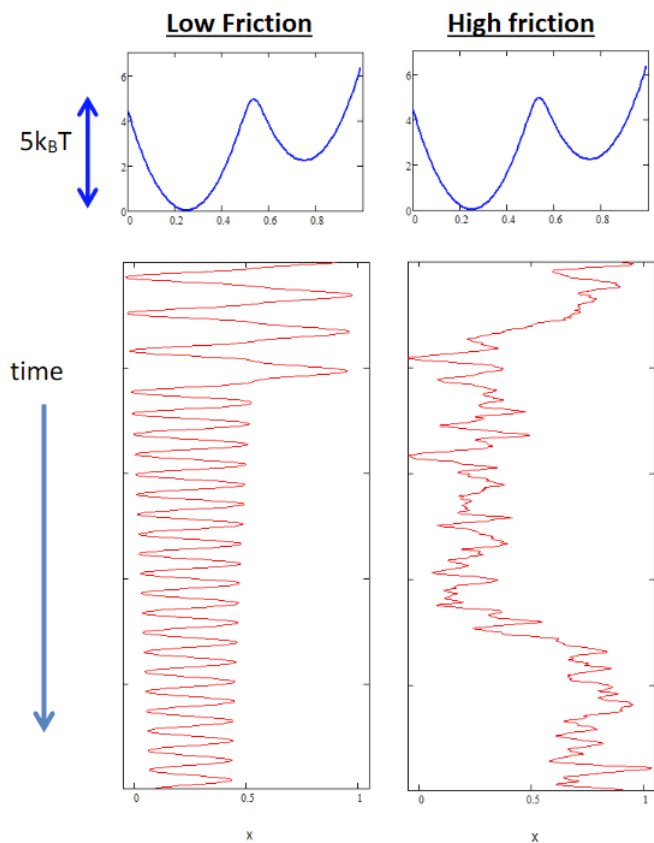
The random force reflects the equilibrium thermal fluctuations acting on the particle, and is the source of the friction on the particle. In the Markovian limit, the friction coefficient ζ and the random force $f_r(t)$ are related through a fluctuation-dissipation relationship:

$$\langle f_r(t) \rangle = 0 \quad (22.2.3)$$

$$\langle f_r(t) f_r(t_0) \rangle = 2\zeta k_B T \delta(t - t_0) \quad (22.2.4)$$

Also, the diffusion constant is $D = k_B T / \zeta$, and the time scale for loss of velocity correlations is $\tau_c = \gamma - 1 = m / \zeta$. The Langevin equation has high and low friction limits. In the low friction limit ($\zeta \rightarrow 0$), the influence of friction and random force is minimal, and the behavior is dominated by the inertial motion of the particle. In the high friction limit, the particle's behavior, being dominated by ζ , is diffusive. The limit is defined by any two of the following four linearly related variables: ζ , D , T , and $\langle f_r^2 \rangle$. The high and low friction limit are also referred to as the low and high temperature limits: $\langle f_r^2 \rangle / 2\zeta = k_B T$.

Example: Trajectory for a particle on a bistable potential from Langevin dynamics



This page titled [22.2: Computing Dynamics](#) is shared under a [CC BY-NC-SA 4.0](#) license and was authored, remixed, and/or curated by [Andrei Tokmakoff](#) via [source content](#) that was edited to the style and standards of the LibreTexts platform.

22.3: Representations of Dynamics

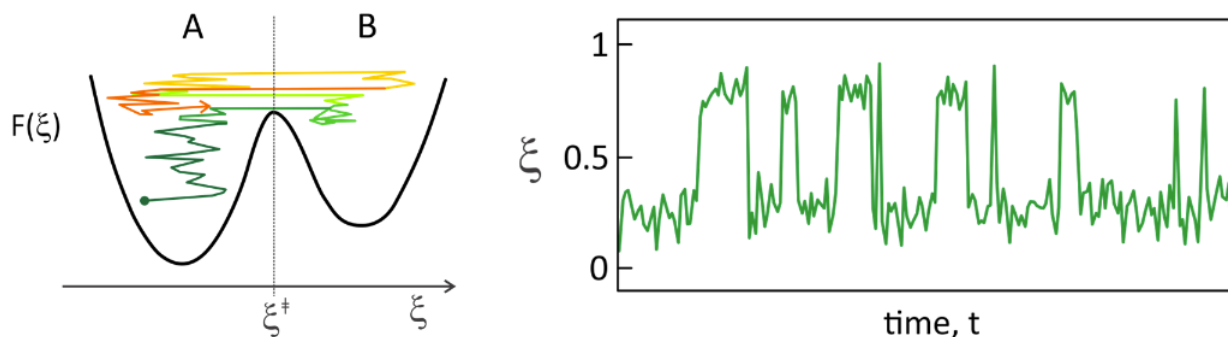
We will survey different representation of time-dependent processes using examples from one-dimension.

Trajectories

Watch the continuous time-dependent behavior of one or more particles/molecules in the system.

Time-dependent structural configurations

A molecular dynamics trajectory will give you the position of all atoms as a function of time $\{\mathbf{r}^N, t\}$. Although there is an enormous amount of information in such a trajectory, the raw data is often overwhelming and not of particularly high value itself. However, it is possible to project this high dimensional information in structural coordinates onto one or more collective variables ξ that forms a more meaningful representation of the dynamics, $\xi(t)$. Alternatively, single molecule experiments can provide a chronological sequence of the states visited by molecule.

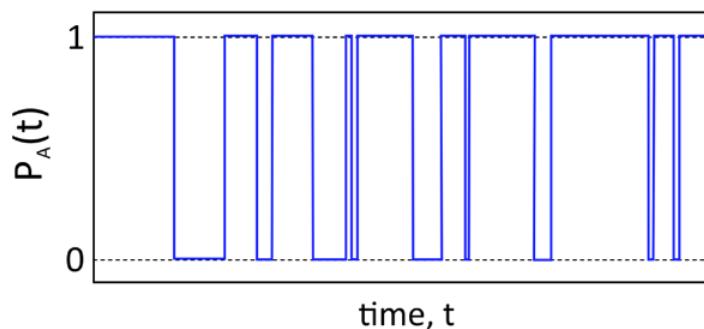


State trajectories: Time-dependent occupation of states

A discretized representation of which state of the system the particle occupies. Requires that you define the boundaries of a state.

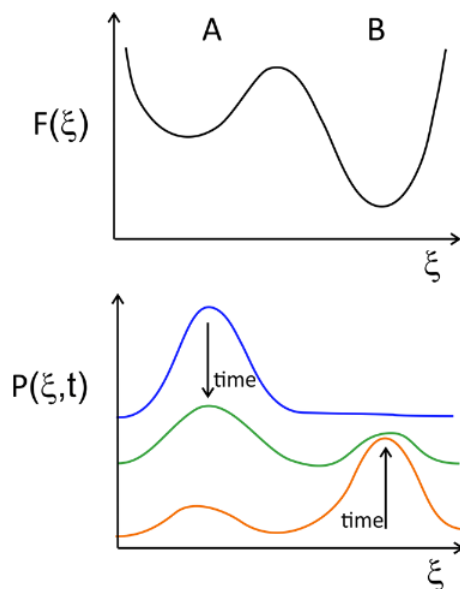
Example: A two state trajectory for an equilibrium $A \rightleftharpoons B$, where the time-dependent probability of being in state A is:

$$P_A(t) = \begin{cases} 1 & \text{if } \xi(t) < \xi^\ddagger \\ 0 & \text{if } \xi(t) > \xi^\ddagger \end{cases} \quad (22.3.1)$$



Time-Dependent Probability Distributions and Fluxes

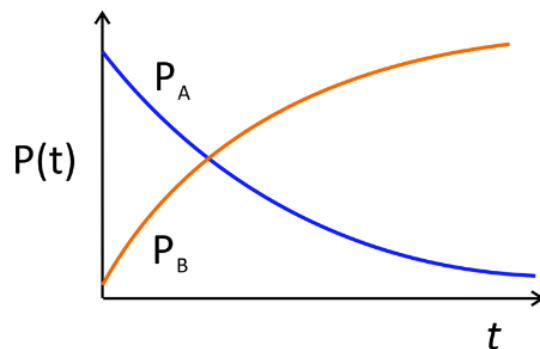
With sufficient sampling, one can average over trajectories in order to develop a time-dependent probability distribution $P(\xi, t)$ for the non-equilibrium evolution of an initial state.



State Populations: Kinetics

- Average over states to get time-dependent populations of those states.

$$\int_{\text{state A}} P(\xi, t) d\xi = P_A(t) \quad (22.3.2)$$



- Alternatively, one can obtain the same information by analyzing waiting time distributions from state trajectories, as described below.
- The kinetics can be modeled with rate equations/master equation: $\dot{P} = \mathbf{k}P$.

Time-Correlation Functions

Time-correlation functions are commonly used to characterize trajectories of a fluctuating observable. These are described next

This page titled [22.3: Representations of Dynamics](#) is shared under a [CC BY-NC-SA 4.0](#) license and was authored, remixed, and/or curated by [Andrei Tokmakoff](#) via [source content](#) that was edited to the style and standards of the LibreTexts platform.

22.4: Analyzing Trajectories

Analyzing Trajectories

Waiting-Time Distributions, P

τ_w : Waiting time between arriving and leaving a state or $P(k,t)$

P_k : Probability of making k jumps during a time interval, t . \rightarrow Survival probability

P_w : Probability of waiting a time τ_w between jumps? Waiting time distribution \rightarrow FPT distribution

Let's relate these...

Assume independent events. No memory of history – where it was in trajectory.

$$\text{Flux: } \frac{dP_R}{dt} = J$$

J : Probability of jump during Δt . Δt is small enough that $J \ll 1$, but long enough to lose memory of earlier configurations.

The probability of seeing k jumps during a time interval t , where t is divided into N intervals of width Δt ($t = N\Delta t$) is given by the binomial distribution

$$P(k, N) = \frac{N!}{k!(N-k)!} J^k (1-J)^{N-k} \quad (22.4.1)$$

Here $N \gg k$. Define rate λ in terms of the average number of jumps per unit time

$$\lambda = \frac{\langle k \rangle}{t} = \frac{1}{\langle \tau_w \rangle}$$

$$J = \lambda \Delta t \rightarrow J = \frac{\lambda t}{N}$$

Substituting this into eq. (22.4.1) Error! Reference source not found.. For $N \gg k$, recognize

$$(1-J)^{N-k} \approx (1-J)^N = \left(1 - \frac{\lambda t}{N}\right)^N \approx e^{-\lambda t}$$

The last step is exact for $\lim N \rightarrow \infty$.

Poisson distribution for the number of jumps in time t .

$$\langle P(k, t) \rangle = \langle \lambda t \rangle = \frac{\lambda t}{\langle P^2(k, t) \rangle^{1/2}} = (\lambda t)^{1/2}$$

Fluctuations: $\sigma / \langle P(k, t) \rangle = (\lambda t)^{-1/2}$

OK, now what about P_w the waiting time distribution?

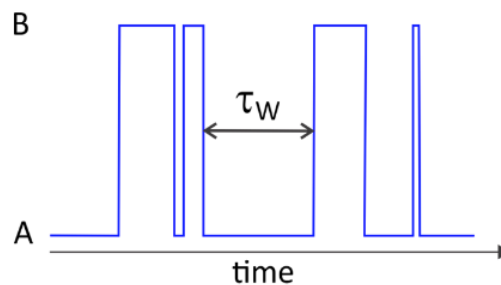
Consider the probability of not jumping during time t :

$$P_k(0, t) = e^{-\lambda t}$$

As you wait longer and longer, the probability that you stay in the initial state drops exponentially. Note that $P_k(0, t)$ is related to P_w by integration over distribution of waiting times.

$$\int_t^\infty P_w(t') dt' = P(0, t) = e^{-\lambda t}$$

$$\int_t^\infty P_w dt \rightarrow \text{probability of staying for } t$$



$$\int_0^t P_w dt \rightarrow \text{probability of jumping within } t$$

Probability of jumping between t and $t+\Delta t$:

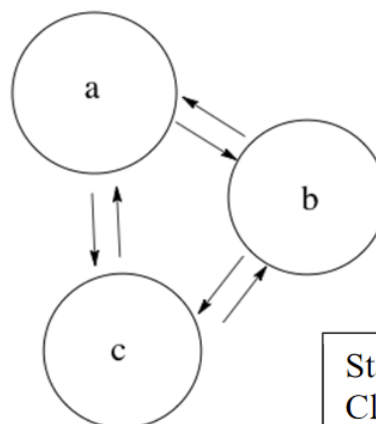
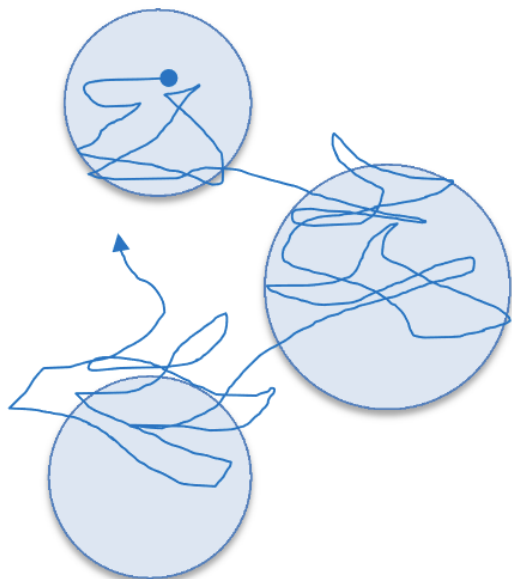
$$P_w(t)\Delta t = \overbrace{(1 - \langle k \rangle \Delta t_1)}^{\text{Probability of no decay for time } <t} \overbrace{(1 - \langle k \rangle \Delta t_2) \dots (1 - \langle k \rangle \Delta t_N)}^{\text{decay on last}} \overbrace{k \Delta t}^{\text{jump}} \\ = (1 - \langle k \rangle \Delta t)^N k \Delta t \approx k e^{-kt} \Delta t$$

$$P_w = \lambda e^{-\lambda t} \\ \langle \tau \rangle = \int_0^\infty t p_w(t) dt$$

$$\langle \tau_w \rangle = 1/\lambda \rightarrow \text{the average waiting time is the lifetime}(1/\lambda) \\ \langle \tau_w^2 \rangle - \langle \tau_w \rangle^2 = (1/\lambda)^2$$

Reduction of Complex Kinetics from Trajectories

- Integrating over trajectories gives probability densities.
- Need to choose a region of space to integrate over and thereby define states:



States:
Clustered regions of phase space that have high probability or long persistence.

- States: Clustered regions of phase space that have high probability or long persistence.
- Markovian states: Spend enough time to forget where you came from.
- Master equation: Coupled first order differential equations for the flow of amplitude between states written in terms of probabilities.

$$\frac{dP_m}{dt} = \sum_n k_{n \rightarrow m} P_n - \sum_n k_{m \rightarrow n} P_m$$

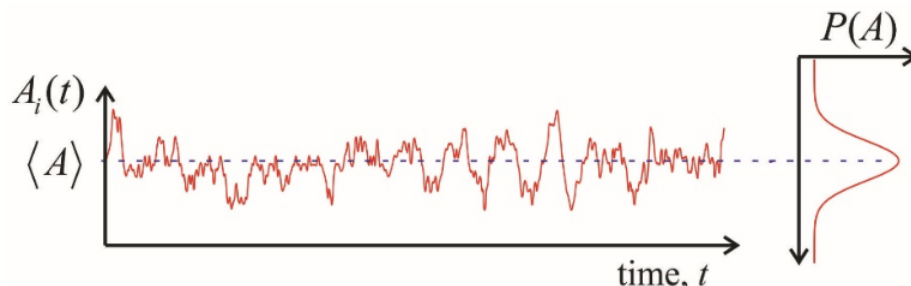
$k_{n \rightarrow m}$ is rate constant for transition from state n to state m . Units: probability/time. Or in matrix form: $\dot{P} = \mathbf{k}P$ where \mathbf{k} is the transition rate matrix. With detailed balance, conservation of population all initial conditions will converge on equilibrium

This page titled [22.4: Analyzing Trajectories](#) is shared under a [CC BY-NC-SA 4.0](#) license and was authored, remixed, and/or curated by [Andrei Tokmakoff](#) via [source content](#) that was edited to the style and standards of the LibreTexts platform.

22.5: Time-Correlation Functions

Time-Correlation Functions

Time-correlation functions are commonly used to characterize the dynamics of a random (or stochastic) process. If we observe the behavior of an internal variable A describing the behavior of one molecule at thermal equilibrium, it may be subject to microscopic fluctuations.



Although there may seem to be little information in this noisy trajectory, this dynamics is not entirely random, since they are a consequence of time-dependent interactions with the environment. We can provide a statistical description of the characteristic time scales and amplitudes to these changes by comparing the value of A at time t with the value of A at a later time t' . We define a time-correlation function as the product of these values averaged over an equilibrium ensemble:

$$C_{AA}(t-t') \equiv \langle A(t)A(t') \rangle \quad (22.5.1)$$

Correlation functions do not depend on the absolute point of observation (t and t'), but rather the time interval between observations (for stationary random processes). So, we can define the time interval $\tau \equiv t - t'$, and express our function as $C_{AA}(\tau)$.

We can see that when we evaluate C_{AA} at $\tau=0$, we obtain the mean square value of A , $\langle A^2 \rangle$. At long times, as thermal fluctuations act to randomize the system, the values of A become uncorrelated: $\lim_{\tau \rightarrow \infty} C_{AA}(\tau) = \langle A \rangle^2$. It is therefore common to redefine the correlation function in terms of the deviation from average

$$\delta A = A - \langle A \rangle \quad (22.5.2)$$

$$C_{\delta A \delta A}(t) = \langle \delta A(t) \delta A(0) \rangle = C_{AA}(t) - \langle A \rangle^2 \quad (22.5.3)$$

Then $C_{\delta A \delta A}(0)$ gives the variance for the random process, and the correlation function decays to zero as $\tau \rightarrow \infty$. The characteristic time scale for this relaxation is the correlation time, τ_c , which we can obtain from

$$\tau_c = \frac{1}{\langle \delta A^2 \rangle} \int_0^\infty dt \langle \delta A(t) \delta A(0) \rangle \quad (22.5.4)$$

The classical correlation function can be obtained from an equilibrium probability distribution as

$$C_{AA}(t-t') = \int dp \int dq A(p, q; t) A(p, q; t') P_{eq}(p, q) \quad (22.5.5)$$

In practice, correlation function are more commonly obtained from trajectories by calculating it as a time average

$$C_{AA}(\tau) = \overline{A(\tau)A(0)} = \lim_{T \rightarrow \infty} \frac{1}{T} \int_0^T dt' A_i(\tau+t') A_i(t') \quad (22.5.6)$$

If the time-average value of C is to be equal to the equilibrium ensemble average value of C , we say the system is ergodic.

Example: Velocity Autocorrelation Function for Gas

A dilute gas of molecules has a Maxwell-Boltzmann distribution of velocities, for which we will focus on the velocity component along the \hat{x} direction, v_x . We know that the average velocity is $\langle v_x \rangle = 0$. The velocity correlation function is

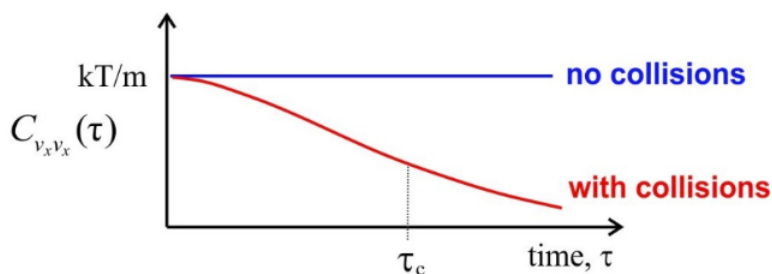
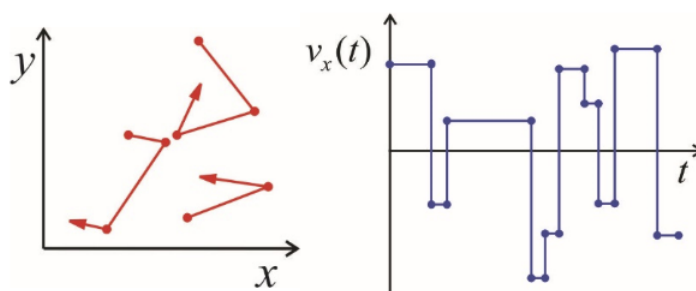
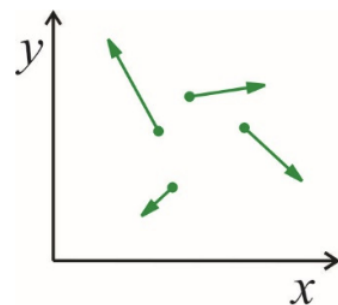
$$c_{v_x v_x}(\tau) = \langle v_x(\tau) v_x(0) \rangle$$

The average translational energy is $\frac{1}{2}m\langle v_x^2 \rangle = k_B T/2$, so

$$C_{v_x v_x}(0) = \langle v_x^2(0) \rangle = \frac{k_B T}{m}$$

For time scales that are short compared to the average collision time between molecules, the velocity of any given molecule remains constant and unchanged, so the correlation function for the velocity is also unchanged at $k_B T/m$. This non-interacting regime corresponds to the behavior of an ideal gas.

For any real gas, there will be collisions that randomize the direction and speed of the molecules, so that any molecule over a long enough time will sample the various velocities within the Maxwell–Boltzmann distribution. From the trajectory of x-velocities for a given molecule we can calculate $C_{v_x v_x}(\tau)$ using time averaging. The correlation function will drop on with a correlation time τ_c , which is related to mean time between collisions. After enough collisions, the correlation with the initial velocity is lost and $C_{v_x v_x}(\tau)$ approaches $\langle v_x^2 \rangle = 0$. Finally, we can determine the diffusion constant for the gas, which relates the time and mean square displacement of the molecules: $\langle x^2(t) \rangle = 2D_x t$. From $D_x = \int_0^\infty dt \langle v_x(t)v_x(0) \rangle$ we have $D_x = k_B T \tau_c / m$. In viscous fluids τ_c / m is called the mobility.



Calculating a Correlation Function from a Trajectory

We can evaluate eq. (22.5.6) for a discrete and finite trajectory in which we are given a series of N observations of the dynamical variable A at equally separated time points t_i . The separation between time points is $t_{i+1} - t_i = \delta t$, and the length of the trajectory is $T = N \delta t$. Then we have

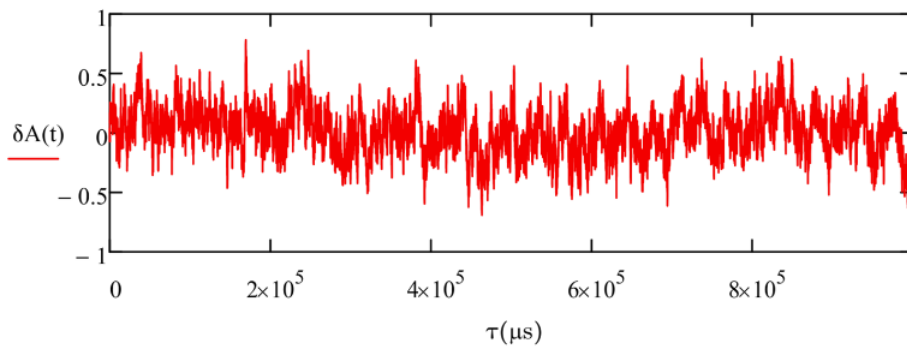
$$C_{AA} = \frac{1}{T} \sum_{i,j=1}^N \delta t A(t_i) A(t_j) = \frac{1}{N} \sum_{i,j=1}^N A_i A_j \quad (22.5.7)$$

where $A_i = A(t_i)$. To make this more useful we want to express it as the time interval between points $\tau = t_j - t_i = (j - i)\delta t$, and average over all possible pairwise products of A separated by τ . Defining a new count integer $n = j - i$, we can express the delay as $\tau = n\delta t$. For a finite data set there are a different number of observations to average over at each time interval (n). We have the most pairwise products— N to be precise—when the time points are equal ($t_i = t_j$). We only have one data pair for the maximum delay $\tau = T$. Therefore, the number of pairwise products for a given delay τ is $N - n$. So we can write eq. (22.5.7) as

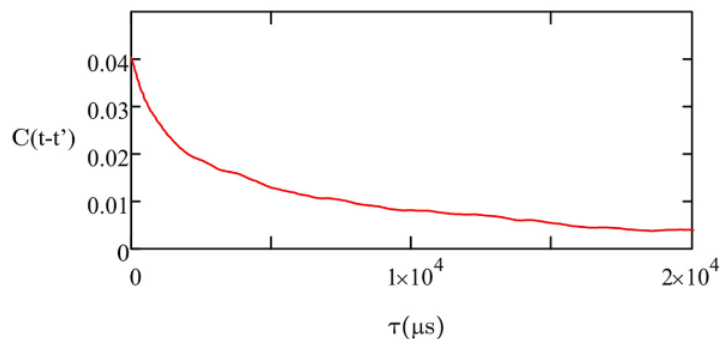
$$C_{AA}(\tau) = C(n) = \frac{1}{N - n} \sum_{i=1}^{N-n} A_{i+n} A_i \quad (22.5.8)$$

Note that this expression will only be calculated for positive values of n , for which $t_j \geq t_i$.

As an example consider the following calculation for fluctuations in fluorescence intensity in an FCS experiment. This trajectory consists of 32000 consecutive measurements separated by 44 μs , and is plotted as a deviation from the mean $\delta A(t) = A(t) - A$.



The correlation function obtained from eq. (22.5.8) is



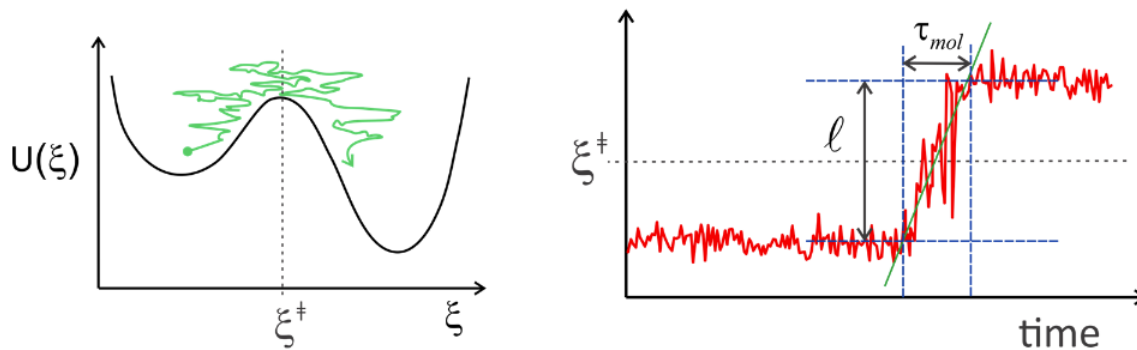
We can see that the decay of the correlation function is observed for sub-ms time delays. From eq. (22.5.4) we find that the correlation time is $\tau_C = 890 \mu\text{s}$.

This page titled [22.5: Time-Correlation Functions](#) is shared under a [CC BY-NC-SA 4.0](#) license and was authored, remixed, and/or curated by [Andrei Tokmakoff](#) via [source content](#) that was edited to the style and standards of the LibreTexts platform.

CHAPTER OVERVIEW

23: Barrier Crossing and Activated Processes

"Rare but important events"



The rates of chemical reaction are obtained by calculating the forward flux of reactant molecules passing over the transition state, i.e. the time rate of change of concentration, population, or probability for reactants passing over the transition state.

$$\langle J_f^\ddagger \rangle = dP_R^\ddagger / dt \quad (23.1)$$

‡

[23.1: Transition State Theory](#)

[23.2: Kramers' Theory](#)

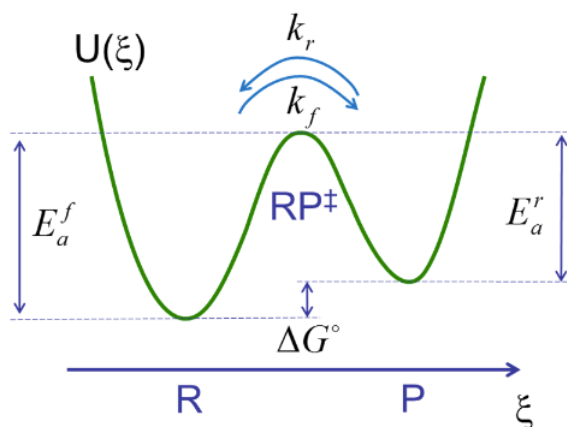
This page titled [23: Barrier Crossing and Activated Processes](#) is shared under a [CC BY-NC-SA 4.0](#) license and was authored, remixed, and/or curated by [Andrei Tokmakoff](#) via [source content](#) that was edited to the style and standards of the LibreTexts platform.

23.1: Transition State Theory

Transition state theory is an equilibrium formulation of chemical reaction rates that originally comes from classical gas-phase reaction kinetics. We'll consider a two-state system of reactant R and product P separated by a barrier $\gg k_B T$:



which we obtain by projecting the free energy of the system onto a reaction coordinate ξ (a slow coordinate) by integrating over all the other degrees of freedom. There is a time-scale separation between the fluctuations in a state and the rare exchange events. All memory of a trajectory is lost on entering a state following a transition.



Our goal is to describe the rates of crossing the transition state for the forward and reverse reactions. At thermal equilibrium, the rate constants for the forward and reverse reaction, k_f and k_r , are related to the equilibrium constant and the activation barriers as

$$K_{eq} = \frac{[P]}{[R]} = \frac{P_{P,eq}}{P_{R,eq}} = \frac{k_f}{k_r} = \exp\left(-\frac{(E_a^f - E_a^r)}{k_B T}\right)$$

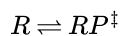
E_a^f , E_a^r are the activation free energies for the forward and reverse reactions, which are related to the reaction free energy through $E_a^f - E_a^r = \Delta G_{rxn}^0$. P_i refers to the population or probability of occupying the reactant or product state.

The primary assumptions of TST is that the transition state is well represented by an activated complex RP^\ddagger that acts as an intermediate for the reaction from R to P, that all species are in thermal equilibrium, and that the flux across the barrier is proportional to the population of the activated complex.



Then, the steady state population of the activated complex can be determined by an equilibrium constant that we can express in terms of the molecular partition functions.

Let's focus on the rate of the forward reaction considering only the equilibrium



We relate the population of reactants within the reactant well to the population of the activated complex through an equilibrium constant

$$K_{eq}^\ddagger = \frac{[RP^\ddagger]}{[R]}$$

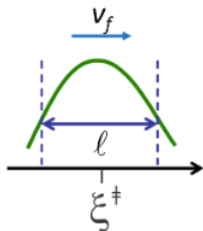
which we will evaluate using partition functions for the reactant and activated complex

$$K_{eq}^\ddagger = \frac{q^\ddagger/V}{q_R/V} e^{-E_a^f/k_B T}$$

Then we write the forward flux in eq. (23.1) proportional to the population of activated complex

$$\begin{aligned}\langle J^\ddagger \rangle &= v[RP^\ddagger] \\ &= vK_{eq}^\ddagger[R]\end{aligned}$$

Here v is the reaction frequency, which is the inverse of the transition state lifetime $\tau_{mol} \cdot v^{-1}$ or τ_{mol} reflects the time it takes to cross the transition state region.



To evaluate v , we will treat motion along the reaction coordinate ξ at the barrier as a translational degree of freedom. When the reactants gain enough energy (E_a^f), they will move with a constant forward velocity v_f through a transition state region that has a width ℓ . (The exact definition of ℓ will not matter too much).

$$\tau_{mol} = \frac{\ell}{v_f}$$

Then we can write the average flux of population across the transition state in the forward direction

$$\begin{aligned}\langle J^\ddagger \rangle &= K_{eq}^\ddagger[R] \frac{v_f}{\ell} \\ &= \frac{q^\ddagger}{q_R} e^{-E_a^f/k_B T} [R] \frac{1}{\ell} \sqrt{\frac{k_B T}{2\pi m}}\end{aligned}\tag{23.1.1}$$

where v_f is obtained from a one-dimensional Maxwell–Boltzmann distribution.

For a multidimensional problem, we want to factor out the slow coordinate, i.e., reaction coordinate (ξ) from partition function.

$$q^\ddagger = q_\xi q'^\ddagger$$

q'^\ddagger contains all degrees of freedom except the reaction coordinate. Next, we calculate q_ξ by treating it as translational motion:

$$q_\xi(\text{trans}) = \int_0^\ell d\xi e^{-E_{\text{trans}}/k_B T} = \sqrt{\frac{2\pi m k_B T}{h^2}} \ell\tag{23.1.2}$$

Substituting (23.1.2) into (23.1.1):

$$\langle J_f^\ddagger \rangle = \frac{k_B T}{h} \frac{q'^\ddagger}{q_R} e^{-E_a^f/k_B T} [R]$$

We recognize that the factor $v = k_B T/h$ is a frequency whose inverse gives an absolute lower bound on the crossing time of 10^{-13} seconds. If we use the speed of sound in condensed matter this time is what is needed to propagate 1–5 Å. Then we can write

$$\langle J_f^\ddagger \rangle = k_f [R]$$

where the forward rate constant is

$$k_f = A e^{-E_a^f/k_B T}\tag{23.1.3}$$

and the pre-exponential factor is

$$A = v \frac{q^\ddagger}{q_R}$$

A determines the time that it takes to cross the transition state in the absence of barriers ($E_a \rightarrow 0$). k_f is also referred to as k_{TST} .

To make a thermodynamic connection, we can express eq. (4) in the Eyring form

$$k_f = v e^{\Delta S^\ddagger/k_B} e^{-\Delta E_f^\ddagger/k_B T}$$

where the transition state entropy is

$$\Delta S^\ddagger = k \ln \frac{q^\ddagger}{q_R}$$

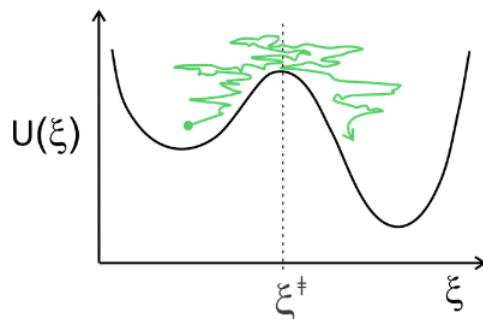
ΔS^\ddagger represents a count (actually ratio) of the reduction of accessible microstates in making the transition from the reactant well to the transition state. For biophysical phenomena, the entropic factors are important, if not dominant!

Also note implicit in TST is a dynamical picture in which every trajectory that arrives with forward velocity at the TST results in a crossing. It therefore gives an upper bound on the true rate, which may include failed attempts to cross. This is often accounted for by adding a transmission coefficient $\kappa < 1$ to k_{TST} : $k_f = \kappa k_{\text{TST}}$. Kramers' theory provides a physical basis for understanding κ .

This page titled [23.1: Transition State Theory](#) is shared under a [CC BY-NC-SA 4.0](#) license and was authored, remixed, and/or curated by [Andrei Tokmakoff](#) via [source content](#) that was edited to the style and standards of the LibreTexts platform.

23.2: Kramers' Theory

In our treatment the motion of the reactant over the transition state was treated as a free transitional degree of freedom. This ballistic or inertial motion is not representative of dynamics in soft matter at room temperature. **Kramers' theory** is the leading approach to describe diffusive barrier crossing. It accounts for friction and thermal agitation that reduce the fraction of successful barrier crossings. Again, the rates are obtained from the flux over barrier along reaction coordinate, Equation (23.1).



One approach is to treat diffusive crossing over the barrier in a potential using the **Smoluchowski equation**. The diffusive flux under influence of potential has two contributions:

1. Concentration gradient $dC/d\xi$. Proportional to diffusion coefficient, D .
2. Force from gradient of potential.

$$J(\xi) = -D \frac{dC(\xi)}{d\xi} - \frac{C(\xi)}{\zeta} \frac{dU(\xi)}{d\xi}$$

As discussed earlier ζ is the **friction coefficient** and in one dimension:

$$\zeta = \frac{k_B T}{D}$$

Written in terms of a probability density P

$$\begin{aligned} J &= D \left(-\frac{P}{k_B T} \frac{dU}{d\xi} - \frac{dP}{d\xi} \right) \\ &= -D e^{-U/k_B T} \frac{d}{d\xi} \left(P e^{U/k_B T} \right) \end{aligned}$$

or

$$J e^{U/k_B T} = -D \frac{d}{d\xi} P e^{U/k_B T} \quad (23.2.1)$$

Here we have assumed that D and ζ are not functions of ξ .

The next important assumption of Kramers' theory is that we can solve for the diffusive flux using the steady-state approximation. This allows us to set: $J = \text{constant}$. Integrate along ξ over barrier.

$$\begin{aligned} J \int_a^b e^{U/k_B T} d\xi_* &= -D \int_a^b dP e^{U/k_B T} \\ J \int_a^b e^{U(\xi)/k_B T} d\xi &= D \left\{ P_R e^{U_R/k_B T} - P_P e^{U_P/k_B T} \right\} \end{aligned}$$

P_i are the probabilities of occupying the R or P state, and U_i are the energies of the R and P states. The right hand side of this equation describes net flux across barrier.

Let's consider only flux from $R \rightarrow P$: $J_{R \rightarrow P}$, which we do by setting $P_P \rightarrow 0$. This is just a barrier escape problem. Also as a reference point, we set $U_R(\xi_R) = 0$.

$$J_{R \rightarrow P} = \frac{DP_R}{\int_a^b e^{U(\xi)/k_B T} d\xi} \quad (23.2.2)$$

The flux is linearly proportional to the diffusion coefficient and the probability of being in the reactant state. The flux is reduced by a factor that describes the energetic barrier to be overcome. Now let's evaluate with a specific form of the potential. The simplest form is to model $U(\xi)$ with parabolas. The reactant well is given by

$$U_R = \frac{1}{2} m \omega_R^2 (\xi - \xi_R)^2 \quad (23.2.3)$$

and we set $\xi_R \rightarrow 0$. The barrier is modeled by an inverted parabola centered at the transition state with a barrier height for the forward reaction E_f and a width given by the barrier frequency ω_{bar} :

$$U_{bar} = E_f - \frac{1}{2} m \omega_{bar}^2 (\xi - \xi^\ddagger)^2$$

In essence this is treating the evolution of the probability distribution as the motion of a fictitious particle with mass m .

First we evaluate the denominator in Equation 23.2.2 $e^{U_{bar}/k_B T}$ is a probability density that is peaked at ξ^\ddagger , so changing the limits on the integral does not affect things much.

$$\int_a^b e^{U_{bar}/k_B T} d\xi \approx \int_{-\infty}^{+\infty} d\xi \exp\left[-\frac{m\omega_B^2 (\xi - \xi^\ddagger)^2}{2k_B T}\right] = \sqrt{\frac{2\pi k_B T}{m\omega_B^2}}$$

Then Equation 23.2.2 becomes

$$J_{R \rightarrow P} = \omega_{bar} D \sqrt{\frac{m}{2\pi k_B T}} e^{-E_f/k_B T} P_R \quad (23.2.4)$$

Next, let's evaluate P_R . For a the Gaussian well in Equation 23.2.3 the probability density along ξ is $P_R = e^{-U_R/k_B T}$:

$$P_R(\xi) = \exp\left[-\frac{1}{2} m \omega_R^2 (\xi - \xi_R)^2 / k_B T\right]$$

$$P_R \approx \int_{-\infty}^{+\infty} P_R(\xi) d\xi = \omega_R \sqrt{\frac{m}{2\pi k_B T}}$$

Substituting this into Equation 23.2.4 we have

$$J_{R \rightarrow P} = \omega_R \omega_{bar} D \left(\frac{m}{2\pi k_B T}\right) e^{-E_f/k_B T}$$

Using the Einstein relation $D = k_B T / \zeta$, we find that the forward flux scales inversely with friction (or viscosity).

$$J_{R \rightarrow P} = \frac{\omega_R}{2\pi} \frac{\omega_{bar}}{\zeta} e^{-E_f/k_B T} \quad (23.2.5)$$

Also, the factor of m disappears when the problem is expressed in mass-weighted coordinates $\omega_{bar} = \sqrt{m} \omega_{bar}$. Note the similarity of Equation (9) to transition state theory. If we associate the period of the particle in the reactant well with the barrier crossing frequency,

$$\frac{\omega_R}{2\pi} \Rightarrow v = \frac{k_B T}{h}$$

then we can also find that we an expression for the transmission coefficient in this model:

$$k_{diff} = \kappa_{diff} k_{TST}$$

$$\kappa_{diff} = \frac{\omega_{bar}}{\zeta} \ll 1$$

This is the reaction rate in the strong damping, or diffusive, limit. Hendrik Kramers actually solved a more general problem based on the [Fokker-Planck Equation](#) that described intermediate to strong damping. The reaction rate was described as

$$k_{Kr} = \kappa_{Kr} k_{TST}$$

$$\kappa_{Kr} = \frac{1}{\omega_{bar}} \left(-\frac{\zeta}{2} + \sqrt{\frac{\zeta^2}{4} + \omega_{bar}^2} \right)$$

$$\zeta = \frac{1}{mk_B T} \int_0^\infty dt \langle \xi(0)\xi(t) \rangle$$

This shows a crossover in behavior between the strong damping (or diffusive) behavior described above and an intermediate damping regime:

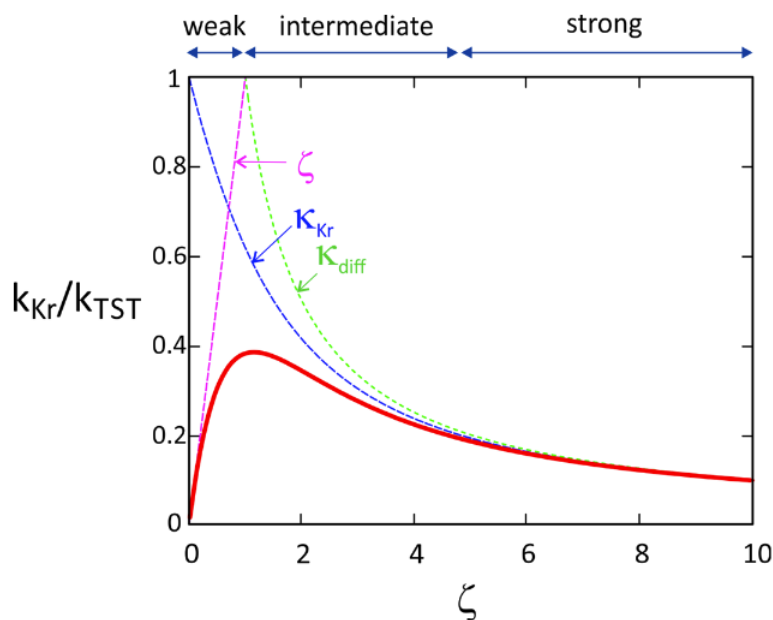
- Strong damping/friction: $\zeta \rightarrow \infty$ $\kappa_{Kr} \rightarrow \frac{\omega_{bar}}{\zeta}$
- Intermediate damping: $\zeta \ll 2\omega_B$ $\kappa_{Kr} \rightarrow 1$ and $k_{Kr} \rightarrow k_{TST}$

In the weak friction limit, Kramers argued that the reaction rate scaled as

$$k_{weak} \sim \zeta k_{TST}$$

That is, if you had no friction at all, the particle would just move back and forth between the reactant and product state without committing to a particular well. You need some dissipation to relax irreversibly into the product well. On the basis of this we expect an optimal friction that maximizes κ , which balances the need for some dissipation but without so much that barrier crossing is exceedingly rare. This “**Kramers turnover**” is captured by the interpolation formula

$$\kappa^{-1} = \kappa_{Kr}^{-1} + \kappa_{weak}^{-1}$$



This page titled [23.2: Kramers' Theory](#) is shared under a [CC BY-NC-SA 4.0](#) license and was authored, remixed, and/or curated by [Andrei Tokmakoff](#) via [source content](#) that was edited to the style and standards of the LibreTexts platform.

Index

A

aggregation number
 19.1: Micelle Formation
 amphiphilic
 19.1: Micelle Formation

B

Brownian dynamics
 13.2: Brownian Dynamics
 Brownian motion
 10.1: Continuum Diffusion
 Brownian ratchet
 17.3: Brownian Ratchet

C

configurational entropy
 5.1: Hydrophobic Solvation - Thermodynamics
 critical micelle concentration
 19.1: Micelle Formation
 critical nucleation cluster size
 19.2: Classical Nucleation Theory

D

Debye length
 6.6: Debye–Hückel Theory
 dielectric constant
 6.2: Dielectric Constant and Screening
 diffusion
 10.1: Continuum Diffusion
 diffusion constant
 10.1: Continuum Diffusion
 DNA hybridization
 21.3: DNA Hybridization
 drag force
 14.3: Laminar and Turbulent Flow

E

entropy of mixing
 2.3: Binary Fluid
 excluded volume
 1.3: Excluded Volume

F

facilitated diffusion
 15.2: Facilitated Diffusion
 Fick's first law of diffusion
 10.1: Continuum Diffusion
 Fick's second law of diffusion
 10.1: Continuum Diffusion
 Flory characteristic ratio
 7.1: Segment Models
 Flory–Huggins model
 8.4: Flory–Huggins Model of Polymer Solutions
 fluctuation–dissipation theorem
 13.1: Langevin Equation
 fluid
 1.1: What is a Fluid?
 fluorescence correlation spectroscopy
 11.3: Fluorescence Correlation Spectroscopy

Fluorescence Recovery After
 Photobleaching (FRAP)
 10.2: Solving the Diffusion Equation
 freely jointed chain model
 7.1: Segment Models

G

Gaussian random coil
 7.1: Segment Models
 Gouy–Chapman layer
 6.7: Ion Distributions Near a Charged Interface
 Gouy–Chapman model
 6.7: Ion Distributions Near a Charged Interface
 Green–Kubo relationship
 13.1: Langevin Equation

H

Helix–Coil transition
 18.1: Helix–Coil Transition
 20.1: Models for Simulating Folding
 hydrophobic solvation
 5.1: Hydrophobic Solvation - Thermodynamics
 hydrophobicity
 5.1: Hydrophobic Solvation - Thermodynamics

J

Jarzynski equality
 9.1: Force and Work

K

Kramers turnover
 23.2: Kramers' Theory
 Kramers' theory
 23.2: Kramers' Theory

L

laminar flow
 14.3: Laminar and Turbulent Flow
 Langevin equation
 13.1: Langevin Equation
 13.2: Brownian Dynamics

lattice gas
 2.2: Ideal Lattice Gas
 lattice model
 2.1: Lattice Models

M

Markov chain
 11.2: Markov Chain and Stochastic Processes
 micelles
 19.1: Micelle Formation

N

Newtonian fluid
 14.1: Newtonian Fluids
 nucleation theory
 19.2: Classical Nucleation Theory

O

orientational diffusion
 11.4: Orientational Diffusion
 orientational diffusion constant
 11.4: Orientational Diffusion
 Overton relation
 10.3: Steady-State Solutions

P

persistence length
 7.1: Segment Models
 Poisson–Boltzmann equation
 6.5: Poisson–Boltzmann Equation
 polymer loops
 7.3: Polymer Loops
 potential of mean force
 1.2: Radial Distribution Function

R

radial distribution function
 1.2: Radial Distribution Function
 radius of gyration
 7.1: Segment Models
 random walk
 11.1: Random Walk and Diffusion
 reorganization energy
 4.3: Solvation Dynamics and Reorganization Energy
 Reynolds number
 14.3: Laminar and Turbulent Flow

S

screening
 6.2: Dielectric Constant and Screening
 Smoluchowski equation
 12.3: Diffusion in a Potential
 solute's solvent accessible surface area
 4.2: Solvation Thermodynamics
 solvation
 4.1: Solvation
 4.2: Solvation Thermodynamics
 solvation dynamics
 4.3: Solvation Dynamics and Reorganization Energy
 solvation free energy
 6.3: Free Energy of Ions in Solution
 Stern layer
 6.7: Ion Distributions Near a Charged Interface
 stochastic process
 13.1: Langevin Equation
 Stochastic processes
 11.2: Markov Chain and Stochastic Processes
 Stokes' law
 14.2: Stokes' Law

T

transition state theory
 23.1: Transition State Theory
 turbulent flow
 14.3: Laminar and Turbulent Flow
 two-state sliding mechanism
 15.3: Search Times in Facilitated Diffusion

V

viscosity

[14.1: Newtonian Fluids](#)

W

writhe

[9.2: Worm-like Chain](#)

Z

Zimm–Bragg model

[18.1: Helix–Coil Transition](#)

Detailed Licensing

Overview

Title: Concepts in Biophysical Chemistry (Tokmakoff)

Webpages: 121

Applicable Restrictions: Noncommercial

All licenses found:

- [CC BY-NC-SA 4.0](#): 91.7% (111 pages)
- [Undeclared](#): 8.3% (10 pages)

By Page

- [Concepts in Biophysical Chemistry \(Tokmakoff\) - CC BY-NC-SA 4.0](#)
 - [Front Matter - Undeclared](#)
 - [TitlePage - Undeclared](#)
 - [InfoPage - Undeclared](#)
 - [Table of Contents - Undeclared](#)
 - [Licensing - Undeclared](#)
 - [1: Water and Aqueous Solutions - CC BY-NC-SA 4.0](#)
 - [1: Fluids - CC BY-NC-SA 4.0](#)
 - [1.1: What is a Fluid? - CC BY-NC-SA 4.0](#)
 - [1.2: Radial Distribution Function - CC BY-NC-SA 4.0](#)
 - [1.3: Excluded Volume - CC BY-NC-SA 4.0](#)
 - [2: Lattice Model of a Fluid - CC BY-NC-SA 4.0](#)
 - [2.1: Lattice Models - CC BY-NC-SA 4.0](#)
 - [2.2: Ideal Lattice Gas - CC BY-NC-SA 4.0](#)
 - [2.3: Binary Fluid - CC BY-NC-SA 4.0](#)
 - [3: Water's Physical Properties - CC BY-NC-SA 4.0](#)
 - [3.1: Water Structure - CC BY-NC-SA 4.0](#)
 - [3.2: Water Dynamics - CC BY-NC-SA 4.0](#)
 - [3.3: Electrical Properties of Pure Water - CC BY-NC-SA 4.0](#)
 - [4: Solvation - CC BY-NC-SA 4.0](#)
 - [4.1: Solvation - CC BY-NC-SA 4.0](#)
 - [4.2: Solvation Thermodynamics - CC BY-NC-SA 4.0](#)
 - [4.3: Solvation Dynamics and Reorganization Energy - CC BY-NC-SA 4.0](#)
 - [5: Hydrophobicity - CC BY-NC-SA 4.0](#)
 - [5.1: Hydrophobic Solvation - Thermodynamics - CC BY-NC-SA 4.0](#)
 - [5.2: Hydrophobic Solvation- Solute Size Effect - CC BY-NC-SA 4.0](#)
 - [5.3: Hydrophobic Collapse - CC BY-NC-SA 4.0](#)
 - [6: Electrical Properties of Water and Aqueous Solutions - CC BY-NC-SA 4.0](#)
 - [6.1: Electrostatics - CC BY-NC-SA 4.0](#)
 - [6.2: Dielectric Constant and Screening - CC BY-NC-SA 4.0](#)
 - [6.3: Free Energy of Ions in Solution - CC BY-NC-SA 4.0](#)
 - [6.4: Ion Distributions in Electrolyte Solution - CC BY-NC-SA 4.0](#)
 - [6.5: Poisson–Boltzmann Equation - CC BY-NC-SA 4.0](#)
 - [6.6: Debye–Hückel Theory - CC BY-NC-SA 4.0](#)
 - [6.7: Ion Distributions Near a Charged Interface - CC BY-NC-SA 4.0](#)
 - [6.8: Ion Distributions Near a Charged Sphere - CC BY-NC-SA 4.0](#)
 - [2: Macromolecules - CC BY-NC-SA 4.0](#)
 - [7: Statistical Description of Macromolecular Structure - CC BY-NC-SA 4.0](#)
 - [7.1: Segment Models - CC BY-NC-SA 4.0](#)
 - [7.2: Excluded Volume Effects - CC BY-NC-SA 4.0](#)
 - [7.3: Polymer Loops - CC BY-NC-SA 4.0](#)
 - [8: Polymer Lattice Models - CC BY-NC-SA 4.0](#)
 - [8.1: Entropy of Single Polymer Chain - CC BY-NC-SA 4.0](#)
 - [8.2: Self-Avoiding Walks - CC BY-NC-SA 4.0](#)
 - [8.3: Conformational Changes with Temperature - CC BY-NC-SA 4.0](#)
 - [8.4: Flory–Huggins Model of Polymer Solutions - CC BY-NC-SA 4.0](#)
 - [8.5: Polymer–Solvent Interactions - CC BY-NC-SA 4.0](#)
 - [9: Macromolecular Mechanics - CC BY-NC-SA 4.0](#)
 - [9.1: Force and Work - CC BY-NC-SA 4.0](#)
 - [9.2: Worm-like Chain - CC BY-NC-SA 4.0](#)
 - [9.3: Polymer Elasticity and Force–Extension Behavior - CC BY-NC-SA 4.0](#)
 - [3: Diffusion - CC BY-NC-SA 4.0](#)
 - [10: Diffusion - CC BY-NC-SA 4.0](#)

- 10.1: Continuum Diffusion - [CC BY-NC-SA 4.0](#)
- 10.2: Solving the Diffusion Equation - [CC BY-NC-SA 4.0](#)
- 10.3: Steady-State Solutions - [CC BY-NC-SA 4.0](#)
- 11: Brownian Motion - [CC BY-NC-SA 4.0](#)
 - 11.1: Random Walk and Diffusion - [CC BY-NC-SA 4.0](#)
 - 11.2: Markov Chain and Stochastic Processes - [CC BY-NC-SA 4.0](#)
 - 11.3: Fluorescence Correlation Spectroscopy - [CC BY-NC-SA 4.0](#)
 - 11.4: Orientational Diffusion - [CC BY-NC-SA 4.0](#)
- 12: Diffusion in a Potential - [CC BY-NC-SA 4.0](#)
 - 12.1: Diffusion with Drift - [CC BY-NC-SA 4.0](#)
 - 12.2: Biased Random Walk - [CC BY-NC-SA 4.0](#)
 - 12.3: Diffusion in a Potential - [CC BY-NC-SA 4.0](#)
- 13: Friction and the Langevin Equation - [CC BY-NC-SA 4.0](#)
 - 13.1: Langevin Equation - [CC BY-NC-SA 4.0](#)
 - 13.2: Brownian Dynamics - [CC BY-NC-SA 4.0](#)
- 4: Transport - [CC BY-NC-SA 4.0](#)
 - 14: Hydrodynamics - [CC BY-NC-SA 4.0](#)
 - 14.1: Newtonian Fluids - [CC BY-NC-SA 4.0](#)
 - 14.2: Stokes' Law - [CC BY-NC-SA 4.0](#)
 - 14.3: Laminar and Turbulent Flow - [CC BY-NC-SA 4.0](#)
 - 15: Passive Transport - [CC BY-NC-SA 4.0](#)
 - 15.1: Dimensionality Reduction - [CC BY-NC-SA 4.0](#)
 - 15.2: Facilitated Diffusion - [CC BY-NC-SA 4.0](#)
 - 15.3: Search Times in Facilitated Diffusion - [CC BY-NC-SA 4.0](#)
 - 16: Targeted Diffusion - [CC BY-NC-SA 4.0](#)
 - 16.1: Diffusion to Capture - [CC BY-NC-SA 4.0](#)
 - 16.2: Diffusion to Capture with Interactions - [CC BY-NC-SA 4.0](#)
 - 16.3: Mean First Passage Time - [CC BY-NC-SA 4.0](#)
 - 17: Directed and Active Transport - [CC BY-NC-SA 4.0](#)
 - 17.1: Motor Proteins - [CC BY-NC-SA 4.0](#)
 - 17.2: Passive vs Active Transport - [CC BY-NC-SA 4.0](#)
 - 17.3: Brownian Ratchet - [CC BY-NC-SA 4.0](#)
 - 17.4: Polymerization Ratchet and Translocation Ratchet - [Undeclared](#)
- 5: Cooperativity - [CC BY-NC-SA 4.0](#)
 - 18: Cooperativity - [CC BY-NC-SA 4.0](#)
 - 18.1: Helix-Coil Transition - [CC BY-NC-SA 4.0](#)
 - 18.2: Two-State Thermodynamics - [CC BY-NC-SA 4.0](#)
- 6: Dynamics and Kinetics - [CC BY-NC-SA 4.0](#)
 - 19: Self-Assembly - [CC BY-NC-SA 4.0](#)
 - 19.1: Micelle Formation - [CC BY-NC-SA 4.0](#)
 - 19.2: Classical Nucleation Theory - [CC BY-NC-SA 4.0](#)
 - 19.3: Why Are Micelles Uniform in Size? - [CC BY-NC-SA 4.0](#)
 - 19.4: Shape of Self-Assembled Amphiphiles - [CC BY-NC-SA 4.0](#)
 - 20: Protein Folding - [CC BY-NC-SA 4.0](#)
 - 20.1: Models for Simulating Folding - [CC BY-NC-SA 4.0](#)
 - 20.2: Perspectives on Protein Folding Dynamics - [CC BY-NC-SA 4.0](#)
 - 21: Binding and Association - [CC BY-NC-SA 4.0](#)
 - 21.1: Thermodynamics and Biomolecular Reactions - [CC BY-NC-SA 4.0](#)
 - 21.2: Statistical Thermodynamics of Biomolecular Reactions - [CC BY-NC-SA 4.0](#)
 - 21.3: DNA Hybridization - [CC BY-NC-SA 4.0](#)
 - 21.4: Biomolecular Kinetics - [CC BY-NC-SA 4.0](#)
 - 21.5: Diffusion-Limited Reactions - [CC BY-NC-SA 4.0](#)
 - 21.6: Protein Recognition and Binding - [CC BY-NC-SA 4.0](#)
 - 21.7: Forces Guiding Binding - [CC BY-NC-SA 4.0](#)
 - 21.8: Specificity in Recognition and Binding - [CC BY-NC-SA 4.0](#)
 - 22: Biophysical Reaction Dynamics - [CC BY-NC-SA 4.0](#)
 - 22.1: Concepts and Definitions - [CC BY-NC-SA 4.0](#)
 - 22.2: Computing Dynamics - [CC BY-NC-SA 4.0](#)
 - 22.3: Representations of Dynamics - [CC BY-NC-SA 4.0](#)
 - 22.4: Analyzing Trajectories - [CC BY-NC-SA 4.0](#)
 - 22.5: Time-Correlation Functions - [CC BY-NC-SA 4.0](#)
 - 23: Barrier Crossing and Activated Processes - [CC BY-NC-SA 4.0](#)
 - 23.1: Transition State Theory - [CC BY-NC-SA 4.0](#)
 - 23.2: Kramers' Theory - [CC BY-NC-SA 4.0](#)
- Back Matter - [Undeclared](#)
 - Index - [Undeclared](#)
 - Glossary - [Undeclared](#)
 - Detailed Licensing - [Undeclared](#)

